

Polymerization of reactive *S*-vinyl monomers

Dissertation
(kumulativ)

zur Erlangung des akademischen Grades doctor rerum naturalium
(Dr. rer. nat.)

vorgelegt dem Rat der Chemisch-Geowissenschaftlichen Fakultät der
Friedrich-Schiller-Universität Jena
von M.Sc. Nicole Ziegenbalg
geboren am 09.05.1996 in Leisnig

Gutachter:

1. Dr. Johannes C. Brendel, Friedrich-Schiller-Universität Jena
2. Prof. Dr. Ulrich Schubert, Friedrich-Schiller-Universität Jena

Tag der Verteidigung: 27.06.2023

Table of contents

Documentation of authorship	5
1. Introduction	7
2. Reactivity of <i>S</i> -vinyl monomers.....	9
2.1. Vinyl sulfides.....	9
2.2. Vinyl sulfoxides.....	12
2.3. Vinyl sulfones.....	13
3. Motivation and aim	15
4. Homogeneous radical polymerization of the <i>S</i> -vinyl monomer VME.....	17
4.1. Free radical polymerization	17
4.2. Controlled radical polymerization <i>via</i> RAFT.....	19
4.3. Properties of the polymers.....	23
4.3.1. Oxidation of the homopolymer	23
4.3.2. Thermal properties of the polymers	24
4.3.3. Optical properties of the polymers	26
4.3.4. Mechanical properties of the polymers	26
5. Heterogeneous radical polymerization of the <i>S</i> -vinyl monomer VME.....	29
5.1. Emulsion or dispersion polymerization?	29
5.2. Incorporation of noble metals in the polymer particle	32
5.2.1. Modification of polyvinyl mercaptoethanol particles with silver ions (Ag ⁺ @PVME).....	32
5.2.1. Modification of polyvinyl mercaptoethanol particles with silver nanoparticles (Ag@PVME)	34
5.2.2. Modification of polyvinyl mercaptoethanol particles with gold ions and nanoparticles (AuCl ₄ ⁻ @PVME and Au@PVME).....	36
6. Homogeneous polyaddition of electron-deficient <i>S</i> -monomer VSE.....	38
6.1. Oxa-Michael polyaddition.....	38
6.1.1. Bulk polymerization.....	40
6.1.2. Solution polymerization	43
6.2. Properties of the oxa-Michael polymers.....	45
7. Summary	48
8. Zusammenfassung.....	52
9. References	57
List of abbreviations.....	61
Publication list.....	63
Acknowledgment	65
Declaration of originality	66

Table of contents

Appendix	67
----------------	----

Documentation of authorship

This election contains a list of the individual author's contributions to the publications reprinted in this thesis.

P1 <i>Polymers from S-vinyl monomers: Reactivities and properties</i> N. Ziegenbalg, ¹ L. Elbinger, ² U. S. Schubert, ³ J. C. Brendel, ⁴ <i>Polym. Chem.</i> 2022 , <i>13</i> , 5019-5041.					
Author	1	2	3	4	
Conceptual contribution	×				×
Literature research	×	×			
Preparation of the manuscript	×				
Correction of the manuscript	×	×	×		×
Supervision of N. Ziegenbalg					×
Proposed publication equivalent	0.5				

P2 <i>Vinyl mercaptoethanol as a reactive monomer for preparation of functional homo- and copolymers with (meth)acrylates</i> N. Ziegenbalg, ¹ F. V. Gruschwitz, ² T. Adermann, ³ L. Mayr, ⁴ S. Guriyanova, ⁵ J. C. Brendel, ⁶ <i>Polym. Chem.</i> 2022 , <i>13</i> , 4934-4943.						
Author	1	2	3	4	5	6
Conceptual contribution	×		×			×
Synthesis	×	×				
Polymer characterization	×	×		×	×	
Preparation of the manuscript	×					
Correction of the manuscript	×	×	×	×	×	×
Supervision of N. Ziegenbalg						×
Proposed publication equivalent	1					

Documentation of authorship

<i>Coordination of noble metals in poly(vinyl mercaptoethanol) particles prepared by precipitation/emulsion polymerization</i>									
P3	N. Ziegenbalg, ¹ H. F. Ulrich, ² S. Stumpf, ³ P. Mueller, ⁴ J. Wiethan, ⁵ J. Danner, ⁶ U. S. Schubert, ⁷ T. Adermann, ⁸ J. C. Brendel, ⁹ <i>Macromol. Chem. Phys.</i> 2023 , 224, 2200379.								
Author	1	2	3	4	5	6	7	8	9
Conceptual contribution	×							×	×
Synthesis	×	×							
Polymer characterization	×		×	×	×	×			
Preparation of the manuscript	×								
Correction of the manuscript	×	×	×	×	×	×	×	×	×
Supervision of N. Ziegenbalg									×
Proposed publication equivalent	1								

<i>Oxa-Michael polyaddition of vinylsulfonylethanol for aliphatic polyethersulfones</i>					
P4	N. Ziegenbalg, ¹ R. Lohwasser, ² G. D'Andola, ³ T. Adermann, ⁴ J. C. Brendel, ⁵ <i>Polym. Chem.</i> 2021 , 12, 4337-4346.				
Author	1	2	3	4	5
Conceptual contribution	×	×			×
Synthesis	×				
Polymer characterization	×				
Preparation of the manuscript	×				
Correction of the manuscript	×	×	×	×	×
Supervision of N. Ziegenbalg					×
Proposed publication equivalent	1				

1. Introduction

The development of highly functional polymers has led to more and more innovations coming onto the market in recent years. The potential of functional polymers appears to be almost unlimited, and so polymer research is being pushed ever further. One area that has received less attention so far, but whose development potential is quite foreseeable, is sulfur-containing polymers. They are characterized by a unique combination of properties, such as an increased refractive index,¹⁻⁹ the ability to coordinate metals,¹⁰⁻¹³ and high thermal stability¹⁴⁻¹⁷ for example. Therefore, these materials will be of great interest in the future, for research in general and but also for industrial applications.

The substance class is characterized not only by its unique properties but also by the possibility of modifying it in a quite simple way and thus obtaining substances with completely new properties. An overview of the various modification routes with a selection of applications is shown in Figure 1. Sulfide species can selectively oxidize to sulfoxides or sulfones for example.¹⁸⁻²⁰ This result not only in a changed reactivity but also in completely new properties of the substances because of the now more polar sulfoxide or sulfone group, which greatly expands the range of applications for sulfur-containing polymers. Sulfoxides are predestined, for example, for pharmaceutical applications due to their skin-penetrating properties,^{21, 22} while sulfones seem ideally suited for optical applications because of their increased refractive index and very high Abbe number.^{1-3, 5, 8, 9, 23} However, not only the oxidation of the sulfide group is a simple way to modify the properties of substances. Starting from thiol compounds, these can form reversible disulfide bridges in a reductive environment and thus represent an interesting class of crosslinkers that plays an important role in the biological research of proteins, peptides, and other biomolecules.²⁴⁻²⁶ Furthermore, sulfur-containing materials are not limited to neutrally charged materials.²⁷⁻³⁰ Sulfonates or materials containing sulfonium ions moieties can also be used, for example, as drug delivery systems through their interaction with other charged substances.

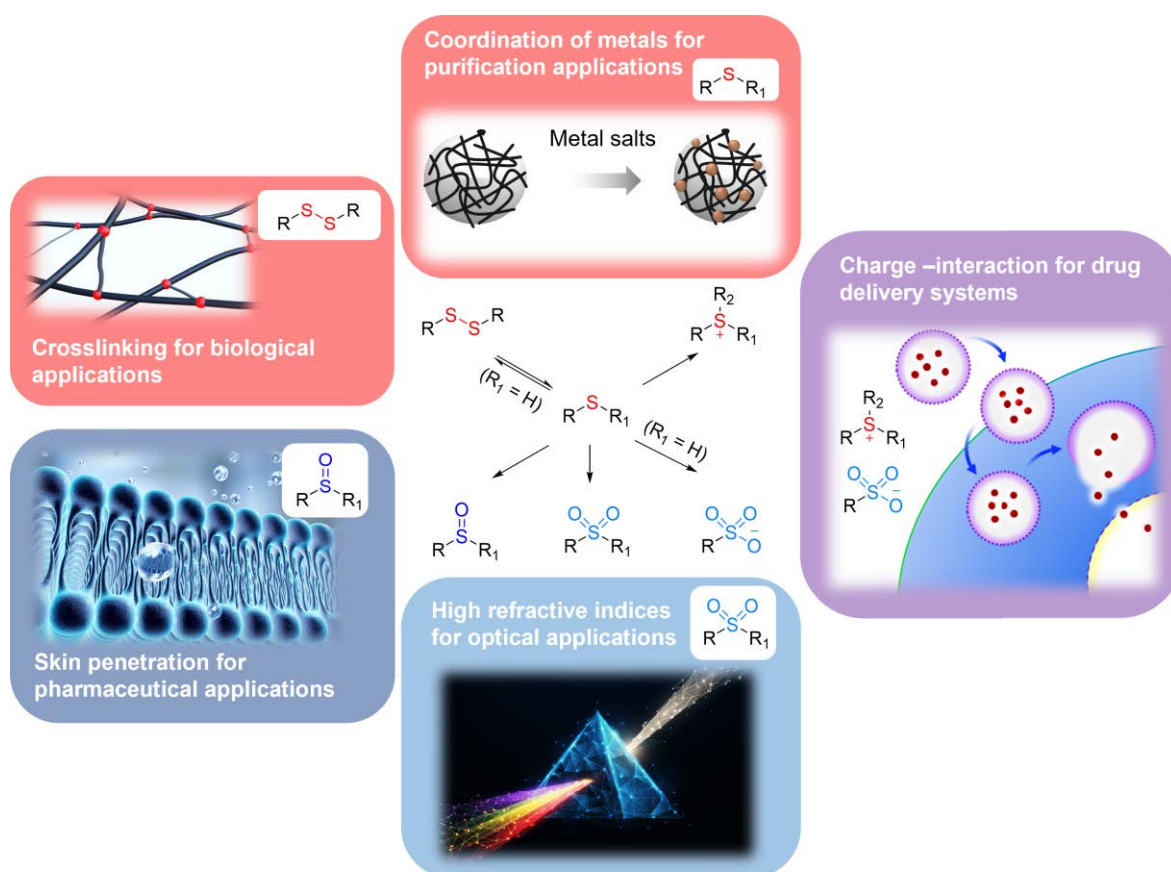


Figure 1: Schematic overview of the different sulfur species and possible applications.

However, polymerization of sulfur-containing monomers proves to be a major challenge because peroxides and redox initiators, which are commonly used in industry, often only lead to oxidation of the sulfur but do not initiate the polymerization process. In addition, frequently occurring side reactions such as chain transfer reactions caused by the presence of sulfur complicate the polymerization on an industrial scale, which significantly limits potential applications. In particular, the polymerization of *S*-vinyl monomers has so far only been a niche in polymer research, because of the challenges already described, but also due to the limited availability of these monomers. Nevertheless, research into this class of compounds is desirable because of their unique properties. Previous publications demonstrated the enormous influence of the oxidation state of the sulfur on the polymerization behavior due to its direct proximity to the vinyl group. For example, increased reactivity has been observed in the free-radical polymerization of vinyl sulfides, while vinyl sulfoxides and vinyl sulfones are usually polymerized by anionic processes. The focus of this thesis was to study the reactivity of *S*-vinyl monomers, in particular, the novel monomer vinyl mercaptoethanol and related derivatives.

2. Reactivity of *S*-vinyl monomers

Parts of this chapter have been published in: P1) N. Ziegenbalg, L. Elbinger, U. S. Schubert, J. C. Brendel, *Polym. Chem.* **2022**, *13*, 5019-5041.

As mentioned at the beginning, the polymerization behavior of *S*-vinyl monomers is strongly dependent on the oxidation state of sulfur. Therefore, the different reactivities and properties of vinyl sulfides, vinyl sulfoxides, and vinyl sulfones will be discussed in more detail in this chapter.

2.1. Vinyl sulfides

Although the monomer class of vinyl sulfides has received little attention in recent years compared to other monomer classes. Vinyl sulfides are characterized above all by an increased reactivity in radical polymerization compared to, for example, the oxygen analogs, which was observed and demonstrated by Price and coworkers as early as 1950.³¹ Due to the 2p-3p conjugation of sulfur with the adjacent carbon atom, a bathochromic shift occurs for the unsaturated vinyl sulfides compared to the saturated sulfides. This conjugation is much weaker than the 2p-2p conjugation in vinyl ethers, which thus favors the attack of radicals. These radicals can then be additionally stabilized in the transition state by the 3d orbital of the sulfur.

Polymerization of vinyl sulfides can be achieved mainly by aza-initiators such as azobisisobutyronitrile (AIBN).³¹⁻³⁹ Peroxides, on the other hand, are not suitable because of their tendency to oxidize the sulfide group and usually are not able to initiate the polymerization. After the initial studies by Alfrey and Coworker, subsequent work focused in particular on the copolymerization of vinyl sulfides, while homopolymerizations played a rather minor role. The determination of the copolymerization parameters for the respective monomers was important in order to be able to make predictions about copolymerization behavior with other monomers. For this purpose, the original composition in the monomer mixture would be compared to the ratio of monomer units in the obtained polymer and inserted into one of the following equations for the determination of the parameters: Mayo-Lewis,⁴⁰ Fineman-Ross⁴¹ or Kelen-Tüdös equation.⁴² With the copolymerization parameters determined, preferably by copolymerization with styrene, the *Q*- and *e*-values can then be calculated according to the Alfrey-Price equation,²⁶ allowing a comparison of the *S*-vinyl monomers with other monomer classes. But these values also provide information about the reactivity and

polarity in radical polymerizations in general, in addition to estimating the copolymerization behavior of unknown monomer combinations. The Q- values for vinyl sulfides are in the range of 0.3 to 0.5, revealing good stabilization of the radicals.^{43, 44} However, this value can also be strongly influenced by the substituents. For example, if the conjugated system is extended, as in the case of divinyl sulfides, the Q-value increases to 0.6,⁴⁵ while if the coplanarity of the molecule is not maintained, as in the case of pentachlorophenylvinyl sulfides, the Q-value decreases to 0.23.⁴⁶ Although there are major differences between the radical polymerization behavior of vinyl sulfides and vinyl ethers, the two classes of monomers exhibit similar polarity, as reflected in the negative e-values in the range of -1.5 .⁴⁵ However, even here the value can be strongly influenced by the substituent and thus electron-accepting groups cause an increase in the e-value.^{34, 47} Various copolymerizations have been carried out in the literature with styrene,^{33, 43, 44} but also with a variety of monomer classes such as acrylates,^{33, 43, 46, 48} methacrylates,^{43, 45, 47} acrylonitrile,⁴³ vinylene carbonates,⁴⁹ vinyl ethers,⁵⁰ maleimides,⁵¹ and diallyl compounds.⁵² The copolymerizations with acrylonitriles, as well as acrylates and methacrylates, worked very well, which is in good agreement with the determined Q- and e-values. However, interest in this class of monomers quickly vanished and did not flare up again until the development of controlled polymerization techniques. In 2013, the first attempts were made to synthesize well-defined homopolymers as well as random copolymers and block copolymers starting from vinyl sulfide monomers *via* reversible-addition-fragmentation chain-transfer (RAFT) polymerization.⁵³⁻⁵⁷ The kind of chain transfer agent (CTA) has a crucial influence on the dispersity of the polymers, as not every CTA seems to be suitable for this class of monomers. For example Abiko *et al.* demonstrated in 2015 that trithiocarbonate-type CTAs were the most suitable for the copolymerization of phenylvinyl sulfide with different comonomers like maleic anhydride, *N*-methyl maleimide, and *N*-phenyl maleimide (PMI), as the obtained polymers have the lowest dispersity (1.3 – 1.4) (Figure 2).⁵⁴ On the other hand the use of xanthate- and dithiocarbamate-type CTAs, which are mostly suitable for vinyl ethers and vinyl esters, resulted in polymers with higher dispersities (1.8 – 2.6). The success of these experiments once again underscores the potential of S-vinyl polymers.

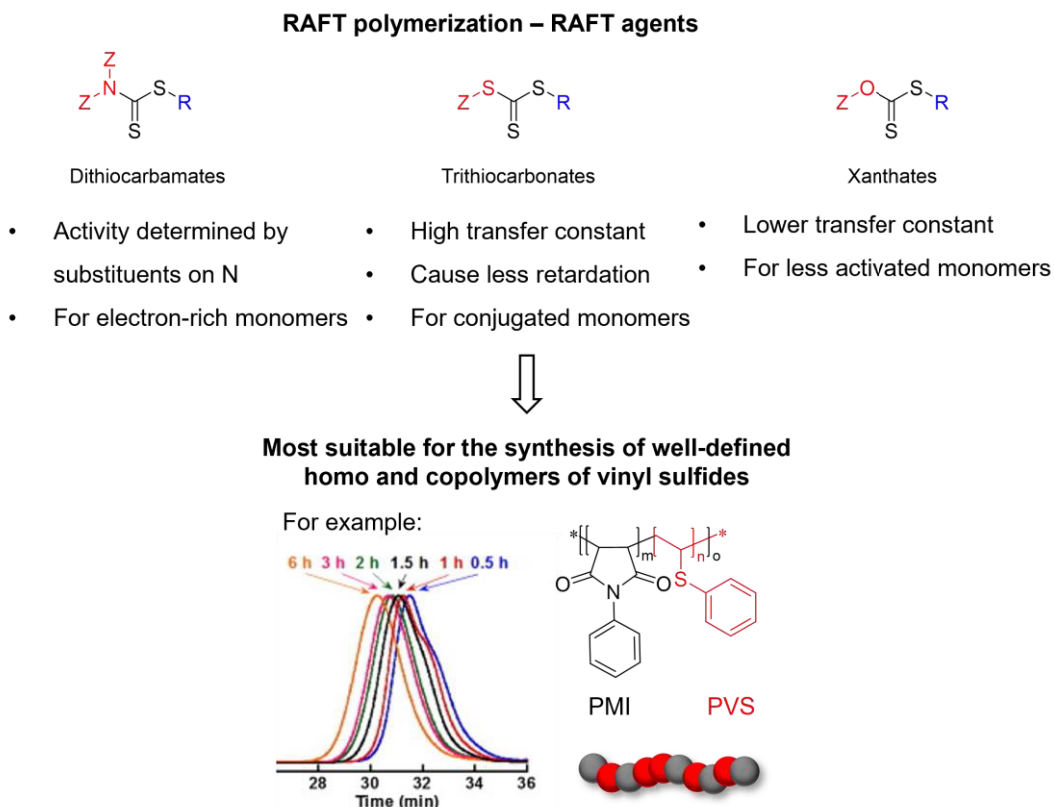
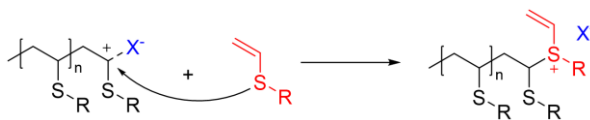


Figure 2: Schematic representation of the different possible CTAs for RAFT polymerizations and the size exclusion chromatography (SEC) traces of the copolymer poly (*N*-phenyl maleimide-*co*-phenylvinyl sulfide) (P(PMI-*co*-PVS)) with a trithiocarbonate-CTA. The figure was adapted from ref. ⁵⁴ with permissions of Elsevier. Copyright 2015.

However, not only radical but also cationic polymerization of vinyl sulfides is feasible because of the high electron density at the vinyl group, as Reppe was able to demonstrate as early as 1956.⁵⁸ Nevertheless, the cationic polymerizations are characterized by more difficulties than radical polymerization.⁵⁹ Often only oligomers are formed or very high temperatures and longer reaction times are required to synthesize polymers, while vinyl ethers react comparatively much faster with less catalyst.⁶⁰ This can be explained by the lower reactivity, but also by the basicity of sulfur, which often leads to the formation of sulfur-metal complexes during polymerization. As a result, the polymerization process is not completely suppressed by the formation of the complex but is at least significantly limited. Another explanation for the low molar masses is the chain-transfer process, in which the sulfur atom of a monomer molecule reacts with the cationic chain-end to the sulfonium ion (Scheme 1).⁶¹ Because of these results and the low chances of success of this polymerization, efforts for further research in this field were discontinued after 1980.



Scheme 1: Schematic representation of the chain transfer reaction of sulfides in cationic polymerizations. The figure was reused from ref. ⁶² with permissions of Royal Society of Chemistry. Copyright 2022.

2.2. Vinyl sulfoxides

As already mentioned in the introduction, vinyl sulfides are versatile and can be selectively oxidized to sulfoxides or sulfones with little effort. This not only changes the properties of the monomer, such as the solubility but also decisively influences the polymerization behavior by changing the polarity of the vinyl group.

In contrast to vinyl sulfides, the free-radical polymerization of vinyl sulfoxide has been reported only sporadically in the literature, partly because the sulfoxide group can also act as an inhibitor. The Q-values determined are in the range of 0.1 to 0.2, demonstrating the significantly lower stabilization of the radicals and explaining the low molar masses of the polymers and the low yields.^{63, 64} The positive e-values in the range of 0.6 to 1.0 reflect the changed polarity compared to the vinyl sulfides, which is caused by the strongly electron-withdrawing sulfoxide group. As a consequence, the electron-poor vinyl group leads to an improved copolymerization behavior for example with the electron-rich monomer vinyl acetate which is completely different from the copolymerizations with vinyl acetate and vinyl sulfides.⁶⁵ Surprisingly, increased reactivities were also observed during copolymerization with the electron-deficient monomers methacrylamides, acrylamides, acrylonitriles, and vinyloximes. This observation could be attributed to the formation of complexes of the functional group with the sulfoxide group, which was confirmed by spectroscopic measurements.

As a consequence of the electron-withdrawing effect of the sulfoxide group and the resulting electron-deficient double bond, vinyl sulfoxides are suitable for anionic polymerization. As early as 1970, Hogen-Esch *et al.* succeeded in carrying out anionic living polymerizations with dispersities of 1.2 to 1.4 of phenylvinyl sulfoxide with various initiators.⁶⁶⁻⁶⁸ However, with longer reaction time and higher temperatures, an increase in side reactions was observed, expressed mainly in bimodal or broader molar mass distributions. Therefore, it can be assumed that the side reactions already have a

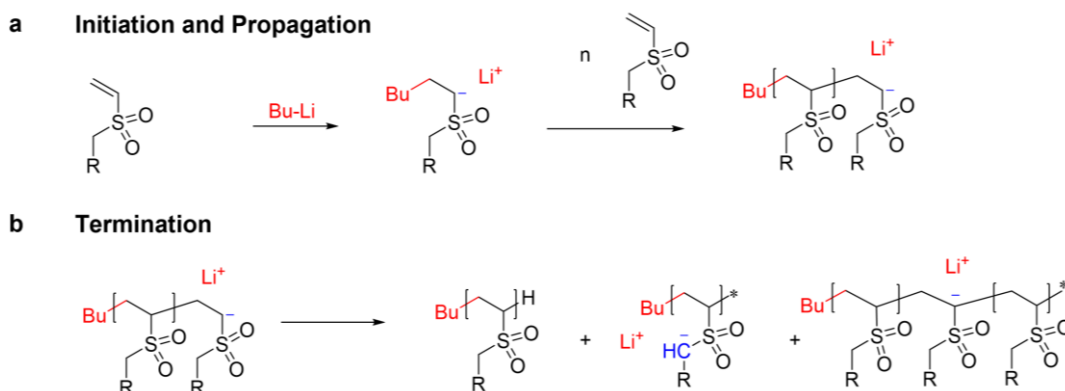
minor influence at lower reaction times and temperatures and thus also explain the dispersities, which are small but not comparable to other anionic living polymerizations.

2.3. Vinyl sulfones

Vinyl sulfones have generally attracted attention, among other things because of the very high dipole moment (4.49 D)⁶⁹ compared to the sulfide group (≈ 1.55 D), but also to the sulfoxide group (≈ 3.96 D).^{70, 71} This property leads to increased adhesion, a change in the barrier and transport properties or an improvement in solvent resistance, which makes the incorporation of vinyl sulfones desirable.⁷²⁻⁷⁴ But also the increased refractive index in combination with a high Abbe number characterizes this class of materials, which makes them ideal for optical applications for example.^{2, 3, 5, 8, 9, 23}

Price and co-workers are also pioneers in the field of radical polymerization of vinyl sulfones, who first investigated the polymerization behavior of methylvinyl sulfone and phenylvinyl sulfone in 1950.^{31, 33} However, the low Q-values ($Q = 0.1$) demonstrate poorer stabilization of the radicals compared to the vinyl sulfides and provide the reason for the difficulties of realizing radical polymerizations with these monomers. An explanation for the lower stabilization of the radicals is the weaker conjugation of the 2p and 2d orbitals in vinyl sulfones, in contrast to the conjugation of the 2p and 3p orbitals in vinyl sulfides. Nevertheless, radical polymerization is feasible in principle, but it only leads to polymers with low molar masses because of the lack of stabilization and the fact that sulfones also can act as a chain transfer agent.

In addition, high e-values in the range of 1.2 were determined, which are related to the electron-withdrawing group and thus, as already mentioned at the beginning, strongly influence the electron density at the double bond, resulting in electron-poor vinyl groups. Instead, vinyl sulfones seem theoretically ideal for anionic polymerization because of the electron-withdrawing group. However, it was demonstrated very early on that anionic polymerizations are difficult because the monomers are too reactive and often prone to side or termination reactions.⁷⁵ For example, the α -proton can be abstracted from the monomer molecule, leading to the inactivation of the active chain (Scheme 2).^{76, 77} However, an α -proton can also be abstracted from the backbone of the polymer, which leads to the same result and does not allow new initiation.



Scheme 2: Schematic representation of the initiation, propagation, and termination of the anionic polymerization of vinyl sulfones. The figure was adapted from ref. ⁶² with permissions of Royal Society of Chemistry. Copyright 2022.

Even though the radical and anionic polymerization of vinyl sulfones are often associated with difficulties, other polymerization processes have become established. For example, sulfone units can be introduced *via* the copolymerization of sulfur dioxide with various comonomers,⁷⁸⁻⁸⁰ or by the much more frequently used Michael polyaddition.⁸¹⁻⁸⁵ Vinyl sulfone is a very reactive Michael acceptor in literature. In particular, the polymerization of divinyl sulfones with bivalent alcohols is a very well-known reaction involving AA/BB polyaddition. However, often only polymers with low molar masses can be obtained in this type of polymerization because the exact adjustment of the stoichiometry, which is essential for high molar masses, is often a major challenge. In this context, side reactions, in particular, can also interfere sensitively. For this reason, it is easier to use an AB-monomer containing both the vinyl sulfone unit as the Michael acceptor and a Michael donor. At present, however, only a few monomers of this type are known, as synthesis in particular often presents difficulties because of the need of a complex manufacturing process or the use of toxic derivatives.⁸⁶⁻⁸⁹ A monomer that has only recently become available is vinyl sulfonylethanol, whose polymerization behavior is discussed in more detail in Chapter 6.

3. Motivation and aim

Further studies of the polymerization behavior and the properties of the sulfur-containing polymers are essential in order to get innovations. However, since the synthesis of *S*-vinyl monomers is often difficult, the number of available monomers is limited. BASF SE has succeeded in producing the new *S*-vinyl monomer vinyl mercaptoethanol which is characterized by long-term stability. It can be produced easily and on a large scale from acetylene and mercaptoethanol using Reppe chemistry.⁹⁰⁻⁹² Thanks to the current availability of the monomer, the polymerization behavior and properties of the polymers can now be studied in detail. The aim of this thesis was the implementation of different polymerization techniques starting from the monomer vinyl mercaptoethanol and the investigation of the properties of the corresponding polymers. An overview of the different research areas is given in Figure 3.

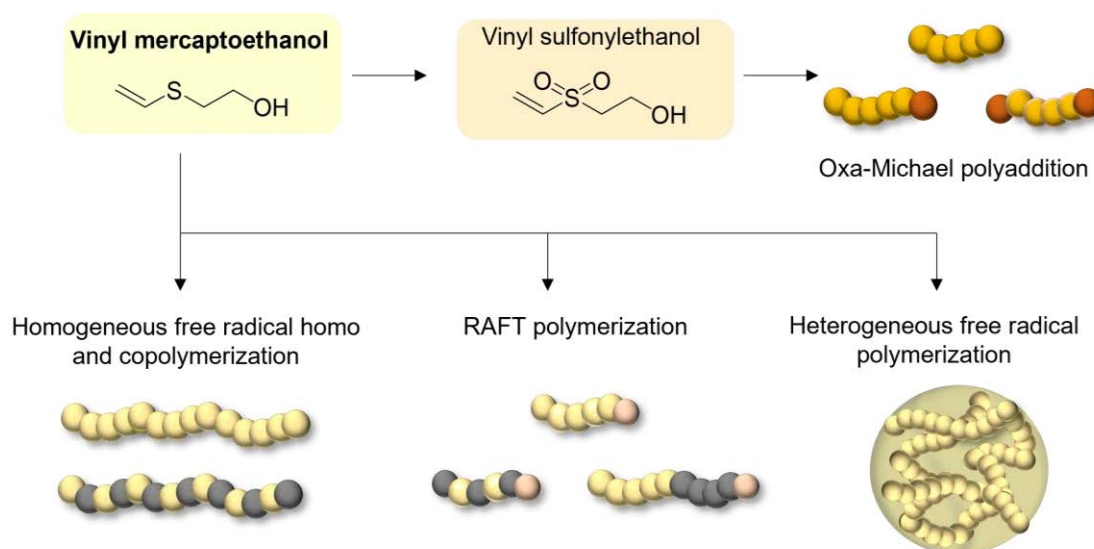


Figure 3: Overview of the different polymerization techniques which was used for the synthesis of sulfur-containing polymers in this work.

In the first part of this work, the radical polymerization behavior of the monomer vinyl mercaptoethanol will be investigated using homogeneous polymerization techniques such as bulk and solution polymerization. The focus of this study was not only on an understanding of the homopolymerization but also of the copolymerization with various monomers such as styrene, methyl methacrylate (MMA), and *n*-butyl acrylate (BA). Subsequently, it should be evaluated whether well-defined homopolymers and copolymers can be produced by controlled polymerization. RAFT polymerization promises the highest chances of success in our opinion because this technique has a high

tolerance to other functionalities and is therefore suitable for a large number of monomers. After the polymerizations were conducted, the thermal, optical, as well as mechanical properties, will be investigated in order to evaluate possible applications of these polymers. However, this work should not be limited to homogeneous polymerization techniques. The possibility of polymerizing the monomer using heterogeneous polymerization techniques should also be examined. The first focus is on the search for suitable conditions that lead to the formation of stable polymer particles. On the one hand, these can be realized by classical emulsifiers, which are also frequently used in industry, for example. On the other hand, the property of sulfur to coordinate noble metals offers the possibility to additionally stabilize particles with metal salts or metal nanoparticles.

In the last part of this work, the possibilities of using other polymerization methods than radical polymerization for the synthesis of novel functional polymers by the selective oxidation of the monomer to the sulfone will be investigated. In particular, oxa-Michael polyaddition appears to be suitable, since oxidation from the sulfide group to the sulfone leads to a monomer characterized by a stable Michael acceptor in the form of the vinyl group and a Michael donor in the form of the hydroxyl group. The influence of different catalysts on the polymerization behavior, but also on the properties of the resulting polymers, should be investigated in detail.

4. Homogeneous radical polymerization of the *S*-vinyl monomer VME

Parts of this chapter have been published in: P2) N. Ziegenbalg, F. V. Gruschwitz, T. Adermann, L. Mayr, S. Guriyanova, J. C. Brendel, *Polym. Chem.* **2022**, *13*, 4934-4943.

A major problem in researching the polymerization behavior of *S*-vinyl monomers is their availability. These can often only be realized through a complex manufacturing process or the use of toxic derivatives.^{86, 88, 93} However, BASF SE has succeeded in establishing the synthesis of the new *S*-vinyl monomer vinyl mercaptoethanol (VME) on an industrial scale by Reppe chemistry⁹² using ethylene and mercaptoethanol as starting materials. This represents an interesting breakthrough for the synthesis also for further *S*-vinyl monomers, and could be another important step for the implementation of sulfur-containing polymers in industrial applications. Up to this point, the synthesis of VME by the reaction of vinyl bromide and the corresponding sodium thiolate as nucleophile was already known,⁸⁹ but could not be realized on a larger scale, which also limited research on this monomer. The polymerization behavior of this monomer, as well as the modification possibilities of the polymers, can now be examined in detail because of the current availability. In the following, the radical homopolymerization and different copolymerization with various monomers will be described. But also, the possibility of the synthesis of well-defined polymers by RAFT polymerization will be discussed in this chapter.

4.1. Free radical polymerization

Polymerization of VME with the aza-initiator AIBN leads to polymers with high molar masses in the range of 100 to 200 kg mol⁻¹, depending on the amount of initiator used. In contrast, the polymerization experiments with peroxides were unsuccessful, which is in good agreement with the literature of other *S*-vinyl monomers, since the oxidation of sulfur occurs preferentially in the presence of hydrogen peroxide. The polymerization rate of VME proved to be very similar to the polymerization rate of methyl methacrylates under comparable conditions. However, the limited solubility of the obtained polymers posed a major challenge in handling and also restrict the possible characterization methods. The limited solubility is most likely a consequence of the formation of hydrogen bonds, which is the reason why only the polar solvents dimethyl sulfoxide (DMSO), dimethyl formamide (DMF), and methoxy ethanol proved to be suitable. In addition, a crosslinking process was observed during the initial purification process while

the polymers were drying under reduced pressure and slightly elevated temperatures (40 °C). But crosslinking can also be observed during long storage (> 1 year) at room temperature or high temperatures. In consequence, the crosslinking behavior was investigated with simultaneous thermal analysis (STA-MS). This analysis revealed a steady release of water molecules with increasing temperature, which is a clear indication of etherification *via* the hydroxyl group (Figure 4). But also, a release of acetaldehyde at temperatures above 110 °C can be observed which can be explained by the formation of a sulfonium polymer.

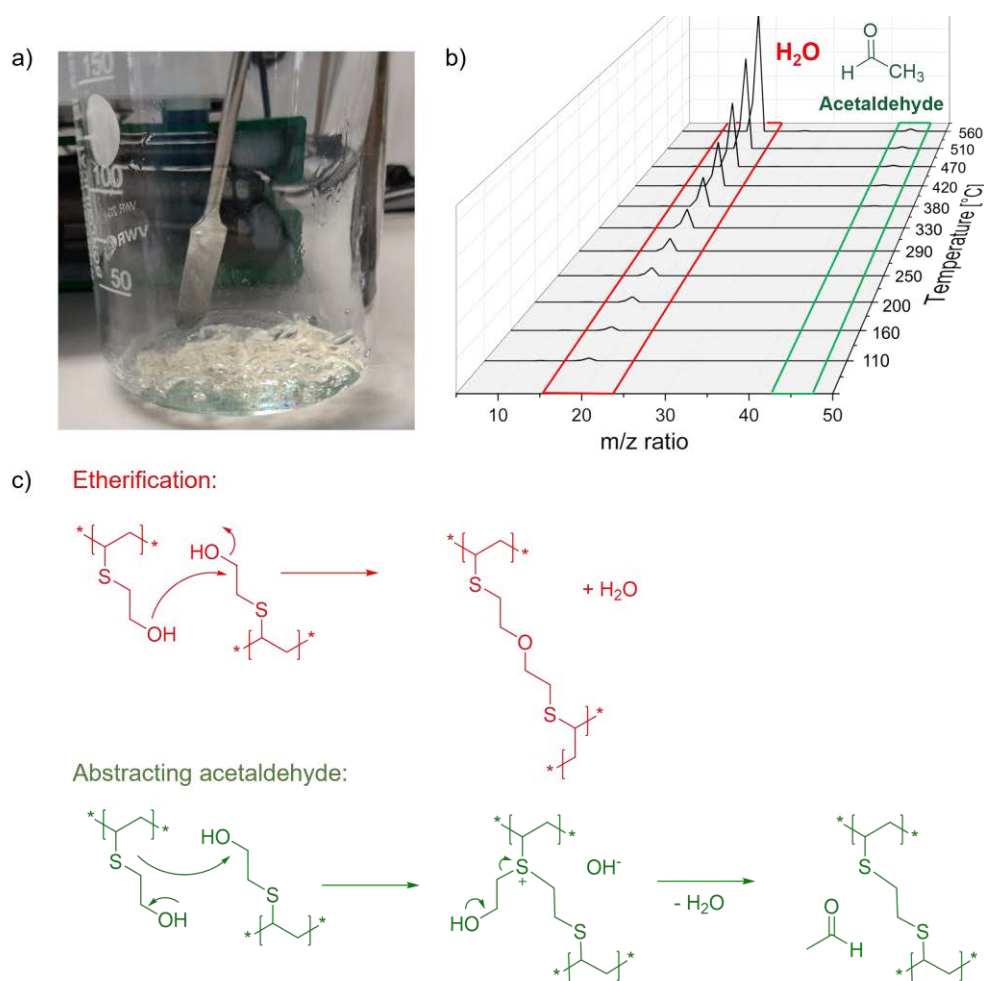


Figure 4: a) Photography of the generated crosslinked gel b) STA-measurement (He) of the homopolymer and c) schematic representation of a possible mechanism of crosslinking. The figure was adapted from ref. ⁹⁴ with permissions of Royal Society of Chemistry. Copyright 2022.

In the following, also copolymerizations with different comonomers were investigated. Styrene, methyl methacrylate (MMA), *n*-butyl acrylate (BA), vinyl pyrrolidone (VP), and vinyl acetate (VA) were selected as representatives of the various monomer classes. The polymerization of MMA and BA reveals increased reactivity, characterized mainly by a very high polymerization rate which is demonstrated by the rapidly increasing viscosity

due to the high molar masses. Lower reactivities, on the other hand, were observed for the copolymerizations with styrene, vinyl pyrrolidone, and vinyl acetate. Nevertheless, it was possible to determine the copolymerization parameters for all copolymerizations by the Fineman-Ross equation and thus establish the respective copolymerization type (Table 1).

Table 1: Determined copolymerization parameter and the kind of copolymerization.

	Copolymerization parameter r_1^a	Copolymerization parameter r_2^a	Kind of copolymerization
Styrene	0.04	5.88	statistical (ideal) non-azeotropic copolymerization
Methyl methacrylate (MMA)	0.07	0.48	random (non-ideal) azeotropic copolymerization
<i>n</i> -Butyl acrylate (BA)	0.05	0.13	random (non-ideal) azeotropic copolymerization
Vinyl pyrrolidone (VP)	0.22	3.28	statistical (ideal) non-azeotropic copolymerization
Vinyl acetate (VA)	15.09	0.15	statistical (ideal) non-azeotropic copolymerization

^a Determination *via* the Fineman-Ross equation.

In addition, the Q- and e-values could be calculated based on the copolymerization parameters determined during the copolymerization with styrene. The monomer is characterized by a high Q-value of 0.45, suggesting increased stability of the radicals during polymerization, and a low e-value of -2 , which is similar to vinyl ethers and indicate the high electron density at the vinyl group due to the neighboring sulfur. Thus, the new monomer is located in the 4th quadrant of the Q- and e-scheme⁹⁵ defined by Alfrey and Price and thus also demonstrates the feature of this monomer since not many already known monomers are located in this quadrant.

4.2. Controlled radical polymerization *via* RAFT

In recent years, controlled polymerization techniques in particular have attracted much attention, as they offer the possibility of producing well-defined homopolymers, but also, for example, block copolymers with unique properties. With this in mind, we also investigated whether the monomer is suitable for controlled polymerization. We chose

the RAFT method because of its high tolerance to many functional groups. For this purpose, three different RAFT-agents 2-(((butylthio)carbonothioyl)thio)propanoic acid (CTA I), 4-cyano-4-(((ethylthio)carbonothioyl)thio)pentanoic acid (CTA II) and cyanomethyl-*N*-methyl-*N*-phenyl-dithiocarbamate (CTA III) were tested (Figure 5). While the use of CTA I and CTA II leads to polymers with narrowly distributed molar masses (dispersities below 1.2), the use of CTA III had an insignificant effect on the dispersities compared to the free radical polymerization. The similarity of VME to other vinyl ethers has made it interesting to evaluate whether CTA III has an influence. However, it has been confirmed that the character of the monomer is more like that of (meth)acrylates. Nevertheless, differences could also be observed for the first two CTAs. While the use of CTA I resulted in polymers with very low dispersities even after a reaction time of 24 h, a slight loss of control is observed with CTA II over time, manifested by a slight increase in dispersity after 24 h. But a general statement cannot yet be made in this regard because of the higher conversion in this polymerization. Both CTAs are suitable for the synthesis of well-defined polyvinyl mercaptoethanol (PVME), as they are characterized by a linear increase in molar mass with conversion.

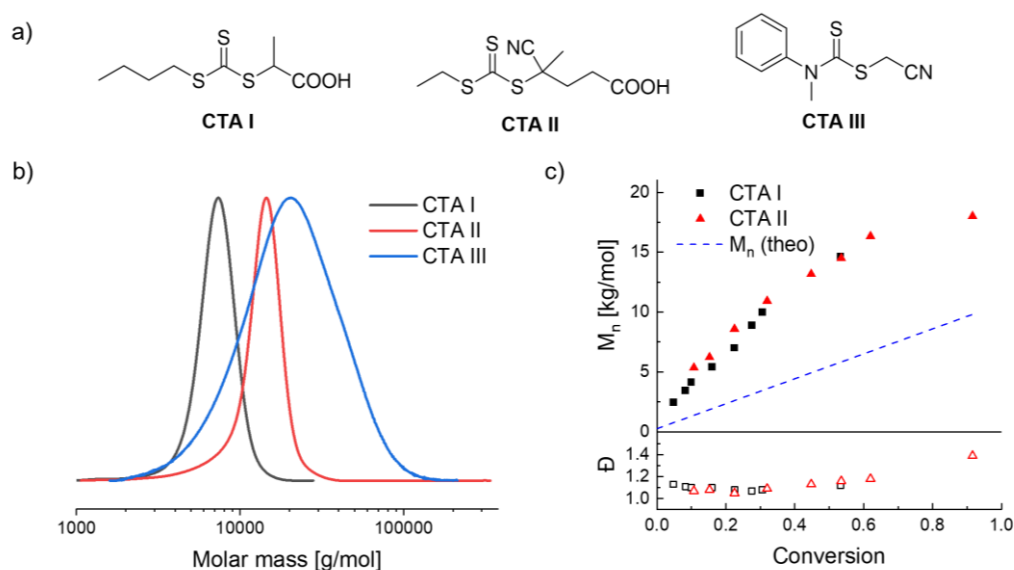


Figure 5: a) Schematic representation of the different used CTAs, b) SEC (DMAc (+ 0.21wt% LiCl), PMMA standards) traces of PVME synthesized with different CTAs, and c) evolution of M_n (filled symbols) and dispersity (empty symbols) with increasing conversion during the polymerization with CTA I (black squares) or CTA II (red triangles). The figure was adapted from ref. ⁹⁴ with permissions of Royal Society of Chemistry. Copyright 2022.

Based on the good results obtained in homopolymerization with CTA I, various copolymerizations were also carried out with this chain transfer agent. Both MMA and BA showed good control over time, resulting in narrowly distributed polymers. However,

while this CTA is well suited for polymerization with BA, it is known in the literature that controlled polymerization with MMA does not seem to be possible with this CTA. We explain the observed control by the fact that the nearly alternating incorporation of the monomers can compensate the unsuitable transfer.

In addition, the possibility of synthesizing block copolymers was also investigated (Figure 6). A shortened reaction time of 4 h was used, since 24 h reaction time resulted in more side reactions in form of recombinations, *e.g.*, in the synthesis of BA blocks, or inactive chain ends in the synthesis of VME blocks. First, PVME₆₂ was synthesized with CTA I and successfully extended with BA to form PVME₆₂-*b*-PBA₈₃ after purification of the macro-CTA. The SEC data revealed a clear shift to higher molecular weights while maintaining low dispersities. However, the elongation of PVME₆₂ with MMA did not result in well-defined block copolymers. We attribute this to the lack of uniform rapid reinitiation of the macro-CTA compared to propagation, as the initial equilibrium in the RAFT process does not favor a sufficient transfer. For a deeper understanding of RAFT-polymerizations with VME, the sequence of blocks was reversed, and a macro-CTA with BA was successfully extended with VME to PBA₉₂-*b*-PVME₂₁. In addition, a macro-CTA with CTA II and MMA was also synthesized and could then be extended with VME successfully.

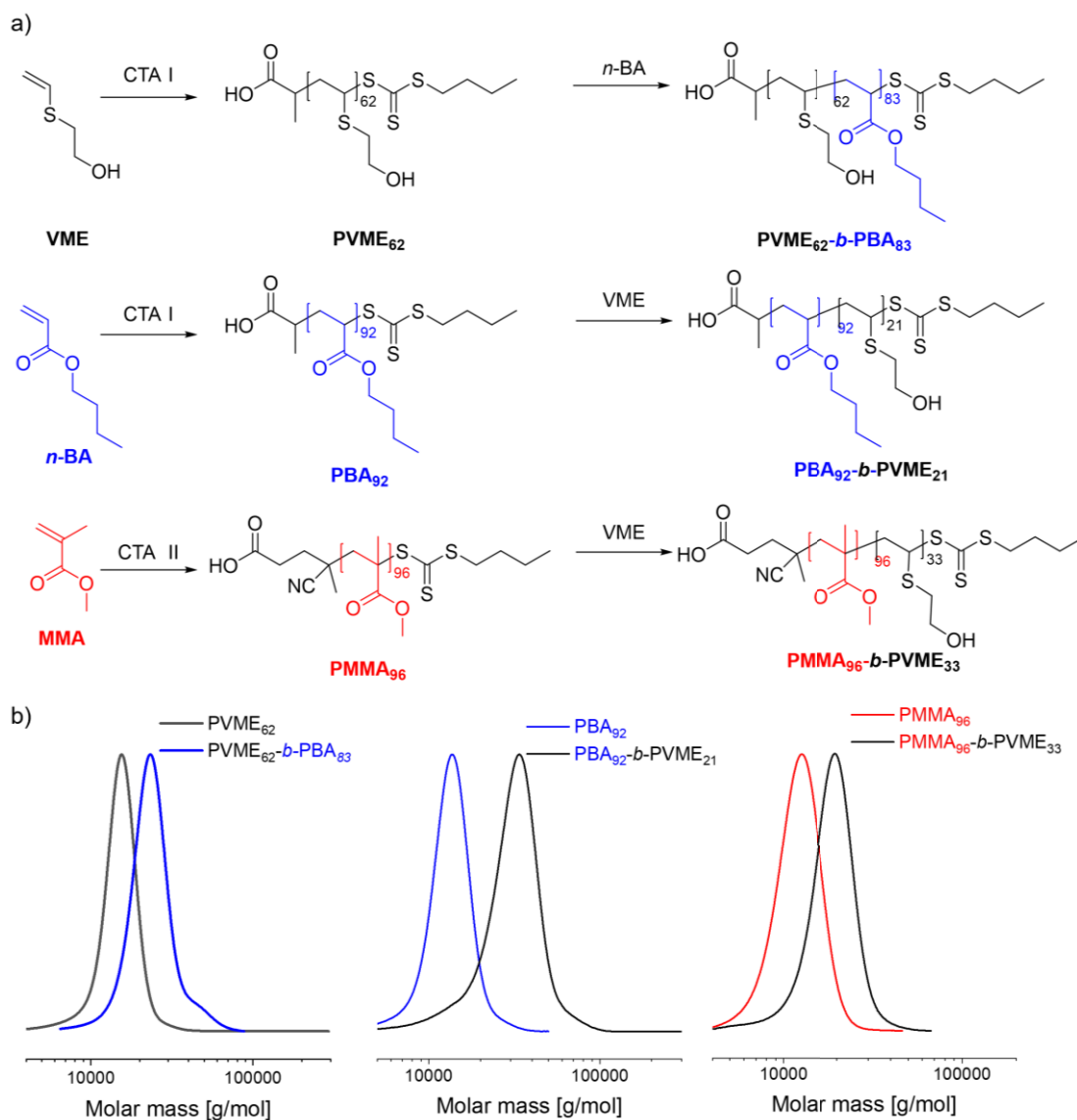


Figure 6: a) Schematic representation of the synthesis of the different block-copolymer and b) SEC (DMAc (+ 0.21wt% LiCl), PMMA standards) traces of the different block-copolymers. The figure was adapted from ref. ⁹⁴ with permissions of Royal Society of Chemistry. Copyright 2022.

In summary, we were able to demonstrate that the monomer is very well suited for controlled polymerization and that the different functionalities in the monomer do not negatively influence polymerization. Not only well-defined homopolymers but also various random copolymers and even block copolymers could be successfully synthesized. Although controlled polymerization techniques are not yet of great importance on an industrial scale because of cost inefficiencies, these experiments nevertheless show their potential for further research work.

4.3. Properties of the polymers

4.3.1. Oxidation of the homopolymer

As already described in the second chapter, it is possible to change the properties of the polymers, such as polarity and solubility, by simple oxidation of the sulfide group, for example with hydrogen peroxide. Initially, attempts were made to polymerize the oxidized monomers vinyl sulfinylethanol (sulfoxide species) and vinyl sulfonylethanol (sulfone species) by radical polymerization. Unfortunately, no polymerization was observed for the sulfoxide species, and only extremely low conversions were reached for the sulfone. Nevertheless, the polymer obtained in the latter could be used as a reference substance for the following post-polymerization oxidation starting from PVME, which is an alternative to the direct polymerization of oxidized monomers. For this purpose, the polymer was dissolved in DMF, an excess of hydrogen peroxide was added, and the reaction kinetics were recorded over time. It was observed that after 4 h the sulfide groups were almost completely oxidized, which could be verified by ^1H -nuclear magnetic resonance (NMR) spectroscopy. However, a distinction between the two oxidized species, sulfoxide, and sulfone, was not possible because of the similar chemical shifts in the ^1H -NMR spectra. In order to accurately determine the oxidation state of sulfur, different reaction conditions were tested, and a detailed study of the polymers was performed using infrared (IR) spectroscopy and heteronuclear single quantum coherence (HSQC) NMR spectroscopy. On the one hand, the polymer was oxidized once with hydrogen peroxide at room temperature over a reaction time of 24 h. On the other hand, the polymer was oxidized in the presence of the catalyst sodium tungstate at slightly elevated temperatures of 60 °C but otherwise unchanged reaction conditions, and the differences in the resulting polymers were investigated. Significant differences in the IR spectra were observed. The band at $\approx 1280\text{ cm}^{-1}$, which corresponds to the SO_2 stretching band, is more dominant in the oxidized polymers which were synthesized with the catalyst. However, a clear statement about the selectivity can only be made using the HSQC-NMR spectroscopy. Only one species is visible in the NMR-spectra for the different reaction conditions confirming the selectivity of the oxidations under these conditions, as can be seen in Figure 7. When a catalyst was used at higher temperatures, the sulfone species is present, characterized by a chemical shift of the $\text{SO}_2\text{-CH}_2$ group at 3.44 ppm and 53.65 ppm. At room temperature, on the other hand, the sulfoxide is selectively formed, as evidenced by the signal at 3.29 ppm, and 49.49 ppm corresponding to the SO-CH_2 group.

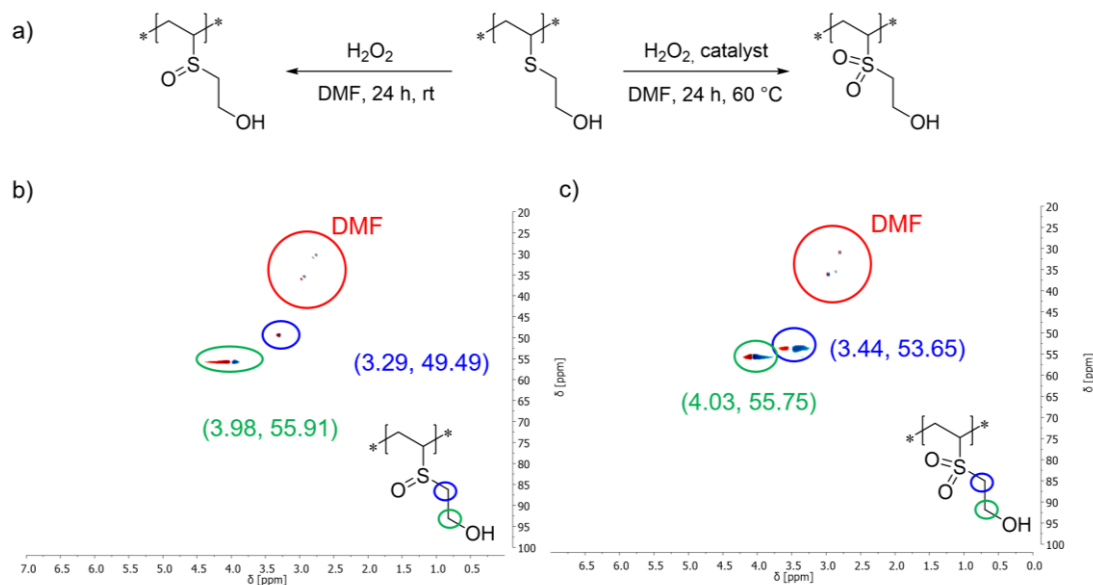


Figure 7: a) Schematic representation of the oxidation of PVME under different conditions, b) zoomed HSQC-NMR-spectrum (400 MHz, DMF-d₇, 298 K) of the oxidized species prepared without any catalyst, and c) zoomed HSQC-NMR-spectrum (400 MHz, DMF-d₇, 298 K) of the oxidized species prepared with the catalyst sodium tungstate. The figure was adapted from ref. ⁹⁴ with permissions of Royal Society of Chemistry. Copyright 2022.

4.3.2. Thermal properties of the polymers

The focus of the further course was on the investigation of the properties in order to be able to subsequently evaluate the possibility of using the polymers in potential applications. First, the homopolymer and the oxidized species were investigated for their thermal properties. The non-oxidized polymer possesses increased stability with a decomposition temperature above 300 °C. The sulfoxide polymer, in turn, revealed a decomposition onset at 150 °C, indicating that the polar group leads to the instability of the polymer. The sulfone, on the other hand, revealed remarkably high thermal stability, which can be explained by the lower polarity of the sulfone group and the resulting more stable carbon-sulfur bond. Also, the glass transition temperatures are quite different depending on the oxidation state. The sulfide has a glass transition around room temperature, which is the reason for the very soft and sticky nature of the material. The sulfoxide, on the other hand, is not as soft, but a glass transition temperature could not be determined because of the very low decomposition temperature. The glass transition temperature of the sulfone is in the range of 100 °C, which also shows significant differences from the sulfide.

On the other side the glass transition temperatures of the copolymers prepared by free radical polymerization are strongly dependent on the comonomers and compositions of

the monomer in the polymer (Figure 8a). Thus, for copolymers with MMA, it can be observed that an increased proportion of VME also leads to lower values for the glass transition temperature compared to pure PMMA. The glass transition temperature approaches more and more the glass transition temperature of pure PVME with increasing VME content. Similar behavior was observed for the copolymers with BA. However, with an increasing proportion of VME, the glass transition temperature increases this time compared to pure PBA, because PBA has a glass transition temperature below room temperature. The random copolymers prepared by RAFT revealed a similar behavior mostly independent of the chain lengths. However, the block-copolymers prepared by RAFT differ significantly from the other polymers in their thermal properties. Multiple glass transition temperatures could be determined for block-copolymers with BA for example, which is a clear indication of phase separation in the polymer due to strong polarity differences (Figure 8b). Further investigations were not yet perused in this direction, but an analysis of the polymers using small-angle X-ray scattering (SAXS) measurements could be considered for a better understanding with respect to the morphology.

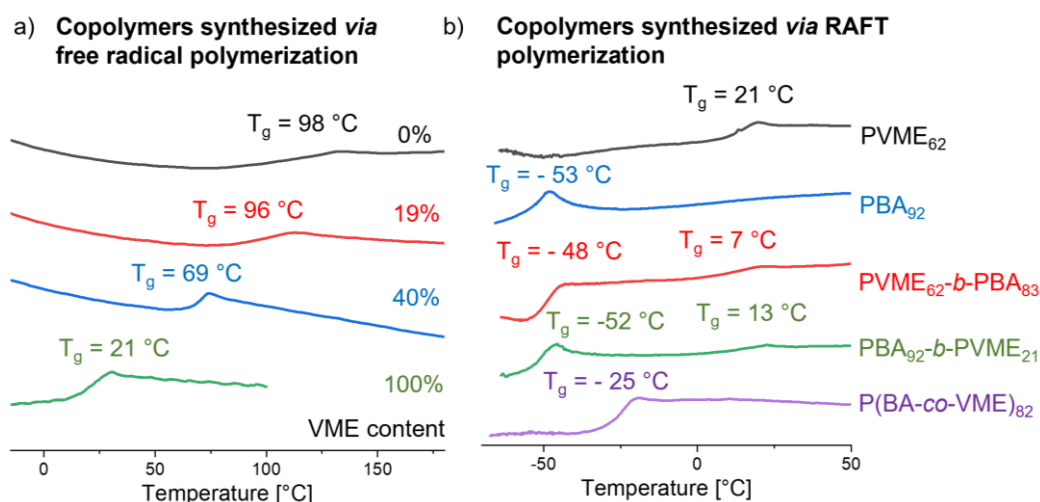


Figure 8: a) Differential scanning calorimetry (DSC) data of the different homo- and copolymers synthesized *via* free radical polymerization and b) DSC-data of the different homo- and copolymers synthesized *via* RAFT polymerization. The figure was adapted from ref. ⁹⁴ with permissions of Royal Society of Chemistry. Copyright 2022.

Thus, it was demonstrated that a wide variety of thermal properties can be obtained depending on the polymerization technique and the composition of the chosen monomers.

4.3.3. Optical properties of the polymers

In addition, the optical properties were investigated since sulfur-containing polymers are known in the literature for their increased refractive index because of the high atomic refraction of sulfur and thus optical applications are conceivable. The focus was on the polymers prepared by free radical polymerization, which are colorless, transparent materials, while the RAFT-polymers have a yellow color as a consequence of the trithiocarbonate end-groups. For the determination of the refractive indices, films of the homopolymer and the different copolymers with a film thickness of about 4 μm were prepared on glass slides by doctor blading and then analyzed by ellipsometry. The pure homopolymer revealed a slightly increased refractive index $n_D = 1.55$ compared to other homopolymers such as PMMA $n_D = 1.48$ and a linear increase in refractive index can be observed with an increase in the VME content in the corresponding copolymers (Figure 9a). This allows precise tuning of the desired properties *via* the incorporated amount of VME in the polymer and demonstrates the potential for applications in the optical field. However, for subsequent applications, not only the increased refractive index but also the optical transparency is crucial. With this in mind, ultraviolet-visible (UV-Vis) spectroscopy was carried out on newly prepared films with a film thickness of 50 to 70 μm , which were produced by drop-casting. The polymers exhibit no absorption in visible light, irrespective of the VME content, and are thus comparable to pure PMMA (Figure 9b).

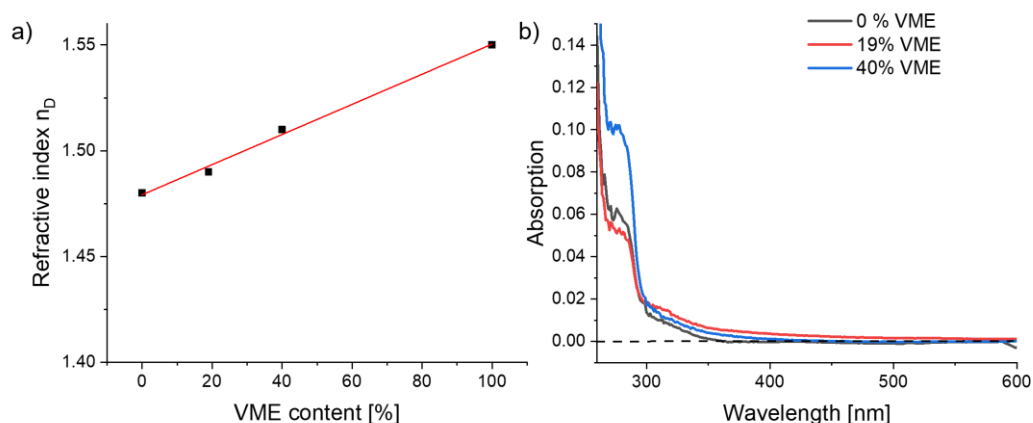


Figure 9: a) Plot of refractive index vs. VME content in the polymer b) UV-Vis spectra of the polymers with different amounts of VME. The figure was adapted from ref. ⁹⁴ with permissions of Royal Society of Chemistry. Copyright 2022.

4.3.4. Mechanical properties of the polymers

In the following, the mechanical properties were also investigated in order to verify the impressions made when handling the polymers and thus to better assess possible

applications. For this purpose, nano-identification measurements were conducted on films with a layer thickness of > 50 micrometers, which were also produced by drop-casting. As a consequence of the very soft nature of the homopolymer, PVME and the copolymer P(BA-*co*-VME), slightly different measurement settings had to be used for the measurements. Thus, a loading of 0.3 mN was chosen for these two polymers (Figure 10d-f), while loading of 1 mN was used for the polymers on MMA basis (Figure 10a-c). As expected, the pure homopolymer PVME showed an extremely low *e*-modulus of 4.4 MPa and a hardness of 0.1 MPa. Interestingly, similar values were obtained for the copolymer P(BA-*co*-VME), although the glass transition temperature was much lower, as described in the previous chapter. Another interesting observation was the creep behavior of the two polymers. While PVME exhibited a much higher indentation of 1000 nm, P(BA-*co*-VME) showed only an indentation of 400 nm with the same load. This unusual behavior can be explained by the higher molar mass of the copolymer. The P(MMA-*co*-VME), on the other hand, did not show much difference from the pure PMMA for *e*-modulus, hardness, and creep behavior, which is quite surprising since we had expected that the incorporation of VME would also lead to a decrease in *e*-modulus and hardness considering the soft nature of PVME. However, the values remained almost constant even at a VME content of 40%, showing that these polymers can maintain the good mechanical properties of PMMA. But in addition, the properties of the sulfur-containing polymer, such as a slightly increased refractive index, can be incorporated into the copolymer.

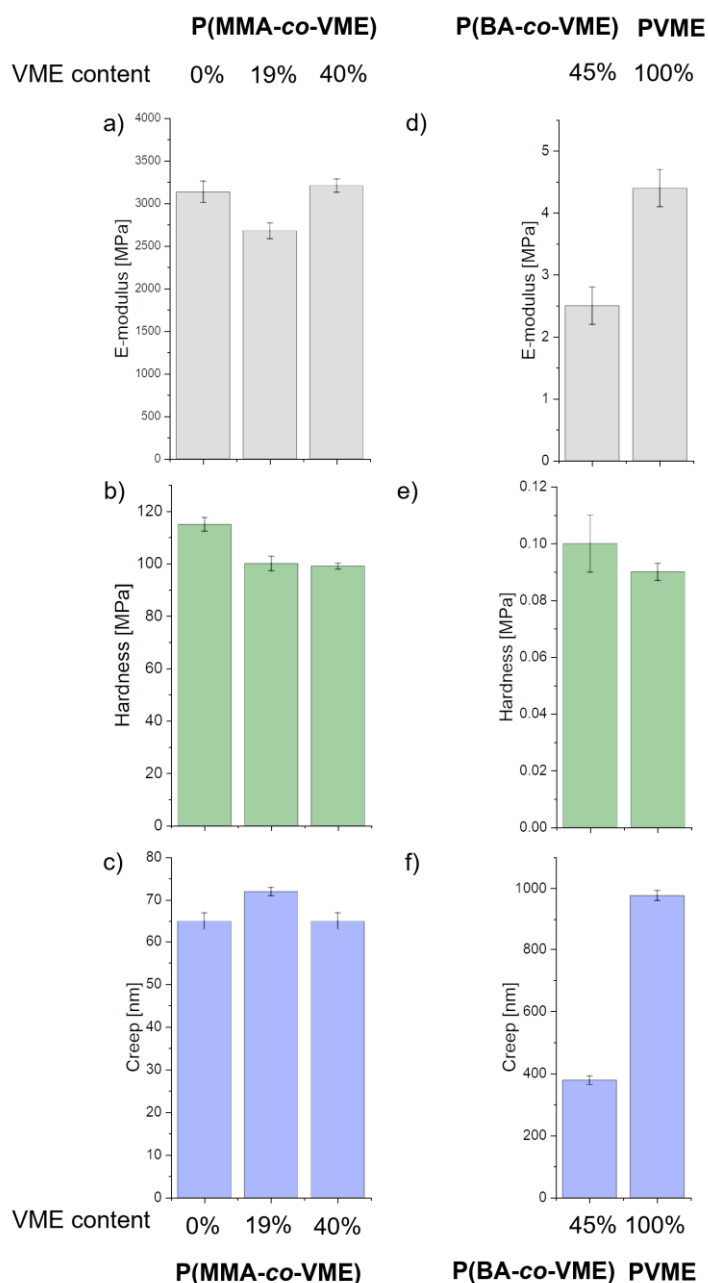


Figure 10: a-c) Mechanical properties of the homopolymer PMMA and the copolymers P(MMA-co-VME) with different amounts of VME which were determined *via* nano-indentation measurements with a load of 1 mN and d-f) mechanical properties of the homopolymer PVME and the copolymer P(BA-co-VME) which were determined *via* nano-indentation measurements with a reduced load of 0.3 mN. The figure was adapted from ref. ⁹⁴ with permissions of Royal Society of Chemistry. Copyright 2022.

5. Heterogeneous radical polymerization of the S-vinyl monomer VME

Parts of this chapter have been published in: P3) N. Ziegenbalg, H. F. Ulrich, S. Stumpf, P. Mueller, J. Wiethan, J. Danner, U. S. Schubert, T. Adermann, J. C. Brendel, *Macromol. Chem. Phys.* **2023**, 224, 2200379.

Heterogeneous polymerization techniques⁹⁶⁻¹⁰⁴ are often preferred in the industry over homogeneous polymerization techniques such as bulk and solution polymerization,¹⁰⁵ and the limited solubility of many of the previously synthesized polymers would be a major challenge on an industrial scale. Nevertheless, due to the unique properties of the polymers, the introduction into commercial products is desirable. For this reason, a new approach to the polymerization of VME was adopted and the possibility of realizing heterogeneous polymerizations was investigated. These have the advantage, especially when using water as the reaction medium, of better heat dissipation, lower cost, and a more environmentally friendly process. In addition, higher molar masses and faster polymerization rates can be achieved through the increased lifetime of radicals confined in the particles.¹⁰⁶⁻¹⁰⁸

5.1. Emulsion or dispersion polymerization?

The monomer vinyl mercaptoethanol is water soluble to a certain extent (105.5 g L⁻¹) as a consequence of the amphiphilic character with a hydrophilic hydroxyl group and a hydrophobic thioether group. This property strongly distinguishes this monomer from other monomers used in heterogeneous polymerization techniques. Therefore, it can be assumed that the following polymerizations are not following the principle of common emulsion polymerization. If higher concentrations are applied it neither can be considered a pure precipitation polymerization, but a mixed process in which the particles are stabilized with suitable surfactants. However, stabilization could be a major challenge because the hydroxyl group is likely to interact with water as the reaction medium, leading to swelling of the polymer particles and thus making stabilization of the particles more difficult.

The polymerizations were conducted using the water-soluble initiator 2,2'-azobis(2-methylpropionamide) dihydrochloride (V-50) and 1wt% of the corresponding surfactant. Initially, one of the most used surfactants in industry, sodium dodecyl sulfate (SDS), was used. Unfortunately, this surfactant did not affect the polymerization, as the

conversion and chain length were similar to a comparative experiment without any stabilizer, and the particles agglomerated and sedimented immediately after polymerization and could not be redispersed. To exclude that these negative results were a consequence of an interaction between the negatively charged surfactant and the positively charged initiator, the neutrally charged polyethylene glycol (PEG) based surfactants TweenTM 80 and TritonTM X-100 were also tested. However, these also did not reveal the desired effect and agglomerated and sedimented very quickly after polymerization. This could indicate that stabilization is not possible because of the different polarities of the hydrophobic aliphatic chains of the surfactants and the hydroxyl group of the polymer. For this reason, the focus was amended to surfactants that should theoretically interact with the hydroxyl group due to their similar polarity. The surfactants PluronicTM F127, commercial polyvinyl pyrrolidone (PVP 40 000 g mol⁻¹), and polyvinyl alcohol (PVA 31 000 g mol⁻¹) were selected. Unfortunately, no improved stabilization behavior was observed with PluronicTM F127 either. The particles with PVP also showed rapid sedimentation after polymerization, but unlike the other surfactants, the particles were partially redispersible. Nevertheless, dynamic light scattering (DLS) measurements showed very large aggregates above 400 nm for all surfactants used. Since the correlograms of the DLS measurements give evidence of aggregates outside the measurable range, a very broad distribution of particle sizes can be assumed.

PVA, on the other hand, shows a completely different stabilization behavior since the resulting particles sediment much slower and a complete redispersion is possible after sedimentation. We assume that sedimentation occurs only because of the size of the particles since these particles are strongly influenced by gravity. This assumption is confirmed by DLS-measurements, which again show very large aggregates. Although stabilization of the particles is a major challenge because of their unique properties, a surfactant was found with PVA that shows a stabilizing effect already at 1wt%. Based on this stabilization behavior with 1wt% PVA, the amount of PVA was increased to study the influence of the surfactant in more detail. When 1wt% or 2wt% PVA was used, no significant differences were observed in the conversion, chain lengths, and sedimentation behavior over time (Figure 11). However, if 4wt% or even 8wt% PVA was initially added to the reaction mixture, increased conversions were observed on the one hand, but also a slightly different molar mass distribution on the other. Basically, a bimodal distribution is always observed, which is an indication of the mixed polymerization process in the

aqueous phase and in the particles (Figure 11c). However, if the amount of PVA is increased, the proportion of longer chains also increases. Theoretically, larger molar masses can be expected in emulsion polymerizations than in precipitation polymerizations, since fewer termination reactions occur. Thus, the change in molar mass distribution could be a consequence of emulsion polymerization becoming more and more dominant at higher PVA amounts in this mixed process. The reason why both processes are possible at all is the partial water solubility of the monomer already mentioned at the beginning.

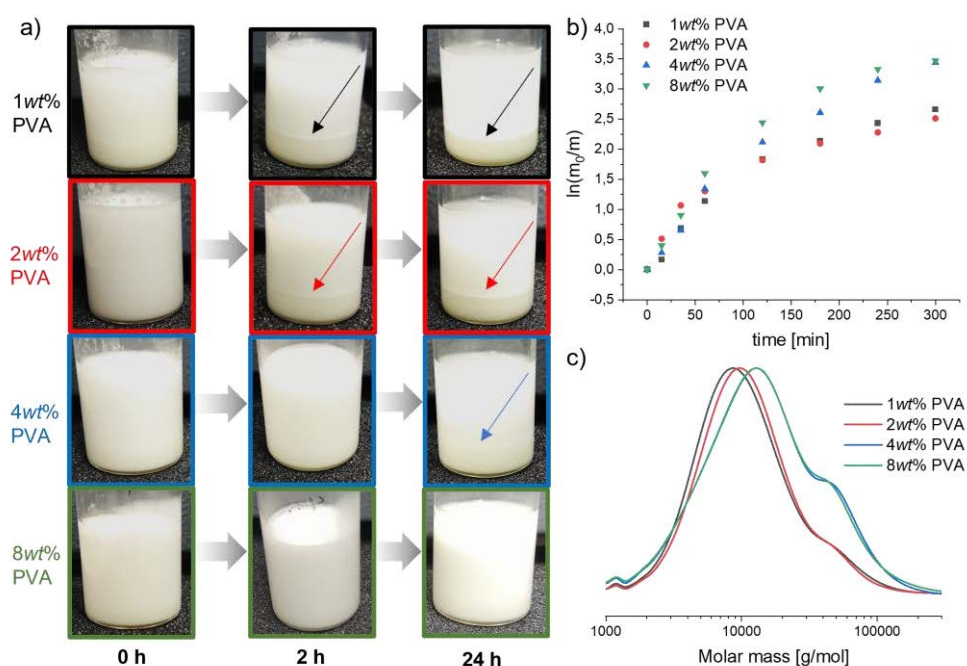


Figure 11: a) Photography of the sedimentation behavior over the time starting directly after the polymerization, b) plot of $\ln(m_0/m)$ vs. reaction time and c) SEC (DMAc (+ 0.21wt% LiCl), PMMA standards) traces of the polymers after 5 h with different amounts of PVA. The figure was adapted from ref. ¹⁰⁹ with permissions of John Wiley and Sons. Copyright 2023.

Even though the DLS-measurements showed some very large aggregates for all particles with different amounts of PVA, it was possible to prove the spherical shape of the particles by SEM images. But the SEM images also confirm that the size of the particles varies greatly, and that the particles collapse on the mica substrate during the drying process (Figure 12a/b).

5.2. Incorporation of noble metals in the polymer particle

Another approach to further stabilize the particles, but also to broaden the area of application of these particles, was to use them as a host matrix for metal ions and nanoparticles. Since sulfur has the property of coordinating well with metals such as silver, gold, or other metals,^{10-13, 110} this possibility should also be investigated further for PVME particles.

5.2.1. Modification of polyvinyl mercaptoethanol particles with silver ions (Ag⁺@PVME)

The initial focus was on silver ions since these have already been shown in the literature to have an antimicrobial effect, with possible applications in the medical field, textile industry, or antifouling for ships for example.¹¹¹⁻¹¹⁶ In addition, silver ions should also lead to a stabilizing effect, since agglomeration should be partially prevented by the positive charge of the silver ions because of electrostatic repulsive forces. In general, there are two synthetic routes to successfully incorporate metal ions or metal nanoparticles - the *in situ* or the *ex situ* process.¹¹⁷ The *in situ* method describes the modification of the pre-existing particles with metal ions or nanoparticles, while in the *ex situ* method the monomer is polymerized in their presence. Both synthetic routes were evaluated, even if we have limited it to the use of the salts for the time being since here the greatest interaction was to be expected. All experiments were performed in the absence of light because of the photosensitivity of silver salts. Unfortunately, polymerization in the presence of silver nitrates or silver acetates (*ex situ* method) did not improve the particle stability. Therefore, the polymer particles were first synthesized with PVA, and, after subsequent purification, the addition of silver ions took place.

Different amounts of silver ions were added to the particles. After 3 h, non-coordinated silver ions were removed by dialysis and the silver content was determined by inductively coupled plasma mass spectrometry (ICP-MS) measurements. And indeed, an increased silver content could be detected with increasing the equivalents of silver ions compared to the sulfur in the polymer. If up to 0.04 equivalents of silver ions were applied compared to the sulfur in the polymer, nearly the same amount of silver was detected after purification, indicating complete incorporation of the silver ions into the polymer particles. However, if the applied amount was increased to 0.1 equivalents, the final amount of silver ions in the particles after purification was decreased in comparison. This

is an indication of the oversaturation of the sulfur since the silver ions were no longer able to fully coordinate to the sulfur. This could have two reasons: either one silver ion coordinates to several sulfur atoms or the other free sulfur atoms are not accessible to the silver ions because of their position within the particle core. Nevertheless, an additional stabilizing effect was observed in these experiments, which, as mentioned above, is a consequence of the repulsive forces between the silver ions.

In addition, the influence of different amounts of PVA on the coordination of the silver was investigated. For this purpose, silver ions were also added to the previously prepared dispersions containing 1wt%, 2wt%, 4wt%, and 8wt% PVA. Here, too, increased stability was observed for all samples, which, moreover, could be confirmed by zeta-potential measurements. These measurements revealed positive values in accordance with the positively charged silver ions. However, not only the stability but also other characteristics of the particles were examined more closely in these samples. DLS-measurements demonstrated the enormous influence of the silver ions on the particles, as these giant aggregates, which were outside the measurable range of the DLS-measurement, are no longer present, which can be explained by the fact that agglomeration is partly prevented by the silver ions, even if complete prevention of agglomeration could not be ensured. The spherical particles were again visible in the SEM images for the aggregates with 1wt% and 2wt% SDS, but this time no collapses of the particle can be observed during the drying process (Figure 12c/d). At 4wt% and 8wt%, however, it was clear that the silver ions were irregularly distributed both inside and outside the polymer particles, which we attribute to shielding of the particles at higher PVA contents so that complete incorporation is no longer possible. For this reason, the following tests focused mainly on the emulsion with 1wt% PVA.

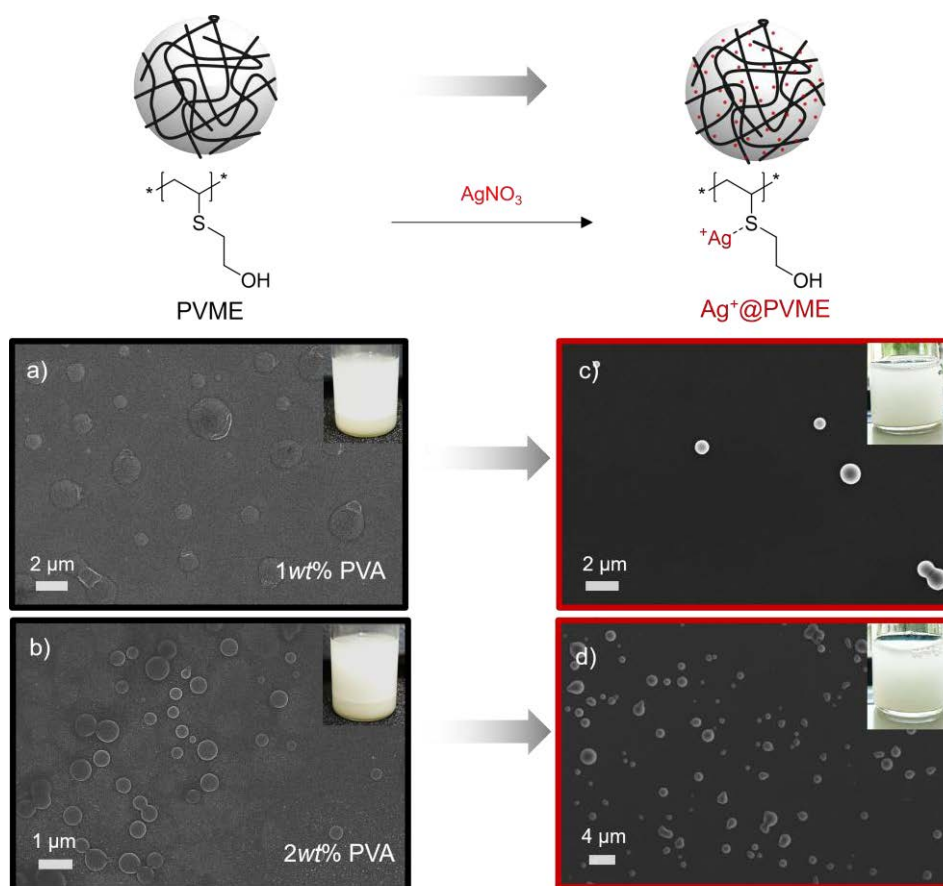


Figure 12: SEM images of a) pure PVME emulsion with 1wt% PVA, b) pure PVME emulsion with 2wt% PVA, c) Ag⁺@PVME with 1wt% PVA and d) Ag⁺@PVME with 2wt% PVA. The figure was adapted from ref. ¹⁰⁹ with permissions of John Wiley and Sons. Copyright 2023.

Subsequently, the coordination of silver ions to sulfur was studied in more detail by monitoring the release of silver ions over 7 days. The emulsion containing the particles was transferred to a controlled dialysis set-up after purification, and the silver ion content was analyzed by ICP-MS before and after the 7 days. The slightly lower silver ion levels after the 7 days indicate a slow release of silver ions and show that the coordination of silver ions to sulfur is reversible. The experiment was then repeated with 0.04 eq. of silver ions compared to sulfur, and the silver content in the filtrated water was determined daily and a linear release of the silver ions was observed.

5.2.1. Modification of polyvinyl mercaptoethanol particles with silver nanoparticles (Ag@PVME)

In the following, an attempt was made to reduce the silver ions to introduce silver nanoparticles (AgNPs) into the polymer particles. Several reducing agents for the reduction of silver ions to silver are known in the literature.¹¹⁸⁻¹²⁰ One of the most

commonly used is sodium borohydride. Unfortunately, the addition of sodium borohydride led to the coagulation of the silver. Even in the case of ascorbic acid, a very mild reducing agent, the transmission electron microscopy (TEM) images showed that the AgNPs were randomly distributed and both free AgNPs and AgNPs in the polymer particle were visible. Controlled reduction of the silver ions within the polymer particles, therefore, appeared a major challenge because a reducing agent had to be found that is not coordinating silver itself or causing further coagulation of the silver. However, the reduction of the silver can lead to a decrease in the stability of the polymers since no repulsive forces can act as a consequence of the lack of charge. Nevertheless, an interesting observation was made that sunlight can interact with the sample and a color change from colorless to brown can be registered after a short time. This is indication of the reduction of the silver, which could be supported by UV-Vis measurements of the highly diluted samples, as the typical shift of the absorption bands of silver ions and AgNP could be detected. TEM-images also confirm the uniform distribution of AgNPs in the polymer particles (Figure 13). These experiments show that no additional reducing agent is necessary for the reduction of the silver ions and that the polymer particles themselves probably function as the reducing agent, because of the reductive nature of thioether groups which can be oxidized to sulfoxides. Unfortunately, an absolute determination of this oxidation was not achieved because of the limited solubility of the particles and the low content of sulfoxides in this case.

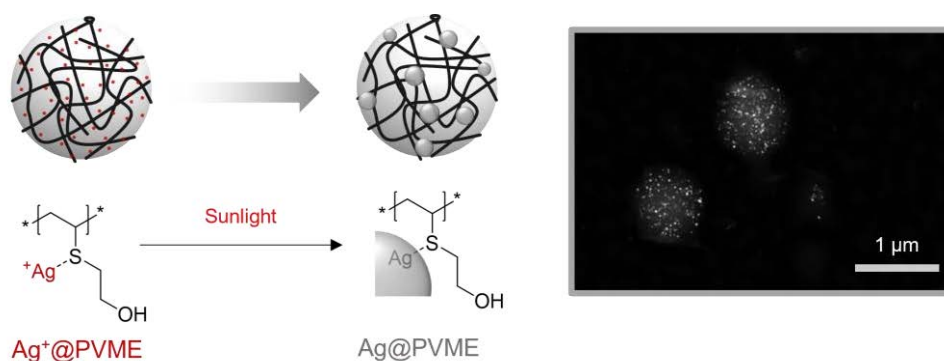


Figure 13: TEM-image of Ag@PVME. The figure was adapted from ref. ¹⁰⁹ with permissions of John Wiley and Sons. Copyright 2023.

Due to the successful synthesis of the AgNP, the antibacterial effect of the pure emulsion, the emulsion modified with silver ions ($Ag^+@PVME$) and silver nanoparticles ($Ag@PVME$) could now also be investigated and compared. For this purpose, bacterial growth of *E. coli* and *S.aureus* was investigated in the presence of the substances and compared with the benchmark Irgaguard B 6000, an antimicrobial agent based on

inorganic silver glass/zeolite. In these experiments, no antibacterial effect was observed with the pure emulsion PVME. Ag@PVME also appears to have a very limited ability to restrict bacterial growth over 24 h. In contrast, a similar behavior to the benchmark was observed for the polymer particles modified with silver ions for the bacterial growth of *E. coli* after 4 h. For *S. aureus*, on the other hand, a significant reduction in bacterial growth was observed both after 4 h and after 24 h, but the bacterial growth is slightly higher than for the optimized benchmark. Nevertheless, a reduced growth rate can be observed for both bacterial species in the presence of Ag⁺@PVME, which opens up the possibility of using them for example in the medical field.

5.2.2. Modification of polyvinyl mercaptoethanol particles with gold ions and nanoparticles (AuCl₄⁻@PVME and Au@PVME)

Not only the incorporation of silver ions with subsequent reduction to AgNP represents an interesting field of research, but gold nanoparticles are also relevant for research because of their broad range of applications. On the one hand, gold nanoparticles can be used for medical applications in the field of diagnostic imaging or cancer therapy.¹²¹⁻¹²⁵ On the other hand applications in the field of catalysis are also more frequently described in the literature.¹²⁶⁻¹²⁹

The first experiments, in which potassium gold(III) chloride was added, did destabilize the system since the particles subsequently tended to agglomerate. However, the addition of chloroauric acid (HAuCl₄) and subsequent purification by dialysis resulted in stable particles whose spherical shape could be confirmed by SEM- and TEM-imaging. Again, no suitable additional reducing agent could be found, as ascorbic acid, for example, led to a random distribution of AuNP in the sample. Therefore, the focus was again on the reduction process in sunlight and a color change from colorless to purple-brown was observed. This color is characteristic of larger AuNP aggregates. This time, however, spherical particles with a deformed surface are still visible in the SEM and TEM images (Figure 14). This could be indicative of homogeneous surface loading and suggests that the gold chloride ions coordinate mostly at the surface and do not diffuse into the particles as in the case of silver, perhaps because of the size, but also because of the interaction of the negative charge with the particles.

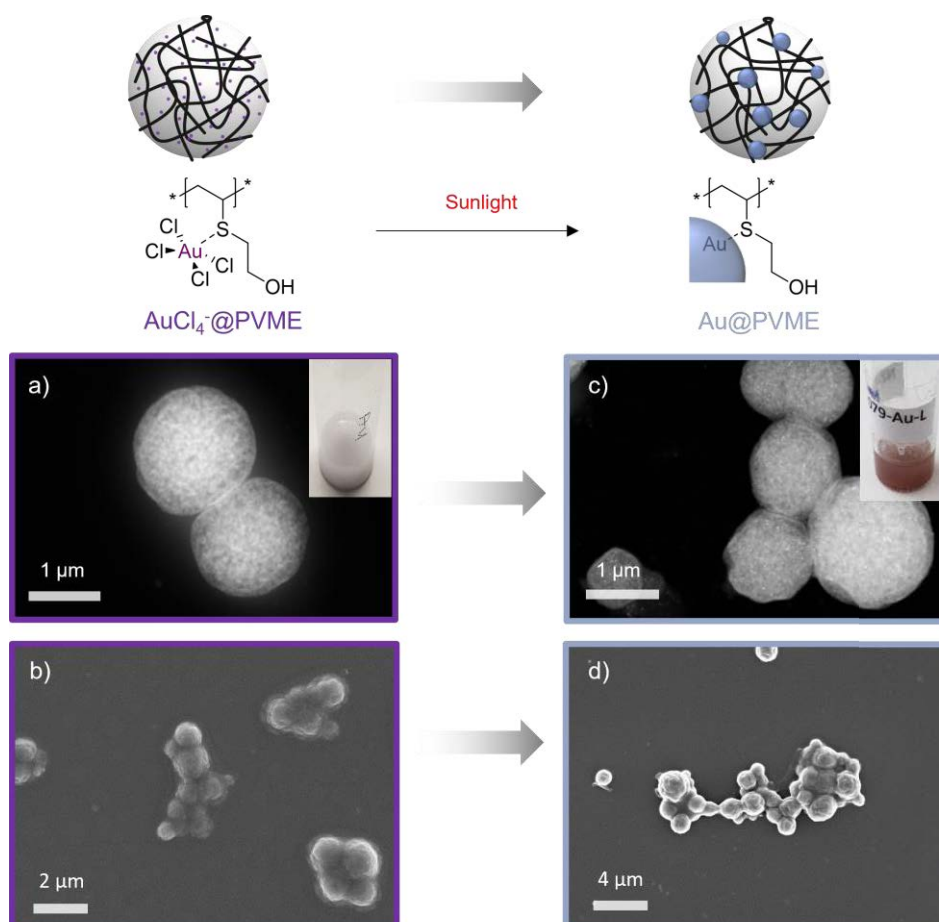


Figure 14: a) TEM-image of $\text{AuCl}_4^-@PVME$, b) SEM-image of $\text{AuCl}_4^-@PVME$, c) TEM-image of $\text{Au}@PVME$ and d) SEM-image of $\text{Au}@PVME$. The figure was adapted from ref. ¹⁰⁹ with permissions of John Wiley and Sons. Copyright 2023.

In summary, stable dispersions as known from commercial emulsions are not possible with PVME. However, the addition of PVA can stabilize the polymer particles, which exhibit sedimentation behavior as a consequence of their micrometer diameter but the particles are redispersible. The addition of metal ions can further stabilize this system because the metal salts are coordinated with the sulfur and the repulsive forces caused by the ions provide additional stability. Based on these research results, possible industrial production of PVME is now conceivable, circumventing the problem of limited solubility and succeeding in the production of polymer particles. Likewise, applications because of the successful incorporation of noble metals are desirable.

6. Homogeneous polyaddition of electron-deficient S-monomer VSE

Parts of this chapter have been published in: P4) N. Ziegenbalg, R. Lohwasser, G. D'Andola, T. Adermann, and J. C. Brendel, *Polym. Chem.* **2021**, *12*, 4337-4346.

Our interest was not only in the polymerization of vinyl sulfides and their subsequent oxidation to obtain polymers with sulfoxide and sulfone units. Our efforts were also in finding a suitable polymerization method starting from the oxidized monomer vinyl sulfonylethanol and investigating the properties of the polymer to obtain a better understanding of the influence of the sulfone group in the polymer compared to the sulfide group. However, as already described in Chapter 2, it is extremely difficult to polymerize monomers radically *via* the vinyl group if a sulfoxide or sulfone is in the immediate vicinity. As a consequence, another polymerization method the oxa-Michael polyaddition was chosen, which is now described in this chapter in more detail. Until recently, often divinyl sulfone/sulfoxides had been polymerized with bivalent alcohols *via* AA/BB-polyaddition.⁸¹⁻⁸³ However, the difficulties of polymers with low molar masses or the formation of only oligomers were often encountered. This can be explained, on the one hand, by the difficulty of accurately adjusting the stoichiometry, which is essential for achieving high molar masses, and, on the other hand, by the fact that the formation of cyclic polymers often cannot be prevented. Nevertheless, this class of polyether sulfones represents an attractive substance class, which requires research and improvement of the polymerization behavior for potential applications.

6.1. Oxa-Michael polyaddition

The monomer vinyl mercaptoethanol was selectively oxidized with hydrogen peroxide first to the sulfoxide and then with the catalyst sodium tungstate to the sulfone (Figure 15). Long-term studies revealed the stability of the monomer for more than a year with the addition of a radical inhibitor and storage at 4 °C. This oxidation has led to the development of an AB-monomer characterized by a strong Michael donor and Michael acceptor because of the aliphatic alcohol and the electron-poor vinyl group, making it ideal for oxa-Michael polyaddition.

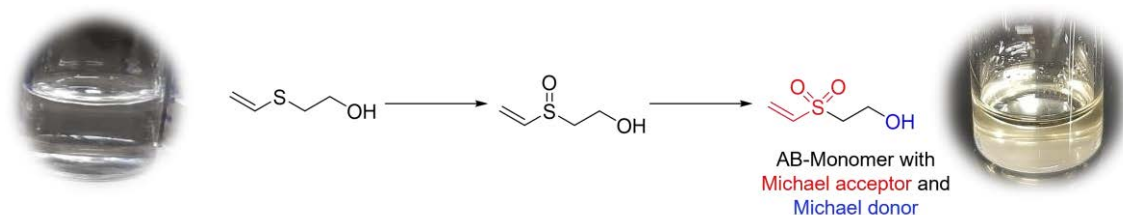
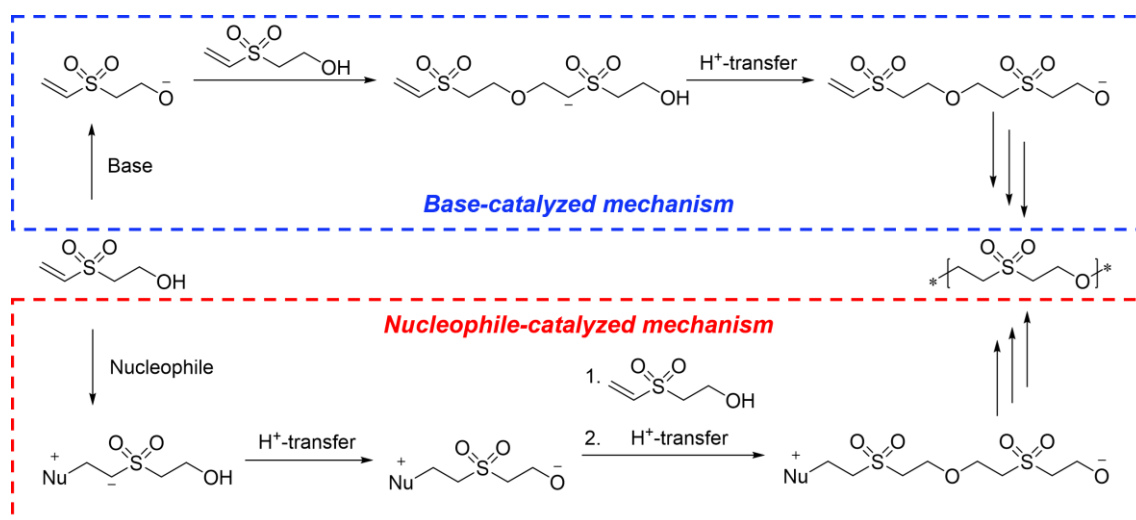


Figure 15: Selective oxidation of vinyl mercaptoethanol to vinyl sulfonylethanol.

Oxa-Michael polyaddition can be realized by two different mechanisms: base-catalyzed and nucleophilic-catalyzed oxa-Michael polyaddition (Scheme 3). In the base-catalyzed mechanism, the hydroxyl group will be deprotonated by the base first. Subsequently, the negatively charged oxygen atom can attack a double bond of the monomer molecules, resulting in a negatively charged carbon atom in the immediate vicinity of the sulfone group. A proton transfer now takes place from another hydroxyl group to the negatively charged carbon atom just described. This proton transfer can either occur from the hydroxyl group of the growing polymer chain (intramolecular), which then leads to the deprotonated hydroxyl end group attacking a new monomer molecule and the chain continuing to grow. However, the proton transfer can also occur from another monomer molecule (intermolecular), which then leads to the growth of a new chain. The nucleophile-catalyzed mechanism is similar to the base-catalyzed mechanism, except that a nucleophile first attacks the double bond, which creates a positive charge on the nucleophile and a negatively charged carbon atom in the immediate vicinity of the sulfone group and then an intra- or intermolecular proton transfer takes place from the hydroxyl group to the negatively charged carbon atom, as described before.



Scheme 3: Schematic representation of the base- and nucleophile catalyzed mechanism of an oxa-Michael polyaddition starting from vinyl sulfonylethanol. The figure was adapted from ref. ⁸⁴ with permissions of Royal Society of Chemistry. Copyright 2021.

In the following, the polymerizations were initiated with the organic catalysts triphenylphosphine (PPh₃), triethylenediamine (TEDA), 4-(dimethylamino)pyridine (DMAP), 1,8-diazabicyclo(5.4.0)-undec-7-ene (DBU) and 1,5,7-triazabicyclo(4.4.0)-dec-5-ene (TBD), as well as with the inorganic catalysts potassium carbonate and cesium carbonate, and the mechanism was investigated.

6.1.1. Bulk polymerization

Initially, bulk polymerizations were conducted, and despite a previously weighed catalyst amount of 0.1 equivalent compared to the monomer, the exact amount of active catalyst could not be determined because most of the catalysts were solids and not completely soluble in the monomer. However, regardless of the catalyst used, a color change from yellow to brown and an increase in viscosity were observed within a few minutes. In all polymerizations, high conversions of the vinyl groups after a few minutes can be confirmed by NMR spectroscopy, and conversions of more than 94% can be obtained after 24 hours, demonstrating the high reactivity of the monomer. Only PPh₃ showed initial retardation of a few minutes compared to the other polymerizations, which is probably because of the steric demands of this nucleophile. However, once attacked, the polymerization proceeds with a polymerization rate similar to the other catalysts. In addition, a continuous increase in chain length with increasing reaction time was observed in the SEC data. The fact that high molar masses, in this case, can only be achieved with almost complete conversion of the functional end groups clearly indicates

the step growth mechanism of these polymerizations. The determined chain lengths are very different from the theoretical chain lengths calculated using the Carothers equation for AB-monomers.¹³⁰ However, it is clearly observed that the theoretical values for the inorganically catalyzed polymers are much closer to the determined values than the values for the polymers created with the organic catalysts. This can be explained, on the one hand, by the fact that the addition of the organic catalysts to the vinyl group leads to an inaccurate stoichiometry of the active end groups for polyaddition, resulting in low molar masses, as described earlier. In addition, however, this can also be an indication that the nucleophilic catalyzed polymerization tends to cyclize, because of the interaction between the positively charged bound catalyst end-group and the negatively charged, deprotonated hydroxyl end-group during polymerization. Even though cyclization can never be ruled out also for the inorganically catalyzed polymerizations. Unfortunately, a quantification of cycles either with NMR, matrix-assisted laser ionization time-of-flight mass spectrometry (MALDI-ToF-MS) or viscosity measurements was not possible. Additionally, the number-average molar masses (M_n) by MALDI-ToF-MS are still significantly lower than the theoretical values and the values determined by SEC. We attribute this to the fact that insufficient ionization takes place, which significantly underestimates the M_n values, and the method is therefore not optimal for the determination of absolute M_n values.

Table 2: Conversions, number average molar masses (M_n), and dispersities (\mathcal{D}) of oxa-Michael polyaddition of vinyl sulfonylethanol after 24 h. The table was adapted from ref. ⁸⁴ with permissions of Royal Society of Chemistry. Copyright 2021.

Catalyst	Conversion [%] ^a	M_n [g mol ⁻¹] (theo.) ^b	M_n [g mol ⁻¹] (SEC) ^c	\mathcal{D} ^c	M_n [g mol ⁻¹] (MALDI) ^d
PPh ₃	99	13 620	3670	1.50	2050
TEDA	98	6 810	2330	1.38	1990
DMAP	97	4 540	2570	1.46	1880
DBU	99	13 620	2200	1.58	2150
TBD	99	13 620	3360	1.28	2310
K ₂ CO ₃	95	2 720	2070	1.38	1040
Cs ₂ CO ₃	96	3 400	2890	1.45	1770

^a ¹H-NMR (300 MHz, DMSO-d₆) after 24 h, determination *via* vinyl groups, ^b Determination with Carothers equation, ^c SEC (DMAc (+ 0.21 wt.% LiCl), PEG standards) after 24 h, ^d Determination from MALDI-ToF-MS spectra.

Nevertheless, the polymers were characterized in more detail after the termination of the polymerization with trifluoroacetic acid (TFA) and purification *via* precipitation by NMR spectroscopy and MALDI-ToF-MS. For the organic catalysts, the ¹H-NMR spectrum of the PPh₃-catalyzed polymer, and for the inorganic catalyzed polymers, the ¹H-NMR spectrum of the Cs₂CO₃-catalyzed polymer was shown in Figure 16 exemplary. For organic catalyzed polymers, on the one hand, vinyl groups and hydroxyl groups can be detected, and on the other hand, the bound catalyst on the polymer can be also detected as end-groups. It could be proven that this signal is assigned to the bound catalyst and not the free PPh₃ species. The protonation of the free PPh₃ can also be excluded because the acid TFA, which was used for the termination of the polymerization, is not strong enough. This is clear evidence that all organic catalysts react also as nucleophiles and the polymerization then proceeds according to the nucleophilic-catalyzed mechanism. For polymers prepared with inorganic catalysts, only the vinyl groups and the hydroxyl group could be detected, which indicates the base-catalyzed mechanism. These results can also be confirmed for the organic and inorganic catalyzed polymers *via* MALDI-ToF-MS measurements.

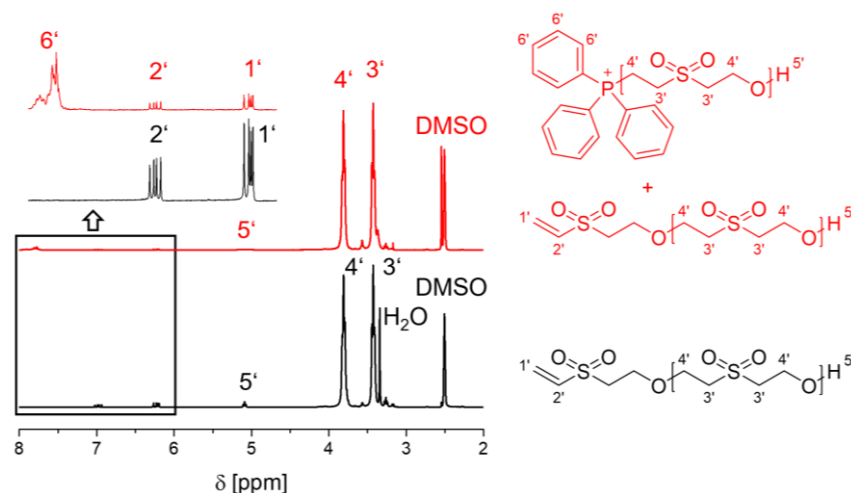


Figure 16: $^1\text{H-NMR}$ spectra (300 MHz, DMSO-d_6 , 298 K) of the PPh_3 -catalyzed (red) and the Cs_2CO_3 -catalyzed (black) polymer. The figure was adapted from ref. ⁸⁴ with permissions of Royal Society of Chemistry. Copyright 2021.

The determination of the molar masses of the purified polymers by SEC measurements is a relative method, which always requires a standard and therefore the values obtained differ from the absolute molar mass of the sample. To determine the real molar masses, an absolute method such as the MALDI-ToF-MS method is required. However, since the MALDI-ToF-MS failed in this context because of insufficient ionization, the absolute molar masses was subsequently determined by vapor pressure osmometry. The determined molar masses of 2110 g mol^{-1} for the K_2CO_3 -catalyzed polymer was in very good agreement with the values determined with SEC measurements (2230 g mol^{-1}). However, the catalyst end-groups of the organically catalyzed polymers influence the measurements, and therefore only the molar masses of the inorganic catalyzed polymers could be determined with this method. In summary, Oxa-Michael polyaddition is a good method to obtain polymers starting from vinyl sulfonylethanol, although the molar masses in the range of 2000 to 4000 g mol^{-1} are still relatively low, mainly because of the incomplete conversion and the inaccurate stoichiometry because of the attack of the nucleophiles on the double bond.

6.1.2. Solution polymerization

As a consequence of the limited solubility of the catalysts in the monomer and the associated imprecise indication of the actual amount of catalyst involved in the polymerization, the polymerizations were also carried out in solution. DMSO was chosen as the solvent for the polymerizations, because of the good solubility of the polymer and the organic catalysts. However, the inorganic catalysts were not fully soluble under these

conditions, so no further studies were performed with these catalysts, and instead, the focus was on the PPh₃, DBU, and DMAP catalysts. Similar to bulk polymerization, high conversion rates were observed at very short reaction times. But as a consequence of the high polymerization rate of PPh₃ and DBU in particular, it was not possible to detect the typical behavior of increasing chain lengths with the reaction time by SEC measurements as with the polymerization described above. In contrast, polymerization with DMAP proceeded slower, so a clear increase in chain length with increasing reaction time could be observed.

Theoretically, the formation of cyclic polymers should occur more frequently or be more likely during solution polymerization due to the dilution effect of the reactive groups compared to those in the bulk. However, no significant change in molar masses was observed, although no quantitative analysis of the cyclic products could be performed because of the known difficulties described in Section 6.1.1. Subsequently, the influence of the concentrations on the polymerization behavior was investigated, but again no significant differences could be observed. Only the polymerization rate is minimally higher, which can be explained by the lower viscosity.

Since homogeneity can be ensured in the solution polymerizations, the influence of the amount of catalyst on the polymerization can also be investigated. For different amounts of PPh₃, no significant change in chain length was observed by SEC measurements. However, the NMR spectra showed that less catalyst used also resulted in fewer end groups with the bonded catalyst after purification. In consequence, the limitation in chain length was not simply because of the nonequivalent stoichiometry as a result of the addition of the catalyst to the polymer but could also be due to a change in reactivity. Also, no significant differences in chain length were observed for DBU with different amounts of catalyst. However, kinetics were performed and monitored *in situ* in an NMR instrument because of the high polymerization rate, to develop an even deeper understanding of the polymerization. For comparison purposes, both DBU-catalyzed polymerization and DMAP-catalyzed polymerization were studied with different amounts of catalyst (Figure 17). As observed earlier, the polymerization with DBU is slightly faster than with DMAP. Nevertheless, it can be observed for both polymerizations that an increased amount of catalyst also leads to an increased reaction rate, which, however, decreases during the individual polymerizations because of the increased viscosity.

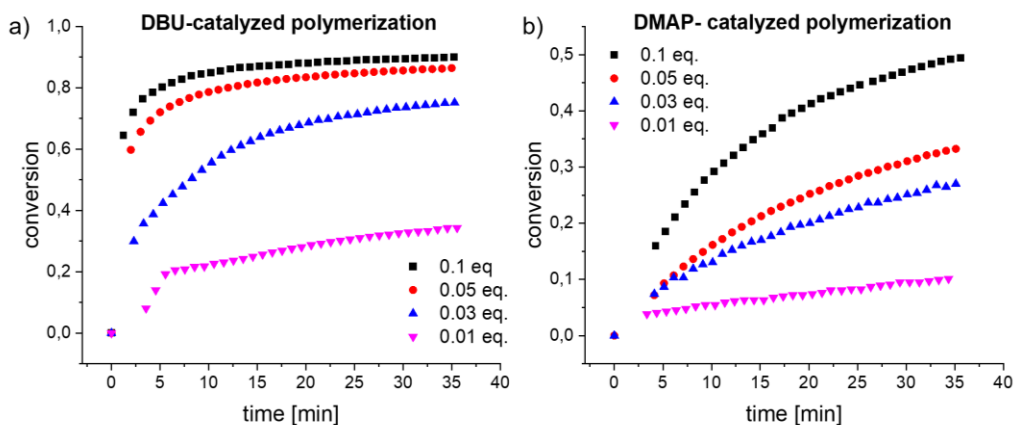


Figure 17: Conversion vs. reaction time of the a) DBU-catalyzed polymerization and b) DMAP-catalyzed polymerization with different amounts of catalyst. The figure was adapted from ref. ⁸⁴ with permissions of Royal Society of Chemistry. Copyright 2021.

6.2. Properties of the oxa-Michael polymers

So far, mostly polyether sulfones based on aromatic units are commercially available and their properties have been investigated in detail. They are characterized by high thermal and chemical resistance but are more difficult to process because of their high glass transition temperatures. Aliphatic polyether sulfones have been studied only sporadically in this regard, which is the reason why the comparison of this new polymer polyvinyl sulfonylethanol with already-known aromatic-based polyether sulfones is so important. Thermogravimetric analysis (TGA) measurements show similar high thermal stability (>300 °C) for the polymers prepared with the inorganic bases under both nitrogen and oxygen atmospheres suggesting that they also exhibit oxidative stability. However, for the organic-catalyzed polymers, the decomposition was highly dependent on the catalyst used but generally lower than for the inorganic catalysts. This may indicate that the catalyst end-groups also catalyzes the degradation. It is conceivable, that a retro-Michael addition occurs during decomposition, but this aspect was not studied in more detail. Although the decomposition temperature of the aromatic polyether sulfones is very similar, they differ greatly in their glass transition temperature. As mentioned before, aromatic polyether sulfones are characterized by very high glass transition temperatures, while polyvinyl sulfonylethanol has a glass transition temperature in the range between 10 and 22 °C, which simplifies processing, because lower temperatures are required. However, the low glass transition temperature is at odds with the solid impression of the polymer if it were an amorphous polymer. Therefore, a semi-crystalline nature of the

polymer was suspected, which was not detectable during the final heating and cooling process (3rd) of the DSC measurement. For this reason, we also examined the first heating process in more detail and were indeed able to detect an endothermic signal corresponding to a melting point (Figure 18). However, the corresponding cooling process shows no sign of recrystallization, suggesting that recrystallization is inhibited. This was supported by experiments involving a lower cooling rate or an annealing sequence at 50 °C for 24 h, which were unsuccessful for the recrystallization. In order to clearly demonstrate the semi-crystalline nature of the polymer, X-ray diffraction (XRD) measurements were performed and indeed, sharp signals were detected confirming the semi-crystalline nature of the polymer after the purification. However, when the polymer is subsequently melted, the sharp signals disappear and only a corona can be observed, which is typical for amorphous materials.

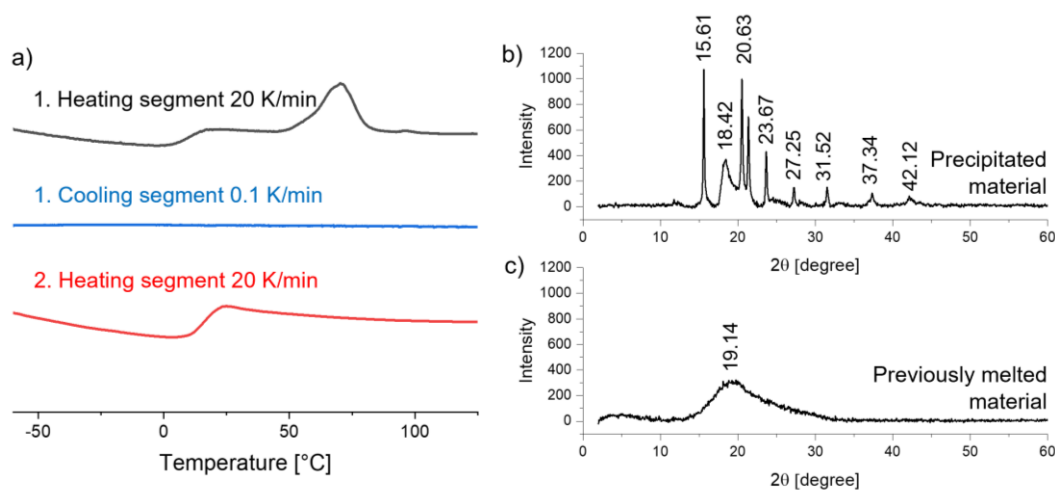


Figure 18: a) DSC-traces of the purified PPh₃-catalyzed polymer with different heating and cooling segments, b) XRD-spectrum of the purified PPh₃-catalyzed polymer after precipitation, and c) XRD-spectrum of the purified PPh₃-catalyzed polymer after precipitation and melting. The figure was adapted from ref. ⁸⁴ with permissions of Royal Society of Chemistry. Copyright 2021.

In summary, although the free radical polymerization of the monomer vinyl sulfonylethanol, as described in Chapter 4, can only be polymerized at low conversions and is therefore unsuitable for industrial-scale production, oxa-Michael polyaddition is a good all-round alternative for the preparation of sulfone-containing polymers. Polyvinyl sulfonylethanol represents a new polyether sulfone characterized by high thermal stability like aromatic analogs. However, additional interesting properties such as a much lower glass transition temperature and a semicrystalline nature were found, which differ significantly from the aromatic commercial polyether sulfones. This could lead to

interesting new applications, which, however, require more detailed investigations in advance. Nevertheless, the results show the potential of these substances.

7. Summary

Sulfur-containing polymers offer the potential for a wide range of applications in an industrial context, because of their unique properties, such as an increased refractive index, the ability to absorb metal, or the possibility of modifying these polymers in a remarkably simple way. Nevertheless, research in this area is not as advanced as for other classes of materials because of difficulties in the polymerization process. In this work, the polymerization behavior of the new *S*-vinyl monomer vinyl mercaptoethanol, which has recently been produced by BASF SE, was investigated in detail and the properties of the polymers were determined for subsequent potential applications (Figure 19).

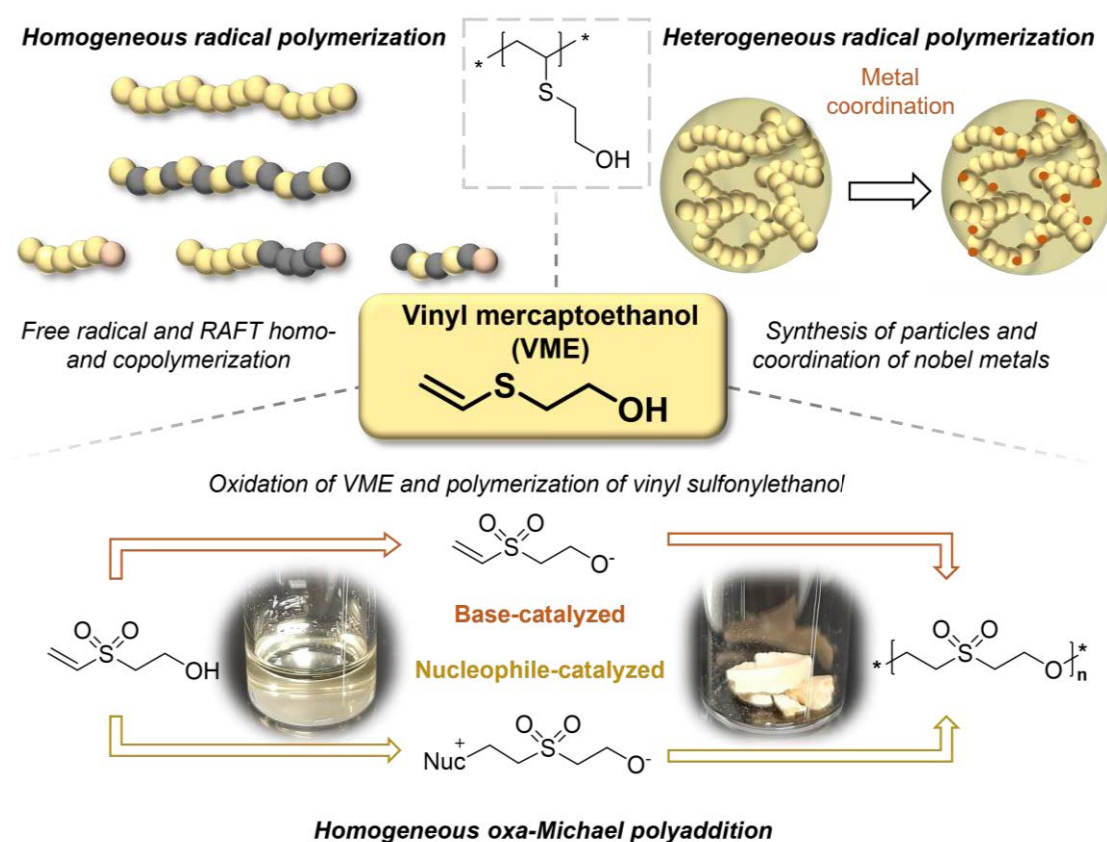


Figure 19: Overview of the different thematic parts in the thesis: homogeneous radical homo- and copolymerization of vinyl mercaptoethanol (upper left), heterogeneous radical homopolymerization and coordination of noble metals (upper right), and the oxidation of vinyl mercaptoethanol to vinyl sulfonylethanol and the subsequent oxa-Michael polyaddition (bottom).

First, radical polymerizations were fundamentally investigated under various conditions in bulk and solution. The polymerization with aza-initiators leads very rapidly to polymers with high molar masses. Initiation by *e.g.*, peroxides was not possible because the thioether group was prone to oxidation. Under similar conditions, the polymerization rate is comparable to that of methyl methacrylate, reflecting the high reactivity of the

monomer in free radical polymerization. However, not only homopolymerization results in polymers with high molar masses. Increased reactivities were also observed during copolymerization with acrylates and methacrylates. In this case, the corresponding copolymerizations proceed even faster than the homopolymerizations and higher molar masses can be achieved, because of the opposite polarities of the monomers. In contrast, polymerizations with vinyl pyrrolidone and vinyl acetate, for example, were very sluggish. Determination of the Q - and e -values, which provide information about the stabilization of the radicals during polymerization, as well as the polarity, revealed that the increased reactivity was a result of the good stabilization of the radicals. In the literature, this stabilization was also observed for other *S*-vinyl monomers and was explained based on the interaction of the 3d orbitals of sulfur. But the monomer not only offers the possibility to produce sulfur-containing polymers by free radical polymerization. Controlled polymerization, such as RAFT polymerization, in this case, could also be successfully conducted and well-defined homopolymers, random copolymers, and block-copolymers with MMA and BA were obtained using suitable trithiocarbonate-CTAs.

Overall, the homopolymer PVME is characterized by a very soft nature with undergoing glass transition at room temperature, but high thermal stability up to 300 °C. The glass transition temperatures of the random copolymers, in turn, vary greatly depending on the composition but are characterized by only one glass transition temperature, whereas the block-copolymers, for example, exhibit several glass transition temperatures, which is an indication of phase separation because of the different polarities of the monomers. The mechanical properties of the copolymers change only slightly even with an increased amount of VME in the copolymers, while a slightly increased refractive index due to the incorporation of sulfur changes the optical properties of these materials. These studies have revealed that the optical properties can be changed without significantly degrading the mechanical properties of the polymer by precisely adjusting the sulfur content and thus, demonstrate the potential of sulfur-containing polymers for possible applications.

Attempts were also made to synthesize the polymers *via* heterogeneous radical polymerization techniques because of the limited solubility of PVME and the resulting issues in processing it. These represent an interesting opportunity to incorporate the polymers into materials on a large scale, especially regarding to industrial applications, since heterogeneous polymerization techniques are often preferred to homogeneous

polymerization techniques in the industry. Various surfactants were evaluated, with polyvinyl alcohol (PVA) proving to be the best stabilizer for this system. Nevertheless, the sedimentation behavior of the generated particles was observed over time, which could be explained by the influence of gravity as a consequence of the size of the particles in the micrometer range. Because of the size of the particles and the sedimentation behavior, we cannot speak of a classical emulsion (particle sizes 100-500 nm) in this case. Therefore, in combination with the partial water solubility of the monomer, we assume a mixed process of emulsion polymerization and precipitation polymerization with PVA, which would also explain the broad distribution of particle sizes. Another interesting possibility is the incorporation of metal ions due to the affinity of sulfur for binding noble metals, which greatly expands the range of applications of these polymers. The focus was on silver ions, which were successfully incorporated ($\text{Ag}^+\text{@PVME}$) and a slow release over time was confirmed. Reduction of the incorporated silver ions to silver nanoparticles (Ag@PVME), on the other hand, was a major challenge because the commonly used reducing agents also interact with the silver and thus compete with the polymer, leading to coagulation of the particles. Interestingly, a color change of the dispersion could be observed in sunlight, indicating a reduction of silver ions. We, therefore, hypothesize that the polymer itself acts as a reducing agent, as the sulfide group is very easy to oxidize, as demonstrated previously. Silver ions and silver nanoparticles are known for their antibacterial effect and are therefore frequently used in medicine, but also, for example, in the textile industry. For this reason, both the pure dispersion and the modified dispersions ($\text{Ag}^+\text{@PVME}$, Ag@PVME) were evaluated for their antibacterial activity, which showed a clear antibacterial effect of $\text{Ag}^+\text{@PVME}$, while the PVME had no effect at all and Ag@PVME had very little effect on the growth of bacteria. However, not only silver ions or silver nanoparticles could be successfully incorporated into the polymer particles, also the coordination of gold ions by the addition of hydrochloric acid could be realized. Here, too, reduction by sunlight provided the best results for uniform distribution of the gold nanoparticles in the polymer particles.

The polymerization of the oxidized vinyl mercaptoethanol species also aroused our interest because of the simplicity of the modification and the associated preparation of substances with completely new properties and altered polymerization behavior. However, radical polymerization of the sulfoxide species was not feasible, and radical polymerization of the sulfone species was only possible with extremely low conversion

rates (<5%). Our aim was then to find a suitable polymerization method for the oxidized monomers, although it was demonstrated that the oxidation of polyvinyl mercaptoethanol can selectively lead to sulfoxide or sulfone polymer under different reaction conditions. And indeed, the oxidized monomer is ideally suited for oxa-Michael polyaddition because of the electron-deficient vinyl group, which is an ideal Michael acceptor, and the hydroxyl group, which is a strong Michael donor. Various organic and inorganic catalysts were tested both in bulk and in solution, initiating either a nucleophilic-catalyzed mechanism or a base-catalyzed mechanism. After only a few minutes, a color change and an increase in viscosity were observed for all catalysts, reflecting the high polymerization rate of this reaction. Polymers with molar masses in the range of 2000 to 4000 g mol⁻¹ were obtained, although the formation of cycles could not be excluded. Interestingly, the end-group analysis demonstrated that all the organic catalysts functioned as nucleophiles, although some of them are strong bases, while the inorganic catalysts triggered the base-catalyzed mechanism. The study of the properties of the polymers revealed a very high thermal stability of the polymers similar to the commercially available aromatic polyether sulfones, but polyvinyl sulfonylethanol, in comparison, has a much lower glass transition temperature depending on the chain length and the end group in the range of 10 to 20 °C. Surprisingly, the polymer further features a semi-crystalline character when processed from solution. Even though the transformation of the crystalline regions into amorphous regions in a subsequent melting process must be considered irreversible. This opens up new possible alternative application profiles because of better processability, but also because of the completely new properties like the semicrystalline nature, especially on an industrial scale.

8. Zusammenfassung

Schwefelhaltige Polymere bieten das Potenzial für eine Vielzahl von Anwendungen in der Industrie, da sie einzigartige Eigenschaften aufweisen, wie einen erhöhten Brechungsindex, die Fähigkeit, Metalle zu absorbieren oder die Möglichkeit, diese Polymere auf sehr einfache Weise zu modifizieren. Dennoch ist die Forschung in diesem Bereich aufgrund von Schwierigkeiten bei der Polymerisation nicht so weit fortgeschritten wie bei anderen Materialklassen. In dieser Arbeit wurde das Polymerisationsverhalten des neuen *S*-Vinylmonomers Vinylmercaptoethanol, das kürzlich von der BASF SE hergestellt wurde, und die Eigenschaften der resultierenden Polymere für spätere potenzielle Anwendungen eingehend untersucht (Abbildung 20).

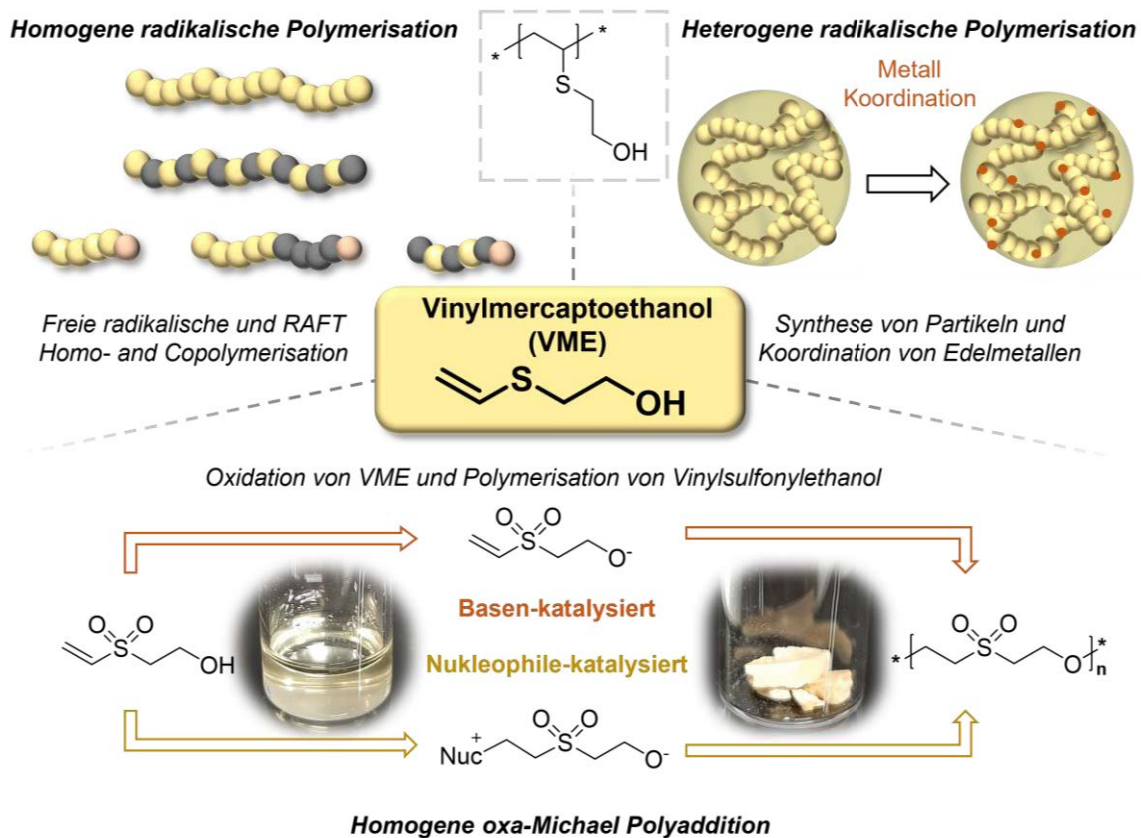


Abbildung 20: Überblick über die verschiedenen thematischen Teile der Arbeit: **homogene radikalische Homo- und Copolymerisation von Vinylmercaptoethanol (oben links), heterogene radikalische Homopolymerisation und Koordination von Edelmetallen (oben rechts) und Oxidation von Vinylmercaptoethanol zu Vinylsulfonylethanol und die anschließende Oxa-Michael-Polyaddition (unten).**

Zunächst wurden radikalische Polymerisationen unter verschiedenen Bedingungen in Bulk und Lösung grundlegend untersucht. Die Polymerisation mit Aza-Initiatoren führt sehr schnell zu Polymeren mit hohem Molekulargewicht. Eine Initiierung durch z.B. Peroxide war stattdessen nicht möglich, da die Thioethergruppe zur Oxidation neigt.

Unter ähnlichen Bedingungen ist die Polymerisationsgeschwindigkeit mit der von Methylmethacrylat vergleichbar, was die hohe Reaktivität des Monomers bei einer radikalischen Polymerisation widerspiegelt. Doch nicht nur die Homopolymerisation führt zu Polymeren mit hohen Molekulargewichten. Erhöhte Reaktivitäten wurden auch bei der Copolymerisation mit Acrylaten und Methacrylaten beobachtet. In diesem Fall verlaufen die entsprechenden Copolymerisationen sogar noch schneller als die Homopolymerisationen und es können aufgrund der entgegengesetzten Polaritäten der Monomere höhere Molmassen erreicht werden. Im Gegensatz dazu verliefen Polymerisationen beispielsweise mit Vinylpyrrolidon und Vinylacetat sehr schleppend. Die Bestimmung der Q - und e -Werte, die Auskunft über die Stabilisierung der Radikale während der Polymerisation sowie der Polarität geben, zeigte, dass die erhöhte Reaktivität auf die gute Stabilisierung der Radikale zurückzuführen ist. In der Literatur wurde diese Stabilisierung auch für andere *S*-Vinylmonomere beobachtet und durch die Wechselwirkung der 3d-Orbitale des Schwefels erklärt. Das Monomer bietet aber nicht nur die Möglichkeit, schwefelhaltige Polymere durch freie Radikalik herzustellen. Auch eine kontrollierte Polymerisation, wie in diesem Fall die RAFT-Polymerisation, konnte erfolgreich durchgeführt werden und es wurden unter Verwendung eines geeigneten Trithiocarbonat-CTAs wohldefinierte Homopolymere, statistische Copolymere und Block-Copolymere mit MMA und BA synthetisiert.

Insgesamt zeichnet sich das Homopolymer PVME durch eine sehr weiche Beschaffenheit mit einem Glasübergang bei Raumtemperatur, aber hoher thermischer Stabilität bis zu 300 °C aus. Die Glasübergangstemperaturen der statistischen Copolymere wiederum variieren je nach Zusammensetzung stark, sind aber durch nur eine Glasübergangstemperatur gekennzeichnet, während z. B. die Blockcopolymere mehrere Glasübergangstemperaturen aufweisen, was auf eine Phasenseparation aufgrund der unterschiedlichen Polaritäten der Monomere hinweist. Die mechanischen Eigenschaften der Copolymere ändern sich auch bei erhöhtem VME-Anteil in den Copolymeren nur geringfügig, während ein leicht erhöhter Brechungsindex durch das Einbringen von Schwefel die optischen Eigenschaften dieser Materialien verändert. Das zeigt, dass durch eine genaue Einstellung des Schwefelgehalts die optischen Eigenschaften verändert werden können, ohne die mechanischen Eigenschaften des Polymers wesentlich zu verschlechtern, und demonstrieren somit das Potenzial der schwefelhaltigen Polymere für mögliche Anwendungen.

Aufgrund der begrenzten Löslichkeit von PVME und der daraus resultierenden Probleme bei der Verarbeitung wurden auch Versuche unternommen, die Polymere mittels heterogener radikalischer Polymerisationstechniken zu synthetisieren. Diese stellen eine interessante Möglichkeit dar, die Polymere in Werkstoffe einzubringen, insbesondere im Hinblick auf industrielle Anwendungen, da heterogene Polymerisationstechniken in der Industrie häufig den homogenen Polymerisationstechniken vorgezogen werden. Es wurden verschiedene Tenside getestet, wobei sich Polyvinylalkohol (PVA) als der beste Stabilisator für dieses System erwies. Dennoch wurde im Laufe der Zeit ein Sedimentationsverhalten der erzeugten Partikel beobachtet, das durch den Einfluss der Schwerkraft infolge der Größe der Partikel im Mikrometerbereich erklärt werden konnte. Aufgrund der Größe der Partikel und des Sedimentationsverhaltens kann in diesem Fall nicht von einer klassischen Emulsion (Partikelgrößen 100-500 nm) gesprochen werden. In Kombination mit der teilweisen Wasserlöslichkeit des Monomers gehen wir daher von einem gemischten Prozess aus Emulsionspolymerisation und Fällungspolymerisation mit PVA aus, was ebenfalls die breite Verteilung der Partikelgrößen erklären würde. Eine weitere interessante Möglichkeit ist die Einbringung von Metallionen aufgrund der Affinität von Schwefel zur Bindung von Edelmetallen, was das Anwendungsspektrum dieser Polymere stark erweitert. Der Schwerpunkt lag auf Silberionen, die erfolgreich eingebaut werden konnten ($\text{Ag}^+\text{@PVME}$) und deren langsame Freisetzung im Laufe der Zeit bestätigt wurde. Die Reduktion der Silberionen zu Silbernanopartikeln (Ag@PVME) stellte hingegen eine große Herausforderung dar, da die üblicherweise verwendeten Reduktionsmittel auch mit dem Silber interagieren und somit mit dem Polymer konkurrieren, was zur Koagulation der Partikel führte. Interessanterweise konnte eine Farbveränderung der Dispersion im Sonnenlicht beobachtet werden, was auf eine Reduktion der Silberionen hinweist. Wir stellen daher die Hypothese auf, dass das Polymer selbst als Reduktionsmittel wirkt, da die Thioethergruppe sehr leicht zu oxidieren ist, wie zuvor schon gezeigt werden konnte. Silberionen und Silbernanopartikel sind für ihre antibakterielle Wirkung bekannt und werden daher häufig in der Medizin, aber auch z. B. in der Textilindustrie eingesetzt. Aus diesem Grund wurden sowohl die reine Dispersion als auch die modifizierten Dispersionen ($\text{Ag}^+\text{@PVME}$, Ag@PVME) auf ihre antibakterielle Aktivität untersucht, wobei sich eine deutliche antibakterielle Wirkung von $\text{Ag}^+\text{@PVME}$ zeigte, während das PVME überhaupt keine und Ag@PVME nur eine sehr geringe Wirkung auf das Wachstum von Bakterien hatte. Aber nicht nur Silberionen oder Silbernanopartikel konnten erfolgreich in die Polymerpartikel eingebaut

werden, sondern auch die Koordination von Goldionen konnte realisiert werden. Auch hier lieferte die Reduktion durch Sonnenlicht die besten Ergebnisse für eine gleichmäßige Verteilung der Gold-Nanopartikel in den Polymerpartikeln.

Die Polymerisation der oxidierten Vinylmercaptoethanol-Spezies weckte ebenfalls unser Interesse, da die Modifikation sich als sehr einfach erwies und damit die Herstellung von Substanzen mit völlig neuen Eigenschaften und verändertem Polymerisationsverhalten verbunden ist. Die radikalische Polymerisation der Sulfoxid-Spezies war jedoch nicht durchführbar, und die radikalische Polymerisation der Sulfon-Spezies war nur mit sehr geringen Umsatzraten (<5%) möglich. Unser Ziel war es dann, eine geeignete Polymerisationsmethode für die oxidierten Monomere zu finden, auch wenn schon gezeigt werden konnte, dass die Oxidation von Polyvinylmercaptoethanol unter verschiedenen Reaktionsbedingungen selektiv zu Sulfoxid- oder Sulfonpolymeren führen kann. Und tatsächlich ist das oxidierte Monomer aufgrund der elektronenarmen Vinylgruppe, die ein idealer Michael-Akzeptor darstellt, und der Hydroxylgruppe, die ein starker Michael-Donor darstellt, ideal für die Oxa-Michael-Polyaddition geeignet. Verschiedene organische und anorganische Katalysatoren wurden sowohl in Bulk als auch in Lösung getestet, wobei entweder ein nukleophil-katalysierter Mechanismus oder ein basen-katalysierter Mechanismus in Gang gesetzt wurde. Bereits nach wenigen Minuten wurden bei Verwendung von allen Katalysatoren ein Farbwechsel und ein Anstieg der Viskosität beobachtet, was die hohe Polymerisationsgeschwindigkeit dieser Reaktion widerspiegelt. Es wurden Polymere mit Molekulargewichten im Bereich von 2000 bis 4000 g mol⁻¹ erhalten, wobei die Bildung von Zyklen nicht ausgeschlossen werden konnte. Interessanterweise zeigte die Endgruppenanalyse, dass alle organischen Katalysatoren als Nukleophile fungierten, obwohl einige von ihnen ebenfalls auch starke Basen sind, während die anorganischen Katalysatoren den basenkatalysierten Mechanismus auslösten. Die Untersuchung der Eigenschaften der Polymere ergab eine sehr hohe thermische Stabilität der Polymere, ähnlich wie bei den handelsüblichen aromatischen Polyethersulfonen. Aber Polyvinylsulfonylethanol hat im Vergleich dazu eine viel niedrigere Glasübergangstemperatur in Abhängigkeit von der Kettenlänge und der Endgruppe im Bereich von 10 bis 20 °C. Überraschenderweise weist das Polymer außerdem einen teilkristallinen Charakter auf, wenn es aus der Lösung verarbeitet wird. Auch wenn bei einem anschließenden Schmelzprozess die Umwandlung der kristallinen Bereiche in amorphe Bereiche als irreversibel angesehen werden musste. Nichtsdestotrotz

eröffnet diese Polymere neue mögliche alternative Anwendungsprofile wegen der besseren Verarbeitbarkeit, aber auch wegen der völlig neuen Eigenschaften wie der teilkristallinen Natur, insbesondere im industriellen Maßstab.

9. References

1. J.-G. Liu, Y. Nakamura, Y. Shibasaki, S. Ando and M. Ueda, *Macromolecules*, 2007, **40**, 4614-4620.
2. J.-G. Liu, Y. Nakamura, Y. Suzuki, Y. Shibasaki, S. Ando and M. Ueda, *Macromolecules*, 2007, **40**, 7902-7909.
3. J.-G. Liu and M. Ueda, *J. Mater. Chem.*, 2009, **19**, 8907-8919.
4. T. Okubo, S. Kohmoto and M. Yamamoto, *J. Macromol. Sci. A*, 1998, **35**, 1819-1834.
5. R. Okutsu, Y. Suzuki, S. Ando and M. Ueda, *Macromolecules*, 2008, **41**, 6165-6168.
6. Y. Sato, S. Sobu, K. Nakabayashi, S. Samitsu and H. Mori, *ACS Appl. Polym. Mater.*, 2020, **2**, 3205-3214.
7. N.-H. You, T. Higashihara, Y. Oishi, S. Ando and M. Ueda, *Macromolecules*, 2010, **43**, 4613-4615.
8. Y. Suzuki, T. Higashihara, S. Ando and M. Ueda, *Polym. J.*, 2009, **41**, 860-865.
9. Y. Suzuki, T. Higashihara, S. Ando and M. Ueda, *Macromolecules*, 2012, **45**, 3402-3408.
10. H. Vahrenkamp, *Angew. Chem. Int. Ed. Engl.*, 1975, **14**, 322-329.
11. K. Suzuki and K. Yamasaki, *I. Inorg. Nucl. Chem.*, 1962, **24**, 1093-1103.
12. C. Vericat, M. E. Vela, G. Corthey, E. Pensa, E. Cortés, M. H. Fonticelli, F. Ibañez, G. E. Benitez, P. Carro and R. C. Salvarezza, *RSC Adv.*, 2014, **4**, 27730-27754.
13. J. A. Rodriguez, J. Dvorak, T. Jirsak, G. Liu, J. Hrbek, Y. Aray and C. González, *J. Am. Chem. Soc.*, 2003, **125**, 276-285.
14. N. Lotti, V. Siracusa, L. Finelli, P. Marchese and A. Munari, *Eur. Polym. J.*, 2006, **42**, 3374-3382.
15. C. Berti, A. Celli and E. Marianucci, *Eur. Polym. J.*, 2002, **38**, 1281-1288.
16. A. A. Basfar and J. Silverman, *Polym. Degrad. Stab.*, 1994, **46**, 1-8.
17. J. P. Kennedy and T. Chou, Berlin, Heidelberg, 1976.
18. M. Geven, R. d'Arcy, Z. Y. Turhan, F. El-Mohtadi, A. Alshamsan and N. Tirelli, *Eur. Polym. J.*, 2021, **149**, 110387-110408.
19. E. Lallana and N. Tirelli, *Macromol. Chem. Phys.*, 2013, **214**, 143-158.
20. R. V. Kupwade, *Journal of Chemical Reviews*, 2019, **1**, 99-113.
21. A. A. Burkey, A. Hillsley, D. T. Harris, J. R. Baltzegar, D. Y. Zhang, W. W. Sprague, A. M. Rosales and N. A. Lynd, *Biomacromolecules*, 2020, **21**, 3047-3055.
22. D. Işık, A. A. Joshi, X. Guo, F. Rancan, A. Klossek, A. Vogt, E. Rühl, S. Hedtrich and D. Klinger, *Biomater. Sci.*, 2021, **9**, 712-725.
23. T. Higashihara and M. Ueda, *Macromolecules*, 2015, **48**, 1915-1929.
24. S. N. Mthembu, A. Sharma, F. Albericio and B. G. de la Torre, *Chem. Bio. Chem.*, 2020, **21**, 1947-1954.
25. A. R. Stasińska, P. Putaj and M. K. Chmielewski, *Bioorg. Chem.*, 2019, **92**, 103223.
26. T. Alfrey Jr. and C. C. Price, *J. Polym. Sci.*, 1947, **2**, 101-106.
27. S. I. Kozhushkov and M. Alcarazo, *Eur. J. Inorg. Chem.*, 2020, **2020**, 2486-2500.
28. D. Kaiser, I. Klose, R. Oost, J. Neuhaus and N. Maulide, *Chem. Rev.*, 2019, **119**, 8701-8780.
29. J. J. Fitzgerald and R. A. Weiss, *J. Macromol. Sci. C*, 1988, **28**, 99-185.
30. R. J. Reddy and A. H. Kumari, *RSC Adv.*, 2021, **11**, 9130-9221.

References

31. C. C. Price and J. Zomlefer, *J. Am. Chem. Soc.*, 1950, **72**, 14-17.
32. A. V. Sviridova and E. N. Prilezhaeva, *Russ. Chem. Rev.*, 1974, **43**, 200-209.
33. C. C. Price and H. Morita, *J. Am. Chem. Soc.*, 1953, **75**, 4747-4750.
34. K. Tsuda, S. Kobayashi and T. Otsu, *J. Macromol. Sci. A*, 1967, **1**, 1025-1037.
35. K. D. Gollmer, F. H. Müller and H. Ringsdorf, *Makromole. Chem.*, 1966, **92**, 122-136.
36. C. C. Price and R. G. Gillis, *J. Am. Chem. Soc.*, 1953, **75**, 4750-4753.
37. J. C. H. Hwa, *J. Am. Chem. Soc.*, 1958, **81**, 3604-3607.
38. M. F. Shostakovskiy, E. N. Prilezhaeva and A. M. Khomutov, *Bull. Acad. Sci. USSR, Div. Chem. Sci.*, 1956, **5**, 1257-1262.
39. J. Kosai, Y. Masuda, Y. Chikayasu, Y. Takahashi, H. Sasabe, T. Chiba, J. Kido and H. Mori, *ACS Appl. Polym. Mater.*, 2020, **2**, 3310-3318.
40. F. R. Mayo and F. M. Lewis, *J. Am. Chem. Soc.*, 1944, **66**, 1594-1601.
41. M. Fineman and S. D. Ross, *J. Polym. Sci.*, 1950, **5**, 259-265.
42. T. Kelen, F. Tüdös and B. Turcsányi, *Polymer Bull.*, 1980, **2**, 71-76.
43. T. Otsu and H. Inoue, *J. Macromol. Sci. A*, 1970, **4**, 35-50.
44. K. Gollmer and H. Ringsdorf, *Kolloid-Z.*, 1967, **216**, 325-329.
45. C. E. Scott and C. C. Price, *J. Am. Chem. Soc.*, 1959, **81**, 2672-2674.
46. E. D. Holly, *J. Polym. Sci.*, 1959, **36**, 329-332.
47. K. Tsuda, S. Kobayashi and T. Otsu, *J. Macromol. Sci. A*, 1968, **6**, 41-48.
48. A. I. Vorob'eva, S. A. Onina, R. R. Muslukhov, S. V. Kolesov, L. Parshina, M. Y. Khil'ko, B. A. Trofimov and Y. B. Monakov, *Polym. Sci. Ser. B*, 2003, **45**, 102-105.
49. J. M. Judge and C. C. Price, *J. Polym. Sci.*, 1959, **41**, 435-443.
50. B. A. Trofimov, L. V. Morozova, A. I. Mikhaleva, M. V. Markova, I. V. Tatarinova and J. Henkelmann, *Russ. Chem. Bull.*, 2008, **57**, 2111-2116.
51. S. Iwatsuki, M. Kubo, M. Wakita, Y. Matsui and H. Kanoh, *Macromolecules* 1991, **24**, 5009-5014.
52. A. I. Vorob'eva, S. A. Onina, I. D. Musina, S. V. Kolesov, R. R. Muslukhov, L. Parshina, L. A. Oparina, B. A. Trofimov and Y. B. Monakov, *Polym. Sci. Ser. B*, 2004, **46**, 364-368.
53. Y. Abiko, A. Matsumura, K. Nakabayashi and H. Mori, *Polymer*, 2014, **55**, 6025-6035.
54. Y. Abiko, A. Matsumura, K. Nakabayashi and H. Mori, *React. Funct. Polym.*, 2015, **93**, 170-177.
55. Y. Abiko, K. Nakabayashi and H. Mori, *Macromol. Symp.*, 2015, **349**, 34-43.
56. K. Nakabayashi, Y. Abiko and H. Mori, *Macromolecules*, 2013, **46**, 5998-6012.
57. K. Nakabayashi, A. Matsumura, Y. Abiko and H. Mori, *Macromolecules*, 2016, **49**, 1616-1629.
58. W. Reppe, *Liebigs Ann. Chem.*, 1956, **601**, 81-138.
59. M. F. Shostakovskii, E. N. Prilezhaeva and V. M. Karavaeva, *Polym. Sci. U.S.S.R.*, 1960, **1**, 200-208.
60. H. Inoue and T. Otsu, *J. Polym. Sci., Polym. Chem. Ed.*, 1976, **14**, 845-861.
61. R. Kroker and H. Ringsdorf, *Makromole. Chem.*, 1969, **121**, 240-257.
62. N. Ziegenbalg, L. Elbinger, U. S. Schubert and J. C. Brendel, *Polym. Chem.*, 2022, **13**, 5019-5041.
63. K. Imai, T. Shiomi, Y. Tezuka and K. Takahashi, *J. Macromol. Sci. A*, 1985, **22**, 1347-1358.
64. C. C. Price and R. D. Gilbert, *J. Am. Chem. Soc.*, 1952, **74**, 2073-2074.
65. G. V. Leplyanin, V. A. Nikonov, A. A. Yelichev and Y. M. Shaul'skii, *Polym. Sci. U.S.S.R.*, 1990, **32**, 237-245.

66. M. A. Buese and T. E. Hogen-Esch, *Macromolecules*, 1987, **20**, 1509-1518.
67. R. S. Kanga, T. E. Hogen-Esch, E. Randrianalimanana, A. Soum and M. Fontanille, *Macromolecules*, 1990, **23**, 4241-4246.
68. R. S. Kanga, T. E. Hogen-Esch, E. Randrianalimanana, A. Soum and M. Fontanille, *Macromolecules*, 1990, **23**, 4235-4240.
69. C. Bouilhac, T. Rünzi and S. Mecking, *Macromolecules*, 2010, **43**, 3589-3590.
70. Y. Toshiyasu, Y. Taniguchi, K. Kimura, R. Fujishiro, M. Yoshihara, W. Tagaki and S. Oae, *Bulletin of the Chemical Society of Japan*, 1969, **42**, 1878-1881.
71. T. Clark, J. S. Murray, P. Lane and P. Politzer, *J. Mol. Model.*, 2008, **14**, 689-697.
72. T. Zhang, M. H. Litt and C. E. Rogers, *J. Polym. Sci. B*, 1994, **32**, 1671-1676.
73. E. Klein, P. D. May, J. K. Smith and N. Leger, *Biopolymers*, 1971, **10**, 647-655.
74. J.-C. Lee, M. H. Litt and C. E. Rogers, *J. Polym. Sci. A Polym. Chem.*, 1998, **36**, 793-801.
75. C. G. Overberger and A. M. Schiller, *J. Org. Chem.*, 1961, **26**, 4230-4232.
76. J. Boor Jr and A. M. T. Finch, *J. Polym. Sci. A-1*, 1971, 249-252.
77. J. P. Schroeder, D. C. Schroeder and S. Jotikasthira, *J. Polym. Sci. A*, 1972, **10**, 2189-2195.
78. T. Sasaki, S. Hashimoto, N. Nogami, Y. Sugiyama, M. Mori, Y. Naka and K. V. Le, *ACS Appl. Mater. Interfaces*, 2016, **8**, 5580-5585.
79. C. M. Possanza Casey and J. S. Moore, *ACS Macro Lett.*, 2016, **5**, 1257-1260.
80. H. Yaguchi and T. Sasaki, *Macromolecules*, 2007, **40**, 9332-9338.
81. S. Strasser and C. Slugovc, *Catal. Sci. Technol.*, 2015, **5**, 5091-5094.
82. S. Strasser, C. Wappl and C. Slugovc, *Polym. Chem.*, 2017, **8**, 1797-1804.
83. H. Wang, F. Cheng, W. He, J. Zhu, G. Cheng and J. Qu, *Biointerphases*, 2017, **12**, 02C414-411-402C414-418.
84. N. Ziegenbalg, R. Lohwasser, G. D'Andola, T. Adermann and J. C. Brendel, *Polym. Chem.*, 2021, **12**, 4337-4346.
85. K. Ratzenböck, M. M. Ud Din, S. M. Fischer, E. Žagar, D. Pahovnik, A. D. Boese, D. Rettenwander and C. Slugovc, *Chem. Sci.*, 2022, **13**, 6920-6928.
86. R. M. Black, K. Brewster, J. M. Harrison and N. Stansfield, *Phosphorus, Sulfur, Silicon Relat. Elem.*, 2006, **71**, 31-47.
87. A. H. Ford-Moore, *J. Chem. Soc.*, 1949, 2433-2440.
88. C. C. Price and O. H. Bullitt, *J. Org. Chem.*, 1947, **12**, 238-248.
89. A. Schöberl and M. Biedermann, *Justus Liebigs Ann. Chem.*, 1968, **716**, 37-46.
90. *German Pat.*, WO/2020/221607, 2020.
91. *German Pat.*, WO/2018/036848, 2018.
92. W. Reppe, *Acetylene chemistry*, CA Meyer, 1949.
93. G. Ayoub, M. Arhangel'skis, X. Zhang, F. Son, T. Islamoglu, T. Frišćić and O. K. Farha, *Beilstein J. Nanotechnol.*, 2019, **10**, 2422-2427.
94. N. Ziegenbalg, F. V. Gruschwitz, T. Adermann, L. Mayr, S. Guriyanova and J. C. Brendel, *Polym. Chem.*, 2022, **13**, 4934-4943.
95. C. C. Price, *J. Polym. Sci.*, 1948, **3**, 772-775.
96. I. Capek, M. Riza and M. Akashi, *J. Polym. Sci. A Polym. Chem.*, 1997, **35**, 3131-3139.
97. J. M. Saenz and J. M. Asua, *J. Polym. Sci. A Polym. Chem.*, 1996, **34**, 1977-1992.
98. H. Bamnolker and S. Margel, *J. Polym. Sci. A Polym. Chem.*, 1996, **14**, 1857-1871.
99. J. M. Asua, *Polymer Reaction Engineering*, Blackwell Publishing, Oxford, 2007.
100. J. M. Asua, *Polymeric Dispersions: Principles and Applications*, Springer, Dordrecht, 1997.

101. C.-S. Chern, *Principles and Applications of Emulsion Polymerization*, John Wiley & Sons, Hoboken, 2008.
102. Y. Saeki and T. Emura, *Prog. Polym. Sci.*, 2002, **27**, 2055-2131.
103. D. Zhang and X. Yang, in *Encyclopedia of Polymeric Nanomaterials*, Springer, Berlin, Heidelberg, 2015, pp. 2108-2116.
104. H. J. M. Wolff, M. Kather, H. Breisig, W. Richtering, A. Pich and M. Wessling, *ACS Appl. Mater. Interfaces*, 2018, **10**, 24799-24806.
105. P. Nesvadba, in *Encyclopedia of Radicals in Chemistry, Biology and Materials*, 2012.
106. P. A. Lovell and F. J. Schork, *Biomacromolecules*, 2020, **21**, 4396-4441.
107. J. M. Asua, *J. Polym. Sci. A Polym. Chem.*, 2004, **42**, 1025-1041.
108. P. B. Zetterlund, Y. Kagawa and M. Okubo, *Chem. Rev.*, 2008, **108**, 3747-3794.
109. N. Ziegenbalg, H. F. Ulrich, S. Stumpf, P. Mueller, J. Wiethan, J. Danner, U. S. Schubert, T. Adermann and J. C. Brendel, *Macromol. Chem. Phys.*, 2023, **224**, 2200379.
110. R. A. Bell and J. R. Kramer, *Environ. Toxicol. Chem.*, 1999, **18**, 9-22.
111. G. Franci, A. Falanga, S. Galdiero, L. Palomba, M. Rai, G. Morelli and M. Galdiero, *Molecules*, 2015, **20**, 8856-8874.
112. N. Durán, M. Durán, M. B. de Jesus, A. B. Seabra, W. J. Fávaro and G. Nakazato, *Nanomed.: Nanotechnol. Biol. Med.*, 2016, **12**, 789-799.
113. I. A.-O. Yin, J. Zhang, I. A.-O. Zhao, M. L. Mei, Q. Li and C. A.-O. Chu, *Int. J. Nanomedicine*, 2020, **15**, 2555-2562.
114. C. Marambio-Jones and E. M. V. Hoek, *J. Nanoparticle Res.*, 2010, **12**, 1531-1551.
115. S. P. Deshmukh, S. M. Patil, S. B. Mullani and S. D. Delekar, *Mater. Sci. Eng. C*, 2019, **97**, 954-965.
116. M. Radetić, *J. Mater. Sci.*, 2013, **48**, 95-107.
117. H. Althues, J. Henle and S. Kaskel, *Chem. Soc. Rev.*, 2007, **36**, 1454-1465.
118. J. García-Barrasa, J. M. López-de-Luzuriaga and M. Monge, *Cent. Eur. J. Chem.*, 2011, **9**, 7-19.
119. E. Abbasi, M. Milani, S. Fekri Aval, M. Kouhi, A. Akbarzadeh, H. Tayefi Nasrabadi, P. Nikasa, S. W. Joo, Y. Hanifehpour, K. Nejati-Koshki and M. Samiei, *Crit. Rev. Microbiol.*, 2016, **42**, 173-180.
120. A. Ravindran, P. Chandran and S. S. Khan, *Colloids Surf. B: Biointerfaces*, 2013, **105**, 342-352.
121. L. E. Cole, R. D. Ross, J. M. R. Tilley, T. Vargo-Gogola and R. K. Roeder, *Nanomedicine*, 2015, **10**, 321-341.
122. P. C. Chen, S. C. Mwakwari and A. K. Oyelere, *Nanotechnol. Sci. Appl.*, 2008, **1**, 45-65.
123. W. Cai, T. Gao, H. Hong and J. Sun, *Nanotechnol. Sci. Appl.*, 2008, **1**, 17-32.
124. X. Huang, P. K. Jain, I. H. El-Sayed and M. A. El-Sayed, *Nanomedicine*, 2007, **2**, 681-693.
125. S. Taghizadeh, V. Alimardani, P. L. Roudbali, Y. Ghasemi and E. Kaviani, *Photodiagnosis Photodyn. Ther.*, 2019, **25**, 389-400.
126. P. Paalanen, B. M. Weckhuysen and M. Sankar, *Catal. Sci. Technol.*, 2013, **3**, 2869-2880.
127. S. S. Dash, I. K. Sen and S. K. Dash, *Int. Nano Lett.*, 2022, **12**, 47-66.
128. J. Zhao and R. Jin, *Nano Today*, 2018, **18**, 86-102.
129. R. Ciriminna, E. Falletta, C. Della Pina, J. H. Teles and M. Pagliaro, *Angew. Chem. Inter. Ed.*, 2016, **55**, 14210-14217.
130. C. H. Carothers, *Trans. Faraday Soc.*, 1936, **32**, 39-49.

List of abbreviations

Ag@PVME	Polyvinyl mercaptoethanol particle modified with silver nanoparticles
Ag ⁺ @PVME	Polyvinyl mercaptoethanol particle modified with silver ions
AgNP	Silver nanoparticle
Au@PVME	Polyvinyl mercaptoethanol particle modified with gold nanoparticles
AuCl ₄ ⁻ @PVME	Polyvinyl mercaptoethanol particle modified with gold tetrachloride ions
AuNP	Gold nanoparticle
AIBN	Azobisisobutyronitrile
BA	<i>n</i> -Butyl acrylate
CTA	Chain-transfer-agent
DBU	1,8-Diazabicyclo[5.4.0]undec-7-ene
DLS	Dynamic light scattering
DMAP	4-(Dimethylamino)pyridin
DMF	Dimethylformamide
DMSO	Dimethyl sulfoxide
DSC	Differential scanning calorimetry
HSQC	Heteronuclear single quantum coherence
ICP-MS	Inductively coupled plasma mass spectrometry
IR	Infrared
MALDI-ToF-MS	Matrix-assisted laser ionization time-of-flight mass spectrometry
MMA	Methyl methacrylate
M _n	Number average molar mass
n _D	Refractive index
NMR	Nuclear magnetic resonance
PBA	Polybutylacrylate
PMI	<i>N</i> -Phenyl maleimide

PMMA	Polymethyl methacrylate
PPh ₃	Triphenylphosphine
PVA	Polyvinyl alcohol
PVME	Polyvinyl mercaptoethanol
PVP	Polyvinyl pyrrolidone
RAFT	Reversible addition–fragmentation chain-transfer
ref	Reference
rt	Room temperature
SAXS	Small angle X-ray scattering
SDS	Sodium dodecyl sulfate
SEC	Size exclusion chromatography
STA-MS	Simultaneous thermal analysis-mass spectroscopy
TBD	Triazabicyclodecene
TEDA	Triethylendiamin
TEM	Transmission electron microscopy
TFA	Trifluoroacetic acid
T _g	Glass transition temperature
TGA	Thermogravimetric analysis
UV-Vis	Ultraviolet–visible
V-50	2,2'-Azobis(2-methylpropionamidine) dihydrochloride
VA	Vinyl acetate
VME	Vinyl mercaptoethanol
VP	Vinyl pyrrolidone
<i>wt</i>	Weight
XRD	X-ray diffraction

Publication list

Peer reviewed publications

N. Ziegenbalg, R. Lohwasser, G. D'Andola, T. Adermann, and J. C. Brendel, "Oxa-Michael polyaddition of vinylsulfonylethanol for aliphatic polyethersulfones", *Polym. Chem.* **2021**, *12*, 4337-4346.

DOI: 10.1039/D1PY00256B

M. K. Farh, F. V. Gruschwitz, N. Ziegenbalg, H. Abul-Futouh, H. Görls, W. Weigand, and J. C. Brendel, "Dual function of β -hydroxy dithiocinnamic esters: RAFT agent and ligand for metal complexation", *Macromol. Rapid Commun.* **2022**, *43*, 2200428.

DOI: 10.1002/marc.202200428

N. Ziegenbalg, F. V. Gruschwitz, T. Adermann, L. Mayr, S. Guriyanova, and J. C. Brendel, "Vinyl mercaptoethanol as a reactive monomer for preparation of functional homo- and copolymers with (meth)acrylates", *Polym. Chem.* **2022**, *13*, 4934-4943.

DOI: 10.1039/D2PY00598K

N. Ziegenbalg, L. Elbinger, U. S. Schubert, and J. C. Brendel, "Polymers from S-vinyl monomers: Reactivities and properties", *Polym. Chem.* **2022**, *13*, 5019-5041.

DOI: 10.1039/D2PY00850E

N. Ziegenbalg, H. F. Ulrich, S. Stumpf, P. Mueller, J. Wiethan, J. Danner, U. S. Schubert, T. Adermann, and J. C. Brendel, "Coordination of noble metals in poly(vinyl mercaptoethanol) particles prepared by precipitation/emulsion polymerization", *Macromol. Chem. Phys.* **2023**, *224*, 2200379.

DOI: 10.1002/macp.202200379

Poster presentations

101 Years of Macromolecular Chemistry - Biennial Meeting of the GDCh Division of Macromolecular Chemistry 2021 (online conference)

T. Klein, F. V. Gruschwitz, F. Hausig, F. H. Sobotta, H. F. Ulrich, N. Ziegenbalg, J. C. Brendel: Synthesis of functional, hierarchically structured polymers.

Bordeaux Polymere Conference 2022 (Bordeaux, France)

N. Ziegenbalg, T. Adermann, J. C. Brendel: Synthesis of functional sulfur containing polymers from vinyl mercaptoethanol (VME).

Acknowledgment

At this point, I would like to take the opportunity to thank the people who were essential to the completion of this thesis. First and foremost, I would like to thank my supervisor, Dr Johannes C. Brendel, who was always there to give me advice and support. I especially appreciate that you gave me the freedom I needed to develop my full potential. Thank you for the years I spent in your group. I wish you all the best for the future and that you get the professorship you desire.

My next thanks go to Prof. Ulrich S. Schubert for the opportunity to work in this highly scientific interdisciplinary environment. The facilities made available to us exceed those at many other universities and have contributed significantly to my successful work.

Then, I would like to thank my collaborative partner BASF SE and in particular the staff members G. D'Andola and T. Adermann. BASF initiated this project and always stands by me with helpful advice in the further course. In addition, several characterization measurements of my compounds were performed at BASF SE. These measurements add value to the publications and thus had a decisive influence on my work as a whole.

I would also like to thank the people who performed measurements for me at the Friedrich Schiller University in Jena or supported me in other ways. These are Renzo Paulus for TGA and DSC measurements, Steffi Stumpf for the SEM images, Rica Patzschke for special NMR measurements, and Dr. Dirk Merten for ICP-MS measurements. But special thanks also go to Yannik Köster, who often implemented my graphical ideas for publications and presentations, and to my office team (Franka Gruschwitz, Franziska Hausig, Marcel Enke, Felix Tzschöckell, and Öykü Şimşek), who always supported me. I would like to thank the APS and the lunch group, without whom the days would not have been half as much fun, and additional Sebastian Städter, Lada Elbinger, and Hans F. Ulrich, who became a kind of second family to me during this time. I will never forget this time.

And last but not least, I would like to thank my family and all the friends I have not yet mentioned by name. Again, through your constant support and encouragement, you have played a big part in enabling me to do this work.

Declaration of originality

Ich erkläre, dass ich die vorliegende Arbeit selbständig und unter Verwendung der angegebenen Hilfsmittel, persönlichen Mitteilungen und Quellen angefertigt habe.

Jena, den

.....

Nicole Ziegenbalg

Appendix

Publications P1 to P4

P1: Reprinted by permission of Royal Society of Chemistry. Copyright 2022.

P2: Reprinted by permission of Royal Society of Chemistry. Copyright 2022.

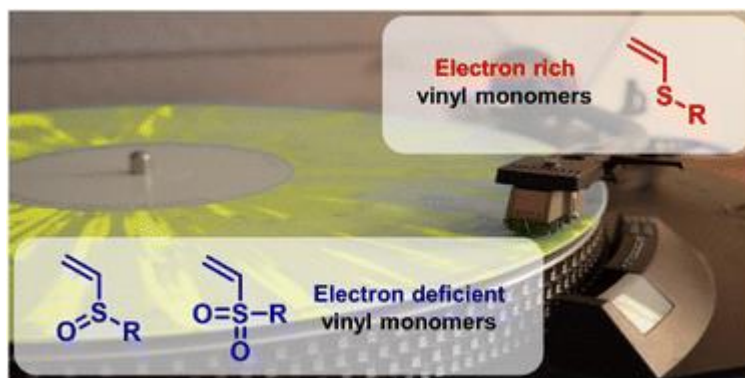
P3: Reproduced by permission of H. F. Ulrich, S. Stumpf, P. Mueller, J. Wiethan, J. Danner, U. S. Schubert, T. Adermann, J. C. Brendel.

P4: Reprinted by permission of Royal Society of Chemistry. Copyright 2021.

Publication P1

Polymers from S-vinyl monomers: reactivities and properties

N. Ziegenbalg, L. Elbinger, U. S. Schubert, J. C. Brendel, *Polym. Chem.* **2022**, *13*, 5019-5041.



Reproduced by permission of Royal Society of Chemistry. Copyright 2022.

The paper is available online: doi.org/10.1039/D2PY00850E



Cite this: *Polym. Chem.*, 2022, **13**, 5019

Polymers from S-vinyl monomers: reactivities and properties

Nicole Ziegenbalg,^{a,b} Lada Elbinger,^{a,b} Ulrich S. Schubert ^{a,b} and Johannes C. Brendel ^{*a,b}

The large variety of available functional groups, their versatility, and the various polymerization techniques have made vinyl monomers the prevalent source for preparation of polymers. Interestingly, among this wide variety of applied structures S-vinyl monomers have remained a niche for the last decades despite their unique set of properties and early reports on their reactivities. An obstacle has been the limited access on a technical scale, but recent developments in sulfur chemistry and the request for more diverse reactivities might lead to a renaissance of these often neglected compounds. In particular, the different variations of sulfur moieties and the correlating diversity of properties render these compounds increasingly attractive for fundamental research as well as applications. A challenge, however, remains the detailed understanding and control of their polymerization behavior, as these S-vinyl compounds might be prone to side reactions depending on the applied reactions. In this regard, this review intends to provide a comprehensive overview of reported polymerization techniques, their challenges and limitations with regard to the sulfur compounds, and the resulting reactivities of the corresponding monomers in homopolymerizations but as well copolymerizations with various other vinyl monomers. We further include reports on characteristic properties and tried to highlight some potential applications of the resulting polymers. Considering the various modifications of sulfur, we distinguished according to electron rich S-vinyl monomers, such as vinyl sulfides and electron deficient compounds including the various oxidized variants. In accordance, the reactivities differ significantly and suitable polymerization techniques are summarized for each class of monomers.

Received 30th June 2022,
Accepted 10th August 2022

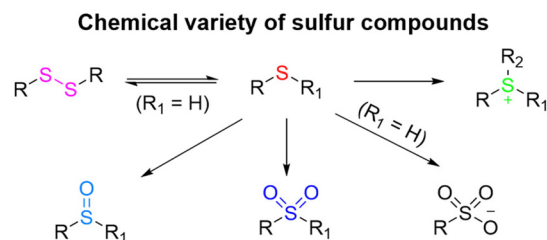
DOI: 10.1039/d2py00850e

rsc.li/polymers

1. Introduction

Due to its unique characteristics, the incorporation of sulfur into polymers creates reactive and functional materials, which are of interest for a variety of applications and makes them not only attractive for academic research but also for industry. One particular example of a specific property the sulfur is impacting is an increased refractive index of these materials. In accordance with the Lorentz–Lorenz equation sulfur features a high atomic refraction, which renders materials with high sulfur content favorable for optical applications such as lenses or anti-reflective coatings.^{1–8} In addition, the incorporation of sulfur may improve flame retarding properties,^{9–11} resulting in materials with a high thermal as well as chemical resistance.^{12–15}

However, sulfur also allows these substances to be modified in a variety of ways, which is shown in detail in Scheme 1. Thus, the corresponding sulfoxide or sulfone can be obtained by selective oxidation, which offers completely new properties, for example changes in polarity and solubility, and this opens up new application areas.^{16–18} It is also possible to form reversible disulfide bridges, which can then often be used as cross-linkers. However, not only neutrally charged monomers and polymers have attracted interest, but also, sulfonium ions as cationic representatives and sulfonates/sulfonates as anionic



Scheme 1 Schematical representation of the modification possibilities of the sulfur.

^aLaboratory of Organic and Macromolecular Chemistry (IOMC), Friedrich Schiller University Jena, Humboldtstraße 10, 07743 Jena, Germany.

E-mail: johannes.brendel@uni-jena.de

^bJena Center for Soft Matter (JCSM), Friedrich Schiller University Jena, Philosophenweg 7, 07743 Jena, Germany

representatives can be used for various interactions with other substances due to their charges.^{19–22} In summary, the sulfur-containing monomers are not limited to the typical sulfides, but there is a great variability of potentially new physical properties due to the simple modifications.

Considering the high reactivity of sulfur-based compounds, it is no surprise that the majority of polymers are created by the reaction on the sulfur moiety, e.g. the radical thiol–ene linking or classic Michael additions of thiols to electron-deficient vinyl units.^{16,23–25} The polymerizations in these cases usually follow a step-growth process. Polymers comprising sulfide groups in the main chain can further be derived by ring opening polymerizations of episulfides or thiranes – the sulfur equivalents of epoxides – which are chain-growth processes and can be considered living polymerizations under appropriate conditions.^{26–30} Of course, also a large variety of vinyl based monomers containing sulfur moieties in the side chain have been reported. However, it has to be mentioned that commercialized and technically used monomers mostly rely on sulfonic acid derivatives, such as styrene sulfonic acid or 2-acrylamido-2-methylpropane sulfonic acid (AMPS). Other sulfur-based moieties such as thioethers or disulfides, which might still be tolerated during polymerizations of vinyl monomers, remain a niche among the large variety of commercial vinyl monomers, but their selective reactivities certainly attract increasing attention in academic research over the last decades. Examples are cleavable crosslinkers based on disulfide groups, which react in a reductive environment, or oxidizable thioethers in the side chains. Excellent overviews on these structures are provided in several comprehensive reviews.^{16,31–34}

Interestingly, a direct covalent attachment of sulfur, in its various states, to a carbon double bond creates a set of interesting vinyl monomers, which feature some unique characteristics. For example, the conjugation with a sulfide group enables a good stabilization of a radical at the neighboring carbon atom, which renders vinyl sulfides much more reactive

in radical polymerization compared to the corresponding vinyl ethers.^{35,36} On the other side, sulfoxides and particularly sulfones induce a strong electron withdrawing effect on the vinyl group favoring anionic polymerizations. Research into the polymerization of *S*-vinyl substances began as early as 1950, and fundamental reactivities were examined in the following years. Unfortunately, scientific interest in these substances waned from 1990 onwards, since their synthesis was fraught with difficulties and that efforts to achieve high molar masses in polymers were often futile due to various side reactions. Nevertheless, *S*-vinyl monomers returned to the focus of research around 2010, partly because of the increasing interest in controlled polymerization techniques, where particularly the reversible addition fragmentation chain-transfer (RAFT) process raised again the interest in sulfur-based compounds for radical polymerization. In this rediscovery of *S*-vinyl monomers, several unique features of the materials became known that certainly aroused scientific, but also industrial interest and showed that the effort spent on researching such systems is well justified.

In this review, we summarized the fundamental knowledge gained during the early era of research on these monomers, which is primarily about the polymerization behavior of these materials and provide an overview on the more recent progress in terms of their characteristics, properties, and potential applications. Fig. 1 depicts the various different classes of *S*-vinyl monomers that are covered in this review. They were distinguished according to the different characteristics of the double bond which depends most of all on the oxidation state of the sulfur. First, monomers comprising bivalent sulfur were described including *S*-vinyl sulfides, -thioacetates, -thioacetals, -thiocarbamates and -thiosilanes. In contrast, derivatives of higher oxidation state, such as found in sulfoxides, sulfones, or sulfonates reduce the electron density at the double bond which leads to quite different polymerization behavior. In the following, we organized this overview according to these



Nicole Ziegenbalg

Nicole Ziegenbalg was born in Leisnig (Germany). After graduating from school, she moved to Jena (Germany) to study chemistry. She successfully completed her B.Sc. degree in 2017. Then she continued her studies within the M.Sc. programme in Jena. In 2018/2019, she spent a semester abroad in Eindhoven (Netherlands) and then returned to Jena for her master thesis and subsequent PhD. In her current research area, she is working on

the polymerization of new sulfur-containing monomers and the investigation of the obtained properties in cooperation with the BASF SE.

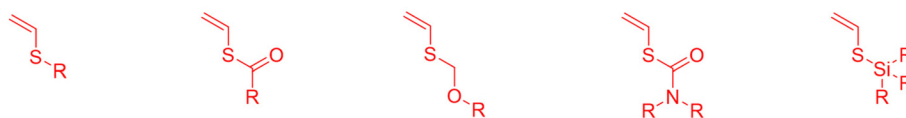


Lada Elbinger

Lada Elbinger obtained her M. Sc. at the Friedrich Schiller University Jena in 2019 within the master programme Chemistry–Energy–Environment. Since 2019, she has been a Ph.D. student in the group of Prof. Dr U. S. Schubert, where she is investigating hydrogel electrolytes and novel active materials for hybrid- and polymer-based organic thin-film batteries.

Electron rich S-vinyl groups

S-vinyl sulfides S-vinyl thioacetates S-vinyl thioacetates S-vinyl thiocarbamates S-vinyl thiosilanes



Electron poor S-vinyl groups

S-vinyl sulfoxides S-vinyl sulfones S-vinyl sulfonic acids S-vinyl sulfonates S-vinyl sulfonamids S-vinyl sulfonylhalides

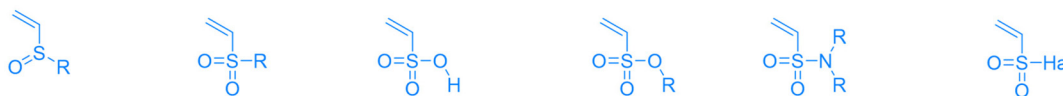


Fig. 1 Schematic representation of the monomer classes discussed in this review.

different classes, starting with electron-rich S-vinyl groups and subdivided the sections for each monomer class according to the different reported polymerization techniques.

2. Electron rich S-vinyl groups

2.1. Vinyl sulfides

Radical polymerization. The free-radical polymerizations of vinyl sulfide derivatives lead to polymers with very high molar masses and also prove to be faster compared to their oxygen analogues, provided that the suitable initiators are used, for example azo initiators such as azobisisobutyronitrile (AIBN).^{31,35–43} Peroxides, on the other hand, appear not to be suitable for polymerization, since the oxidation of the sulfide to the corresponding sulfoxide or sulfone is preferred.⁴⁴

The increased reactivity of vinyl sulfides compared to vinyl ethers was demonstrated early on and already explained by Price and coworkers in 1950,³⁶ who observed a bathochromic shift when unsaturated sulfide molecules were excited with light compared to saturated ones. This effect can be explained by the 2p–3p conjugation of sulfur and the adjacent carbon atom. However, this conjugation is much weaker in the ground state than the 2p–2p conjugation of oxygen to the adjacent carbon in vinyl ethers, so a reaction with radicals is favored and the new electron-distributing conjugation in the transition state leads to the stabilization of the radicals by the participation of the 3d orbitals of sulfur, what could also be confirmed later by Shorygin *et al.*⁴⁵

In the early years, reactivity was studied only in copolymerizations and homopolymerizations played only a supporting role. The reactivity of the monomers can be calculated from



Ulrich S. Schubert

Ulrich S. Schubert was born in Tübingen (Germany) in 1969. He studied chemistry in Frankfurt and Bayreuth (both Germany) and at Virginia Commonwealth University, Richmond (USA). His PhD studies were performed at the Universities of Bayreuth and South Florida. After post-doctoral training with J.-M. Lehn at the University of Strasbourg (France), he moved to the TU Munich (Germany) and obtained his Habilitation in 1999. During

1999 to 2000 he was Professor at the University of Munich and during 2000–2007 Full-Professor at the TU Eindhoven (the Netherlands). Since 2007, he has been Full-Professor at the Friedrich Schiller University Jena, Germany.



Johannes C. Brendel

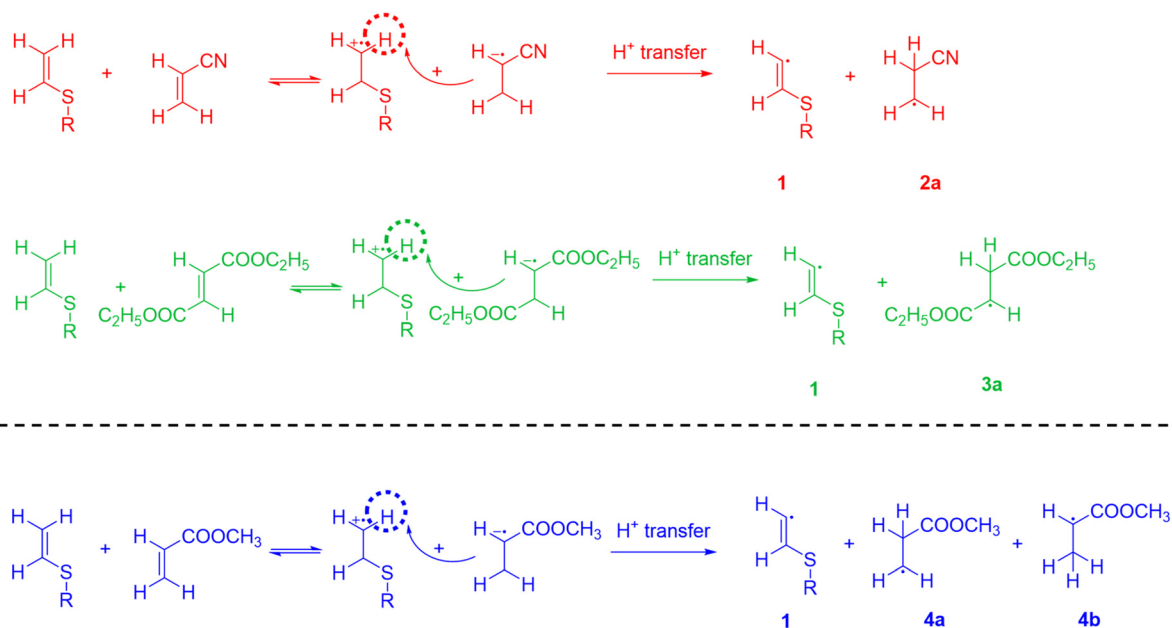
Johannes C. Brendel studied chemistry at the University of Bayreuth (Germany) and received his PhD in 2013 on his studies of semiconducting polymers. From 2014 to 2016 he worked at the University of Warwick (UK) and the Monash Institute of Pharmaceutical Sciences (Australia) as a postdoctoral researcher funded by the German Research Foundation (DFG). In 2016, he established an independent research group at the Friedrich Schiller University Jena (Germany) which became funded within the Emmy Noether Programme in 2017. His research interests include the design of reactive monomers, the synthesis of well-defined polymer architectures, and their self-assembly into complex nanostructures.

the ratio of the different monomers in the polymer compared to the original composition of the monomer mixture. Either the Mayo–Lewis equation,⁴⁶ the Fineman–Ross equation⁴⁷ or the Kelen–Tüdös equation⁴⁸ can be used for this purpose. Using the reactivity values obtained, it is subsequently possible to calculate Q - and e values, which are classified into the Q - e scheme. The Q - and e -scheme is a useful tool for predicting reactivities based on the structures of the monomers and facilitates a simple comparison of the monomers with each other. So far, these values can only be practically determined for copolymerizations, preferably with styrene, and calculated using the Alfrey Price equation.⁴⁹ The Q -values provide information on the stabilization of the resulting radical, and are in the range of 0.3 to 0.5, depending on the substituent for vinyl sulfide monomers,^{50,51} which are significantly higher than comparable vinyl ethers ($Q = 0.015$)⁵² and, thus, indicates good stabilization. The first monomers studied were methyl vinyl sulfide ($Q = 0.34$)³⁶ and phenyl vinyl sulfide with 0.35³⁵ from Price and coworker, which could later also be confirmed by others.^{50,53} Later divinyl sulfide showed a significantly higher Q -value of 0.6 due to the increased resonance stabilization.⁵⁴ However, the crosslinking was not as strong as expected, clearly showing that the reactivity of the double bond in the polymer decreases significantly with respect to the monomer. Another crucial factor that seems to influence the Q -value is coplanarity. If this cannot be maintained in a molecule, it also leads to a decrease in resonance stabilization.³⁹ For example, due to the chloride atoms in *ortho*-position, the coplanarity of pentachloro phenyl vinyl sulfide is cancelled, demonstrating the lower stabilization by the determined Q -value of 0.23.⁵⁵ The other value that can be determined using the Alfrey–Price equation is the e -value, which provides information about the

polarity of the monomers. It was expected that values similar to those obtained for vinyl ethers could be obtained for vinyl sulfides, due to the electron-donating sulfide group and the resulting increased electron density at the double bond.⁵⁴ And indeed negative e -values of about -1.5 were obtained, which are comparable to the values of vinyl ether. However, the substituents also have a strong influence on the value. For example, when electron-accepting substituents are present on the sulfur, the e -values are larger.^{37,56}

However, this monomer class has been shown to copolymerize well not only with styrene^{35,50,51,54–56} but also with a variety of monomer classes such as acrylates,^{35,50,55,57} methacrylates,^{50,54,56} acrylonitriles,⁵⁰ vinylene carbonates,⁵⁸ vinyl ethers,⁵⁹ maleimides,⁶⁰ and diallyl compounds,⁶¹ which is in good agreement with the calculated copolymerization parameters.³¹ The reactivity of the radicals of the various comonomers decreases in relation to the vinyl sulfides in the following order: acrylonitrile > methyl acrylate > methyl methacrylate > styrene.^{49,50,53}

In addition, the directed synthesis of alternating polymers can also be realized due to the electron accepting properties of the monomer.^{50,58,62} Spectroscopic studies have shown, for example, that ethyl vinyl sulfide and phenyl vinyl sulfide with maleic anhydride lead to the formation of charge transfer complexes, which can then initiate copolymerization even without an additional initiator.^{62,63} Another example of such copolymerizations include isobutyl vinyl sulfide with acrylonitrile⁵⁰ Spin trapping was used to investigate the initiation mechanism of these copolymerizations.⁶⁴ It was found that for example for the copolymerization with acrylonitrile and also with diethyl fumarate two types of radicals can be present, namely the vinyl radical (1) and the substituted alkyl radical



Scheme 2 Schematic representation of the initiation mechanism of alternating copolymerization with acrylonitrile (red)/diethyl fumarate (green) and methacrylate (blue) determined by spin trapping technique.⁶⁴

(2a or 3a) (Scheme 2). Both radicals are generated by an intramolecular proton transfer from the β -carbon of the cation radical of the vinyl sulfide species stereospecifically to the α -carbon of the anion radical of the electron accepting monomer in the charge transfer complex. However, during copolymerization with methacrylate, a total of three types of radicals were detected: the vinyl radical (**1**), but also two alkyl radicals (**4a and b**), which show proton migration from the β -carbon of the cation radical of the vinyl sulfide species to the α - or β -carbon of the methacrylate anion radical.

With the development of new controlled polymerization techniques, the possibility of synthesizing narrowly distributed polyvinyl sulfides has also been investigated starting in 2013. Reversible-addition-fragmentation chain-transfer polymerization (RAFT)^{65–70} has been shown to be suitable for generating a variety of homopolymers and copolymers from vinyl sulfide monomers. However, the different types of chain transfer agents (CTAs) have a tremendous effect on the polymerization behavior of vinyl sulfide monomers, as shown by Abiko *et al.* 2015, by performing the copolymerization of phenyl vinyl sulfide and electron-accepting monomers with three different kind of CTAs: xanthate-type, dithiocarbamate-type and trithiocarbonate-type.⁶⁶ In principle, xanthate-CTAs are suitable for the controlled polymerization of non-conjugated *O*-vinyl and *N*-vinyl monomers,⁷¹ whereas dithiocarbamates are mostly used for conjugated monomers or less active monomers, and trithiocarbonates are also used for conjugated monomers. The results of these studies revealed that trithiocarbonate CTAs are most suitable for copolymerizations, as the obtained polymers feature narrow distributions (1.3 to 1.4) compared to the polymers prepared with other CTAs (1.8 to 2.6).

Nevertheless, also narrow distributions with phenyl vinyl sulfide derivatives such as bromophenyl vinyl sulfide (BPVS) and a xanthate-like CTA could be obtained, and based on this example, block copolymers with *N*-isopropylacrylamide (NIPAAm) could be prepared, showing that reinitiation is possible after the formation of the first block and that the RAFT end groups are preserved (Fig. 2).⁶⁵ Micelles were formed when the polymer was dispersed in water, where the hydrophilic NIPAAm forms the stabilizing corona and hydrophobic bromophenyl vinyl sulfide the core. Transition metal-catalyzed reactions not only crosslinked the micelles but also introduced chromophores with different optical properties. In addition, the NIPAAm block caused LCST behavior.

Cationic polymerization. The very first cationic polymerization of vinyl sulfide monomers was described by Reppe in 1956,⁴⁴ who described the formation of polymers using the catalysts sulfur dioxide, boron trifluoride, and zinc chloride (Scheme 3). Already in these early reports, however, a diminished reactivity became apparent when compared to their oxygen analogs.

The cationic polymerization of vinyl sulfides remains a challenge, which was clearly demonstrated in more detailed studies by Shostakovskii *et al.*⁷² using the catalysts SnCl₄ and FeCl₃. Alkyl vinyl sulfides yield only oligomers and require longer reaction times and elevated temperatures even with highly reactive catalysts, while ethers tend to have “explosive” reactions even with traces of the catalysts. Not only the reactivity of the vinyl group is lower than for comparable vinyl ethers due to the lower nucleophilicity, but also the basicity of the sulfur has an influence of the cationic polymerization behavior of these monomers. In the case of *tert*-butyl vinyl sulfides, on

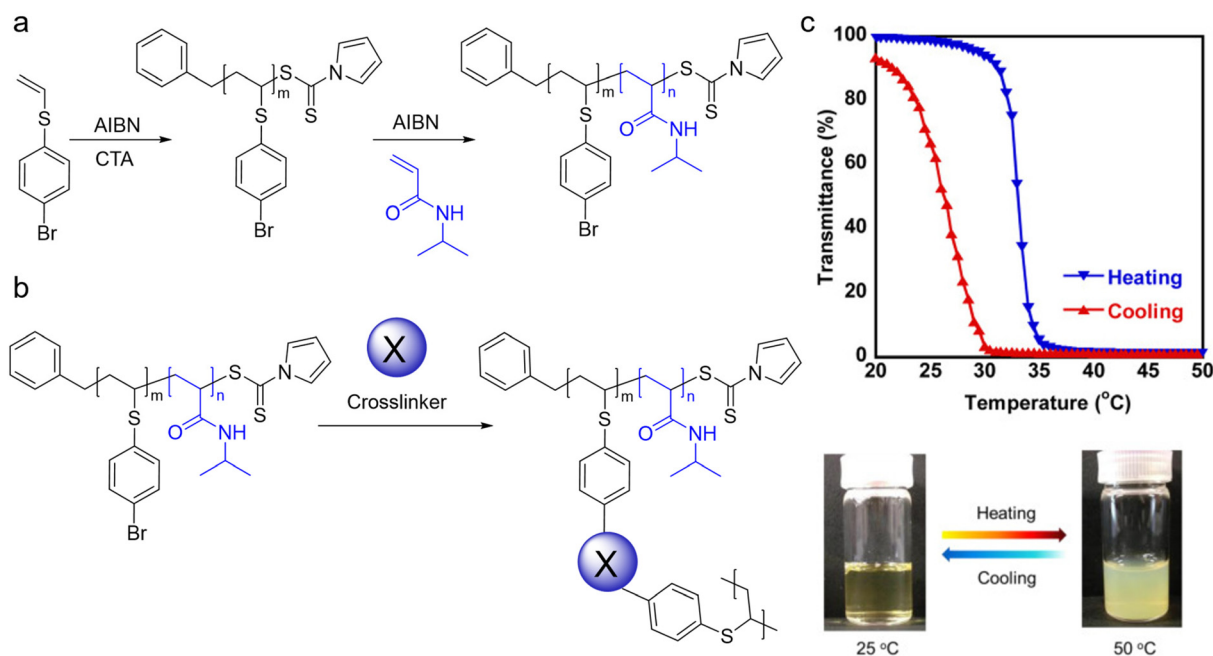
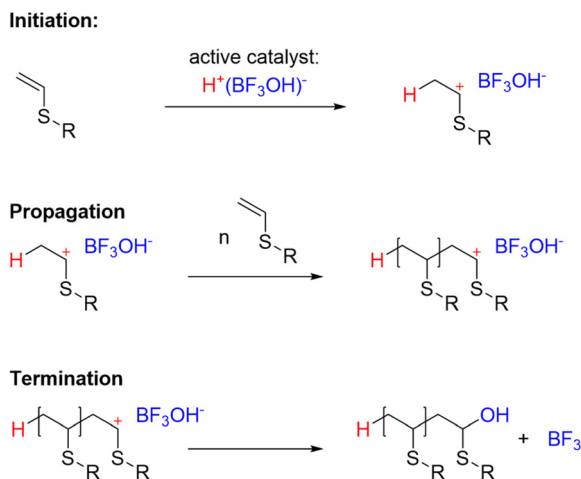


Fig. 2 (a) Schematic representation of the synthesis of the block-copolymer PBPVS-*b*-PNIPAAm, (b) schematic representation of the crosslinking of the bromophenyl moiety (c) LCST behavior of core cross-linked nanoparticle. Figure was adapted from ref. 65 with permission of Elsevier (Copyright 2014).

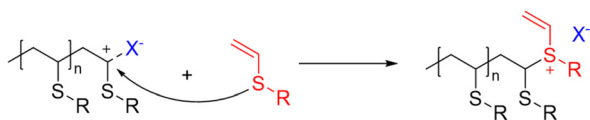


Scheme 3 Schematic representation of the mechanism of the cationic polymerization of vinyl sulfide monomers.

the one hand, only oligomers are formed, which can also be explained by the fact that an unstable sulfur-catalyst complex is formed, which cannot completely inhibit the polymerization, but impedes the process. On the other hand, phenyl vinyl sulfides exhibit higher reactivity in ionic polymerization, which is due to the fact that the free electrons of sulfur are located near the conjugated π -system of the phenyl ring which results in better resonance stabilization.⁷²

Any copolymerizations are similarly affected by the above-mentioned limitations found for homopolymerizations. Thus, significant amounts of polymer are only formed during the polymerization of phenyl vinyl sulfide with styrene in the presence of SnCl_4 and with butyl vinyl ether in the presence of both SnCl_4 and FeCl_3 . Copolymerization of the aliphatic compound ethyl vinyl sulfide with styrene or butyl vinyl ether did yield no polymer at all or only exceptionally low amounts, respectively. Further studies of copolymerizations by Inou *et al.*⁷³ suggested that vinyl sulfides may quench cationic vinyl polymerizations due to a reaction of the carbocation of the propagating chain with the sulfur resulting in the formation of a stable sulfonium ion. This mechanism was also postulated by Ringsdorf *et al.*⁷⁴ for vinyl thioacetals (Scheme 4).

In summary, for vinyl sulfides, cationic polymerization is much more challenging than their radical polymerization. This limited success and the high tendency for side reactions also explain the decay in research efforts on the cationic polymerization of vinyl sulfides after 1980.



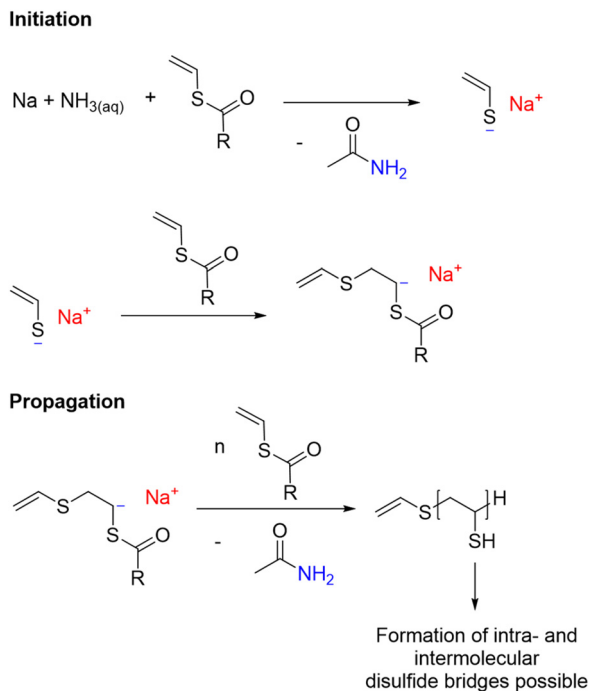
Scheme 4 Schematic representation of possible retarding and chain-transfer mechanism of vinyl sulfides in cationic polymerization.⁷³

2.2. Vinyl thioacetates

Polythiols are frequently used as redox resins or electron exchangers because they can easily react in the presence of strong oxidizing agents to form disulfide bridges or sulfonic acids.^{32,75} In addition, they are also used as protective agents to prevent radiation damage and as model substances to elucidate thiol function in enzymes, which is why this class of substances has aroused quite some interest.^{31,32} However, polymerization of monomers comprising thiol units is almost impossible because in most polymerizations they either act as inhibitors or as chain transfer agents. As a consequence, masking of the thiol groups is generally required. Similar to the preparation of polyvinyl alcohol (PVA), a possibility is the polymerization of thioacetates, which after hydrolysis leads to the equivalent polyvinyl thiol.^{32,76–78}

The polymerization rate is lower for radical homopolymerizations than for vinyl acetates.⁷⁹ However the stabilization of the radicals is greater for copolymerizations due to the inclusion of the 3d-orbitals of sulfur.^{31,80} In 1969, Kinoshita *et al.* were able to determine the Q - and e -values ($Q = 0.25$, $e = -0.8$) from copolymerization with styrene, demonstrating the good stabilization of the radicals but also the strong electron-withdrawing effect of the thioacetate group. On this basis, radical copolymerizations of vinyl thioacetate with various comonomers such as styrene, vinyl acetate, methacrylate⁷⁹ methyl methacrylates⁸¹ N -vinyl succinimide, N -vinyl phthalimide, N -vinyl carbazole⁸² and vinylene carbonate⁸³ have been successfully carried out. In the case of N -vinyl succinimide and N -vinyl phthalimide, a preferential incorporation of vinyl thioacetate was observed, while vinyl carbazole showed rather an alternating incorporation. In addition, an increased incorporation of vinyl thioacetates compared to the monomer vinylene carbonate was also observed. However, it could not be excluded that steric effects also influence the reaction during copolymerization and probably also favor the incorporation of the sterically less demanding vinyl thioacetate. Furthermore, the authors postulated a possible application of the hydrolyzed copolymers as short-lived prophylactics for ionized radiation.

Anionic polymerization. In 1966, Leonard *et al.* reported the anionic polymerization of vinyl thioacetates with sodium in liquid ammonia.⁸⁴ Similar to some tested acrylates with larger side chains, only a small part of the polymerization is directly initiated by the attack of the sodium amide on the double bond. The authors assume in accordance with other studies that in case of the hindered acrylates alkoxides instead initiate the polymerization, which are formed after hydrolysis of the ester.^{85,86} For the vinyl thioacetates, they correspondingly consider that the amide first causes an aminolysis of the monomer to release a vinyl thiolate and acetamide, which could also be detected. The corresponding thiolate then initiates the actual polymerization, which is why end groups of vinyl thioacetates polymers are different compared to other monomers polymerized in these conditions (Scheme 5).⁸⁷ Chain growth is further considered to proceed *via* a common anionic polymerization mechanism, however infrared spectra

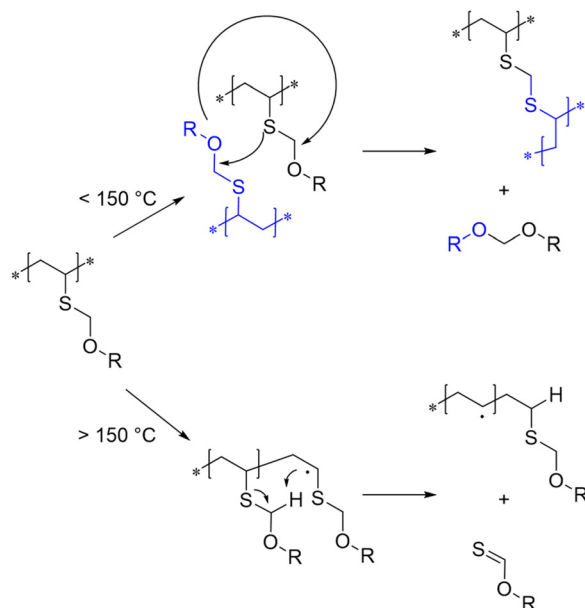


Scheme 5 Schematic representation of the mechanism of the anionic polymerization of vinyl thioacetate monomers.⁸⁴

revealed that none of the acetate groups remain intact and a polythiol is formed instead. The resulting thiol groups appear to be formed during this type of polymerization. The resulting thiols might further get oxidized under the given basic conditions and cause the formation of inter- and intramolecular disulfide bridges. However, to our knowledge, this study is the only example for an anionic polymerization of vinyl thioacetates that has been published.

2.3. Other electron rich S-vinyl groups

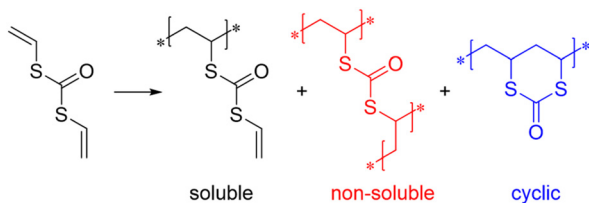
Besides the above-mentioned sulfides and thioacetals, there are a variety of other compounds that comprise a S-vinyl group. Among them vinyl thioacetals are closely related to vinyl sulfides and feature comparable properties, but the acetal unit also induces further reactivities. Vinyl thioacetals have been reported to polymerize with azo-initiators such as AIBN, similar to vinyl sulfides.^{74,88} Polymerization with peroxides can only be carried out in very low yields due to the competitive reaction of peroxide with sulfur. In accordance, the influence of substituents on the polymerization behavior of vinyl thioacetals can be attributed to inductive and steric effects. However, chain transfer may also occur here due to the -S-CH₂-O-group.⁷⁴ Furthermore, it has been observed that these polymers tend to crosslink during storage, which can be accelerated by an increase in temperature.^{41,74} The corresponding reaction mechanism was first described by Hwa⁴¹ in 1958 and refined and confirmed by Gollmer *et al.*⁸⁸ in 1968 (Scheme 6). Up to 150 °C, transacetalization of the polymers occurs almost exclusively, whereas above 150 °C, thioesters and hydrocarbon moieties are formed *via* radicals. Moreover,



Scheme 6 Schematic representation of the crosslinking reaction and further decomposition process observed for poly(vinyl thioacetals).⁸⁸

due to the polarization of the double bond of the vinyl thioacetals, a high polymerization tendency towards cationic initiators was also expected. And indeed, the monomers could be polymerized with BF₃ however, the obtained polymers differed significantly from those prepared by radical polymerization, since various side reactions, such as the cleavage of the S-CH₂-OR group, led to the crosslinking of the polymer.⁷⁴ Overall, research on this class of materials remains limited to the presented reports (1958–1968) and no recent studies have been presented.

Another class of monomers are vinyl thiocarbonates and vinyl thiocarbamates, which are more closely related to vinyl thioacetates and have still to be considered electron rich. Similar to the thioacetates, they can be polymerized with radical azo-initiators, but in addition also peroxides result in the formation of polymers.^{76,89–93} The resulting polymers can be converted into poly thiols as in the case of thioacetates, although this occurs more slowly. For example, free radical polymerization of S-vinyl-O-*t*-butyl thiocarbonate leads to the corresponding polythiocarbonate. This was subsequently converted to the poly thiol with hydrogen bromide or by heating.⁹⁴ A subsequent study of the kinetics of oxidation of poly(vinyl thiol) and low molar masses analogs with molecular oxygen in various aprotic solvents in the presence of iron(II) sulfate⁹⁵ revealed that the reaction rate of polythiols is much faster in comparison, as thiol groups in the vicinity appear to have an influence on it. In most cases, the oxidation of poly thiols leads to the formation of disulfide bridges and thus to the formation of a crosslinked, water-insoluble polymer, which is why these substances are also used as crosslinking agents. Another possibility for the preparation of poly thiols is, for example, the polymerization of S,S'-divinyl thiocarbonate which can also



Scheme 7 Schematic representation of the polymerization of divinyl thiocarbonate.⁹⁶

be converted by subsequent alkane hydrolysis (Scheme 7).^{96,97} However, the properties of the polymers depend very much on the polymerization conditions and the conversion of polymerization. If conversion of more than 20% were recorded, only insoluble polymers could be registered. But if the polymerization was interrupted at low conversion rates, soluble polymers could also be detected. Cyclopolymerization plays a minor role, as demonstrated by IR spectroscopy. The soluble part consists of polymers with *S*-vinyl dithiocarbonate side chains, while the insoluble part consists of crosslinked polymers. The study of thermal properties shows that both kinds of polymers have a decomposition temperature ranging from 260 to 280 °C. However, for the linear polymers, re-solidification was observed at 150 to 180 °C, which led the authors to postulate thermal polymerization of the vinyl side chains.

In studies of various thiocarbamate monomers, *S*-vinyl *N*-diethyl thiocarbamate was found to be more reactive than *S*-ethyl *N*-vinyl thiocarbamate, as expected, which can be explained by the conjugation of sulfur to the adjacent carbon atom and is evidenced by the higher *Q*-value ($Q = 0.33$) compared to the *N*-vinyl monomer ($Q = 0.18$) (Fig. 3).⁹¹ For this purpose, copolymerizations were carried out with styrene and vinyl acetate. Additionally, the *e*-value -1.49 for *S*-vinyl *N*-diethyl thiocarbamate was determined which are comparable to the *N*-vinyl monomer, but also to other *S*-vinyl monomers.

Also vinyl thiosilanes were found to be readily homopolymerized with AIBN.⁹⁸ The UV spectra of different alkyl thiosilanes suggest interaction of the sulfur with the silicon atom, since a shift of the absorption bands to lower wavelengths was

observed for example for $(\text{Me}_3\text{Si})_2\text{S}$ and poly(methyl thiosilanes).⁹⁹ Accordingly, this interaction should also take place with the vinyl thiosilanes and the influence of this interaction on the polymerization behavior was investigated.⁹⁸ The *Q*-value of 0.25 and *e*-value of -1.60 are slightly smaller but still in the range of alkyl and aryl sulfides suggesting a similar stabilization of the growing radical chain ends. Despite a potential interaction of sulfur and silicon in the 3d orbitals, these results indicate that they have only a limited effect on the reactivity of the adjacent vinyl group and, thus, the monomer overall. The silane group can conveniently be removed by acidic hydrolysis to yield polyvinyl thiol (Scheme 8). Similar to the reports on polyvinyl thiols from thioacetates, the polymer can initially be dissolved, for example in chloroform, but then became increasingly insoluble as time progressed. The authors relate this to a partial oxidation of the thiol groups in air resulting in disulfide bridges and thus a crosslinking of the polymer. In addition, cationic polymerization was also studied, but only oligomers are formed.⁹⁸

In addition, it is possible to increase the reactivity or stability of the resulting radicals by using molecules with better conjugation. This has already been shown, for example, with divinyl sulfide, which has a higher *Q*-value than methyl vinyl sulfide. However, better conjugation can also be achieved, for example, by using different heteroaromatic compounds, such as vinyl mercapto benzothiazole (VMBT, $Q = 0.75$), vinyl mercapto 4-methylthiazole (VMMT, $Q = 0.61$), vinyl mercapto benzoxazole (VMBO, $Q = 0.61$), and vinyl mercapto benzimidazole (VMBI, $Q = 0.37$) (Fig. 4).^{6,100–103} The first three can be polymerized with both AIBN or UV-light without any initiator, while the last can only be initiated by azo-initiators. Furthermore, the properties of the homopolymers were investigated. The TGA curves reveal that both VMBT (200 °C) and VMMT (170 °C) decompose at much lower temperatures than, for example, polyvinyl sulfide (280 °C). In addition, the photodegradation of the homopolymers at 30 °C with a mercury lamp was studied, and it was found that the viscosity of all homopolymers decreased significantly as a function of irradiation time, because of the degradation of the polymers. Based on these results, it is quite conceivable that these photodegradable polymers could be used for applications in biomedical engineering, biopatterning technology, photolabeling of biologics, and drug delivery.¹⁰⁴

Various copolymerizations with VMBT were carried out and the reactivity of VMBT in presence of various polymer radicals was found to descend according to the order: vinyl acetates > phenyl vinyl sulfides > acrylonitrile > methyl methacrylate >

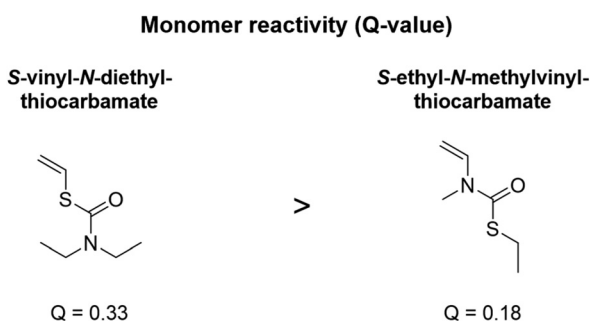
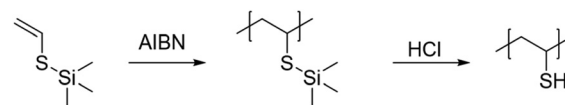


Fig. 3 Schematic representation of the comparison of the *Q*-values of *S*- and *N*-vinyl thiocarbamates.⁹¹



Scheme 8 Schematic representation of the polymerization and subsequent hydrolysis of vinyl thiosilanes.⁹⁸

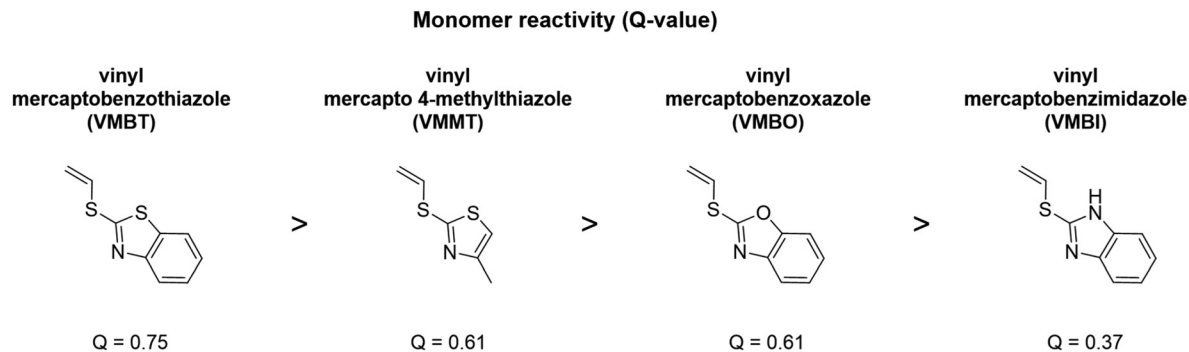


Fig. 4 Schematic representation of the comparison of the Q-values of different cyclic S-vinyl derivatives.^{100–103}

styrene. Again, acrylonitrile tends to copolymerize in an alternating pattern, which is related to the electron-accepting properties. Therefore, the authors also investigated copolymerizations with the sterically hindered and electron-deficient monomer maleic anhydride in more detail. However, these polymerizations were found to be much slower, and as the amount of VMBT in the monomer mixture increased, a higher amount of VMBT was also found in the polymer. Thus, these results differ somewhat from those obtained with alkyl vinyl sulfides. Such a difference seems to be due to an additional interaction between maleic anhydride and the thiazole ring.

3. Electron deficient S-vinyl groups

3.1. Vinyl sulfoxide monomers

Considering the different possible stages of oxidation of sulfur compounds, sulfoxide moieties have gained considerable attention in various aspects of chemistry including the prominent polar solvent dimethyl sulfoxide (DMSO). The sulfoxide moiety is among the most polar, non-ionic groups, which makes corresponding materials usually well-soluble in water or other polar solvents. Indeed, the sulfoxide moiety features characteristics of both a dative bond and a polarized double bond, which is partially reflected in its reactivity.¹⁰⁵ Therefore, it is no surprise that polysulfoxides have also raised some interest in research considering their highly polar character. Among other applications, they are used as catalysts in two- or three-phase systems,¹⁰⁶ but also exhibit antifouling behavior^{107,108} and are conceivable for medical applications due to their low cytotoxicity, good biocompatibility and skin penetration properties.^{109,110}

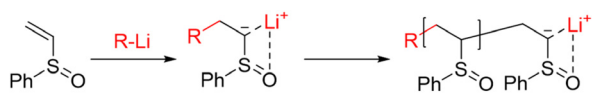
Radical polymerization. Despite several examples for polymers comprising sulfoxide moieties, synthesis and applications of polymers in which the sulfoxide group is directly bonded to the backbone have been sporadic. One of the reasons may be that a direct radical homopolymerization is restricted because the sulfoxide group acts as an inhibitor. Imai *et al.* studied the homopolymerization of various alkyl vinyl sulfoxides, and only the polymerization of methyl vinyl sulfoxide resulted in polymers of low molar mass and only in low

yields.^{111,112} Ethyl- and butyl vinyl sulfoxides did not polymerize at all under these conditions, which can be explained by a degradative chain transfer process to the sulfoxide unit.¹¹² In the direct copolymerization of methyl vinyl sulfoxide with styrene or MMA yields remained also low and the polymers featured only a low content of sulfoxide groups.¹¹³ However, these experiments allowed at least the determination of *Q*- and *e*-values ($Q = 0.10$, $e = 0.9$). The resonance stabilization of the corresponding radical is much lower compared to methyl vinyl sulfide ($Q = 0.34$),³⁶ indicating that there is little or no conjugation between the sulfoxide moiety and the adjacent carbon atom. In addition, copolymerizations with vinyl acetate were also investigated, showing good polymerization behavior and also in this copolymerization the copolymerization parameters could be determined ($Q = 0.2$ and $e = 1.0$).¹¹¹ Interestingly, an increased activity of these monomers is observed in the copolymerizations with methacrylic acid, acrylamide, acrylonitrile, and vinyl oxime, which can be explained by the ability of sulfoxide moiety to form complexes with carboxylamides and other functional groups, which was confirmed by spectroscopic methods.¹¹⁴ Inoue *et al.* also studied the copolymerization of ethyl vinyl sulfoxide and were able to determine the copolymer parameters $Q = 0.13$ and $e = 0.61$.¹¹² They also found that non-conjugated monomers showed no copolymerization behavior with ethyl vinyl sulfoxide, while polymerization with conjugated comonomers yielded in polymers with a low content of ethyl vinyl sulfoxide. Due to the strong acidity of oxygen in the sulfoxide group, complexes with Lewis acids or hydrogen bonds with proton donors as additives can form very easily, which alters the polymerization behavior and was therefore investigated again in more detail during copolymerization with styrene. It was ensured that no cationic polymerization process takes place. The addition of zinc chloride to benzene increases the incorporation of ethyl vinyl sulfoxide into the polymer. The copolymerization parameters were also determined to be minimally larger (0.15 and 0.72) compared to the previous conditions. Acetic acid as a proton donor also slightly increased the reactivity of ethyl vinyl sulfoxide. It was also shown that the solvent has an influence on the polymerization and that, in particular, the use of phenols and alcohols leads to a higher content of ethyl vinyl sulfoxide in the

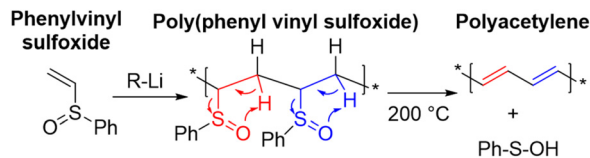
polymer. In addition, the *p*-tolyl vinyl sulfoxide was copolymerized with styrene 1970, even though the incorporation of styrene into the copolymer is preferred here.¹¹⁵ However, again radical homopolymerization was not possible.

Anionic polymerization. But the strongly electron-withdrawing character of the sulfoxide group causes a high acidity of the neighboring methyl groups, which could actually make such monomers suitable for anionic polymerization and indeed polymers could be obtained by anionic polymerization from *p*-tolyl vinyl sulfoxide.^{116,117} The anionic living polymerization of phenyl vinyl sulfoxides was 20 years later studied in detail by Hogen-Esch *et al.*^{118–120} In one of these studies they investigated in detail the polymerization behavior of different enantiomeric pure phenyl vinyl sulfoxide as well as the racemic mixture and tested their influence on the tacticity of the obtained polymers.¹¹⁸ Indeed, stereoregular polymers were found when the enantiomeric pure monomers were used, due to a stereospecific and stereoselective addition of monomer molecules to the specific end groups. If the racemic mixture was used, mostly atactic polymers were obtained. Further polymerizations of racemic phenyl vinyl sulfoxide with various anionic initiators such as (triphenylmethyl)lithium, (triphenylmethyl)potassium and (diphenylhexyl)lithium were also carried out and can lead to the formation of polymers with moderate dispersities in the range of 1.2–1.4.¹²⁰ During the reaction an α -sulfinyl carbanion is formed, which forms a chelated ion-pair structure with the lithium counterion (Scheme 9). Furthermore, such a chelation is also conceivable for potassium as a counterion, although the interaction is weaker.

Temperature was further found to have an enormous influence on polymerization. For example, polymers with a broad or bimodal molar mass distribution were formed at 25 °C, while the monomodal and more narrow distributions mentioned above require low temperatures of –78 °C.¹²⁰ It was also found that more side reactions occurred at longer reaction times, indicating deactivation of the chain ends during the polymerization process. This aspect could also explain why only at short reaction times (30 min) polymers with low dispersities of 1.2 to 1.4 can be obtained, which are nevertheless higher compared to other anionic living polymerizations. Durst *et al.* already showed the two different reaction types of alkyl lithium and various sulfoxides. On the one hand, abstraction of the α -proton can occur, but on the other hand, splitting of the sulfur–carbon bond by an S_N2 displacement is also possible.¹²¹ The resulting polymer has another interesting property. A color change occurred after heating, which can be explained by the formation of polyacetylenes by sigma tropic thermal elimination *via* a cyclic five-membered transition state,^{122,123} which was first described by Kingsbury *et al.* as



Scheme 9 Schematic representation of the mechanism of the anionic living polymerization of phenyl vinyl sulfoxide.¹²⁰



Scheme 10 Schematic representation of the anionic polymerization of phenyl vinyl sulfoxide and subsequent formation of polyacetylene.¹²⁴

early as the 1960s (Scheme 10).¹²⁴ Interestingly, this observation could not be made when the polymer was previously oxidized to sulfone.

Due to the potential living nature of the polymerization, attempts to synthesize block-copolymers with styrene (A) and the vinyl sulfoxide monomer (B) were also carried out.¹²⁰ Both A–B diblock copolymers (styrene – vinyl sulfoxide) and A–B–A triblock copolymers (styrene – vinyl sulfoxide – styrene) were successfully synthesized, proving in principle the presence of the active chain ends even after polymerization with the sulfoxide species. However, in contrast to the homopolymerizations, butyllithium proved to be the best initiator for the preparation of the diblock copolymer and lithium naphthalide was used for the synthesis of the triblock copolymer under these conditions. In comparison, the obtained block copolymers displayed a narrower distribution than the corresponding homopolymers of the sulfoxide, which is, however, related to the fact that the first block polystyrene was well-defined. An increased concentration of the sulfoxide species led to a significant termination of the polymerization and thus to a broadening of the molar mass distribution. Nevertheless, the technique of anionic living polymerization of vinyl sulfoxides for the preparation of block copolymers was again applied several years later. Higashihara *et al.* used the resulting polymer to prepare block copolymers comprising a polyacetylene block by thermal decomposition of the sulfoxide moiety as described above (Fig. 5).¹²⁵ The resulting polymers form continuous nanofibril structures due to the strong tendency of the acetylene block to aggregate.

An alternative pathway to polyvinyl sulfoxides relies on the polymerization of vinyl sulfides monomers and subsequent postpolymerization oxidation.^{31,32,59,126} It has to be kept in mind that during this oxidation, properties of the polymers, such as solubility, thermal stability or glass transition temperature are significantly altered, which is related to the drastic change in polarity of the sulfur moiety.¹²⁷ As mentioned before, such polysulfoxides are very interesting for a variety of applications, and in 2008 Trofimov *et al.* demonstrated the use of an aliphatic polyvinyl sulfoxide copolymer prepared by oxidation of the corresponding polyvinyl sulfide as a matrix for absorbing alkali metals (Scheme 11).⁵⁹ In this case, diethylene glycol divinyl ether and methyl vinyl sulfide were radically polymerized with AIBN to obtain a crosslinked polymer, which was subsequently oxidized with hydrogen peroxide to form the sulfoxide groups. The structure of the polymer was designed to form a porous crown-like structure for complexation of alkali metal ions. The strong binding of the cation in the polymer

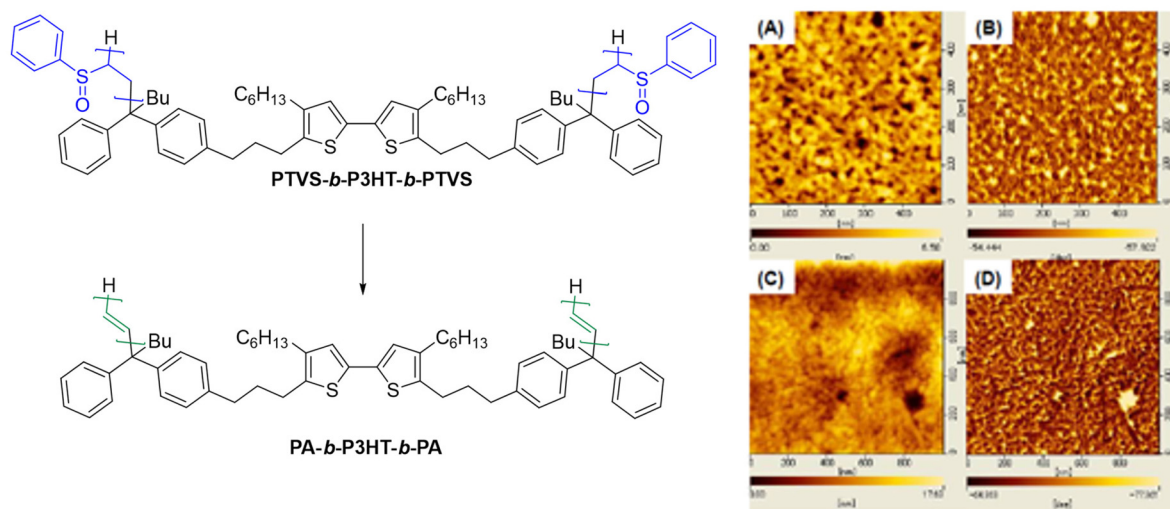
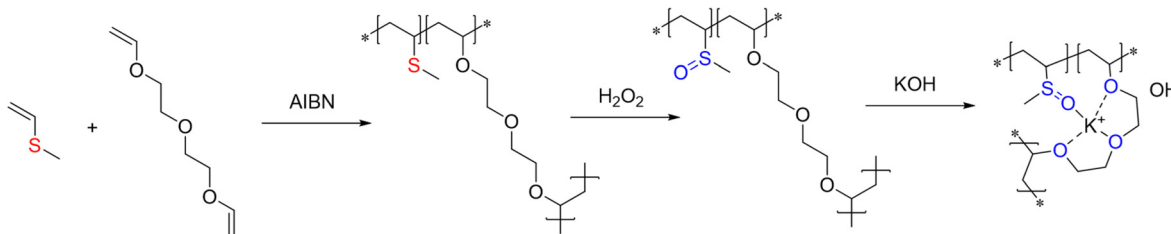


Fig. 5 Tapping-mode AFM images of (A) height image and (B) phase image of PTVS-*b*-P3HT-*b*-PTVS, (C) height image and (D) phase image of PA-*b*-P3HT-*b*-PA. Figure was adapted under the terms of the CC BY 3.0 license from ref. 125.



Scheme 11 Schematic representation of the radical copolymerization of diethylene glycol divinyl ether with methyl vinyl sulfide and the subsequent oxidation of the sulfide moiety to crown ether like matrix for complexation of alkali metal ions.⁵⁹

matrix further leads to an increased activity of the hydroxide ion, which is why the materials are also considered as superbases. The formation of polyacetylenes, as described above, could not be observed under the used conditions.

3.2. Vinyl sulfones

Besides the highly polar sulfoxides, of course, the next oxidation stage of related sulfur compounds *i.e.*, sulfones have attracted considerable attention in terms of forming functional polymers.^{2,5,7,128,129} Sulfone groups possess a high dipole moment (4.49 D),¹³⁰ which are significantly higher than sulfide groups (≈ 1.55 D) and slightly higher than sulfoxide groups (≈ 3.96 D).^{131,132} This makes their incorporation attractive for increasing adhesion, altering barrier and transport properties, or improving solvent resistance.^{133–135} However, it is known in the literature that the hydrophilicity is lower compared to the sulfoxide.^{136,137} Researchers have furthermore been interested in the atomic refraction of the sulfone moiety, which is still considerably higher than for other common groups, although not as high as the corresponding sulfides.^{3,138} However, their atomic dispersion is much lower than for sulfides, which renders sulfones particularly attractive to not only enhance refractive indices of corresponding

materials, but also increase their Abbe number. The latter is indirectly proportional to the materials optical dispersion, *i.e.*, it indicates how much the refractive index changes with different wavelengths of light. This aspect is crucial in designing optical elements with high clarity for the whole spectrum of light. In 2008, Ueda *et al.* demonstrated that their polyether sulfone is characterized by a high refractive index of 1.686, a high Abbe number of 48.6, a glass transition of 152 °C, and high optical transparency (>99%) in the visible light range of 400 to 800 nm, which appears to be well-suited for optical lenses or related applications.^{2,5,7,128} Sulfone moieties are mainly introduced by oxidation of sulfides, by Michael addition on corresponding vinyl sulfones,^{139,140} or by direct radical copolymerization of vinyl monomers with SO₂.^{141–143} The latter was mainly used to create thermally degradable materials due to the thermal instability of the resulting C–S bond. However, direct polymerizations of the vinyl moiety of vinyl sulfone derivatives remain scarcely reported, in particular if radical polymerizations are concerned. Anionic polymerizations are more frequently applied, but also these methods have not been pursued further in the last decades. We nevertheless summarized the related examples in the following, since there is in our opinion more potential for this class of

materials to find application not only in optics but also electronics and membrane technology due to their high polarity and good stability.

Radical polymerization. Price and coworker can be considered pioneers in the field of the direct radical polymerization of vinyl sulfone monomers, as they were the first to homopolymerize methyl vinyl sulfone and phenyl vinyl sulfone.^{35,36} They further investigated their copolymerization with styrene or vinyl acetate. The obtained Q values appeared to be lower ($Q \approx 0.1$) than for sulfides and more similar to vinyl acetate. The low absorption coefficient in the spectroscopic studies revealed that the sulfur–oxygen bond does not have a normal character of a double bond and Price describes it more as a semipolar bond. Related to this aspect, he further describes that conjugation along the C–S bond still occurs in these materials. However, in contrast to vinyl sulfides with an overlap of 2p and 3p orbitals, only 2p and d orbitals interact, which is why this conjugation is less pronounced and provides only a limited stabilization of the growing radical.³⁵ Although radical polymerization is in principle possible, these monomers tend to have a strong tendency for chain transfer reactions, which is why often only polymers of low molar masses are obtained. Apart from the low Q -values, a high e -value of 1.2 was estimated for methyl vinyl sulfone, which is in line with expectations since the vinyl moiety is in conjugation with a strong electron-withdrawing group.³⁶ In addition to free-radical copolymerization with styrene^{35,144,145} to determine Q and e values, copolymerizations with, for example, acrylonitrile and vinyl acetate have also been carried out successfully.¹⁴⁶

A more recent example is given by the work of Choe *et al.* They polymerized divinyl sulfone with the photoinitiator Darocur® at a UV wavelength of 365 nm to form crosslinked polymer films as host matrix for the encapsulation of lithium ions. The sulfone compounds were considered due to their ability to coordinate alkali metal ions and thus could conceivably be used as a solid polymer electrolyte.¹⁴⁷

Anionic polymerization. The strong electron withdrawing character of the sulfone moiety on the adjacent vinyl groups has of course aroused the interest in testing anionic polymerizations of these monomers. In 1952 Foster successfully prepared copolymers of butyl vinyl sulfone and acrylonitrile by an anionic process using sodium in liquid ammonia for the first time.¹⁴⁸ In this reaction, a growing chain end with a terminal vinyl butyl sulfone group was found to react preferentially with an acrylonitrile monomer while the terminal acrylonitrile reacts readily with both the sulfone and itself in equal amounts.

However, most attempts on homopolymerizations revealed that the sulfone groups render these types of monomers too reactive to tolerate an anionic polymerization.¹⁴⁹ Indeed, already in 1961 Overberger and Schiller¹⁵⁰ obtained only dimers when attempting to generate polyvinyl sulfone with potassium, which they attributed to side reactions due to the acidic CH_2 group. The substituent was again found to have a crucial influence on the polymerization behavior, as Diefenbach *et al.*¹⁵¹ showed a few years later. He tested poly-

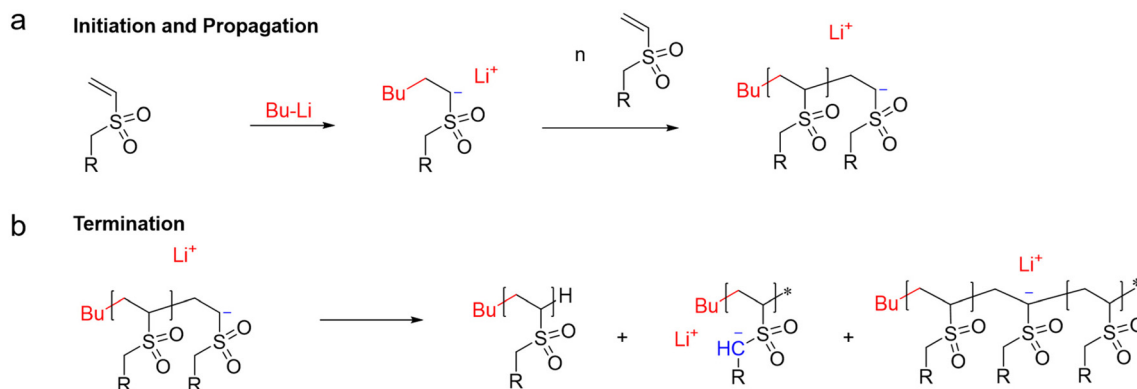
merizations of disulfone derivatives comprising $\text{SO}_2\text{-CH}_2\text{-SO}_2$ adjacent to a vinyl group using potassium *tert*-butylate as initiator. The high acidity of the methylene groups led to a competition between polymerization and polyaddition steps. He then postulated that the more acidic the CH_2 group, the more difficult it is to achieve high molar mass polymers due to increasing transfer reactions. 1971 Boor Jr and Finch¹⁵² demonstrated a successful polymerization of phenyl vinyl sulfone with *n*-BuLi, ZnEt_2 , $\text{LiN}(\text{CH}_3)_2$, NaNH_2 and complexes of *n*-BuLi with ZnEt_2 or AlEt_3 . However, the molar masses remained low for anionic polymerizations (around 10 000 g mol^{-1} , determined *via* the intrinsic viscosity). The polymers are characterized by a high glass transition temperature and exhibit decomposition temperatures of more than 200 °C. 2 years later, Schroeder *et al.* confirmed these results, but they were also able to determine a correlation between the initiator concentration of *n*-BuLi and the polymer yield.¹⁵³ Based on these results, mechanisms for potential side reactions and termination reactions were postulated, which explain the rather low molar masses of the obtained polymers. On the one hand, a termination reaction can occur in which an α -proton is abstracted from a monomer molecule, inactivating the active chain end. On the other hand, it is also conceivable that an α -proton is abstracted in the backbone of the polymer, leading to termination of the polymerization. In both cases the authors assume that the reactivity would then be too low to start a new initiation (Scheme 12).

Coordination polymerization. Although the polymerization of vinyl sulfones can be described as rather difficult, coordination polymerization is another way to obtain sulfone-containing polymers.^{130,154} Zhang *et al.* reported the successful coordination copolymerization of ethylene with methyl vinyl sulfone *via* 2,1-insertion into different catalyst (Scheme 13). The highest molar masses for methyl vinyl sulfone can be obtained with catalyst C1 ($M_w = 10\,000\ \text{g mol}^{-1}$), but the molar mass is lower compared to methyl acrylate ($M_w = 179\,000\ \text{g mol}^{-1}$) under the same conditions.¹⁵⁴ The authors explained this by the stronger polarity and coordination ability of the SO_2 -group with metals compared to the CO_2R -group. Moreover, the polymerizability of phenyl vinyl sulfone and phenyl vinyl sulfoxide was studied and a decreasing catalytic activity was observed in the following order: phenyl vinyl sulfone > methyl vinyl sulfone > phenyl vinyl sulfoxide.

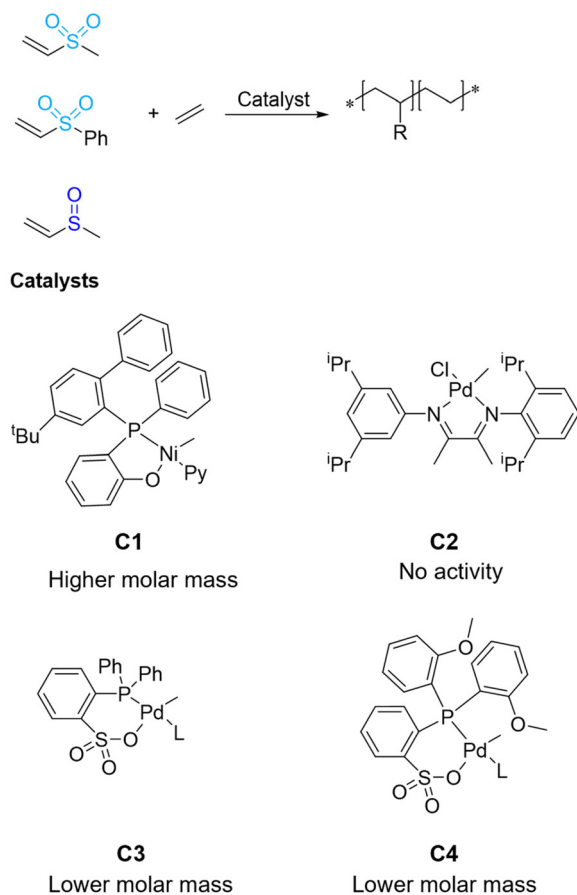
Vinyl sulfones and sulfoxides have indeed only more recently been introduced to coordination polymerizations, which is certainly related to the continuous improvements in the applied catalysts, but there might arise increasing interest in the next years considering the unique characteristics of these monomers.

3.3. Vinyl sulfonic acid and sulfonate salts

Despite the strong difference in the nature of vinyl sulfonic acid and the corresponding sulfonate salts, both materials were summarized in this chapter, since clear distinctions of the state of protonation can often not be clearly differentiated in the many reports in literature. This poor differentiation



Scheme 12 Schematic representation of the mechanism of possible termination processes.¹⁵³



Scheme 13 Schematic representation of the coordinative polymerization of ethylene and different S-vinyl monomers.¹⁵⁴

becomes particularly apparent when the acid is polymerized in aqueous conditions, although it most likely will be deprotonated under most given conditions due to the high acidity of the sulfonic acid group and the associated acid–base reactions. In the following, only the radical polymerization of these monomer classes is considered, since all other variants are not described in the literature. Azo initiators or peroxides such as

AIBN, 4,4'-azobis(4-cyanovaleric acid) or ammonium peroxydisulfate, respectively, can successfully initiate the radical polymerization of vinyl sulfonic acid, although most polymerizations result only in low molar masses compared to other monomer classes.^{155–160} The *Q*- and *e*-values (*Q* = 0.17 and *e* = 1.1) determined in copolymerization with styrene show only a low stabilization of the radicals similar to sulfones, which also explains the difficulties in homopolymerizing this class of substances.¹⁵⁵ Moreover, it can also be copolymerized with methacrylate, methyl methacrylate and acrylonitrile.^{155,158}

Poly sulfonic acids have attracted great interest because they can be used, for example, as a strong cation exchanger or as an acid catalyst,^{157,161,162} since they are characterized by a high ion dissociation, a high proton content and amphiphilicity.^{155,156,163} In addition, they could also replace polystyrene sulfonate as an acid dopant for conductive polymers because the exclusion of the sterically demanding aromatic unit results in lower glass transition temperatures and higher optical transparency.^{163–165}

As early as the 1960s, poly(ethylene sulfonate) was investigated for an application as pharmaceutical agents, *e.g.*, as anti-tumor agents, but failed due to toxicity. The industry expressed strong doubts that a polymer could be a therapeutic agent for diseases where small molecules failed.¹⁶⁶ However, Öztop *et al.* synthesized a hydrogel by copolymerization of acrylamide, vinyl sulfonic acid and a crosslinker and showed increased stability, better swelling properties, and above all improved behavior in the immobilization of invertase (Fig. 6).¹⁵⁹ This is important because isolated enzymes lose their activity over extended periods of time and quickly degrade if not stabilized, which limits their use for industrial applications. Immobilized enzymes, on the other hand, exhibit higher stability and the corresponding hydrogel is suitable to protect the enzyme from denaturation by the environment. In addition, Hussain *et al.* were also able to synthesize a pH-sensitive hydrogel by copolymerization of vinyl sulfonic acid and acrylic acid and ethylene glycol dimethacrylate, which could subsequently be used for drug release. To this end, they demonstrated the successful pH-dependent release of isosorbide mononitrates according to the non-Fickian diffusion mechanism.¹⁶⁷

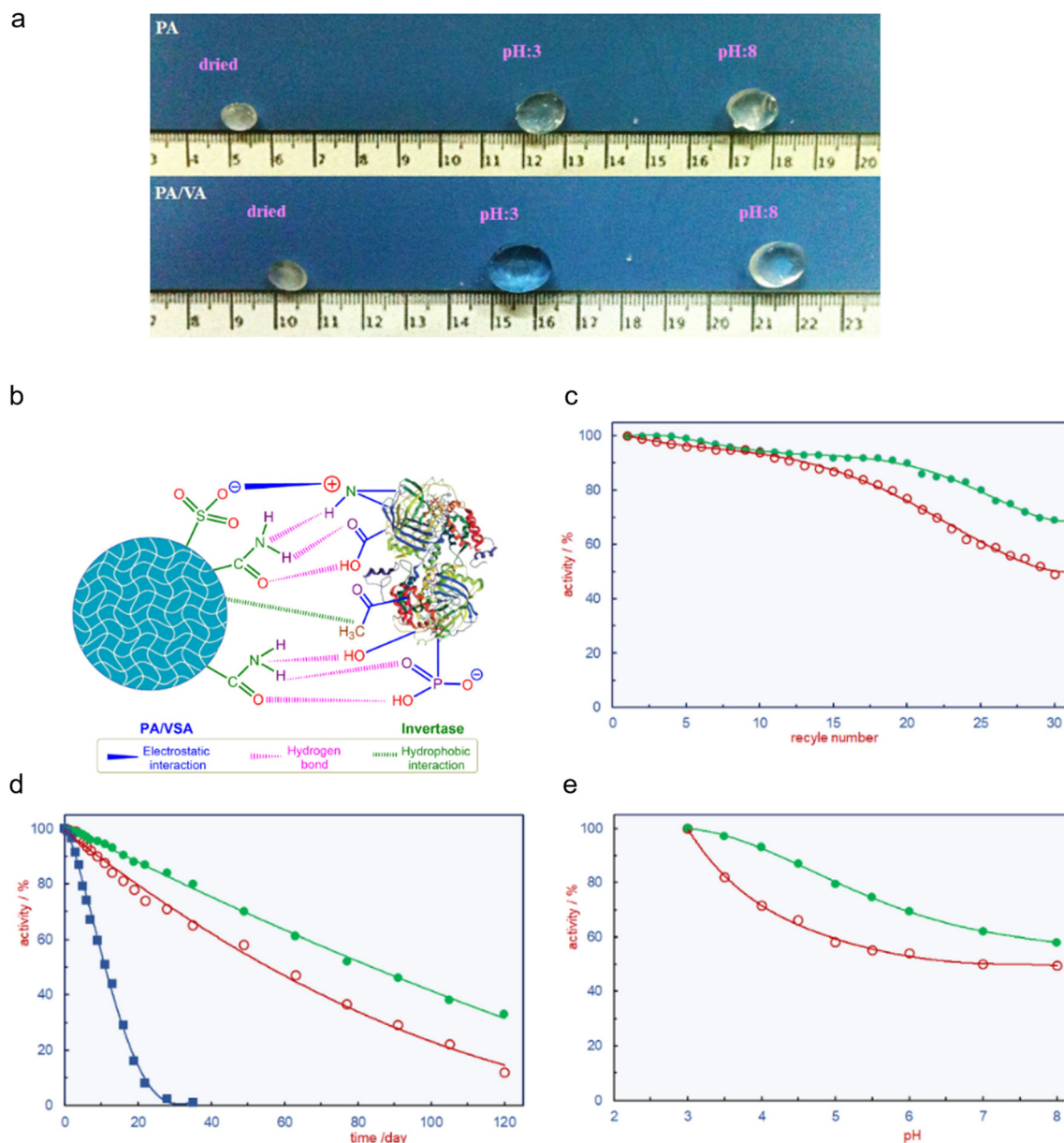


Fig. 6 (a) Swelling behavior of poly acrylamide (PA) and poly(acrylamide-co-vinyl sulfonic acid) (PA/VA) hydrogels, (b) postulated interaction between the hydrogel and invertase (c) operational stability (d) storage stability and (e) pH stability of the free invertase (blue), the invertase immobilized by PA (red) and PA/VA (green). Figure was adapted under the terms of the CC BY 3.0 license from ref. 167.

In general, it is preferable to use an alkali salt of vinyl sulfonic acid to prepare the polymer, although it has to be considered that some of the above-mentioned examples already apply the corresponding salts. The sulfonate salts are convenient to synthesize, can be stored without decomposition and polymerize faster in comparison to the free acid.^{32,168} Due to the negative charge of the sulfonate group, many polyvinyl sulfonates are water soluble and represent a class of anionic polyelectrolytes.¹⁶⁹ For sodium vinyl sulfonate, for example, there are numerous literature reports showing the initiation of polymerization with peroxides, redox systems, UV or γ -irradiation,^{170,171} with an increase in temperature favoring

polymerization. Copolymerizations with acrylamides,^{172–174} acrylic acid and methacrylic acid and their salts^{167,168,172} were also carried out by Breslow *et al.* and resulted in high molar mass polymers. However, it polymerized slowly with acrylonitrile,¹⁶⁸ methacrylates and methyl methacrylate,¹⁶⁸ vinyl acetate^{172,175} and *N*-vinylpyrrolidone.¹⁷² In contrast, copolymerizations with butadiene, isobutylene, α -methyl styrene, *n*-butyl vinyl ether, allyl alcohol, *N*-allyl acetamide, maleic acid, and fumaric acid were not successful.¹⁶⁸ Since Breslow *et al.* were also unable to perform a successful copolymerization with styrene, the *Q*- and *e*-value ($Q = 0.19$, $e = 1.51$) were calculated using acrylamide as a reference rather than styrene.

The stabilization factor of 0.19, corresponds to an increased stability of the resulting radicals compared to sulfones and explains why they are easier to polymerize, but nevertheless explain the still low reactivity compared to vinyl sulfides or other more activated monomers.

Due to the large variety of possible applications, we cannot describe all of them in detail here and have therefore limited ourselves to a few relevant examples. One potential application is the use of sodium vinyl sulfonate copolymers as delivery systems for cationic drugs, as shown by Wang *et al.* 2008.¹⁷⁶ The authors synthesized poly(vinyl sulfonate-*co*-vinyl alcohol) *graft* poly(D,L-lactic acid-*co*-glycolic acid) nanoparticles with a spherical shape and then monitored the degradation process. It was found that higher sulfonate content resulted in faster decomposition. It was possible to encapsulate a positively charged drug in the spherical particles through electrostatic interactions and then release it through the decomposition process. Al-Hussain *et al.* were able to draw attention to another possible application of these substances and show that they can be used for water treatment of industrial wastewater.¹⁷³ They used sodium vinyl sulfonate-*co*-2-acrylamido-2-methylpropane sulfonic acid sodium salt (Na-VS-*co*-Na-AMPS) cryogels with magnetite, coordinated to the sulfonate group. The effectiveness of the cryogel in adsorbing methylene blue was tested, which already proceeds at room temperature *via* a chemical adsorption mechanism. Substituted ammonium sulfonate monomers also belong to the vinyl sulfonates but allow the introduction of further functionality by the ammonium counterion. They can be prepared, for example, by acid-base neutralization of sulfonic acid and a tertiary amine or a substituted imidazole.¹⁷⁷ Similar to other vinyl sulfonates, polymerization can be initiated by radicals using AIBN or other radical initiators.^{178,179} These polymers are useful for a wide range of applications, as they combine the properties of ionic liquids and those of polymers for electrotechnical applications. Among others, they are applied in the preparation of solid electrolytes, organo-chelators and ionic amphiphilic copolymers.

Related to the above-mentioned sulfonic acid are the corresponding sulfonate esters. However, their polymerization behavior differs to sulfonate salts as described above. In general, homo- or copolymerization have been demonstrated to be initiated by azo initiators but as well by peroxides.^{180–184} The studies on the copolymerization behavior of butyl vinyl sulfonate in 1950 revealed a similar reactivity as observed for vinyl acetate and vinyl chloride.¹⁸¹ However, it can also be copolymerized with styrene, methacrylates, and vinylidene chloride, although the copolymerization is significantly retarded. Still these experiments allow the determination of a *Q* value of 0.02, which was obtained from a copolymerization with vinylidene chloride.¹⁸¹ The low value compared to the related sodium vinyl sulfate (*Q* = 0.19) suggests that the negative charge in the latter case must induce an increased stabilizing effect on the corresponding radical chain end, which is diminished in case of the ester. The authors assumed that this could be due to the fact that the electron-withdrawing effect of the sulfone group can be compensated somewhat by the negative

charge of the sodium sulfonate. Similarly, the *e*-value of butyl vinyl sulfonate is lower compared to the correlated sodium sulfonate, indicating an enhanced polarization of the double bond in case of the ester.

In retrospect, research on this class of monomers also came to a standstill after 1970. It was not until 2010 that these materials again gained some attention with the development of controlled polymerization techniques such as the RAFT polymerization. In this context, Mori *et al.*^{169,185–187} demonstrated not only the directed synthesis of well-defined homopolymers of ethyl ethenesulfonate with xanthate-type CTAs, but also the synthesis of block copolymers, for example, with NIPAAm (Fig. 7). By hydrolyzing the sulfonate ester in such block copolymers, they synthesized a thermo-responsive block copolymer that self-assembles at elevated temperatures due to the LCST behavior of the poly(NIPAAm) block. The phase separating poly(NIPAAm) block thus forms the core of a micelle and the hydrophilic poly(lithium vinyl sulfonate) resembles a highly charged shell. In addition to temperature, the size of the particle can also be influenced by adding salts or changing the pH - value, which had an influence on the charge repulsion of the sulfonate block.

3.4. Vinyl sulfonamides and vinyl sulfonimides

Although related to above-described sulfonate esters, vinyl sulfonamides represent an own class of monomers with different properties as the sulfonates. The direct polymerization of vinyl sulfonamides proved to be quite challenging and only a few reports were found on this monomer class, but we nevertheless liked to include this short chapter to provide a comprehensive overview. Most reported poly(vinyl sulfonamides) are indeed prepared by the polymerization of vinyl sulfonyl halogens/vinyl sulfonyl esters which are subsequently transformed into the corresponding amides by postpolymerization reaction with amines.¹⁸⁸ The route *via* the vinyl sulfonyl halogen, will be described in more detail in the next chapter.

The radical homopolymerization of vinyl sulfonamides with an unsubstituted amide is generally described to be difficult, and the lead only to polymers of low molar mass.¹⁸⁹ However, specific substituents attached to the nitrogen have been found to tremendously impact the polymerization behavior and to substantially improve it as well in some cases. For example *N*-allyl vinyl sulfonamides can be polymerized using radical initiators¹⁹⁰ while many alkyl vinyl sulfonamides cannot be polymerized under these conditions.¹⁸⁸ A kind of copolymerization occurs between the different vinyl groups in the monomer during this polymerization, and also the formation of cycles is possible (Scheme 14).¹⁹⁰ The authors conclude that no crosslinking occurred based on the observed solubility, but also note that crosslinking would be very likely if no cyclic repeat units had formed. However, they were unable to quantify the cyclic repeat units because a suitable solvent was not available for the measurements and the hydrolysis experiments were unsuccessful.

Similarly, copolymerizations with other monomers proved to be much easier. Iwakura *et al.* for example described a suc-

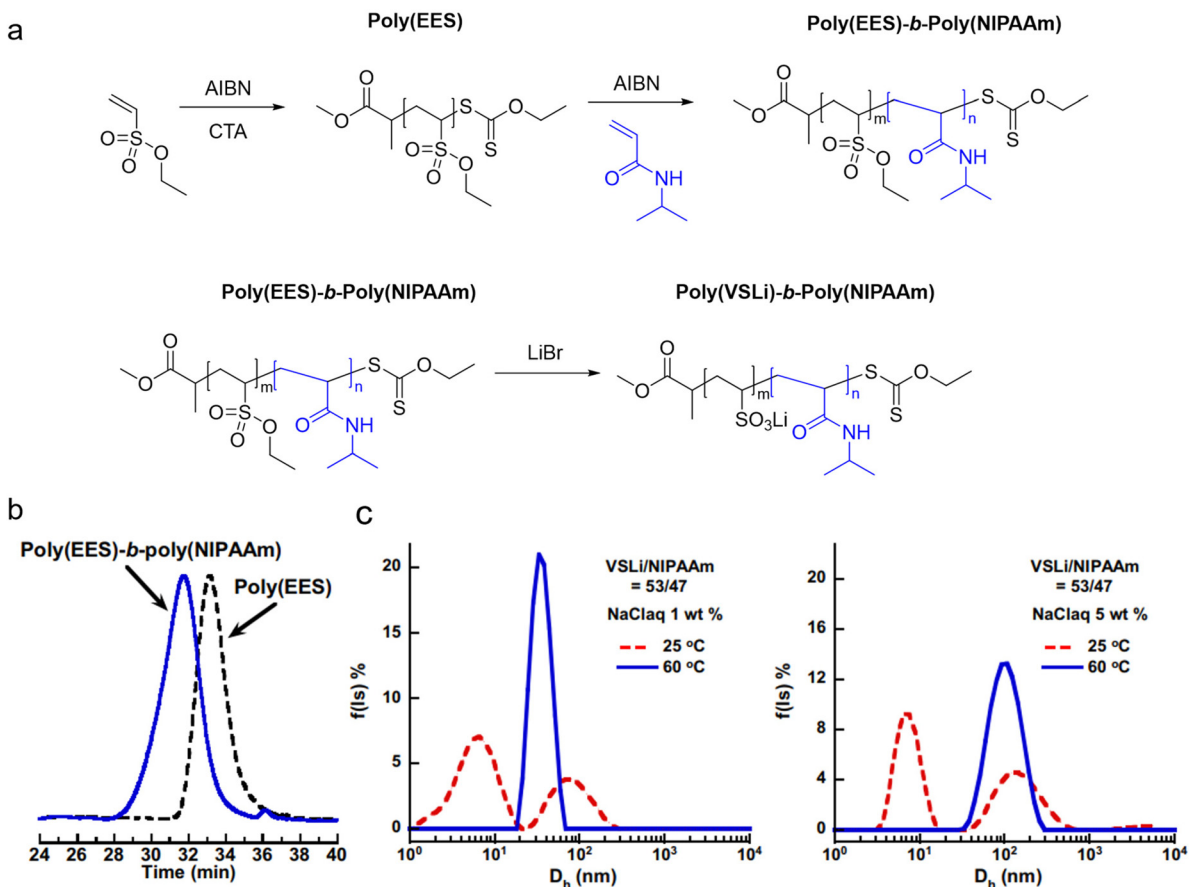
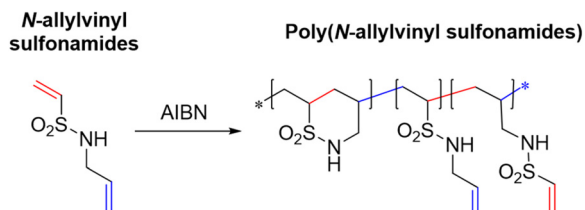


Fig. 7 (a) Schematic representation of the synthesis of the *block*-copolymer poly(VSLi)-*b*-poly(NIPAAm), (b) SEC-traces of the poly(EES) and poly(EES)-*b*-poly(NIPAAm) (c) hydrodynamic diameter distributions of poly(VSLi)-*b*-poly(NIPAAm) at different temperature and different salt content. Figure was adapted from ref. 186 with permission of Elsevier (Copyrights 2012).



Scheme 14 Schematic representation of the polymerization of *N*-allyl vinyl sulfonamide.¹⁸⁸

successful radical copolymerization of vinyl sulfonamides with styrene, ethylene and acrylonitrile.^{188,191} Copolymerization of vinyl sulfonyl-(β -chloroethyl)amide with styrene demonstrated that the incorporation of styrene was preferred, and the *Q*- and *e*-values obtained (*Q* = 0.13 and *e* = 0.42) indicated only a low stabilization of the radical chain ends by the sulfonamide group. Nevertheless, the high *e*-value confirms the high electron withdrawing effect induced by the sulfonamide group.¹⁹¹ In 1957, also an attempt of an anionic polymerization of vinyl sulfonamides was reported.¹⁹² However, only a very soft

material with low molar mass and a melting point range of 100 to 160 °C could be obtained. To our knowledge, no further experiments on this polymerization technique have been published.

In contrast to the limited yield during polymerizations with peroxide or azo initiators, an effective, but rather special method proved to be the γ -induced radiation polymerization of vinyl sulfonamide.^{193–195} In this context, vinyl sulfonamide in particular revealed a high polymerization rate with an increase of conversion of 1.5% per minute at 4200 rpm.¹⁹⁴ The sulfonamides appear to absorb the γ -ray energy quite effectively, while in contrast to other monomers dissipation by other pathways is limited. In further studies, Wiley *et al.*¹⁹⁵ however, reported that *N,N*-dimethyl vinyl sulfonamide did not exhibit such a high polymerization rate. This decrease was related to an enhanced instability of the *N,N*-dimethyl substituted structure, which is similar to corresponding amides and *N*-methylamides in carbon tetrachloride.

In comparison, the compound class of vinyl sulfonimides is found only sporadically in the literature, although lithium sulfonimides, for example, show good suitability as electrolytes for lithium battery applications.^{196–198} Baik *et al.* prepared

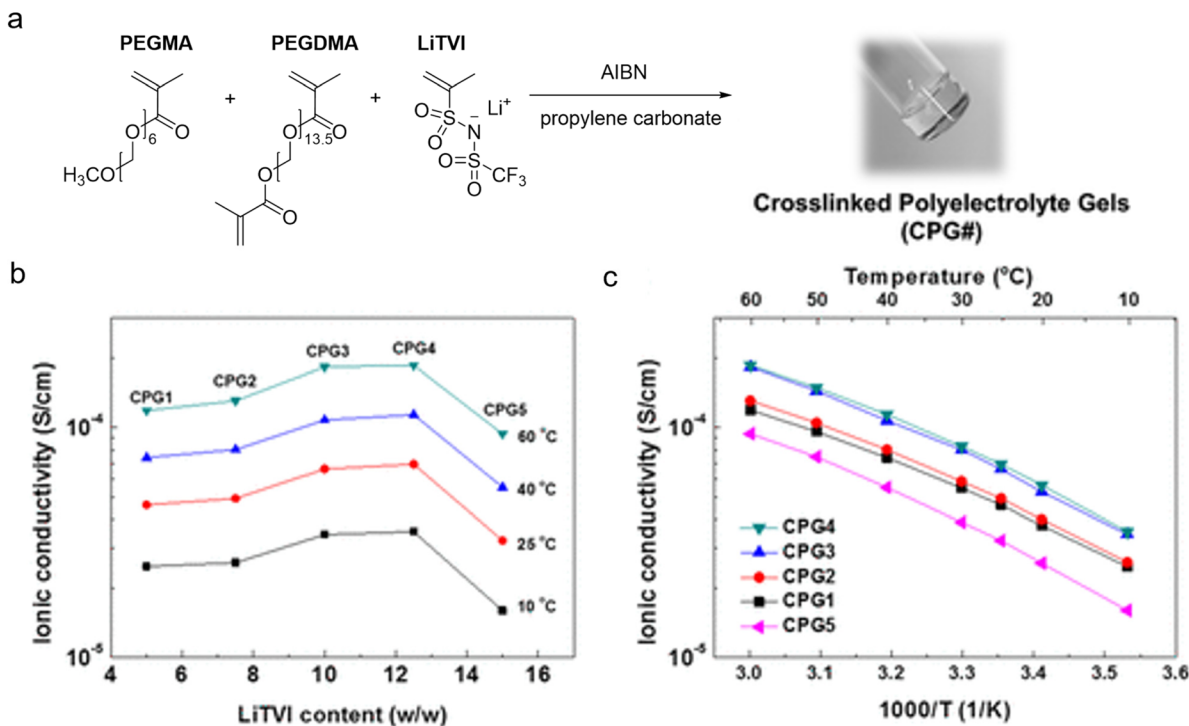


Fig. 8 (a) Schematic representation of the polymerization of LiTVA (b) ionic conductivity vs. LiTVA content and (c) Arrhenius plot of ionic conductivities. Figure was adapted from ref. 196 with permission of the American Chemical Society (Copyright 2019).

stable gel polymer electrolytes (CPGs) using lithium (trifluoromethane sulfonyl)(vinyl sulfonyl)imide (LiTVA) by radical polymerization with poly(ethylene glycol) methyl ether methacrylate (PEGMA), poly(ethylene glycol) dimethacrylate (PEGDMA), and propylene carbonate and investigated their ionic conductivity (Fig. 8).¹⁹⁶ Depending on the LiTVA content, ionic conductivity values of up to $6.7 \times 10^{-4} \text{ S cm}^{-1}$ at 25 °C and $1.8 \times 10^{-3} \text{ S cm}^{-1}$ at 60 °C were found. They are also characterized by high electrochemical stability and large lithium-ion transfer number.

3.5. Vinyl sulfonyl halides

Reactive polymers are generally considered attractive precursors for postpolymerization modifications providing access to otherwise challenging materials.^{199–202} In terms of ester and amide formation, acid halides are often considered as precursors and indeed several reports on poly((meth)acryloyl chloride) confirm the high reactivity of these polymers.^{203,204} Similarly, vinyl sulfonyl halides have been evaluated as reactive precursors for postpolymerization modification. As already mentioned above, these compounds can be converted into polyvinyl sulfonamides with addition of the corresponding amines. The resulting sulfonamides from, for example, *p*-aminophenol, *p*-dimethylaniline, aniline, *m*-chloroaniline and β -naphthylamine were then coupled with diazo-compounds and used as red and brown dyes.¹⁷⁰

Vinyl sulfonyl chloride and vinyl sulfonyl fluoride, for example, can be polymerized into soluble polymers using

radical initiators, although peroxides appeared to be not suitable for the fluoride compound.^{188,205} However, using azo initiators surprisingly high conversions and reasonable molar masses can be reached with vinyl sulfonyl fluoride, while conversions and degrees of polymerization remain low for the chloride analogue. The difference might be related to the relatively high transfer constant of sulfonyl chlorides as later reported.²⁰⁶ More recently also Sharpless and coworkers confirm an increased stability of sulfonyl fluorides, which is related to an energetic inaccessibility of the fluoride radical.²⁰⁷ This combination of stability and reactivity renders sulfonyl fluorides attractive for incorporation into radical polymerizations and subsequent modification *via* a sulfur(vi) fluoride exchange (SuFEx) reaction.²⁰⁸ However, the monomer vinyl sulfonyl fluoride is further considered as one of the strongest Michael acceptors, which has to be considered to avoid unintended side reactions.²⁰⁹ In contrast to radical azo initiators, homopolymerization attempts with Friedel–Crafts catalysts (aluminum trichloride, tin tetrachloride) or with redox systems such as benzene sulfinic acid/benzoyl peroxide and dimethylaniline/benzoyl peroxide were not yielding polymers.¹⁷⁰ It must be said, that after 1960 interest in the polymerization of vinyl sulfonyl halides quickly waned and not much was invested in research on these substances. However, the advent of SuFEx chemistry and the increased accessibility of corresponding vinyl compounds such as vinyl sulfonyl fluoride might again raise the interest in related polymerizations and the corresponding materials as reactive precursors.²¹⁰

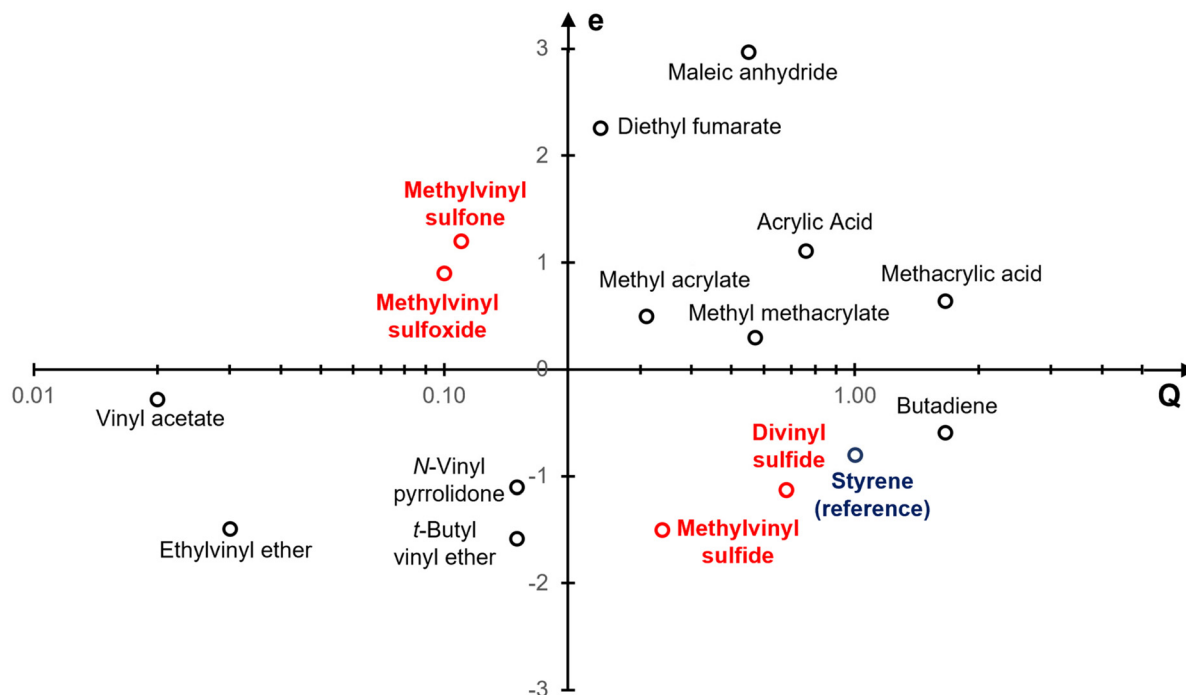


Fig. 9 Q- and e-scheme of selected representatives of different monomer classes.

4. Conclusion and outlook

Considering the broad scope and the vast number of reports on vinyl-based polymers, *S*-vinyl monomers certainly have to be considered a niche among the large variety of general vinyl monomers. However, the chemical versatility of sulfur derivatives and the interesting reactivity of the corresponding vinyl compounds, endow them with unique characteristics, which might again raise increasing interest of researchers if compatibility with established polymerization techniques and, most of all, sufficient accessibility is provided. With respect to the availability of those monomers, the report on the large scale preparation of vinyl sulfonyl fluoride or the adaption of industrially established processes, such as the Reppe chemistry, might represent the required turning point on the way to a broader application of *S*-vinyl monomers.^{210,211} Quite recently, BASF SE, as one of the leading chemical companies, has realized a scalable process to prepare vinyl mercaptoethanol (VME) in an aqueous process providing large scale access to such a monomer at reasonable costs.^{212,213} We therefore considered this the right time to reflect on the already reported investigations on the polymerization behavior of *S*-vinyl monomers, which date back to the very early days of polymer chemistry and found a peak during the 50s and 60s of the last century. In the subsequent decades the research interest in most of these monomers had ceased, but with the advent of controlled radical polymerizations, in particular the RAFT technique, which also heavily relies on sulfur chemistry, a renewed focus has been turned on some of the *S*-vinyl compounds.

In our review, we tried to provide a comprehensive overview of all *S*-vinyl monomers and the reported polymerization processes. The monomers were classified as electron rich or deficient according to the electron donating or withdrawing character of the adjacent sulfur species, respectively, which should also reflect the corresponding density at the double bond. The electron-rich *S*-vinyl monomers such as vinyl sulfides, vinyl thioacetates, or vinyl thioacetals appear generally suitable for radical and cationic polymerization, although their oxidation sensitivity limits the use of peroxides and mostly azo initiators were applied. The electron-poor sulfur-containing monomers, on the other hand, are less sensitive to peroxides, but are often reported to be generally more difficult to be polymerized in a radical process. However, several examples for anionic polymerizations have been reported, which is related to the potential resonance stabilization of the carbanion by the electron withdrawing SO_x species conjugated to the vinyl moiety. Interestingly, sulfone groups are already too reactive for anionic polymerizations, since the high acidity of adjacent methylene units cause frequent transfer or even termination processes.

Comparing all reported techniques, radical polymerizations are most frequently applied and detailed studies of the homo- and copolymerization behavior for most monomers are available. Indeed, in many cases not only copolymerization parameters for specific monomer combinations are provided, but also Q- and e-values according to the definitions of Alfrey and Price are calculated.⁴⁹ These values allow not only an estimation of the expected copolymerization parameters of unknown monomer combinations, but also reflect the reactivity and the polarity of these monomers in radical processes. The first can also be understood

as a measure of the stabilization of the radical at a corresponding active chain end, while the latter reflects the electron density on the double bond. Although the initial Q - e scheme proposed by Alfrey and Price has some shortcomings,²¹⁴ which the authors indeed acknowledged themselves,²¹⁵ and several more accurate methods have been reported,^{216–218} we stick to the initial representation by Alfrey and Price, since most of the discussed monomers have been evaluated before these new methods were proposed. Fig. 9 provides a typical plot of some common representatives of different monomer classes in this Q/e -scheme, where we included further key examples from the monomers discussed in this review (in red).

This graphical presentation reveals quite nicely that the discussed S -vinyl monomers are found separated from the more common monomer classes, which reflects their unique character in terms of reactivity and polarity. In copolymerizations, combinations of monomers with similar Q -values but opposing e -values are interesting, since these cases promise a high tendency to form copolymers and might even lead to alternating structures.²¹⁹ Therefore, vinyl sulfides represent ideal matches for radical copolymerization with acrylates and methacrates. Other more reactive monomers (e.g. styrenes or dienes) featuring a high electron density (low e -value) usually have much higher Q -values. On the other side, vinyl sulfones or related electron deficient S -vinyl compounds might be interesting comonomers in polymerizations with the less reactive N -vinyl or O -vinyl monomers. Although the given Q - and e -values might not allow an accurate prediction of real copolymerization parameters, the general correlations drawn above hold true and reflect the potential of S -vinyl monomers for designing various copolymers.

Reflecting on the overall research on S -vinyl monomers, we can conclude that their polymerization behavior has become well understood. But in terms of potential applications of corresponding polymers researchers have so far only scratched the surface, although these sulfur containing materials feature a variety of interesting properties including a high affinity for various metals, unique optical properties, or flame retardation. Increasing efforts to scale up synthesis and commercialization of further derivatives might therefore induce another turning point in research on these monomers and related polymers. In any case, we are convinced that there is unexploited potential in these S -vinyl compounds and unforeseen applications might still arise, which, however, require a more detailed evaluation of structure–property relations of the corresponding homo- and copolymers.

Conflicts of interest

There are no conflicts to declare.

Acknowledgements

J. C. B. thanks the German Science Foundation (DFG) for generous funding within the Emmy-Noether Programme (Project-ID: 358263073).

References

- J.-g. Liu, Y. Nakamura, Y. Shibasaki, S. Ando and M. Ueda, *Macromolecules*, 2007, **40**, 4614–4620.
- J.-g. Liu, Y. Nakamura, Y. Suzuki, Y. Shibasaki, S. Ando and M. Ueda, *Macromolecules*, 2007, **40**, 7902–7909.
- J.-g. Liu and M. Ueda, *J. Mater. Chem.*, 2009, **19**, 8907–8919.
- T. Okubo, S. Kohmoto and M. Yamamoto, *J. Macromol. Sci., Part A: Pure Appl. Chem.*, 1998, **35**, 1819–1834.
- R. Okutsu, Y. Suzuki, S. Ando and M. Ueda, *Macromolecules*, 2008, **41**, 6165–6168.
- Y. Sato, S. Sobu, K. Nakabayashi, S. Samitsu and H. Mori, *ACS Appl. Polym. Mater.*, 2020, **2**, 3205–3214.
- Y. Suzuki, T. Higashihara, S. Ando and M. Ueda, *Polym. J.*, 2009, **41**, 860–865.
- N.-H. You, T. Higashihara, Y. Oishi, S. Ando and M. Ueda, *Macromolecules*, 2010, **43**, 4613–4615.
- H. Mutlu and P. Theato, *Macromol. Rapid Commun.*, 2020, **41**, 2000181.
- K. Dai, Z. Deng, G. Liu, Y. Wu, W. Xu and Y. Hu, *Polymers*, 2020, **12**, 1441–1456.
- Y. Lyu, Y. Zhang and H. Ishida, *Eur. Polym. J.*, 2020, **133**, 109770–109778.
- N. Lotti, V. Siracusa, L. Finelli, P. Marchese and A. Munari, *Eur. Polym. J.*, 2006, **42**, 3374–3382.
- C. Berti, A. Celli and E. Marianucci, *Eur. Polym. J.*, 2002, **38**, 1281–1288.
- A. A. Basfar and J. Silverman, *Polym. Degrad. Stab.*, 1994, **46**, 1–8.
- J. P. Kennedy and T. Chou, *Poly(isobutylene-co- β -pinene) a new sulfur vulcanizable, ozone resistant elastomer by cationic isomerization copolymerization*, Berlin, Heidelberg, 1976.
- M. Geven, R. d'Arcy, Z. Y. Turhan, F. El-Mohtadi, A. Alshamsan and N. Tirelli, *Eur. Polym. J.*, 2021, **149**, 110387–110408.
- E. Lallana and N. Tirelli, *Macromol. Chem. Phys.*, 2013, **214**, 143–158.
- R. V. Kupwade, *J. Chem. Rev.*, 2019, **1**, 99–113.
- S. I. Kozhushkov and M. Alcarazo, *Eur. J. Inorg. Chem.*, 2020, **2020**, 2486–2500.
- D. Kaiser, I. Klose, R. Oost, J. Neuhaus and N. Maulide, *Chem. Rev.*, 2019, **119**, 8701–8780.
- J. J. Fitzgerald and R. A. Weiss, *J. Macromol. Sci., Chem.*, 1988, **28**, 99–185.
- R. J. Reddy and A. H. Kumari, *RSC Adv.*, 2021, **11**, 9130–9221.
- C. E. Hoyle and C. N. Bowman, *Angew. Chem., Int. Ed.*, 2010, **49**, 1540–1573.
- W. R. Algar, P. Dawson and I. L. Medintz, *Chemoselective and Bioorthogonal Ligation Reactions: Concepts and Applications*, Wiley, 2017.
- C. E. Hoyle, A. B. Lowe and C. N. Bowman, *Chem. Soc. Rev.*, 2010, **39**, 1355–1387.
- A. Rehor, N. Tirelli and J. A. Hubbell, *Macromolecules*, 2002, **35**, 8688–8693.

- 27 A. Napoli, N. Tirelli, G. Kilcher and A. Hubbell, *Macromolecules*, 2001, **34**, 8913–8917.
- 28 C. D. Vo, C. J. Cadman, R. Donno, J. A. Goos and N. Tirelli, *Macromol. Rapid Commun.*, 2013, **34**, 156–162.
- 29 M. Kuhlmann, S. Singh and J. Groll, *Macromol. Rapid Commun.*, 2012, **33**, 1482–1486.
- 30 C. D. Vo, G. Kilcher and N. Tirelli, *Macromol. Rapid Commun.*, 2009, **30**, 299–315.
- 31 A. V. Sviridova and E. N. Prilezhaeva, *Russ. Chem. Rev.*, 1974, **43**, 200–209.
- 32 E. J. Goethals, *J. Macromol. Sci., Part C: Polym. Rev.*, 1968, **2**, 73–144.
- 33 A. Kausar, S. Zulfiqar and M. I. Sarwar, *Polym. Rev.*, 2014, **54**, 185–267.
- 34 A. Kultys, in *Encyclopedia of Polymer Science and Technology*, John Wiley & Sons, Inc., 2010.
- 35 C. C. Price and H. Morita, *J. Am. Chem. Soc.*, 1953, **75**, 4747–4750.
- 36 C. C. Price and J. Zomlefer, *J. Am. Chem. Soc.*, 1950, **72**, 14–17.
- 37 K. Tsuda, S. Kobayashi and T. Otsu, *J. Macromol. Sci., Part A: Pure Appl. Chem.*, 1967, **1**, 1025–1037.
- 38 K. D. Gollmer, F. H. Müller and H. Ringsdorf, *Makromol. Chem.*, 1966, **92**, 122–136.
- 39 C. C. Price and R. G. Gillis, *J. Am. Chem. Soc.*, 1953, **75**, 4750–4753.
- 40 M. F. Shostakovskiy, E. N. Prilezhaeva and N. I. Uvarova, *Russ. Chem. Bull.*, 1954, **3**, 447–454.
- 41 J. C. H. Hwa, *J. Am. Chem. Soc.*, 1958, **81**, 3604–3607.
- 42 J. Kosai, Y. Masuda, Y. Chikayasu, Y. Takahashi, H. Sasabe, T. Chiba, J. Kido and H. Mori, *ACS Appl. Polym. Mater.*, 2020, **2**, 3310–3318.
- 43 M. F. Shostakovskiy, E. N. Prilezhaeva and A. M. Khomutov, *Bull. Acad. Sci. USSR, Div. Chem. Sci.*, 1956, **5**, 1257–1262.
- 44 W. Reppe, *Liebigs Ann. Chem.*, 1956, **601**, 81–138.
- 45 P. P. Shorygin, M. F. Shostakovskii, E. N. Prilezhaeva, T. N. Shkurina, L. G. Stolyarova and A. P. Genich, *Bull. Acad. Sci. USSR, Div. Chem. Sci.*, 1961, **10**, 1468–1472.
- 46 F. R. Mayo and F. M. Lewis, *J. Am. Chem. Soc.*, 1944, **66**, 1594–1601.
- 47 M. Fineman and S. D. Ross, *J. Polym. Sci.*, 1950, **5**, 259–265.
- 48 T. Kelen, F. Tüdös and B. Turcsányi, *Polym. Bull.*, 1980, **2**, 71–76.
- 49 T. Alfrey Jr. and C. C. Price, *J. Polym. Sci.*, 1947, **2**, 101–106.
- 50 T. Otsu and H. Inoue, *J. Macromol. Sci., Part A: Pure Appl. Chem.*, 1970, **4**, 35–50.
- 51 K. Gollmer and H. Ringsdorf, *Kolloid-Z.*, 1967, **216**, 325–329.
- 52 J. Brandrup, E. H. Immergut and W. A. Grulke, *Polymer Handbook*, John Wiley & Sons, Inc., Hoboken, New Jersey, 1999.
- 53 V. M. Karavaeva, E. N. Prilezhaeva and M. F. Shostakovskiy, *Bull. Acad. Sci. USSR, Div. Chem. Sci.*, 1957, **6**, 663–665.
- 54 C. E. Scott and C. C. Price, *J. Am. Chem. Soc.*, 1959, **81**, 2672–2674.
- 55 E. D. Holly, *J. Polym. Sci.*, 1959, **36**, 329–332.
- 56 K. Tsuda, S. Kobayashi and T. Otsu, *J. Macromol. Sci., Part A: Pure Appl. Chem.*, 1968, **6**, 41–48.
- 57 A. I. Vorob'eva, S. A. Onina, R. R. Muslukhov, S. V. Kolesov, L. Parshina, M. Y. Khil'ko, B. A. Trofimov and Y. B. Monakov, *Polym. Sci., Ser. B*, 2003, **45**, 102–105.
- 58 J. M. Judge and C. C. Price, *J. Polym. Sci.*, 1959, **41**, 435–443.
- 59 B. A. Trofimov, L. V. Morozova, A. I. Mikhaleva, M. V. Markova, I. V. Tatarinova and J. Henkelmann, *Russ. Chem. Bull.*, 2008, **57**, 2111–2116.
- 60 S. Iwatsuki, M. Kubo, M. Wakita, Y. Matsui and H. Kanoh, *Macromolecules*, 1991, **24**, 5009–5014.
- 61 A. I. Vorob'eva, S. A. Onina, I. D. Musina, S. V. Kolesov, R. R. Muslukhov, L. Parshina, L. A. Oparina, B. A. Trofimov and Y. B. Monakov, *Polym. Sci., Ser. B*, 2004, **46**, 364–368.
- 62 T. Otsu and H. Inoue, *Makromol. Chem.*, 1969, **128**, 31–40.
- 63 H. Inoue and T. Otsu, *Makromol. Chem.*, 1972, **153**, 21–36.
- 64 T. Sato, M. Abe and T. Otsu, *J. Macromol. Sci., Part A: Pure Appl. Chem.*, 1981, **15**, 367–379.
- 65 Y. Abiko, A. Matsumura, K. Nakabayashi and H. Mori, *Polymer*, 2014, **55**, 6025–6035.
- 66 Y. Abiko, A. Matsumura, K. Nakabayashi and H. Mori, *React. Funct. Polym.*, 2015, **93**, 170–177.
- 67 Y. Abiko, K. Nakabayashi and H. Mori, *Macromol. Symp.*, 2015, **349**, 34–43.
- 68 K. Nakabayashi, Y. Abiko and H. Mori, *Macromolecules*, 2013, **46**, 5998–6012.
- 69 K. Nakabayashi, A. Matsumura, Y. Abiko and H. Mori, *Macromolecules*, 2016, **49**, 1616–1629.
- 70 C.-T. Lo, Y. Abiko, J. Kosai, Y. Watanabe, K. Nakabayashi and H. Mori, *Polymers*, 2018, **10**, 721.
- 71 K. Nakabayashi and H. Mori, *Eur. Polym. J.*, 2013, **49**, 2808–2838.
- 72 M. F. Shostakovskii, E. N. Prilezhaeva and V. M. Karavaeva, *Polym. Sci. U.S.S.R.*, 1960, **1**, 200–208.
- 73 H. Inoue and T. Otsu, *J. Polym. Sci., Polym. Chem. Ed.*, 1976, **14**, 845–861.
- 74 R. Kroker and H. Ringsdorf, *Makromol. Chem.*, 1969, **121**, 240–257.
- 75 K. A. Kun, *J. Polym. Sci., Part A-1: Polym. Chem.*, 1966, **4**, 847–858.
- 76 C. G. Overberger, J. J. Ferraro and F. W. Orttung, *J. Org. Chem.*, 1961, **26**, 3458–3460.
- 77 C. G. Overberger and A. Lebovits, *J. Am. Chem. Soc.*, 1956, **78**, 4792–4797.
- 78 C. G. Overberger and A. Lebovits, *J. Am. Chem. Soc.*, 1955, **77**, 3675–3676.
- 79 M. Kinoshita, T. Irie and M. Imoto, *J. Soc. Chem. Ind., Jpn.*, 1969, **72**, 1210–1211.
- 80 S. R. Sandler, W. Karo and H. H. Wasserman, *Polymer Syntheses: Organic Chemistry: A Series of Monographs*, Elsevier Science, 2013, vol. 3.

- 81 C. G. Overberger and J. J. Ferraro, *J. Org. Chem.*, 1962, **27**, 3539–3545.
- 82 G. Hardy, J. Varga, K. Nytrai, I. Tsajlik and L. Zubonyai, *Polym. Sci. U.S.S.R.*, 1964, **6**, 832–841.
- 83 C. G. Overberger, H. Bilech and R. G. Nickerson, *J. Polym. Sci.*, 1958, **27**, 381.
- 84 F. Leonard, G. A. Hanks and R. K. Kulkarni, *J. Polym. Sci., Part A-1: Polym. Chem.*, 1966, **4**, 449–457.
- 85 M. S. Kharasch, E. Sternfeld and F. R. Mayo, *J. Am. Chem. Soc.*, 1939, **61**, 215–215.
- 86 W. E. Goode, W. H. Snyder and R. C. Fettes, *J. Polym. Sci.*, 1960, **42**, 367–382.
- 87 M. G. Evans, W. C. E. Higginson and N. S. Wooding, *Recl. Trav. Chim. Pays-Bas*, 1949, **68**, 1069–1078.
- 88 K. D. Gollmer, R. Kroker, H. Ringsdorf and U. Zahorszky, *Angew. Chem., Int. Ed. Engl.*, 1968, **10**, 411.
- 89 C. G. Overberger, H. Ringsdorf and B. Avchen, *J. Org. Chem.*, 1965, **30**, 3088–3092.
- 90 C. G. Overberger, H. Ringsdorf and B. Avchen, *J. Med. Chem.*, 1965, **8**, 862–864.
- 91 H. Ringsdorf, N. M. Weinshenker and C. G. Overberger, *Macromol. Chem. Phys.*, 1963, **64**, 126–134.
- 92 C. G. Overberger, H. Ringsdorf and N. Weinshenker, *J. Org. Chem.*, 1962, **27**, 4331–4337.
- 93 W. H. Daly and C.-D. S. Lee, *J. Polym. Sci., Part A-1: Polym. Chem.*, 1971, **9**, 1723–1739.
- 94 C. G. Overberger and W. H. Daly, *J. Am. Chem. Soc.*, 1964, **86**, 3402–3403.
- 95 C. G. Overberger, K. H. Burg and W. H. Daly, *J. Am. Chem. Soc.*, 1965, **87**, 4125–4130.
- 96 S. G. Matsuyan, *Russ. Chem. Rev.*, 1966, **35**, 32–43.
- 97 H. Ringsdorf and C. G. Overberger, *Makromol. Chem.*, 1961, **44**, 418–426.
- 98 S.-i. Nozakura, Y. Yamamoto and S. Murahashi, *Polym. J.*, 1973, **5**, 55–61.
- 99 C. W. N. Cumper, A. Melnikoff and A. I. Vogel, *J. Chem. Soc. A*, 1966, 242–245.
- 100 H. Ohnishi and T. Otsu, *J. Macromol. Sci., Part A: Pure Appl. Chem.*, 1980, **14**, 1015–1027.
- 101 H. Ohnishi and T. Otsu, *J. Macromol. Sci., Part A: Pure Appl. Chem.*, 1978, **12**, 1491–1500.
- 102 H. Ohnishi and T. Otsu, *J. Macromol. Sci., Part A: Pure Appl. Chem.*, 1979, **13**, 1–12.
- 103 T. Otsu and H. Ohnishi, *J. Macromol. Sci., Part A: Pure Appl. Chem.*, 2006, **12**, 1477–1490.
- 104 G. Pasparakis, T. Manouras, P. Argitis and M. Vamvakaki, *Macromol. Rapid Commun.*, 2012, **33**, 183–198.
- 105 T. P. Cunningham, D. L. Cooper, J. Gerratt, P. B. Karadakov and M. Raimondi, *J. Chem. Soc., Faraday Trans.*, 1997, **93**, 2247–2254.
- 106 S. Kondo, K. Ohta, R. Ojika, H. Yasui and K. Tsuda, *Makromol. Chem.*, 1985, **186**, 1–9.
- 107 X. Xu, X. Huang, Y. Chang, Y. Yu, J. Zhao, N. Isahak, J. Teng, R. Qiao, H. Peng, C.-X. Zhao, T. P. Davis, C. Fu and A. K. Whittaker, *Biomacromolecules*, 2021, **22**, 330–339.
- 108 Y. Yu, W. Xu, X. Huang, X. Xu, R. Qiao, Y. Li, F. Han, H. Peng, T. P. Davis, C. Fu and A. K. Whittaker, *ACS Macro Lett.*, 2020, **9**, 799–805.
- 109 A. A. Burkey, A. Hillsley, D. T. Harris, J. R. Baltzegar, D. Y. Zhang, W. W. Sprague, A. M. Rosales and N. A. Lynd, *Biomacromolecules*, 2020, **21**, 3047–3055.
- 110 D. Işık, A. A. Joshi, X. Guo, F. Rancan, A. Klossek, A. Vogt, E. Rühl, S. Hedtrich and D. Klinger, *Biomater. Sci.*, 2021, **9**, 712–725.
- 111 K. Imai, T. Shiomi, Y. Tezuka and K. Takahashi, *J. Macromol. Sci., Part A: Pure Appl. Chem.*, 1985, **22**, 1347–1358.
- 112 H. Inoue, I. Umeda and T. Otsu, *Makromol. Chem.*, 1971, **147**, 271–286.
- 113 C. C. Price and R. D. Gilbert, *J. Am. Chem. Soc.*, 1952, **74**, 2073–2074.
- 114 G. V. Leplyanin, V. A. Nikonov, A. A. Yelichev and Y. M. Shaul'skii, *Polym. Sci. U.S.S.R.*, 1990, **32**, 237–245.
- 115 J. E. Mulvaney and R. A. Ottaviani, *J. Polym. Sci., Part A-1: Polym. Chem.*, 1970, **8**, 2293–2308.
- 116 N. Kunieda, M. Kinoshita and M. Imoto, *J. Polym. Sci., Part B: Polym. Lett.*, 1971, **9**, 241–245.
- 117 N. Hadjichristidis and A. Hira, *Anionic Polymerization*, Springer, Tokyo, 2015.
- 118 M. A. Buese and T. E. Hogen-Esch, *Macromolecules*, 1987, **20**, 1509–1518.
- 119 R. S. Kanga, T. E. Hogen-Esch, E. Randrianalimanana, A. Soum and M. Fontanille, *Macromolecules*, 1990, **23**, 4241–4246.
- 120 R. S. Kanga, T. E. Hogen-Esch, E. Randrianalimanana, A. Soum and M. Fontanille, *Macromolecules*, 1990, **23**, 4235–4240.
- 121 T. Durst, M. J. LeBelle, R. V. d. Elzen and K. C. Tin, *Can. J. Chem.*, 1974, **52**, 761–766.
- 122 L. M. Leung and K. H. Tan, *Polymer*, 1994, **35**, 1556–1560.
- 123 L. M. Leung and W.-D. He, *Synth. Met.*, 2001, **122**, 263–266.
- 124 C. A. Kingsbury and D. Cram, *J. Am. Chem. Soc.*, 1960, **82**, 1810–1819.
- 125 T. Higashihara, C.-L. Liu, W.-C. Chen and M. Ueda, *Polymers*, 2011, **3**, 236–251.
- 126 K. H. Büchel, P. K. Claus, L. Ellinghaus, J. Falbe and G. Fengler, *Houben-Weyl Methods of Organic Chemistry vol. E 11, 4th edn Supplement: Organic Sulfur Compounds*, Thieme, 2014.
- 127 N. Ziegenbalg, F. V. Gruschwitz, T. Adermann, L. Mayr, S. Guriyanova and J. C. Brendel, *Polym. Chem.*, 2022, DOI: [10.1039/D2PY00598K](https://doi.org/10.1039/D2PY00598K).
- 128 Y. Suzuki, T. Higashihara, S. Ando and M. Ueda, *Macromolecules*, 2012, **45**, 3402–3408.
- 129 D. Mokude, A. Takasu and M. Higuchi, *Polymer*, 2017, **117**, 243–248.
- 130 C. Bouilhac, T. Rünzi and S. Mecking, *Macromolecules*, 2010, **43**, 3589–3590.
- 131 Y. Toshiyasu, Y. Taniguchi, K. Kimura, R. Fujishiro, M. Yoshihara, W. Tagaki and S. Oae, *Bull. Chem. Soc. Jpn.*, 1969, **42**, 1878–1881.

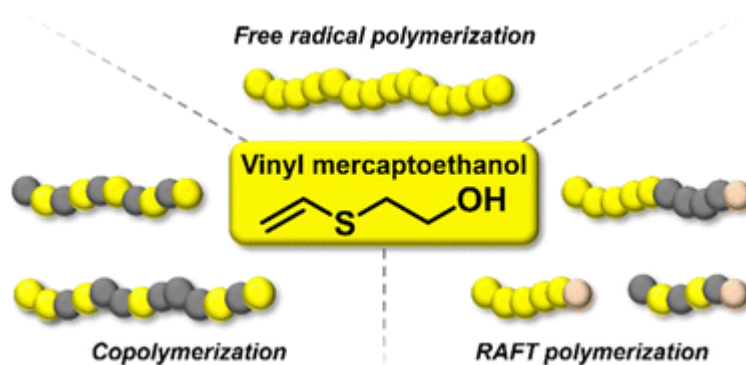
- 132 T. Clark, J. S. Murray, P. Lane and P. Politzer, *J. Mol. Model.*, 2008, **14**, 689–697.
- 133 T. Zhang, M. H. Litt and C. E. Rogers, *J. Polym. Sci., Part B: Polym. Phys.*, 1994, **32**, 1671–1676.
- 134 E. Klein, P. D. May, J. K. Smith and N. Leger, *Biopolymers*, 1971, **10**, 647–655.
- 135 J.-C. Lee, M. H. Litt and C. E. Rogers, *J. Polym. Sci., Part A: Polym. Chem.*, 1998, **36**, 793–801.
- 136 J. Choi and H.-i. Lee, *Bull. Korean Chem. Soc.*, 2021, **42**, 1143–1150.
- 137 D. Işık, E. Quaaş and D. Klinger, *Polym. Chem.*, 2020, **11**, 7662–7676.
- 138 T. Higashihara and M. Ueda, *Macromolecules*, 2015, **48**, 1915–1929.
- 139 N. Ziegenbalg, R. Lohwasser, G. D'Andola, T. Adermann and J. C. Brendel, *Polym. Chem.*, 2021, **12**, 4337–4346.
- 140 K. Ratzenböck, M. M. Ud Din, S. M. Fischer, E. Žagar, D. Pahovnik, A. D. Boese, D. Rettenwander and C. Slugovc, *Chem. Sci.*, 2022, **13**, 6920–6928.
- 141 T. Sasaki, S. Hashimoto, N. Nogami, Y. Sugiyama, M. Mori, Y. Naka and K. V. Le, *ACS Appl. Mater. Interfaces*, 2016, **8**, 5580–5585.
- 142 C. M. Possanza Casey and J. S. Moore, *ACS Macro Lett.*, 2016, **5**, 1257–1260.
- 143 H. Yaguchi and T. Sasaki, *Macromolecules*, 2007, **40**, 9332–9338.
- 144 T. Konstantinova and A. Draganov, *J. Appl. Polym. Sci.*, 1976, **20**, 351–355.
- 145 US2538100A, 1951.
- 146 E. J. Goethals, *Makromol. Chem.*, 1967, **109**, 132–142.
- 147 H. S. Choe, J. Giaccari, M. Alamgir and K. M. Abraham, *Electrochim. Acta*, 1995, **40**, 2289–2293.
- 148 F. C. Foster, *J. Am. Chem. Soc.*, 1952, **74**, 2299–2302.
- 149 A. Hirao, S. Loykulnant and T. Ishizone, *Prog. Polym. Sci.*, 2002, **27**, 1399–1471.
- 150 C. G. Overberger and A. M. Schiller, *J. Org. Chem.*, 1961, **26**, 4230–4232.
- 151 H. Diefenbach, F. H. Müller and H. Ringsdorf, *Kolloid-Z.*, 1966, **209**, 141–151.
- 152 J. Boor Jr. and A. M. T. Finch, *J. Polym. Sci., Part A-1: Polym. Chem.*, 1971, 249–252.
- 153 J. P. Schroeder, D. C. Schroeder and S. Jotikasthira, *J. Polym. Sci., Part A-1: Polym. Chem.*, 1972, **10**, 2189–2195.
- 154 Y. Zhang, F. Wang, L. Pan, B. Wang and Y. Li, *Macromolecules*, 2020, **53**, 5177–5187.
- 155 T. Okayasu, T. Hibino and H. Nishide, *Makromol. Chem. Phys.*, 2011, **212**, 1072–1079.
- 156 T. Okayasu, K. Saito, H. Nishide and M. T. W. Hearn, *Chem. Commun.*, 2009, **31**, 4708–4710.
- 157 T. Okayasu, K. Saito, H. Nishide and M. T. W. Hearn, *Green Chem.*, 2010, **12**, 1981–1989.
- 158 D. S. Breslow and G. E. Hulse, *J. Am. Chem. Soc.*, 1954, **76**, 6399–6401.
- 159 H. N. Öztö, F. Akyıldız and D. Saraydin, *Microsc. Res. Tech.*, 2020, **83**, 1487–1498.
- 160 A. Sepehrianazar and O. Güven, *Polym. Bull.*, 2022, DOI: [10.1007/s00289-022-04190-6](https://doi.org/10.1007/s00289-022-04190-6).
- 161 A. Rahmatpour, *Catal. Lett.*, 2012, **142**, 1505–1511.
- 162 Y. Nabae, J. Liang, X. Huang, T. Hayakawa and M.-a. Kakimoto, *Green Chem.*, 2014, **16**, 3596–3602.
- 163 K. Takahashi and H. Nishide, *Chem. Lett.*, 2013, **42**, 218–219.
- 164 H. Yamakita and S. Fujii, *J. Soc. Chem. Ind., Jpn.*, 1968, **71**, 430–432.
- 165 B. D. Smith, M. B. Soellner and R. T. Raines, *J. Biol. Chem.*, 2003, **278**, 20934–20938.
- 166 P. K. Dhal, S. R. Holmes-Farley, C. C. Huval and T. H. Jozefiak, in *Polymer Therapeutics I*, ed. R. Satchi-Fainaro and R. Duncan, Springer Berlin Heidelberg, Berlin, Heidelberg, 2006, pp. 9–58.
- 167 T. Hussain, M. Ansari, N. M. Ranjha, I. U. Khan and Y. Shahzad, *Sci. World J.*, 2013, **2013**, 340737–340746.
- 168 D. S. Breslow and A. Kutner, *J. Polym. Sci.*, 1958, **27**, 295–312.
- 169 H. Mori, E. Kudo, Y. Saito, A. Onuma and M. Morishima, *Macromolecules*, 2010, **43**, 7021–7032.
- 170 W. Kern and R. C. Schulz, *Angew. Chem., Int. Ed. Engl.*, 1957, **69**, 153–171.
- 171 D. Breslow, in *Encyclopedia Of Polymer Science and Technology*, John Wiley & Sons, Inc., 2011.
- 172 K. Sakaguchi and K. Nagase, *J. Soc. Chem. Ind., Jpn.*, 1966, **69**, 1204–1207.
- 173 S. A. Al-Hussain, A. M. Atta, H. A. Al-Lohedan, A. O. Ezzat and A. M. Tawfeek, *Nanomaterials*, 2018, **8**, 878.
- 174 J. Cao, Y. Tan, Y. Che and Q. Ma, *J. Polym. Res.*, 2011, **18**, 171–178.
- 175 J. Rottstegge, P. Kindervater, M. Wilhelm, K. Landfester, C. Heldmann, J. P. Fischer and H. W. Spiess, *Colloid Polym. Sci.*, 2003, **281**, 1111–1120.
- 176 X. Wang, X. Xie, C. Cai, E. Rytting, T. Steele and T. Kissel, *Macromolecules*, 2008, **41**, 2791–2799.
- 177 K. A. Cavicchi, *ACS Appl. Mater. Interfaces*, 2012, **4**, 518–526.
- 178 M. Yoshizawa-Fujita, W. Ogihara and H. Ohno, *Polym. Adv. Technol.*, 2002, **13**, 589–594.
- 179 H. Ohno, M. Yoshizawa and W. Ogihara, *Electrochim. Acta*, 2004, **50**, 255–261.
- 180 S. Yoshikawa, O.-K. Kim and T. Hori, *Bull. Chem. Soc. Jpn.*, 1966, **39**, 1937–1941.
- 181 C. G. Overberger, D. E. Baldwin and H. P. Gregor, *J. Am. Chem. Soc.*, 1950, **72**, 4864–4866.
- 182 J. C. Sauer and J. D. C. Wilson, *J. Am. Chem. Soc.*, 1955, **77**, 3793–3795.
- 183 C. S. Marvel, V. C. Menikheim, H. K. Inskip, W. K. Taft and B. G. Labbe, *J. Polym. Sci.*, 1953, **10**, 39–48.
- 184 E. De Witte and E. J. Goethals, *Makromol. Chem.*, 1968, **115**, 234–244.
- 185 T. H. Nguyen, S. J. Paluck, A. J. McGahran and H. D. Maynard, *Biomacromolecules*, 2015, **16**, 2684–2692.
- 186 H. Mori, Y. Saito, E. Takahashi, K. Nakabayashi, A. Onuma and M. Morishima, *Polymer*, 2012, **53**, 3861–3877.

- 187 H. Mori, Y. Saito, E. Takahashi, K. Nakabayashi, A. Onuma and M. Morishima, *React. Funct. Polym.*, 2013, **73**, 658–667.
- 188 W. Kern, R. C. Schulz and H. Schlesmann, *Makromol. Chem.*, 1960, **39**, 1–13.
- 189 A. S. Matlack, *J. Org. Chem.*, 1958, **23**, 729–731.
- 190 E. J. Goethals, J. Bombeke and E. d. Witte, *Makromol. Chem.*, 1967, **108**, 312–314.
- 191 Y. Iwakura, K. Uno, N. Nakabayashi and W.-Y. Chiang, *Bull. Chem. Soc. Jpn.*, 1969, **42**, 741–745.
- 192 D. S. Breslow, G. E. Hulse and A. S. Matlack, *J. Am. Chem. Soc.*, 1957, **79**, 3760–3763.
- 193 R. H. Wiley and F. B. Alvey, *J. Polym. Sci.*, 1962, **56**, 11–18.
- 194 R. H. Wiley and D. E. Gensheimer, *J. Polym. Sci.*, 1960, **42**, 119–123.
- 195 R. H. Wiley and P. Jäger, *J. Polym. Sci., Part A: Gen. Pap.*, 1964, **2**, 3327–3331.
- 196 J.-H. Baik, S. Kim, D. G. Hong and J.-C. Lee, *ACS Appl. Mater. Interfaces*, 2019, **11**, 29718–29724.
- 197 V. Aravindan, J. Gnanaraj, S. Madhavi and H. K. Liu, *Chemistry*, 2011, **17**, 14326–14346.
- 198 Y. Matsumura, T. Shiraiwa, T. Hayasaka, S. Yoshida and B. Ochiai, *J. Electrochem. Soc.*, 2018, **165**, B3119–B3121.
- 199 M. A. Gauthier, M. I. Gibson and H.-A. Klok, *Angew. Chem., Int. Ed.*, 2009, **48**, 48–58.
- 200 A. Das and P. Theato, *Chem. Rev.*, 2016, **116**, 1434–1495.
- 201 P. Espeel and F. E. Du Prez, *Macromolecules*, 2015, **48**, 2–14.
- 202 A. S. Goldmann, M. Glassner, A. J. Inglis and C. Barner-Kowollik, *Macromol. Rapid Commun.*, 2013, **34**, 810–849.
- 203 H. Müller, O. Nuyken and P. Strohriegel, *Makromol. Chem., Rapid Commun.*, 1992, **13**, 125–133.
- 204 P. Strohriegel, *Makromol. Chem.*, 1993, **194**, 363–387.
- 205 W. Kern, R. C. Schulz and D. Braun, *J. Polym. Sci.*, 1960, **48**, 91–99.
- 206 M. Iino, M. Igarashi and M. Matsuda, *Macromolecules*, 1979, **12**, 697–699.
- 207 J. Dong, L. Krasnova, M. G. Finn and K. B. Sharpless, *Angew. Chem., Int. Ed.*, 2014, **53**, 9430–9448.
- 208 J. C. Brendel, L. Martin, J. Zhang and S. Perrier, *Polym. Chem.*, 2017, **8**, 7475–7485.
- 209 Q. Chen, P. Mayer and H. Mayr, *Angew. Chem., Int. Ed.*, 2016, **55**, 12664–12667.
- 210 Q. Zheng, J. Dong and K. B. Sharpless, *J. Org. Chem.*, 2016, **81**, 11360–11362.
- 211 W. Reppe, *Acetylene chemistry*, CA Meyer, 1949.
- 212 V. Wascholowski, F. N. Windlin, P. Tuzina and P. Fournier, *German Pat.*, WO/2018/036848, 2018.
- 213 R. Lohwasser, P. Tuzina, F. Bienewald and D. P. Kunsmann-Keitel, *German Pat.*, 2020/221607, 2020.
- 214 A. D. Jenkins, *J. Polym. Sci., Part A: Polym. Chem.*, 1999, **37**, 113–126.
- 215 C. C. Price, *J. Polym. Sci.*, 1948, **3**, 772–775.
- 216 C. H. Bamford, A. D. Jenkins and R. Johnston, *Trans. Faraday Soc.*, 1959, **55**, 418–432.
- 217 S. Kawauchi, A. Akatsuka, Y. Hayashi, H. Furuya and T. Takata, *Polym. Chem.*, 2022, **13**, 1116–1129.
- 218 O. Ito and M. Matsuda, *Prog. Polym. Sci.*, 1992, **17**, 827–874.
- 219 S. Koltzenburg, M. Maskos and O. Nuyken, *Polymer Chemistry*, Springer Berlin, Heidelberg, 2017.

Publication P2

Vinyl mercaptoethanol as a reactive monomer for preparation of functional homo- and copolymers with (meth)acrylates

N. Ziegenbalg, F. V. Gruschwitz, T. Adermann, L. Mayr, S. Guriyanova and J. C. Brendel,
Polym. Chem., **2022**, *13*, 4934-4943.



Reproduced by permission of Royal Society of Chemistry. Copyright 2022.

The paper as well as the supporting information is available online:

doi.org/10.1039/D2PY00598K



Cite this: *Polym. Chem.*, 2022, **13**, 4934

Vinyl mercaptoethanol as a reactive monomer for the preparation of functional homo- and copolymers with (meth)acrylates†

Nicole Ziegenbalg,^{a,b} Franka V. Gruschwitz,^{a,b} Torben Adermann,^c Lukas Mayr,^c Svetlana Guriyanova^c and Johannes C. Brendel[✉]^{a,b}

In contrast to common more activated monomers (MAMs), such as (meth)acrylates or styrenes, vinyl thioethers remain a niche, despite their unique character featuring an electron rich vinyl moiety, which in contrast to vinyl ethers still enables good stabilization of a propagating radical. The sulfur-group further induces a variety of unique properties, for example, the ability to coordinate metals or increase the refractive index, but their limited availability certainly remained a major bottleneck in a wide range of applications of these monomers. Based on recent progress in the direct vinylation of mercaptans, we here demonstrate that vinyl mercaptoethanol (VME) represents a scalable reactive building block for the preparation of functional homo- and copolymers. The former are easily accessible by radical polymerization resulting in transparent, soft and very adhesive homopolymers with enhanced refractive indices compared to other non-aromatic polymers. The high density of hydroxyl groups renders the polymers polar and only soluble in corresponding solvents, but not in water. Only the further oxidation of the sulfide moiety to the more polar sulfoxide creates a water soluble and even slightly hygroscopic polymer. Copolymerizations of VME with common MAMs confirmed previous reports on the *Q*- and *e*-values of comparable vinyl thioethers and statistical copolymers with electron deficient vinyl monomers such as *n*-butylacrylate (BA) or methyl methacrylate (MMA) can be prepared with a tendency towards an alternating sequence. The resulting copolymers were tested for their optical and mechanical properties. The comparable reactivity of the radicals further facilitates the preparation of defined homo- and (block) copolymers with tunable lengths by the reversible addition fragmentation chain transfer (RAFT) process. Overall, the various reactivities of VME and the good compatibility with other MAMs in radical polymerizations render this industrially producible monomer certainly attractive for future materials design.

Received 9th May 2022,
Accepted 2nd August 2022

DOI: 10.1039/d2py00598k

rsc.li/polymers

Introduction

Poly(vinyl ethers) find widespread applications as coatings, adhesives, printing inks, or plasticizers and are commonly prepared by cationic polymerization.^{1–3} More recently, also radical polymerizations were adapted to prepare these polymers.^{4–6} Nevertheless, their ability to copolymerize with more activated monomers (MAMs), such as (meth)acrylate or styrene deriva-

tives, remains limited and only low amounts of vinyl ether monomers are incorporated.^{7,8} Interestingly, vinyl thioethers are generally more suitable for radical (co)polymerizations, as the 3d-orbital resonance of sulfur stabilizes the radicals at the adjacent carbon atom. Despite the early reports on the polymerization process and their ability to copolymerize, mostly by the groups of Ringsdorf and Otsu,^{9–14} this class of monomers have remained a niche in polymer chemistry. The sulfide group, however, further introduces unique characteristics into the corresponding polymers or materials, which, for example, comprises an increased refractive index,^{15–20} strong Raman signals for biomedical diagnostics,²¹ or the ability to coordinate a variety of transition metals.^{22–25} More recent reports on vinyl thioethers not only mostly focus on aromatic derivatives, such as the commercially available phenyl vinyl sulfide, but also include various other functionalities. In particular, the group of Mori is pursuing this research further and

^aLaboratory of Organic and Macromolecular Chemistry (IOMC), Friedrich Schiller University Jena, Humboldtstraße 10, 07743 Jena, Germany.

E-mail: johannes.brendel@uni-jena.de

^bJena Center for Soft Matter (JCSM), Friedrich Schiller University Jena, Philosophenweg 7, 07743 Jena, Germany

^cBASF SE, Carl-Bosch-Straße 38, 67056 Ludwigshafen/Rhein, Germany

† Electronic supplementary information (ESI) available. See DOI: <https://doi.org/10.1039/d2py00598k>

has demonstrated controlled radical polymerizations using reversible addition–fragmentation chain transfer (RAFT)^{26–30} and atom transfer radical polymerization (ATRP)^{31,32} techniques.

Limiting factors for a more widespread application of different types of these monomers are firstly their incompatibility with peroxide initiators, which are most commonly applied in industry.³³ Secondly, the synthesis of particular aliphatic derivatives proceeds either *via* toxic intermediates or requires harmful and malodorous reagents,^{34,35} which both complicate large scale productions. However, BASF SE has recently realized a scalable synthesis procedure to prepare vinyl mercaptoethanol (VME) based on the industrially established Reppe process.^{36–38} This approach opens up the possibility of producing the functional monomer VME on an industrial scale giving access to large quantities at reasonable costs and enabling the use of such vinyl thioethers in polymer chemistry. In this study, we investigated the polymerization behavior of this monomer in detail, which includes the ability to form defined polymers and block copolymers by the RAFT process. In addition, the resulting homo- and copolymers were examined in terms of their physical and mechanical properties.

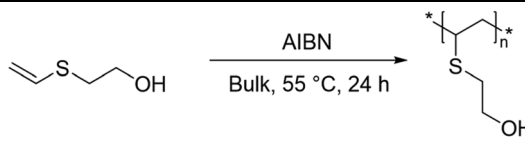
Results and discussion

Homo- and copolymerization behavior

In a first attempt, the monomer was polymerized in bulk using azo-initiators. The previous observations on the incompatibility with peroxide initiators could be confirmed and no polymerization occurred applying a common peroxide initiator (data not shown). The conversions were monitored using nuclear magnetic resonance spectroscopy (NMR) and size exclusion chromatography (SEC) (see ESI Fig. S1/S3†). The apparent polymerization rates determined for different amounts of AIBN are comparable with methacrylates under these conditions ($k_{\text{app}} = 0.003 \text{ min}^{-1}$ for the polymerization of MMA with 1% AIBN at 55 °C, see ESI Fig. S2†). An overview of the polymer characteristics is given in Table 1.

The prepared homopolymers were subsequently examined for their solubility. Despite the polar hydroxy groups, water appears to be a non-solvent for PVME, but nevertheless, these groups necessitate highly polar solvents to break potential hydrogen bonds they form. Therefore, only DMSO, DMF or methoxy ethanol appeared to be suitable solvents for the homopolymer. It is further worth mentioning that our first attempt to thoroughly dry the homopolymer resulted in a crosslinked material (gel formation upon addition of DMF as a good solvent, see ESI Fig. S4a†). A closer look at the drying conditions revealed that crosslinking (see the ESI, shoulder at higher molar masses in SEC, Fig. S5†) only occurs when the substances are kept at elevated temperatures (>40 °C) under vacuum. Simultaneous Thermal Analysis-Mass Spectrometry (STA-MS) measurements were performed to shed light on the underlying mechanism of this reaction (ESI, Fig. S4b†). At elev-

Table 1 Amount of initiator, polymerization rate, conversion, number average molar mass (M_n) and dispersity (D) values of the free radical polymerization of VME after 24 h



Initiator	k_{app}^a [min^{-1}]	Conversion ^b 24 h [%]	M_n^c [kg mol^{-1}]	D^c
0.1%	0.001	63	115.4	2.11
0.2%	0.002	81	140.2	2.2
1%	0.005	93	93.7	2.56

^a Determination from a linear increase of the graph in Fig. S1a.† ^b ¹H NMR (300 MHz, DMSO- d_6) after 24 h, determination *via* a hydroxyl group. ^c SEC (DMAc (+0.21 wt% LiCl), PMMA standards) after 24 h.

ated temperatures (>110 °C) water is released from the material. While it could still be entrapped in the material, the continuous increase in intensity also indicates release due to a condensation reaction (ESI Fig. S4c†), which results in the formation of ether links. But a further increase in temperature leads to another signal arising from the sample. The mass could be assigned to acetaldehyde, whose release can be explained by the second mechanism depicted in ESI Fig. S4c†. Both reactions are certainly accelerated in a vacuum, which explains the observed crosslinking at lower temperatures. To the best of our knowledge this phenomenon has not yet been observed with other hydroxide polymers, we assume that the sulfur has an activating effect on these crosslinking reactions.

In accordance with some previous studies on this monomer,^{39–41} we further investigated its copolymerization behavior with different vinyl monomers including styrene, methyl methacrylate (MMA), *n*-butyl acrylate (BA), vinyl pyrrolidone (VP) and vinyl acetate (VA) as representatives of different classes. The copolymerization parameters were determined according to the method established by Fineman and Ross (Table 2, further details in Fig. S6/7†).⁴² The results confirm a strong tendency to alternate with electron deficient MAMs such as acrylates, but also reveal a limited tendency to copolymerize with either electron rich MAMs (styrene) or LAMs such as vinyl acetate.^{13,14,39–41,43–45}

Table 2 Copolymerization parameters^a of VME with different comonomers

Comonomer	r_1	r_2
Styrene	0.04	5.88
Methyl methacrylate	0.07	0.48
<i>n</i> -Butyl acrylate	0.05	0.13
Vinyl pyrrolidone	0.22	3.28
Vinyl acetate	15.09	0.15

^a Determination according to the method of Fineman and Ross.⁴²

A classification of the monomer is possible by the determination of the corresponding Q and e values,⁴⁶ which mainly correspond to the ability of the reactive polymer end group to stabilize the radical and the polarity of the monomer, respectively. Similar to previous studies on vinyl thioethers, a reasonable stabilization of the radicals was confirmed by a Q -value of 0.45, which is close to methacrylates. The determined e -value ($e = -2.0$) is however more similar to vinyl ethers and reflects the high electron density of the vinyl group on this monomer, which confirms the tendency to alternate with electron deficient (meth)acrylates (see ESI Fig. S8†).

Reversible addition–fragmentation chain transfer (RAFT) polymerization

In addition, we investigated whether it is possible to prepare defined polymers by controlled polymerization techniques. Reversible addition–fragmentation chain transfer (RAFT) polymerization appeared as the most suitable method, since it tolerates a variety of functional moieties. In accordance with the previous observation on the stabilization of the radical end group, three different chain transfer agents (CTA) were tested: 2-(((butylthio)carbonothioyl)thio)propanoic acid (CTA I), 4-cyano-4-(((ethylthio)carbonothioyl)thio)pentanoic acid (CTA II), and cyanomethyl-*N*-methyl-*N*-phenyl-dithiocarbamate (CTA III). While the first is optimized for acrylate or styrene monomers, the second is required to control methacrylates due to a better transfer constant. CTA III is considered suitable for less activated monomers (LAMs) such as vinyl acetate or vinyl amides, which, however, appears unsuitable for the polymerization of VME, since molar masses do not increase with conversion and only broad distributions were obtained (see Fig. S11†). The other two CTAs instead result in well-defined polymers with dispersities below 1.2 (Fig. 1). Interestingly, the

molar mass distribution using CTA II appears to broaden towards higher conversions indicating some side reactions, which is also corroborated by enhanced tailing towards lower molar masses in the SEC traces (ESI Fig. S9 and S10†). Nevertheless, both CTAs result in a linear increase of molar mass with conversion.

The deviation of the experimental M_n with the theoretical value is related to the calibration of the SEC based on PMMA standards, which therefore only provides relative values. Absolute molar masses could however be derived from ¹H NMR spectroscopy comparing the signal of protons of the CTA end groups with the signal of the OH-group in the polymer (NMR spectra are given in Fig. S12,† the corresponding integrals are summarized in Table S7†). Since the dispersity of the RAFT polymerization with CTA II increased for the 24 h sample, the sample after 6 h of reaction time was exemplarily used to calculate the average molar mass. In the case of CTA I the sample is taken after 24 h was used. The determined molar masses agree well with the theoretical values (Table 3).

Based on the good control obtained with CTA I, we further extended the experiment to controlled copolymerizations of VME with BA and MMA (ESI Scheme S1†). Both cases resulted in narrowly distributed polymers (ESI, BA: Table S8/9 and Fig. S13, MMA: Table S10/11 and Fig. S14†). While the CTA is well suitable for the polymerization of BA, the observed good control in the case of MMA must be related to the high tendency for alternating incorporation of the monomers, which compensates for the inapt transfer expected for this CTA.

Another interesting aspect in this context was the synthesis of block copolymers (Scheme 1). Of particular interest is the sequence of monomer additions, which still enables the preparation of well-defined block copolymers.

Therefore, VME was first polymerized for 4 h in the presence of CTA I resulting in the narrowly distributed polymer PVME₆₂. After removal of the remaining monomer by precipitation, the macro-CTA was chain extended with BA. The low dispersity of the obtained block copolymer and the clear shift of the SEC traces towards higher molar mass prove the successful chain extension of the first block resulting in PVME₆₂-*b*-PBA₈₃ (Fig. 2a). It is noteworthy to mention that extended polymerization times (24 h) for the first block seems to strongly impact the ability of the macro-CTA to reinitiate during the block formation (ESI, Fig. S15†). We assume that the RAFT end groups are not fully retained after 24 h and are

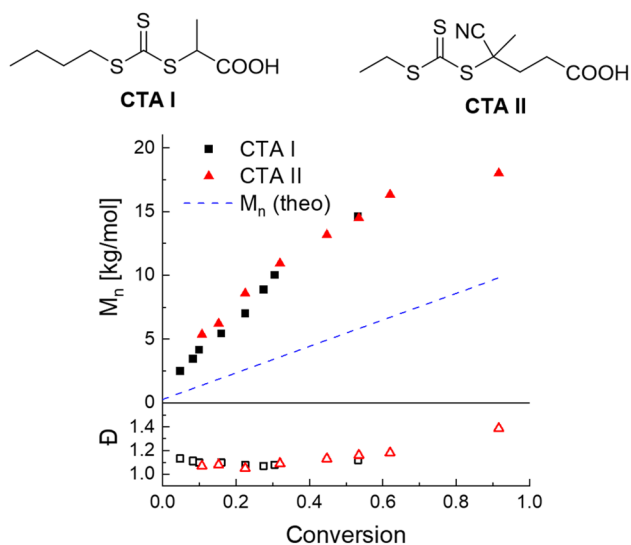
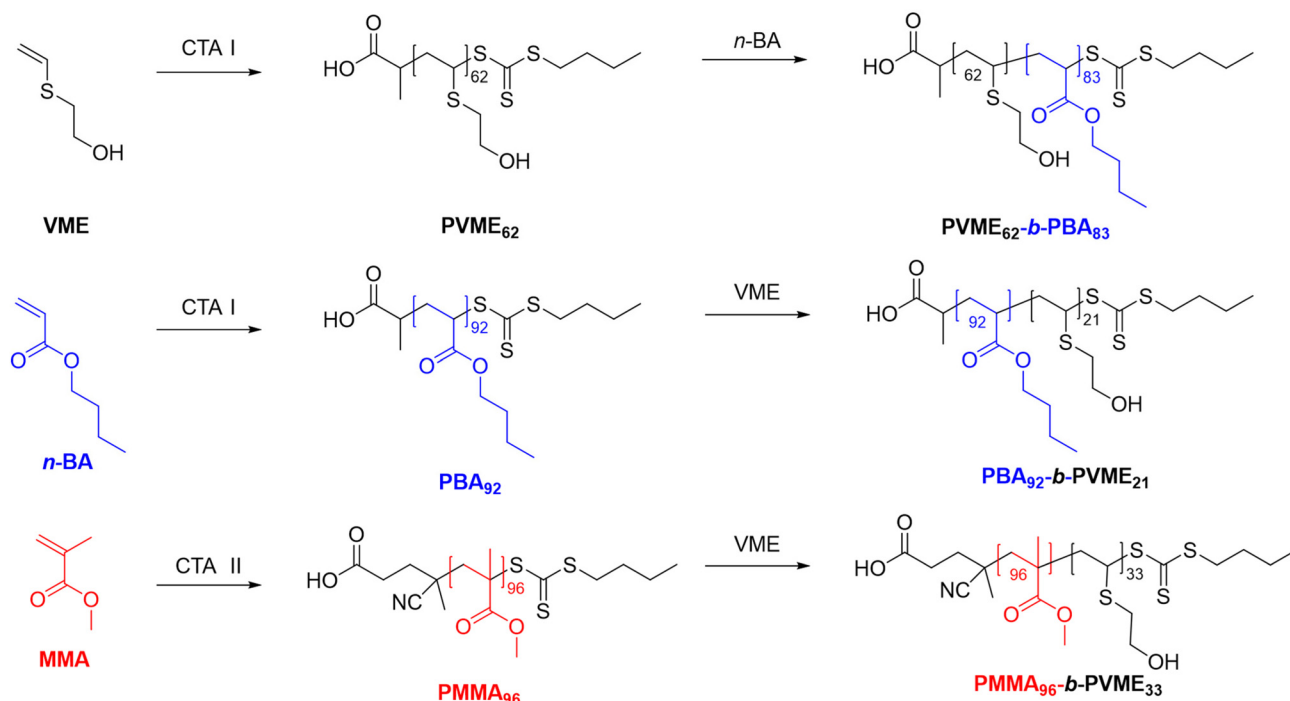


Fig. 1 Evolution of M_n (filled symbols) and dispersity (empty symbols) with increasing conversion during polymerization with CTA I (black squares) or CTA II (red triangles).

Table 3 Theoretical and practical determined values of the molar masses of the RAFT polymers

	M_n (SEC) ^a [g mol ⁻¹]	M_n (NMR) ^b [g mol ⁻¹]	M_n (theo.) ^c [g mol ⁻¹]
CTA I (24 h)	14 600	5800	6000
CTA II (6 h)	16 300	6700	7100

^a SEC (DMAc (+0.21 wt% LiCl), PMMA standards). ^b Determined by ¹H NMR (300 MHz)-spectroscopy comparing the signals specific for the CTA end group with signals of the repeating unit. ^c Determination from the conversion and the ratio of CTA and the monomer.



Scheme 1 Schematic representation of the different block copolymers.

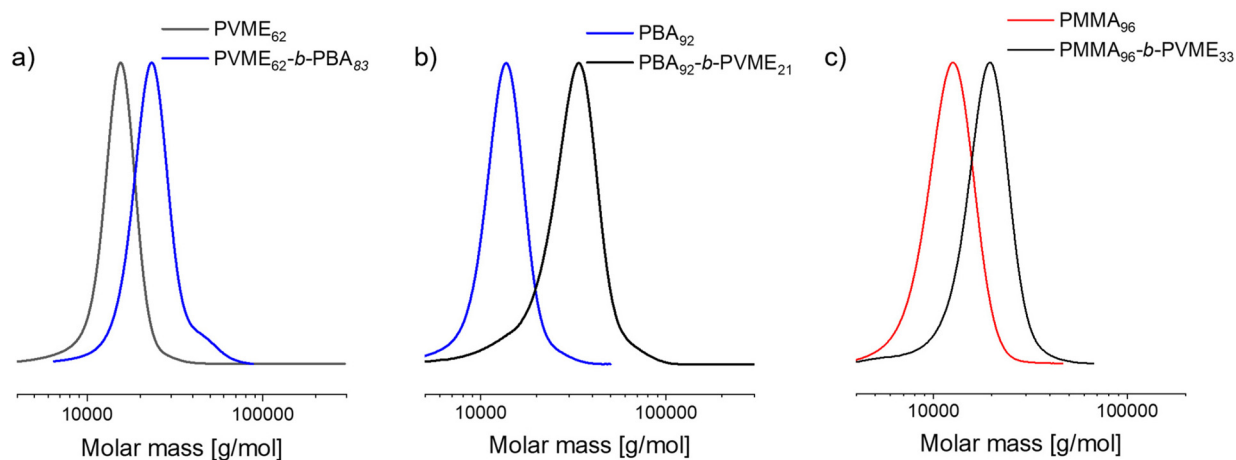


Fig. 2 SEC (DMAc (+0.21 wt% LiCl), PMMA standards) traces of the different block copolymers (a) PVME₆₂ and PVME₆₂-*b*-PBA₈₃, (b) PBA₉₂ and PBA₉₂-*b*-PVME₂₁, and (c) P(MMA₉₂) and PMMA₉₂-*b*-PVME₃₃.

cleaved either by additional radicals being formed or hydrolysis. In contrast to BA, the polymerization of MMA with the P(VME) macro-CTA did not form defined block copolymers despite the good copolymerization (see ESI Fig. S15[†]). Similar to macro-CTAs based on acrylates, we assume that the initial equilibrium in the RAFT process does not favour a sufficient transfer and the chains are not reinitiated equally fast compared to the propagation. Although we were not able to calculate transfer constants due to signals overlapping in the NMR, the obtained data suggest low transfer constants (<1) under these conditions. Considering the successful chain extension

with the acrylate monomer, these results further hint at a comparable stabilization of the radical chain end by a terminal VME unit as expected for acrylates or acrylamides despite the previously found *Q*-values, which were closer to methacrylates.

To gain a more detailed understanding of the block formation, we further reversed the order of blocks and started with BA or MMA instead. The first was polymerized in the presence of CTA I and then extended with VME. This order also resulted in successful block formation indicated by the nearly complete shift of the SEC trace (Fig. 2b) and the polymer PBA₉₂-*b*-PVME₂₁ was obtained. Due to the rather low

propagation rate of VME only low conversions could be achieved in 4 h, which was again chosen to minimize any side reactions. The macro-CTA PMMA₉₂ was successfully synthesized using CTA II, and again a well-controlled second block was formed starting the polymerization of VME in the presence of this macro-CTA (Fig. 2c). The successful chain extension in this case further corroborates the previous assumptions on the reactivity of the different chain ends.

Modification of homopolymers by oxidation

The polarity and thus the solubility of the presented sulfur-based polymers changes fundamentally if the sulfide groups are oxidized to sulfoxides or sulfones.^{48,47,49} We have already reported that the monomer can be selectively oxidized to sulfoxide or sulfone using hydrogen peroxide as the oxidizing agent.⁵⁰ The resulting electron-poor vinyl compounds were, however, not suitable for direct radical polymerizations or showed only low reactivity. While the vinyl sulfinylethanol monomer did not polymerize at all, the conversions of vinyl sulfonylethanol (VSE) remain very low (<5%) and also the molar mass is considerably lower (10 600 g mol⁻¹ after 48 h at 65 °C, see Fig. S16†) than the molar mass (67 100 g mol⁻¹ after 24 h at 65 °C, see ESI Fig. S3†) of PVME obtained under comparable conditions. An alternative route is the post-polymerization oxidation of the homopolymer PVME (Fig. 3). Dissolving the polymer in DMF the oxidation can mildly be induced by the addition of hydrogen peroxide ($c_{\text{final}} = 0.2 \text{ g mL}^{-1}$). The conversion calculation was performed using the integrals of the hydroxide group ($\delta = 5.05$ and 4.85 ppm), which showed a clear low field shift of the oxidized species compared to the PVME (Fig. 3c). The kinetics of the reaction indicate a rapid conversion of approximately 20% of the sulfide within the first minutes, which is followed by slower but continuous oxidation of nearly all thioether moieties (>90%) (Fig. 3b). While the NMR spectra indicate conversion of the sulfide an unequivocal identification of the resulting species (sulfoxide or sulfone) was not possible in these ¹H NMR spectra. Therefore, we conducted additional experiments to analyze the observed state of oxidation under different conditions for the oxidation. Firstly, the initial oxidation with only hydrogen peroxide was repeated and kept for 24 hours at room temperature. Similarly, we also tested the reaction at elevated temperatures (60 °C) and in the presence of the catalyst sodium tungstate, which was used to convert the monomer VME to the corresponding sulfone. The resulting polymers were purified and analyzed in detail by Infrared (IR)- and Heteronuclear single quantum coherence (HSQC)-NMR-spectroscopy. A closer look at the latter revealed high selectivity of the different oxidation procedures. While the initially used, milder conditions almost selectively form sulfoxide moieties, a clear shift of the signal of the SO-CH₂ group (3.29 ppm, 49.49 ppm) with respect to the signal of the SO₂-CH₂ group (3.44 ppm, 53.65 ppm) was observed for the reaction at elevated temperatures and with the catalyst (Fig. S17†). The additional IR-spectra confirmed these clear differences between the two samples, as distinctive signals for the sulfoxide and sulfone groups are observed (Fig. 3d and e,

SO stretching $\approx 1020 \text{ cm}^{-1}$, SO₂ stretching $\approx 1280 \text{ cm}^{-1}$). The comparison with polyvinyl sulfonylethanol prepared by the radical polymerization of the sulfone monomer substantiates that the oxidation without a catalyst leads to sulfoxide, while the one with the catalyst and higher temperatures creates the sulfone, as these signals overlap well.

Thermal properties of the prepared homo- and copolymers

For a more detailed examination of the thermal properties of the polymers, larger batches of different homopolymers, the most interesting copolymers and block copolymers were prepared and purified (for NMR spectra see Fig. S18†). We first focused on PVME and its oxidized analogues. Interestingly, TGA measurements revealed that the original sulfide-based polymer exhibits high thermal stability (>300 °C), while the analysis of the oxidized PVME results in a significant loss of mass at around 150 °C (see ESI Fig. S18a†). The more polar sulfoxide groups seem to destabilize the integrity of the polymer. In contrast, the sulfone moiety as in the directly prepared PVSE appears to increase the stability again. As verified by DSC measurements, the glass transition temperatures (T_g) of the polymers shift significantly with the oxidation of the polymer. While PVME features a T_g of around room temperature (ESI Fig. S18b†) corresponding to its soft appearance, the glass transition of the oxidized variant could not be found below the decomposition temperature. However, PVSE reveals a glass transition at 97 °C.

We further examined the different copolymers prepared by free radical polymerization. Similar to the homopolymer, all copolymers showed high thermal stability with significant mass losses only occurring at temperatures >300 °C (data not shown). The glass transition temperatures, in turn, change in comparison with the pure homopolymers as expected for random copolymers (Table S12 and ESI Fig. S20†). In comparison to pure PMMA an increasing content of VME leads to a corresponding shift of the glass transition temperature to lower values. Considering the T_g value of PVME, a linear correlation between the composition and glass transition can be estimated, as observed for other random copolymers (Fig. 4). A similar shift of T_g , but in the opposite direction, is observed for the copolymers of VME with BA. In this case an increase of the glass transition temperature to -17 °C is observed compared to the homopolymer PBA.

We further examined the more defined polymers prepared by RAFT (ESI Table S13/14 and Fig. S21/22†). The random copolymers displayed a similar trend and were mostly independent of the overall molar mass of the polymer and an average T_g value between both homopolymers is observed (Fig. 6). However, if the block copolymers are considered, the results differ significantly. In particular for the block copolymers of VME with BA, multiple glass transition temperatures are found, which correspond to the T_g estimated for the individual homopolymers (Fig. 5). This data indicates a micro-phase separation in the bulk of these polymers. Surprisingly, two clear glass transition temperatures and thus phase separation can even be observed for the block copolymer PBA₉₂-*b*-PVME₂₁ with a very short block of VME. This result exemplifies

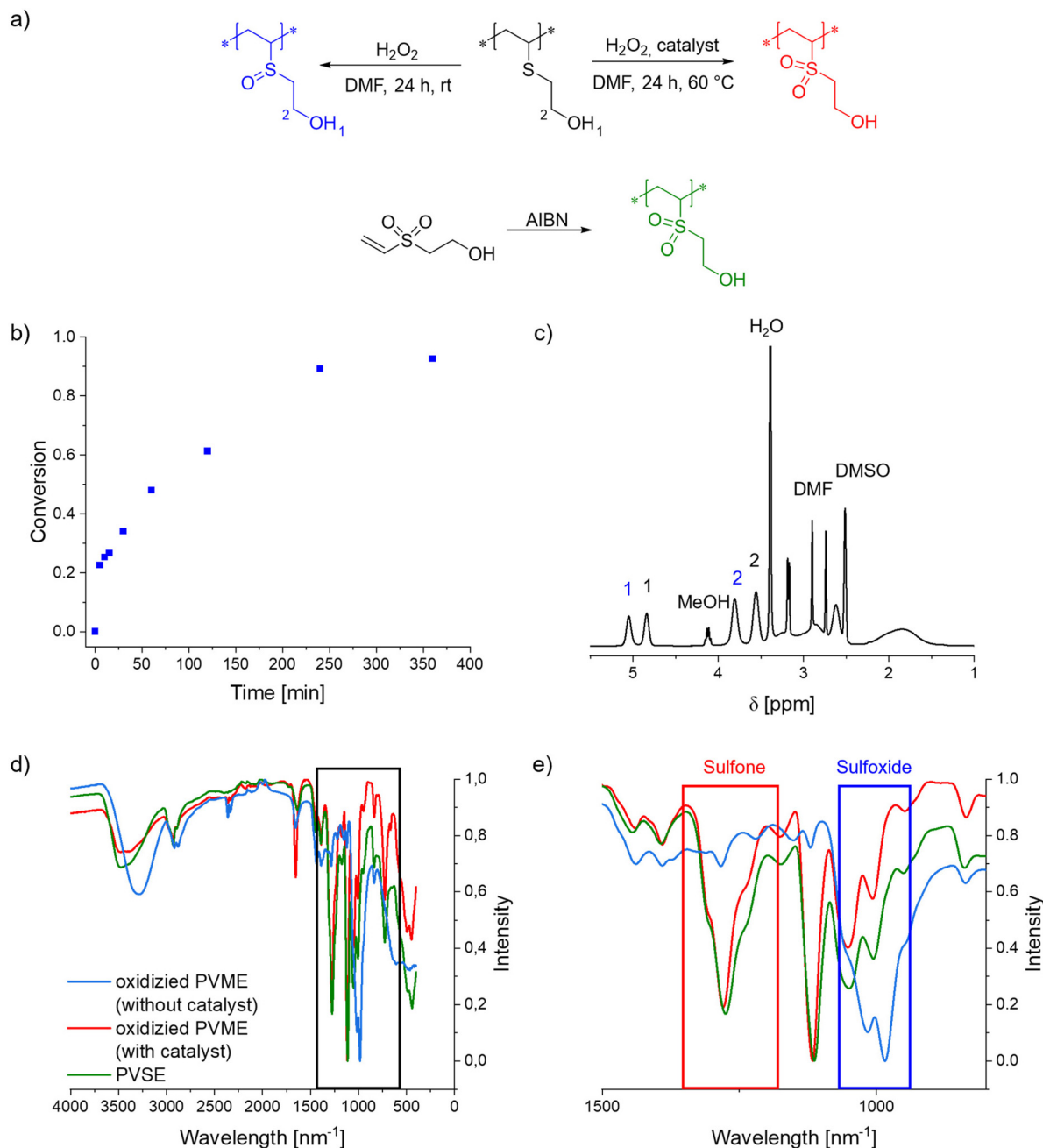


Fig. 3 (a) Schematic representation of the oxidation of PVME at different conditions and the radical polymerization of vinyl sulfonylethanol, (b) Plot of conversion versus time of the oxidation of PVME without a catalyst, (c) ^1H NMR-spectrum (300 MHz, DMSO-d_6 , 298 K) of the kinetic sample of the oxidation of PVME after 60 min without a catalyst, (d) IR-spectra and (e) enlarged section of the IR-spectra of the different oxidized polymers.

a strong difference in the polarity of the polymers and further hints at a rather high χ parameter for these polymers. Further investigations by small angle X-ray scattering (SAXS) would be required to analyze the resulting morphology, but this aspect was beyond the scope of this study. Nevertheless, the data already indicate interesting potential for the creation of very small domains in block copolymer bulk materials or thin films, which could be of interest for future applications in nanolithography or surface patterning.^{51–53}

Optical and mechanical properties of homo- and copolymers

Considering the similar thermal properties and the easier access to larger amounts, we further focused on the homo- and copolymers prepared by free radical polymerization to study their material characteristics in more detail. In contrast to the yellow polymers prepared by RAFT polymerization (the color is induced by the trithiocarbonate moiety of the CTA end group), the homopolymers and copolymers prepared by free

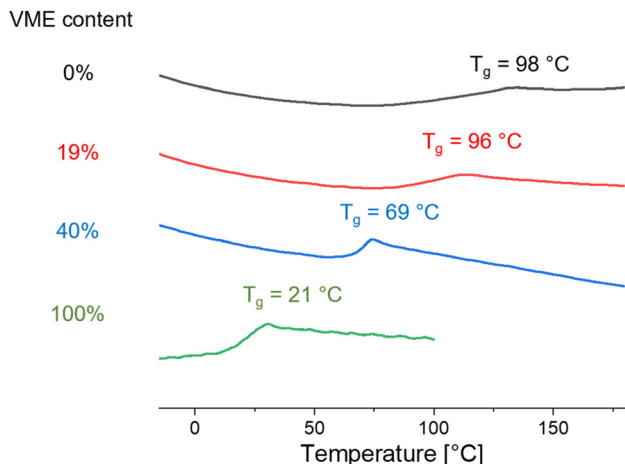


Fig. 4 DSC-data of the different copolymers P(MMA-co-VME) containing 10% VME (P2) or 40% VME (P3) in comparison to the corresponding homopolymers PMMA and PVME (P1). All polymers were synthesized by free radical polymerization.

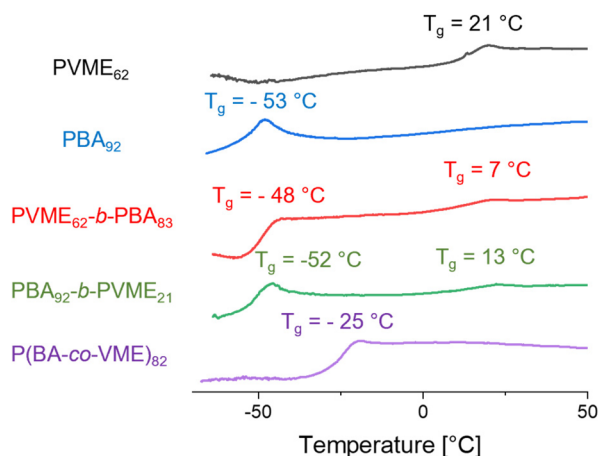


Fig. 5 DSC-data of the block copolymers PVME₆₂-b-PBA₈₃ (R14) and PBA₉₂-b-PVME₂₁ (R16) in comparison to the homopolymers PVME₆₂ (R13) and PBA₉₂ (R15), as well as the random copolymer P(BA-co-VME)₈₂ (R3). All polymers were synthesized using RAFT.

radical polymerization appear colorless and highly transparent. The refractive indices of these polymers were first estimated by ellipsometry measurements of thin films prepared on glass slides with thicknesses of approximately 4 μm . According to the Lorentz–Lorentz equation, high refractive indices can be expected for sulfur-containing substances because of the high atomic refraction^{17,54} However, ellipsometry measurements revealed that the homopolymer PVME had only a slightly increased refractive index ($n_D = 1.55$) compared to other common acrylates or methacrylates (e.g. PMMA: $n_D = 1.48$). It has to be mentioned that issues with reflections during the measurements have led to relatively high uncertainties in the absolute values, but the overall trend remains valid.

In accordance, we estimated the refractive indices of the copolymers, which are in between both values for the homopolymers and following a linear trend with increasing amounts of VME (Fig. S23[†]). While exceptional refractive indices cannot be achieved by incorporation of VME, good copolymerization allows fine-tuning of these properties by incorporating different amounts of VME. In addition to the refractive index, we further examined whether the incorporation of VME alters the high optical transparency of PMMA. Therefore, thicker films (50–70 μm) were prepared by drop casting and their absorption in the visible range was analyzed by UV-Vis spectroscopy (Fig. 6b). Neither additional absorption bands nor a significant increase of the general absorption in the visible range becomes apparent from these measurements, which can also visually be confirmed by the high transparency of the material.

Since not only the optical properties are important for application, we also examined the mechanical properties of the polymer films at room temperature by nanoindentation measurements. These investigations provide information on elastic modulus, hardness, and creep of the materials and were performed on very thick (>50 μm) drop cast films (Fig. 6 and ESI Table S15[†]). First measurements on PVME confirmed the soft nature of the polymer with an elastic modulus of only 4.4 MPa and a hardness of only around 0.1 MPa. Interestingly, the copolymer of VME with BA resulted in comparable values with only a slightly lower modulus of 2.5 MPa, although the glass transition temperature is nearly 40 $^\circ\text{C}$ lower and far below room temperature. Similar surprising characteristics are observed when comparing the creep of both materials by applying a constant load of 0.3 mN. While the copolymer was deformed by less than 400 nm, the homopolymer PVME resulted in a much higher indentation of nearly 1000 nm at the same load. We assume that the unexpected hardness and low creep of the copolymer despite its much lower T_g might be induced by the higher average molar mass of the copolymer, but it might also arise from additional inter-chain interactions within the nearly alternating sequence of low polar BA and more polar VME units. In addition to the previously described soft polymers, we tested the impact of increasing VME content on the mechanical properties of MMA-based polymers. Considering the characteristics of the homopolymer, we initially expected that the incorporation of VME might deteriorate the good mechanical stability of PMMA. However, both elastic modulus and hardness remain nearly constant even when 40% of VME is incorporated into the copolymer. The result is further corroborated by a nearly identical creep behavior of all three tested polymers. The results, therefore, rebut any detrimental effects of even a quite high content of VME on the mechanical properties of P(MMA-co-VME) copolymers, which renders these polymers still well suited for common applications of PMMA but where reduced glass transition temperatures, slightly increased refractive indices, or increased polarity of the polymers might be of further advantage.

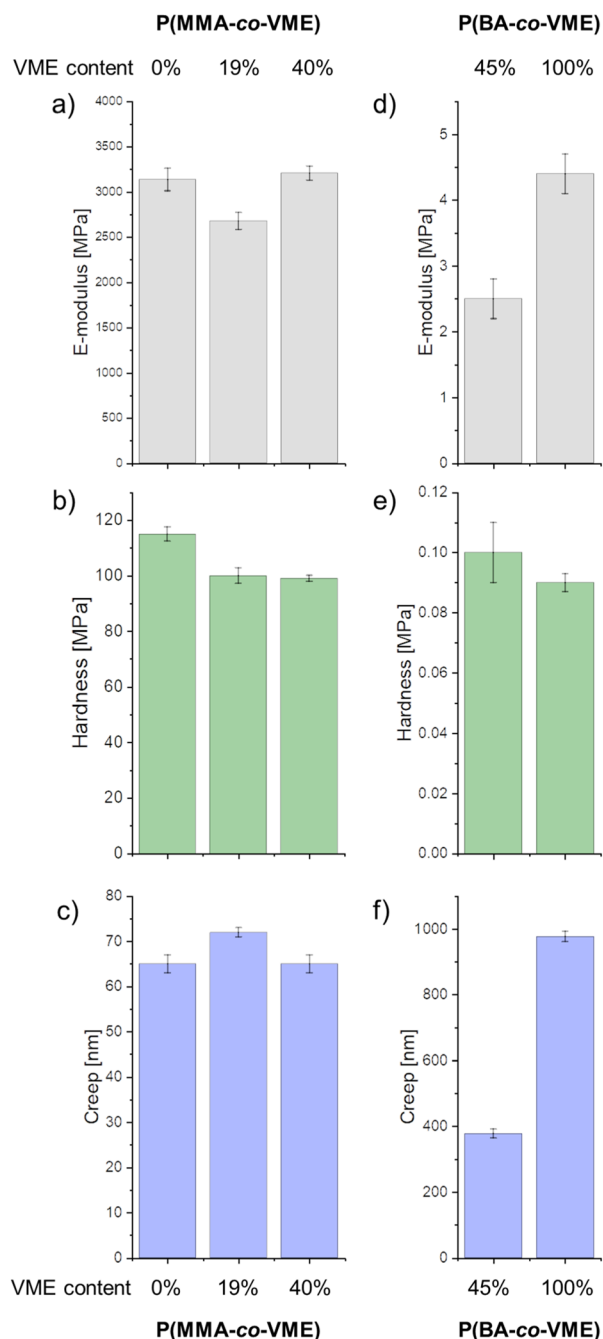


Fig. 6 Mechanical properties of (a–c) the homopolymer PMMA and the copolymers P(MMA-co-VME) containing 10% VME (P2) or 40% VME (P3), which were determined via nano-indenter measurements with a load of 1 mN. Similarly, the homopolymer PVME (P4) and the copolymer P(BA-co-VME) (P1) (d–f) were tested with with a reduced load of 0.3 mN.

Conclusion

In conclusion, we have investigated the behavior of vinyl mercaptoethanol (VME), an industrially scalable vinyl thioether, in free and controlled radical polymerizations. The thioether or sulfide unit induces similar stabilization of the radical chain end as observed for acrylates, while the apparent polymerization rate is

reduced in comparison. The high electron density on the vinyl group favors good copolymerization with electron deficient vinyl monomers such as acrylates or methacrylates with a tendency to alternating monomer incorporation. The RAFT polymerization further enables access to well-defined homo- and copolymers, as well as block copolymers. While during block formation with *n*-butyl acrylate both orders of monomer addition result in well-defined block copolymers, the polymerization of MMA cannot be controlled by a PVME macro-CTA, which again exemplifies similar stabilization of the radical chain end compared to acrylates. The homopolymer PVME is only soluble in very polar solvents but despite the high density of hydroxyl units not in water. The high reactivity of the thioether moiety further allowed the post polymerization oxidation of PVME by hydrogen peroxide. The resulting sulfoxide moieties render the polymer well-soluble in water and induce even a hygroscopic character. Direct preparation of this polymer is otherwise not possible by radical polymerization of the oxidized monomers.

In addition to the (co)polymerization behavior of VME we examined the resulting thermal, optical, and mechanical properties of the different polymers. The homopolymer appears very soft with its glass transition temperature around room temperature and features a slightly increased refractive index compared to other aliphatic vinyl polymers. Nanoindentation measurements further corroborated the soft nature of the material. As expected, average T_g s were observed for the copolymers with BA and MMA correlating with the content of the incorporated VME. To our surprise, all block copolymers featured two glass transition temperatures even in the case of very small blocks of VME (DP = 21). This proof of microphase separation at even low degrees of polymerization opens up an interesting opportunity to access very small domain sizes, but more detailed studies are certainly required to gain a detailed understanding of the morphology evolution. An interesting feature is further observed for the copolymers with MMA. While an increasing content of VME reduced the glass transition temperature, the mechanical properties at room temperature and optical transparency appear not to be impaired even with 40% VME incorporation. These modifications not only enable the adjustment of the refractive index, but further introduce increased polarity and additional functionalities (sulfide and hydroxyl units) to the material, which certainly alter its physical properties. In summary, the improved accessibility of VME by the industrially scalable process by BASF SE makes this monomer attractive not only for modifications of common and technically applied acrylates and methacrylates but also features interesting characteristics as a homopolymer due to its unique reactivity. The incompatibility with peroxide initiators certainly remains a limitation for commodity products, but this aspect might be less relevant if speciality chemicals are considered, where the unique properties can open up interesting potential for applications.

Conflicts of interest

There are no conflicts to declare.

Acknowledgements

The presented study is part of a research project funded by BASF SE to identify and develop applications for vinyl mercaptoethanol (VME). J. C. B. thanks the German Science Foundation (DFG) for generous funding within the Emmy-Noether Programme (Project-ID: 358263073). Prof. U. S. Schubert is furthermore acknowledged for his continuous support and access to excellent research facilities. In addition, the authors thank BASF SE's Material Physics department for the ellipsometry and nano-indentation measurements, R. Paulus for the TGA and DSC measurements, and H. F. Ulrich for the IR measurements.

References

- G. Schröder, *Ullmann's Encyclopedia of Industrial Chemistry*, Wiley-VCH, 2000.
- G. Mengoli and G. Vidotto, *Eur. Polym. J.*, 1972, **8**, 671–680.
- E. Kirillov, K. Rodygin and V. Ananikov, *Eur. Polym. J.*, 2020, **136**, 109872.
- S. Sugihara, Y. Kawamoto and Y. Maeda, *Macromolecules*, 2016, **49**, 1563–1574.
- S. Sugihara, A. Yoshida, T.-a. Kono, T. Takayama and Y. Maeda, *J. Am. Chem. Soc.*, 2019, **141**, 13954–13961.
- Q. Lee, D. J. T. Hill, T. Le, F. Rasoul and A. K. Whittaker, *Polym. Int.*, 2009, **58**, 348–353.
- J. C. Bevington, B. J. Hunt and A. D. Jenkins, *J. Macromol. Sci., Part A: Pure Appl. Chem.*, 2000, **37**, 609–619.
- H. Braun, Y. Yagci and O. Nuyken, *Eur. Polym. J.*, 2002, **38**, 151–156.
- C. C. Price and J. Zomlefer, *J. Am. Chem. Soc.*, 1950, **72**, 14–17.
- K. Tsuda, S. Kobayashi and T. Otsu, *J. Macromol. Sci., Part A: Pure Appl. Chem.*, 1967, **1**, 1025–1037.
- K. Gollmer and H. Ringsdorf, *Colloid Polym. Sci.*, 1967, **216**, 325–329.
- K. D. Gollmer, F. H. Müller and H. Ringsdorf, *Makromol. Chem.*, 1966, **92**, 122–136.
- T. Otsu and H. Inoue, *Makromol. Chem.*, 1969, **128**, 31–40.
- T. Otsu and H. Inoue, *J. Macromol. Sci., Part A: Pure Appl. Chem.*, 1970, **4**, 35–50.
- J.-g. Liu, Y. Nakamura, Y. Shibasaki, S. Ando and M. Ueda, *Macromolecules*, 2007, **40**, 4614–4620.
- J.-g. Liu, Y. Nakamura, Y. Suzuki, Y. Shibasaki, S. Ando and M. Ueda, *Macromolecules*, 2007, **40**, 7902–7909.
- J.-g. Liu and M. Ueda, *J. Mater. Chem.*, 2009, **19**, 8907–8919.
- N.-H. You, T. Higashihara, Y. Oishi, S. Ando and M. Ueda, *Macromolecules*, 2010, **43**, 4613–4615.
- R. Okutsu, Y. Suzuki, S. Ando and M. Ueda, *Macromolecules*, 2008, **41**, 6165–6168.
- Y. Suzuki, T. Higashihara, S. Ando and M. Ueda, *Polym. J.*, 2009, **41**, 860–865.
- R. Perez-Pineiro, S. Dai, R. Alvarez-Puebla, J. Wigginton, B. J. Al-Hourani and H. Fenniri, *Tetrahedron Lett.*, 2009, **50**, 5467–5469.
- G. R. Anpilogova, A. I. Vorob'eva, S. A. Onina, R. A. Khisamutdinov, Y. I. Murinov and Y. B. Monakov, *Russ. J. Appl. Chem.*, 2006, **79**, 1593–1599.
- K. Furukawa, K. Ebata, H. Nakashima, Y. Kashimura and K. Torimitsu, *Macromolecules*, 2003, **36**, 9–11.
- H.-M. Huang, C.-Y. Chang, I. C. Liu, H.-C. Tsai, M.-K. Lai and R. C.-C. Tsiang, *J. Polym. Sci., Part A: Polym. Chem.*, 2005, **43**, 4710–4720.
- E. B. Troughton, C. D. Bain, G. M. Whitesides, R. G. Nuzzo, D. L. Allara and M. D. Porter, *Langmuir*, 1988, **4**, 365–385.
- Y. Abiko, A. Matsumura, K. Nakabayashi and H. Mori, *Polymer*, 2014, **55**, 6025–6035.
- Y. Abiko, A. Matsumura, K. Nakabayashi and H. Mori, *React. Funct. Polym.*, 2015, **93**, 170–177.
- Y. Abiko, K. Nakabayashi and H. Mori, *Macromol. Symp.*, 2015, **349**, 34–43.
- K. Nakabayashi, Y. Abiko and H. Mori, *Macromolecules*, 2013, **46**, 5998–6012.
- K. Nakabayashi, A. Matsumura, Y. Abiko and H. Mori, *Macromolecules*, 2016, **49**, 1616–1629.
- T. Kameyama and A. Takasu, *Polym. Chem.*, 2015, **6**, 4336–4342.
- T. Kameyama and A. Takasu, *Key Eng. Mater.*, 2015, **654**, 37–41.
- V. K. Gollmer and H. Ringsdorf, *Makromol. Chem.*, 1969, **121**, 227–239.
- A. Schöberl and M. Biedermann, *Justus Liebigs Ann. Chem.*, 1968, **716**, 37–46.
- S. V. Amosova, A. S. Atavin and B. A. Trofimov, *Bull. Acad. Sci. USSR, Div. Chem. Sci.*, 1967, **16**, 596–600.
- V. Wascholowski, F. N. Windlin, P. Tuzina and P. Fournier, WO2018/036848A1, 2018.
- R. Lohwasser, P. Tuzina, F. Bienewald and D. P. Kunsmann-Keitel, WO2020/221607A1, 2020.
- W. Reppe, *Acetylene chemistry*, CA Meyer, 1949.
- A. I. Vorob'eva, M. N. Gorbunova, R. R. Muslukhov and S. V. Kolesov, *Russ. J. Appl. Chem.*, 2011, **84**, 1940–1944.
- A. I. Vorob'eva, S. A. Onina, I. D. Musina, S. V. Kolesov, R. R. Muslukhov, L. Parshina, L. A. Oparina, B. A. Trofimov and Y. B. Monakov, *Polym. Sci., Ser. B*, 2004, **46**, 364–368.
- A. I. Vorob'eva, S. A. Onina, R. R. Muslukhov, S. V. Kolesov, L. Parshina, M. Y. Khil'ko, B. A. Trofimov and Y. B. Monakov, *Polym. Sci., Ser. B*, 2003, **45**, 102–105.
- M. Fineman and S. D. Ross, *J. Polym. Sci.*, 1950, **5**, 259–265.
- C. C. Price and H. Morita, *J. Am. Chem. Soc.*, 1953, **75**, 4747–4750.
- C. E. Scott and C. C. Price, *J. Am. Chem. Soc.*, 1959, **81**, 2672–2674.
- K. Tsuda, S. Kobayashi and T. Otsu, *J. Macromol. Sci., Part A: Pure Appl. Chem.*, 1968, **6**, 41–48.
- T. Alfrey Jr. and C. C. Price, *J. Polym. Sci.*, 1947, **2**, 101–106.
- E. Lallana and N. Tirelli, *Macromol. Chem. Phys.*, 2013, **214**, 143–158.
- F. H. Sobotta, F. Hausig, D. O. Harz, S. Hoepfener, U. S. Schubert and J. C. Brendel, *Polym. Chem.*, 2018, **9**, 1593–1602.

- 49 D. Jeanmaire, J. Laliturai, A. Almalik, P. Carampin, d. A. Richard, E. Lallana, R. Evans, R. E. P. Winpenny and N. Tirelli, *Polym. Chem.*, 2014, **5**, 1393–1404.
- 50 N. Ziegenbalg, R. Lohwasser, G. D'Andola, T. Adermann and J. C. Brendel, *Polym. Chem.*, 2021, **12**, 4337–4346.
- 51 J. Bang, U. Jeong, D. Y. Ryu, T. P. Russell and C. J. Hawker, *Adv. Mater.*, 2009, **21**, 4769–4792.
- 52 S.-J. Jeong, J. Y. Kim, B. H. Kim, H.-S. Moon and S. O. Kim, *Mater. Today*, 2013, **16**, 468–476.
- 53 S. Krishnamoorthy, C. Hinderling and H. Heinzlmann, *Mater. Today*, 2006, **9**, 40–47.
- 54 J. G. Speight, N. A. Lange and J. A. Dean, *Lange's Handbook of Chemistry*, McGraw-Hill Professional Publishing, New York, USA, 2005.

Supplementary Information for

Vinyl mercaptoethanol as a reactive monomer for preparation of functional homo- and copolymers with (meth)acrylates

Nicole Ziegenbalg,^{a,b} Franka V. Gruschwitz,^{a,b} Torben Adermann,^c Lukas Mayr,^c Svetlana Guriyanova,^c Johannes C. Brendel,^{a,b,*}

a Laboratory of Organic and Macromolecular Chemistry (IOMC), Friedrich Schiller University Jena, Humboldtstraße 10, 07743 Jena, Germany

b Jena Center for Soft Matter (JCSM), Friedrich Schiller University Jena, Philosophenweg 7, 07743 Jena, Germany

c BASF SE, Carl-Bosch-Straße 38, 67056 Ludwigshafen/Rhein, Germany

*corresponding author: johannes.brendel@uni-jena.de

Experimental part

Materials and Methods

All reagents and solvents were commercially purchased from Sigma-Aldrich, TCI Chemicals, and abcr, or were provided by BASF SE. All were used without further purification.

¹H-NMR spectra were measured with a Bruker spectrometer (300 MHz) equipped with an Avance I console, a dual ¹H and ¹³C sample head and a 120 x BACS automatic sample changer and a Bruker spectrometer (400 MHz) equipped with an Avance III console, a BBO sample head and a 60 x BACS automatic sample changer. The chemical shifts of the peaks were determined by using the residual solvent signal as a reference and are given in ppm in comparison to TMS. Deuterated solvents were commercially purchased from EURISO-TOP GmbH.

Size-exclusion chromatography (SEC) of polymers was performed on an Agilent system (series 1200) equipped with a PSS degasser, a G1310A pump, a G1362A refractive index detector and a

PSS GRAM 30 and 1000 column with DMAc (+ 0.21 wt.% LiCl) as eluent at a flow rate of 1 mL/min. The column oven was set to 40 °C and poly(methyl methacrylate) (PMMA) standards were used for calibration.

The differential scanning calorimetry (DSC) measurements were performed on a DSC 204 F1 Phoenix[®] from Netzsch under a nitrogen atmosphere with a heating rate of 10 K/min. The thermal gravimetric analysis (TGA) was carried under nitrogen using a Netzsch TG 209F1.

Simultaneous Thermal Analysis (STA) measurements were carried out using an Netzsch 449 F3 Jupiter[®] and Netzsch QMS 403 D Aëolos[®] with a quadrupole mass analyzer.

IR spectra were recorded on an Invenio S Fourier transform infrared spectrophotometer equipped with a platinum ATR setup from Bruker.

Nanoindentation measurements were conducted on the film surface using a diamond Berkovich tip by applying a max load of 1 mN or 0.3 mN. The apparatus used was a Nanoindenter G200 (KLA). The applied load was controlled and the resulting penetration depth was detected, so that hardness, Young modulus and creep can be determined from the load vs. displacement curve.

Film thickness and optical constants were determined by spectroscopic ellipsometry. Data were collected by a Woollam Alpha-SE[®] between 380 nm and 900 nm wavelength. For data analysis, CompleteEase[®] version 6.51 was used. The substrate is described with a Cauchy layer. To avoid backside-reflection, a tape was applied to the backside of the substrate. For fitting of the polymer, a layer was converted to a B-spline and fitted over the entire spectral range. An ideal model considering sample roughness was applied. Polymer layer thickness and optical constants were fitted simultaneously.

Synthetic procedures:

General procedure for the free radical homopolymerizations of vinyl mercaptoethanol (VME): Vinyl mercaptoethanol (12 g, 116 mmol) and azobisisobutyronitrile (AIBN) were mixed, and the resulting solution was split into 11 different vials. Every solution was purged for 20 min with nitrogen and immersed into a preheated oil bath. The different polymerizations were stopped at different time points to evaluate the kinetics of the reaction.

Table S1: Temperatures and applied amounts of initiator for the free radical homopolymerizations.

Temperature [°C]	m _{AIBN} [mg]	n _{AIBN} [mmol]
55	19.0	0.1
55	37.8	0.2
55	189.0	1.2
65	19.1	0.1
65	189.0	1.2

General procedure for synthesis of a bigger batch of PVME (P1): Vinyl mercaptoethanol (10 g, 96 mmol) and AIBN (189 mg, 1.2 mmol) were added in a microwave vial and the solution was purged for 20 min with nitrogen. Afterwards the solution was stirred at 55 °C for 4 h. Then DMF was added, and the polymers were precipitated in ether, centrifuged, redissolved in DMF and precipitated in ether again. Finally, the polymers were dried under vacuum.

Synthetic procedure for the oxidation of polyVME to the sulfoxide: PolyVME (0.2 g, 1 eq.) and was dissolved in DMF (3 mL) and 50 wt.% H₂O₂-solution (1.3 g, 22 mmol, 10 eq.) was added and stirred for 24 h at rt. The polymer was precipitated in methanol, centrifuged and dried under vacuum.

Synthetic procedure for the oxidation of polyVME to the sulfone: PolyVME (0.2 g, 1 eq.) and a spatula tip of sodium tungstate were dissolved in DMF (3 mL) and 50 wt.% H₂O₂-solution (1.3 g, 22 mmol, 10 eq.) was added and stirred for 24 h at 60 °C. The polymer was precipitated in methanol, centrifuged and dried under vacuum.

Vinyl sulfonylethanol (VSE): Vinyl mercaptoethanol (30.00 g, 288 mmol, 1 eq.), sodium tungstate (0.04 g, 0.12 mmol, 0.0004 eq.) and hydroxyanisol (0.05 g, 0.40 mmol, 0.001 eq.) were dispersed in water (15 mL). Afterwards, 50% hydrogen peroxide solution (19.61 g, 288 mmol, 1 eq.) was added dropwise so that the temperature did not exceed 40 °C. The solution was further stirred for 1 h at 40 °C. Subsequently, 50% hydrogen peroxide solution (19.61 g, 288 mmol, 1 eq.) was added dropwise at 40 °C and the solution was stirred overnight at 60 °C. Finally, manganese oxide was added, the solution was centrifuged, and the solvent was removed in a continuous stream of air at 40 °C.

$^1\text{H-NMR}$ (300 MHz, DMSO-d_6): δ [ppm] = 6.93 (dd, $J = 16.2, 9.8$ Hz, 1H), 6.18 (dd, $J = 12.7, 8.9$ Hz, 2H), 5.06 (s, 1H), 3.74 (s, 2H), 3.24 (s, 2H).

$^{13}\text{C-NMR}$ (75 MHz, DMSO-d_6) δ [ppm] = 138.09, 128.30, 56.19, 54.84.

Synthetic procedure for the for the free radical homopolymerization of VSE: VSE (4.0 g, 29.4 mmol, 1 eq.) and AIBN (50.0 mg, 0.30 mmol, 0.01 eq.) were added in microwave vial and purged with nitrogen for 20 min. The reaction was started by immersion of the solution into a preheated oil bath at 65 °C and was further stirred for 48 h. The polymer was then precipitated in methanol, centrifuged, dissolved in methoxy ethanol, and precipitated in methanol again. The polymer was dried under vacuum. Because of the low yields two batches had to be prepared for the characterization. The first batch was used for the determination of thermal properties and the second batch for SEC measurements and IR-spectroscopy measurements.

General procedure for the RAFT-homopolymerizations: Vinyl mercaptoethanol (1.0 g, 9.6 mmol, 1 eq.) was added to a 2wt% stock solution of AIBN (1.5 mg, 0.009 mmol, 0.01 eq.) in dioxane and the CTA (0.1 eq.). The reaction mixture was degassed for 20 min. Afterwards the reaction mixture was heated at 65 °C for 24 h and samples were taken at different time points to examine the kinetics of the reaction.

Table S2: Applied amounts of RAFT-agents for the RAFT-polymerizations.

RAFT-agent	m_{CTA} [mg]	n_{CTA} [mmol]
2-(((butylthio)carbonothioyl)thio)propanoic acid	24	0.1
4-cyano-4-(((ethylthio)carbonothioyl)thio)pentanoic acid	25	0.1

General procedure for the determination of the copolymerization parameters: Vinyl mercaptoethanol and comonomer 2 were dissolved in DMF (1 mL) in different ratios and a stock solution of AIBN in vinyl mercaptoethanol was added. The reaction mixtures were purged for 20 min with nitrogen and then immersed into a preheated oil bath 65 °C. After short reaction times (see Table S3) the polymers were precipitated, centrifuged, redissolved in DMF, and precipitated again. The polymers were dried under vacuum and characterized by NMR-spectroscopy.

Table S3: Applied amounts of monomers and initiator, applied solvents and time for the determination of the copolymerization parameters.

Comonomer	No.	m_{VME} [g]	$m_{comonomer\ 2}$ [g]	m_{AIBN} [mg]	Solvent for precipitating	Time [min]
Styrene	1	2.66	1.36	3.12	Isopropanol	50
	2	2.35	1.65	3.12	Isopropanol	50
	3	2.02	2.00	3.12	Isopropanol	48
	4	1.35	2.67	3.12	Isopropanol	46
	5	1.01	3.00	3.12	Isopropanol	44
	6	0.66	3.34	3.12	Isopropanol	42
	7	0.50	3.51	3.12	Isopropanol	40
MMA	1	3.81	0.19	0.31	Diethyl ether	25
	2	3.66	0.36	0.31	Diethyl ether	20
	3	2.70	1.30	0.31	Diethyl ether	15
	4	2.04	2.00	0.31	Diethyl ether	12
	5	1.37	2.63	0.31	Diethyl ether	10
	6	1.04	3.00	0.31	Diethyl ether	7
	7	0.70	3.33	0.31	Diethyl ether	5
BA	1	3.77	0.23	0.31	Diethyl ether	16
	2	3.50	0.44	0.31	Diethyl ether	14
	3	2.45	1.52	0.31	Diethyl ether	12
	4	1.79	2.21	0.31	Diethyl ether	10
	5	1.16	2.85	0.31	Diethyl ether	8
VP	1	3.79	0.21	0.31	Diethyl ether	24
	2	3.61	0.40	0.31	Diethyl ether	22
	3	2.61	1.40	0.31	Diethyl ether	20
	4	1.93	2.07	0.31	Diethyl ether	18
	5	1.27	2.73	0.31	Diethyl ether	16
	6	0.61	3.37	0.31	Diethyl ether	12
VA	1	3.86	0.16	3.12	Diethyl ether	40
	2	2.83	1.16	3.12	Diethyl ether	40

Comonomer	No.	m_{VME} [g]	$m_{\text{comonomer 2}}$ [g]	m_{AIBN} [mg]	Solvent for precipitating	Time [min]
2	3	2.22	1.80	3.12	Diethyl ether	40
	4	1.15	2.85	3.12	Diethyl ether	40
	5	0.77	3.30	3.12	Diethyl ether	40
	6	0.62	3.43	3.12	Diethyl ether	40
	7	0.51	3.54	3.12	Diethyl ether	40

General procedure for the free radical copolymerization targeting higher conversions: Vinyl mercaptoethanol and comonomer 2 were dissolved in DMF (1 mL) and a stock solution of AIBN in vinyl mercaptoethanol was added. The reaction mixtures were purged for 20 min with nitrogen and then immersed into a preheated oil bath 65 °C, where they were kept for 4 h. Afterwards the polymers were precipitated, centrifuged, dissolved in DMF, and precipitated again. The polymers were dried under vacuum.

Table S4: Applied amounts of monomers and initiator for the copolymerizations with higher conversion.

		m_{VME} [g]	n_{VME} [mmol]	$m_{\text{comonomer 2}}$ [g]	$n_{\text{comonomer 2}}$ [mmol]	m_{AIBN} [mg]	n_{AIBN} [mmol]	Solvent for precipitating
P2	MMA	0.38	3.6	3.6	36.2	0.31	0.002	Methanol
P3	MMA	2.1	20.1	2.0	20.0	0.31	0.002	Methanol
P4	BA	1.8	17.2	2.2	17.2	0.31	0.002	THF

General procedure for the experiments on the RAFT copolymerization with BA: *N*-butyl acrylate, vinyl mercaptoethanol, a 5wt% stock solution of AIBN in DMF, a 20wt% stock solution of CTA I in DMF and a few drops of mesitylene as a standard were added into a microwave vial and purged with nitrogen for 20 min. Afterwards the reaction mixtures were stirred for 24 h at 65 °C. The polymers were precipitated in water:methanol-mixture (1:1), centrifuged, washed with water:methanol-mixture (1:1) and dried under vacuum.

Table S5: Applied amounts of monomers and initiator for the RAFT copolymerizations with BA.

Ratio	m_{VME}	n_{VME}	$m_{n\text{-BA}}$	$n_{n\text{-BA}}$	m_{AIBN}	n_{AIBN}	m_{CTAI}	n_{CTAI}
-------	------------------	------------------	-------------------	-------------------	-------------------	-------------------	-------------------	-------------------

	VME: BA	[g]	[mmol]	[g]	[mmol]	[mg]	[mmol]	[mg]	[mmol]
R1	3:1	2.13	20.49	0.88	6.85	4.50	0.03	64.90	0.27
R2	2:1	1.86	17.89	1.15	8.97	4.60	0.03	64.50	0.27
R3	1:1	1.34	12.90	1.65	12.90	4.20	0.03	61.2	0.26
R4	0.5:1	0.87	8.39	2.14	16.72	4.10	0.02	60.10	0.25
R5	1:1	1.35	12.92	1.64	12.80	8.10	0.05	122.50	0.51
R6	1:1	1.34	12.90	1.65	13.83	2.08	0.02	30.70	0.13

General procedure for the experiments on the RAFT copolymerization with MMA: Methyl methacrylate, vinyl mercaptoethanol, a 5wt% stock solution of AIBN in DMF, a 20wt% stock solution of CTA I in DMF and a few drops of mesitylene as a standard were added into a microwave vial and purged with nitrogen for 20 min. Afterwards the reaction mixtures were stirred for 24 h at 65 °C. The polymers were precipitated in diethylether, centrifuged, washed with diethylether and dried under vacuum.

Table S6: Applied amounts of monomers and initiator for the RAFT copolymerizations with MMA.

	Ratio VME:M MA	m _{VME} [g]	n _{VME} [mmol]	m _{MMA} [g]	n _{MMA} [mmol]	m _{AIBN} [mg]	n _{AIBN} [mmol]	m _{CTAI} [mg]	n _{CTAI} [mmol]
R7	3:1	2.28	21.92	0.73	7.29	4.90	0.03	68.22	0.29
R8	2:1	2.03	19.46	0.97	9.72	4.72	0.03	71.80	0.30
R9	1:1	1.52	14.64	1.47	14.72	4.80	0.03	70.20	0.29
R10	0.5:1	1.03	9.89	1.98	19.76	4.80	0.03	71.50	0.30
R11	1:1	1.54	14.78	1.47	14.66	9.50	0.06	140.72	0.59
R12	1:1	1.53	14.71	1.46	14.62	3.06	0.02	35.10	0.15

RAFT polymerization of poly[vinyl mercaptoethanol] [PVME₆₂]: Vinyl mercaptoethanol (6.12 g, 58.8 mmol, 182 eq.), 20wt% stock solution of CTA I (76.8 mg, 0.32 mmol, 1 eq.) in DMF and 5wt% stock solution of AIBN (5.34 mg, 0.03 mmol, 0.1 eq.) in DMF, DMF (2.0 g) and a few drops mesitylene as a standard were added into a microwave vial and purged for 20 min with nitrogen. Afterwards the solution was heated to 65 °C and kept for 4 h. Then the polymer was

precipitated in diethylether, centrifuged, dissolved in methanol and precipitated again in diethylther, centrifuged and dried under vacuum.

Synthesis of poly[vinyl mercaptoethanol-*block*-*n*-butyl acrylate] [PVME₆₂-*b*-PBA₈₃]: PVME₆₂ (253.5 mg, 0.038 mmol, 1 eq.), *n*-butyl acrylate (477.0 mg, 3.72 mmol, 100 eq.) and 5wt% stock solution of AIBN (0.87 mg, 0.005 mmol, 0.13 eq.) in DMF, DMF (1.25 g) and a few drops mesitylene as a standard were added into a microwave vial and purged for 20 min with nitrogen. Afterwards the solution was heated to 65 °C and kept for 4 h. Then the polymer was precipitated in water:methanol-mixture (1:1), centrifuged, washed with water:methanol-mixture (1:1) and dried under vacuum.

RAFT polymerization of poly[*n*-butyl acrylate] [PBA₉₂]: *N*-butyl acrylate (3.30 g, 25.7 mmol, 100 eq.), 20wt% stock solution of CTAI (61.86 mg, 0.26 mmol, 1 eq.) in DMF and 5wt% stock solution of AIBN (2.05 mg, 0.01 mmol, 0.05 eq.) in DMF, DMF (2.0 g) and a few drops mesitylene as a standard were added into a microwave vial and purged for 20 min with nitrogen. Afterwards, the solution was heated to 65 °C and kept for 4 h. Then the polymer was precipitated in water:methanol-mixture (1:1), centrifuged, washed with water:methanol-mixture (1:1) and dried under vacuum.

Synthesis of poly[*n*-butyl acrylate-*block*-vinyl mercaptoethanol] [PBA₉₂-*b*-PVME₂₁]: PBA₉₂ (249.8 mg, 0.02 mmol, 1 eq.), vinyl mercaptoethanol (863.8 mg, 8.28 mmol, 400 eq.) and 5wt% stock solution of AIBN (0.55 mg, 0.003 mmol, 0.17 eq.) in DMF, DMF (250.8 mg) and a few drops mesitylene as a standard were added into a microwave vial and purged for 20 min with nitrogen. Afterwards the solution was heated to 65 °C and kept for 4 h. Then the polymer was precipitated in water:methanol-mixture (1:1), centrifuged, washed with water:methanol-mixture (1:1) and dried under vacuum.

RAFT polymerization of poly[methyl methacrylate] [PMMA₉₆]: Methyl methacrylate (2.95 g, 29.5 mmol, 100 eq.), 20wt% stock solution of CTAII (76.8 mg, 0.29 mmol, 1 eq.) in DMF and 5wt% stock solution of AIBN (2.45 mg, 0.02 mmol, 0.1 eq.) in DMF, DMF (2.0 g) and a few drops mesitylene as a standard were added into a microwave vial and purged for 20 min with nitrogen.

Afterwards, the solution was heated to 65 °C and kept for 4 h. Then the polymer was precipitated in diethylether, centrifuged, washed with diethylther and dried under vacuum.

Synthesis of poly[methyl methacrylate-*block*-vinyl mercaptoethanol] [PMMA₉₆-*b*-PVME₃₂]: PMMA₉₆ (501.0 mg, 0.05 mmol, 1 eq.), vinyl mercaptoethanol (1061.9 mg, 10.2 mmol, 200 eq.) and 5wt% stock solution of AIBN (0.89 mg, 0.005 mmol, 0.1 eq.) in DMF, DMF (2.0 g) and a few drops mesitylene as a standard were added into a microwave vial and purged for 20 min with nitrogen. Afterwards, the solution was heated to 65 °C and kept for 4 h. Then the polymer was precipitated in diethylether, centrifuged, washed with diethylether and dried under vacuum.

Supporting data

Free radical homopolymerization

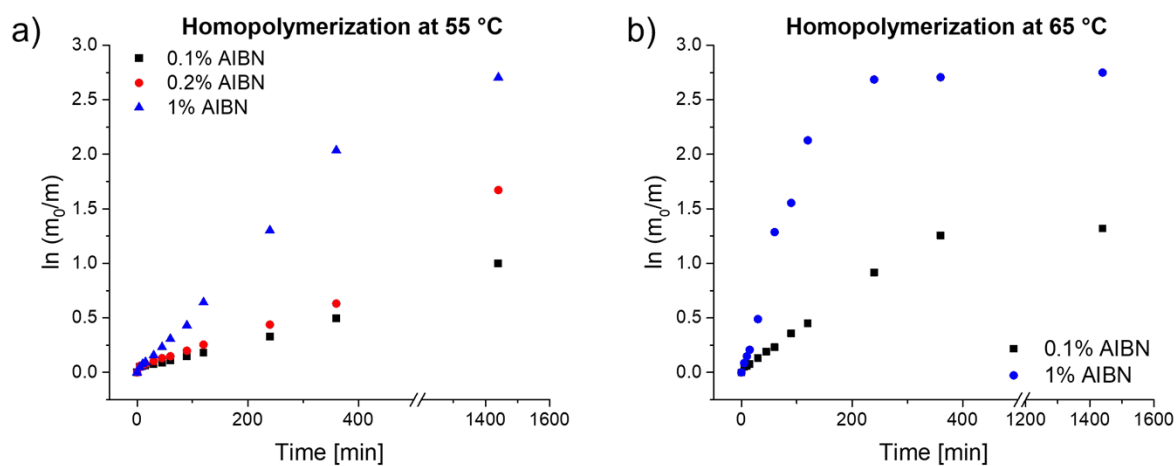


Figure S1: $\ln(m_0/m)$ vs. reaction time for different polymerizations: a) homopolymerization of VME at 55 °C; b) homopolymerization of VME at 65 °C.

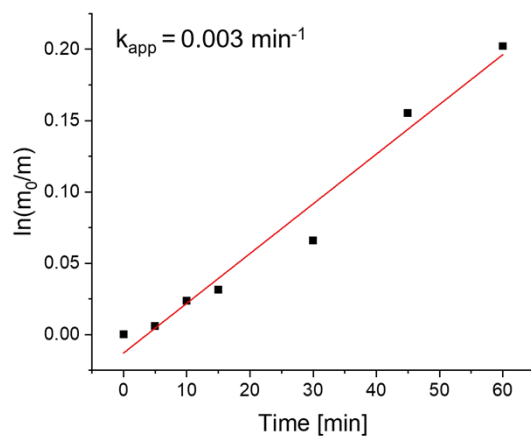


Figure S2: $\ln(m_0/m)$ vs. reaction time for homopolymerization of MMA at 55 °C and 1% AIBN.

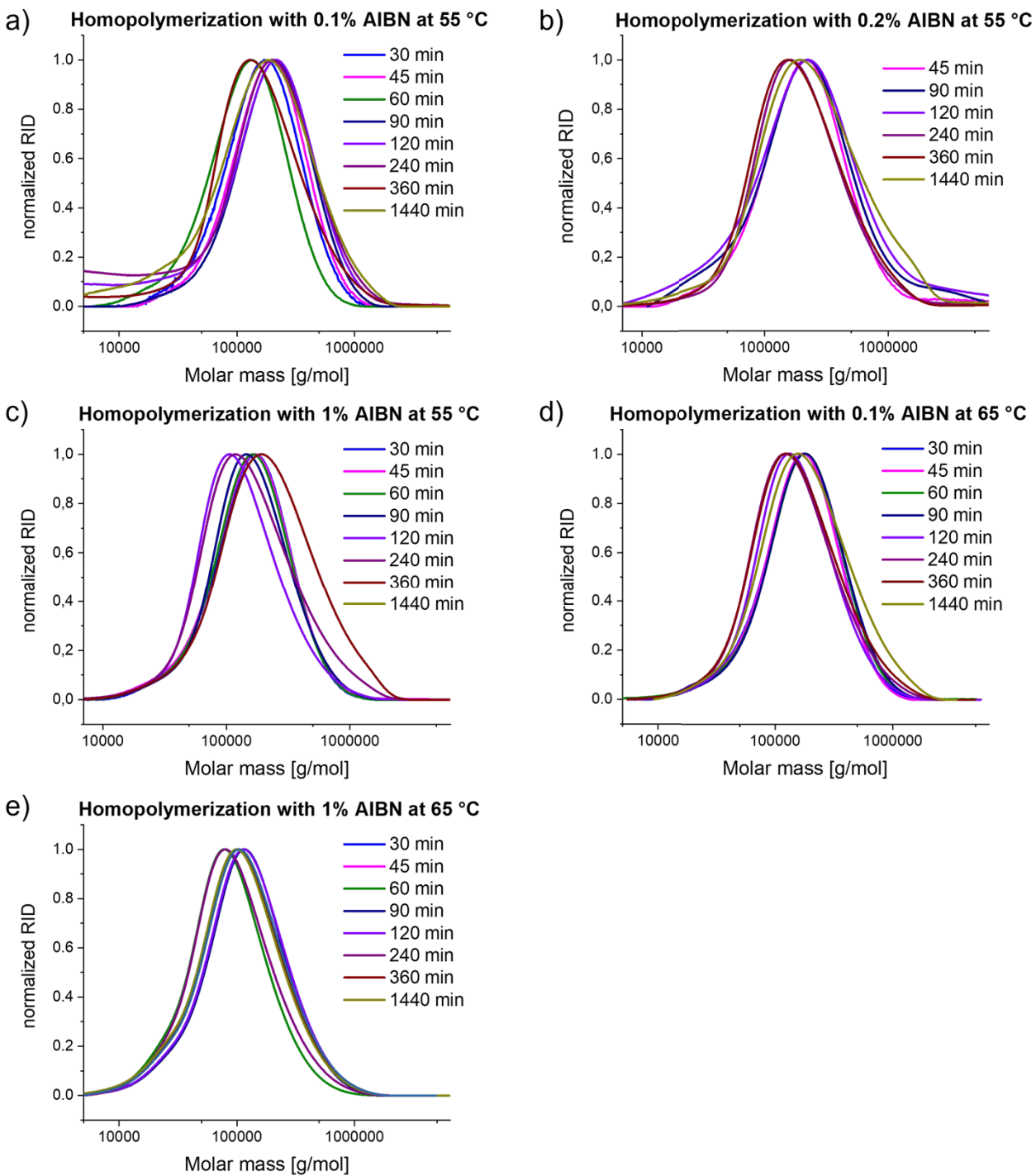


Figure S3: SEC (DMAc (+ 0.21 wt.% LiCl), PMMA standards) traces of the kinetic samples taken after 30 min, 45 min, 60 min, 90 min, 120 min, 240 min, 360 min and 1440 min from the polymerization with a) 0.1 %, b) 0.2%, c) 1% AIBN at 55 °C and d) 0.1%, e) 1% AIBN at 65 °C.

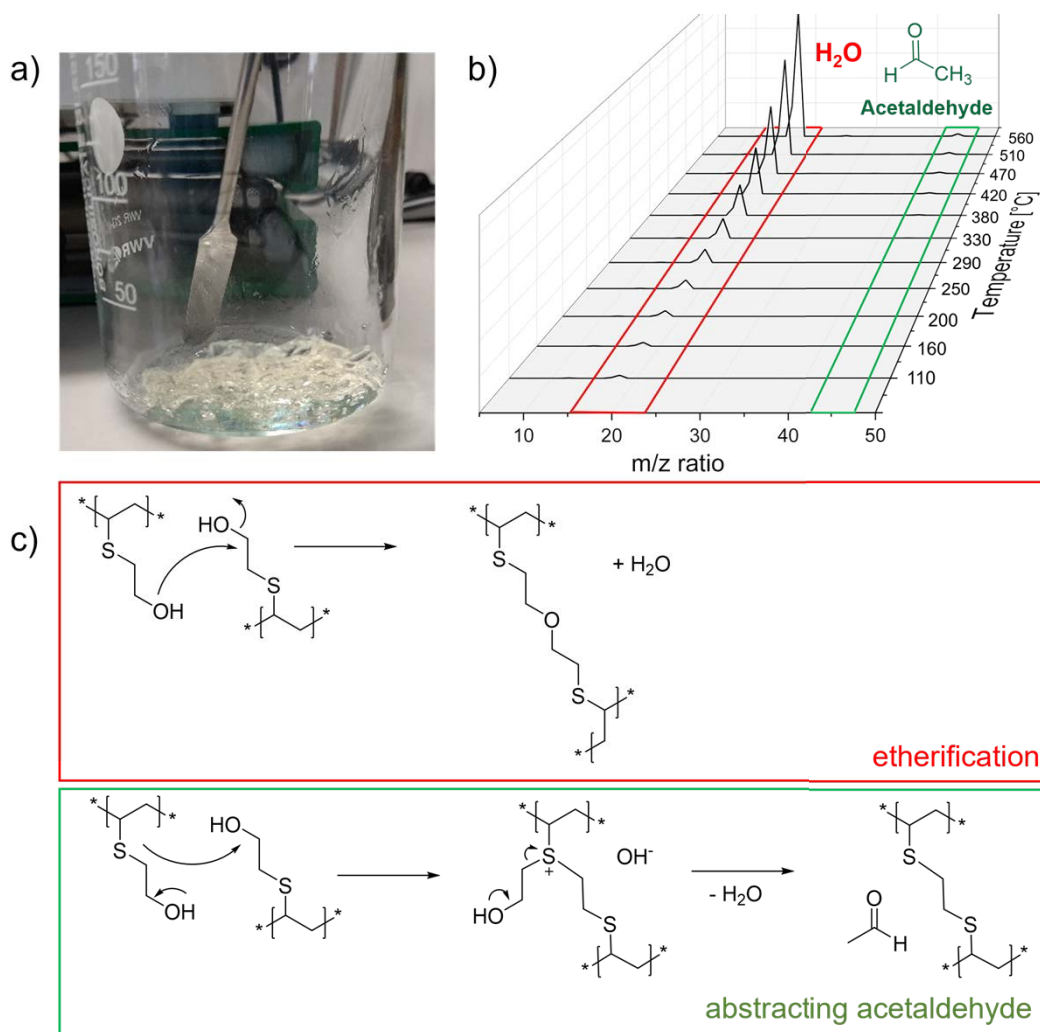


Figure S4: a) Picture of the generated gel b) STA-measurement (He) of the homopolymer c) Scheme of a possible mechanism of crosslinking.

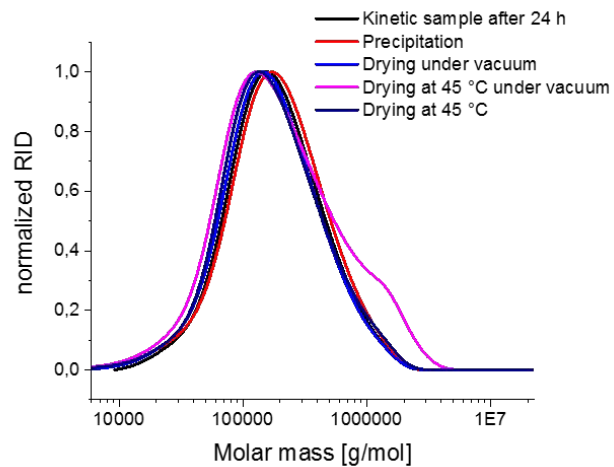


Figure S5: SEC (DMAc (+ 0.21 wt.% LiCl), PMMA standards) traces for the investigation of different influencing variables on cross-linking.

Copolymerization parameter

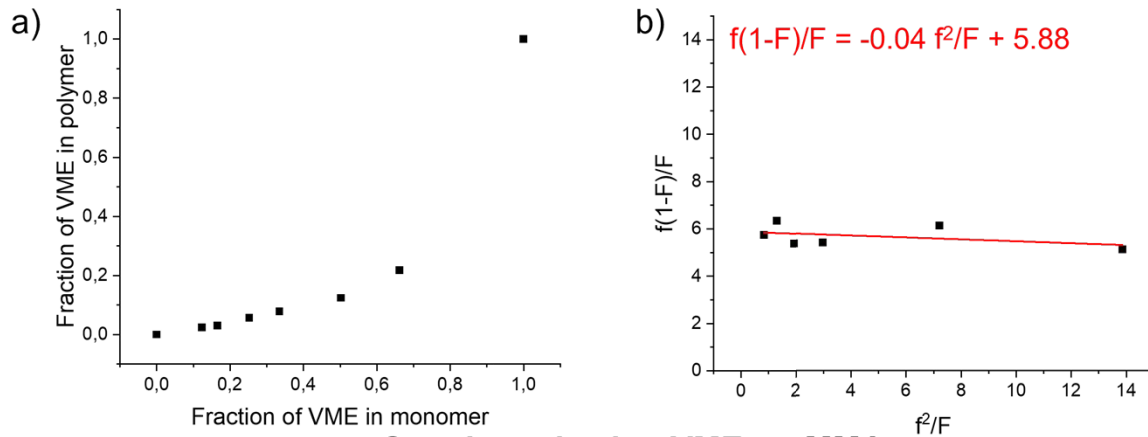
For the determination of the copolymerization parameters, the monomers were weighed in different ratios, dissolved in DMF, degassed for 10 min, and then polymerized at 65 °C. In order to use the Fineman-Ross method for the determination of the copolymer parameters, a conversion of less than 5% must be guaranteed, which in this case was verified with kinetics probes and the respective analysis by NMR spectroscopy. Before reaching a conversion of 5%, the polymerization was stopped by precipitating the polymers into a non-solvent. The polymers were then centrifuged, redissolved, and precipitated/centrifuged again and dried under vacuum. Due to the risk of crosslinking elevated temperatures were avoided during drying. The composition of the monomers (equation (1)) was determined by exact weighing, and the composition of the polymers (equation (2)) was determined by integrating the specific polymer signals for the various repeating units in ¹H-NMR spectra (see SI Figure S19). If these values are now plotted graphically according to equation (3), the values r_1 and r_2 can be determined from the slope and the intercept of the linear fits, respectively (see SI Figure S6/S7).

$$\text{composition monomer } f = \frac{[a]}{[b]} \quad (1)$$

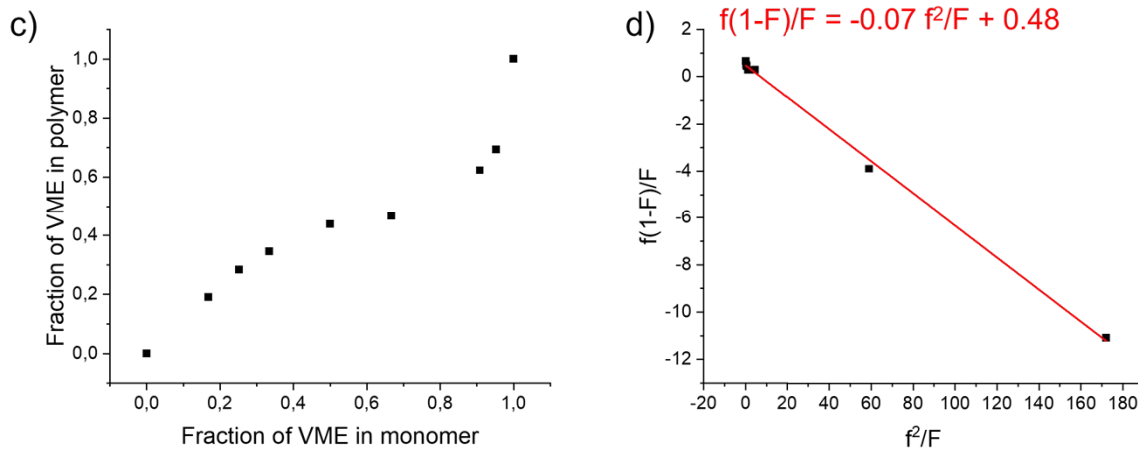
$$\text{composition polymer } F = \frac{[A]}{[B]} \quad (2)$$

$$\frac{f(1-F)}{F} = -r_1 \frac{f^2}{F} + r_2 \quad (3)$$

Copolymerization VME-co-Styrene



Copolymerization VME-co-MMA



Copolymerization VME-co-BA

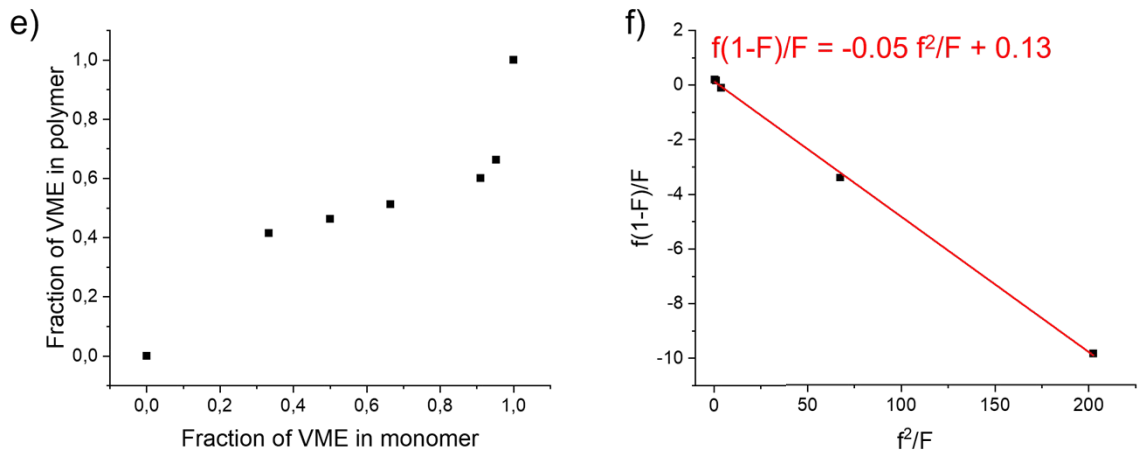
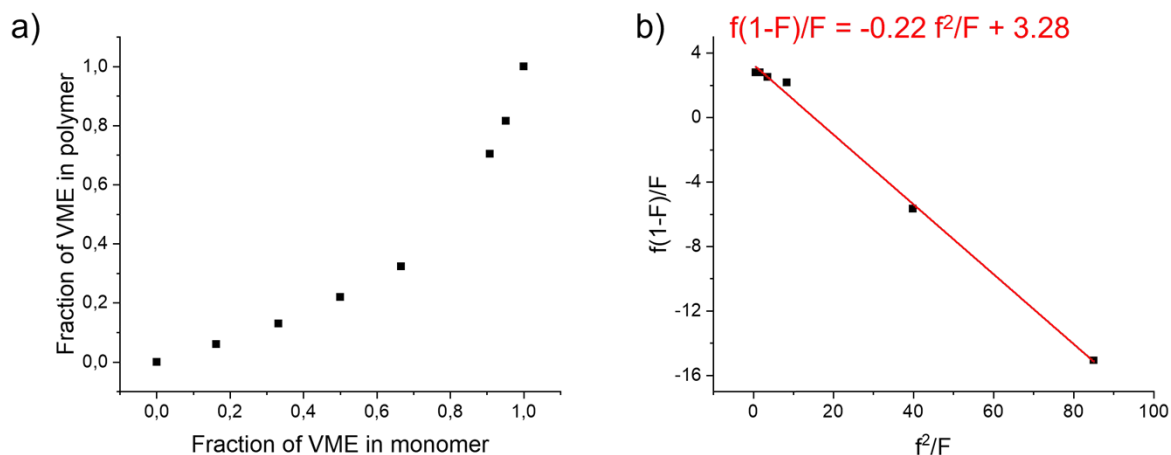


Figure S6: Determination of the copolymer parameters *via* Finemann-Ross method of the copolymerization of a/b) VME-co-Styrene c/d) VME-co-MMA e/f) VME-co-BA.

Copolymerization VME-co-VP



Copolymerization VME-co-VA

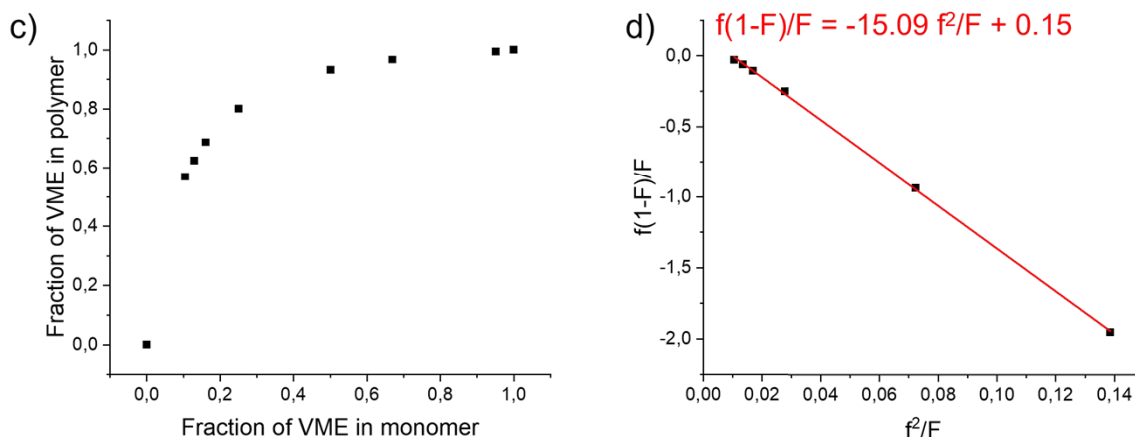


Figure S7: Determination of the copolymer parameters via Finemann-Ross method of the copolymerization of a/b) VME-co-VP c/d) VME-co-VA.

From the copolymer parameters calculated for the copolymerization with styrene, the Q - and e -values could be determined *via* equations (4) and (5), where Q describes the reactivity of the monomer (resonance stabilization) and e the polarity, which varies for each monomer due to the effect of the functional groups on the vinyl group. This allows the new monomer to be classified and compared with other monomers.

$$r_1 = \frac{k_{11}}{k_{12}} = \frac{P_1 Q_1 \exp(-e_1 e_1)}{P_1 Q_2 \exp(-e_1 e_2)} = \frac{Q_1}{Q_2} \exp\left(\frac{e_1(e_1 - e_2)}{1}\right) \quad (4)$$

$$r_2 = \frac{Q_1}{Q_2} \exp\left(\frac{e_1(e_1 - e_2)}{Q_1}\right) \quad (5)$$

$$Q = 0.45$$

$$e = -2.0$$

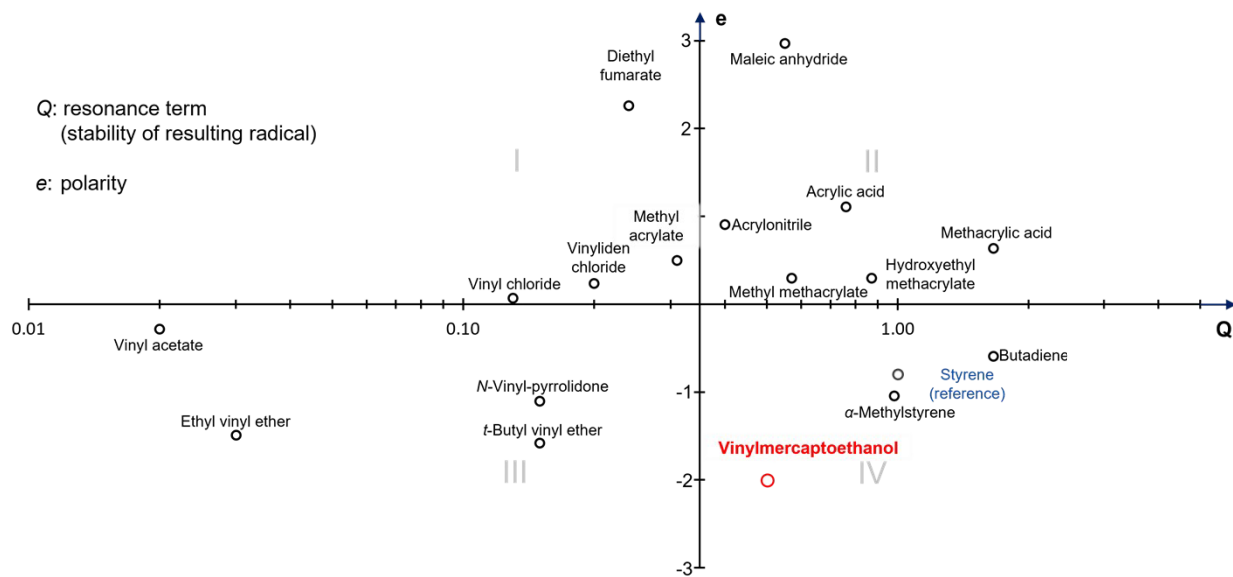


Figure S8: Q-e Scheme with different monomers.¹

RAFT-homopolymerization

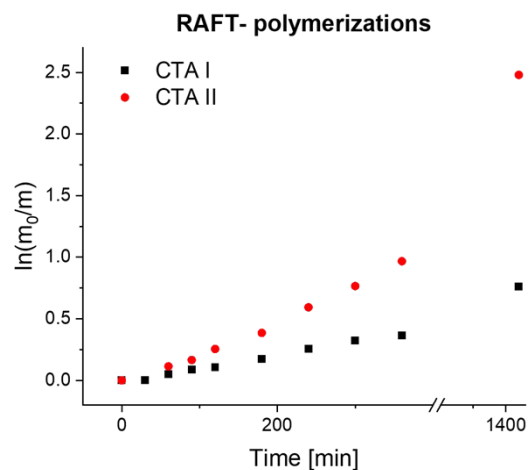


Figure S9: $\ln(m_0/m)$ vs. reaction time for different RAFT-polymerizations with CTA I and CTA II at 65 °C.

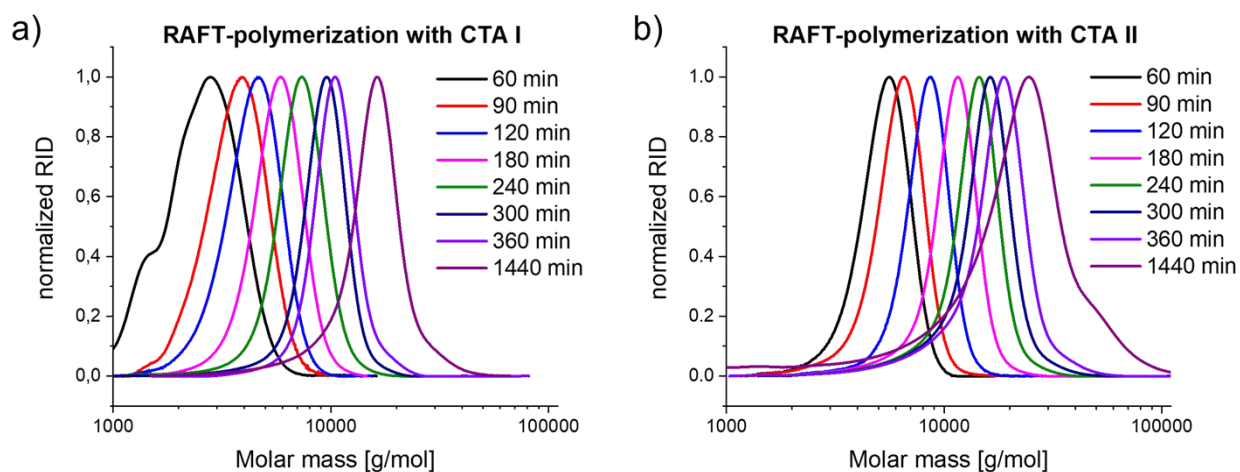


Figure S10: SEC (DMAc (+ 0.21 wt.% LiCl), PMMA standards) traces of the kinetic samples taken after 60 min, 90 min, 120 min, 240 min, 300 min, 360 min and 1440 min from the RAFT-polymerization with a) CTA I, b) CTA II at 65 °C.

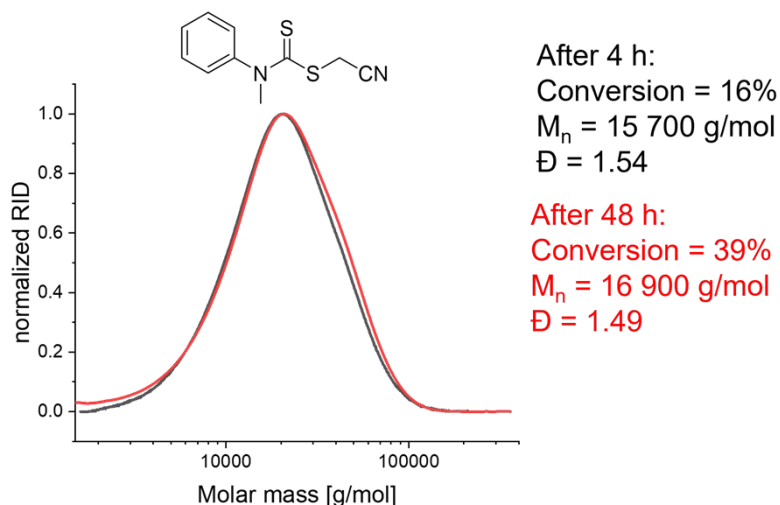


Figure S11: SEC (DMAc (+ 0.21 wt.% LiCl), PMMA standards) traces of the kinetic samples taken after 4 h and 48 h from the polymerization with a carbamate-RAFT agent.

Determination of M_n with $^1\text{H-NMR}$ spectroscopy:

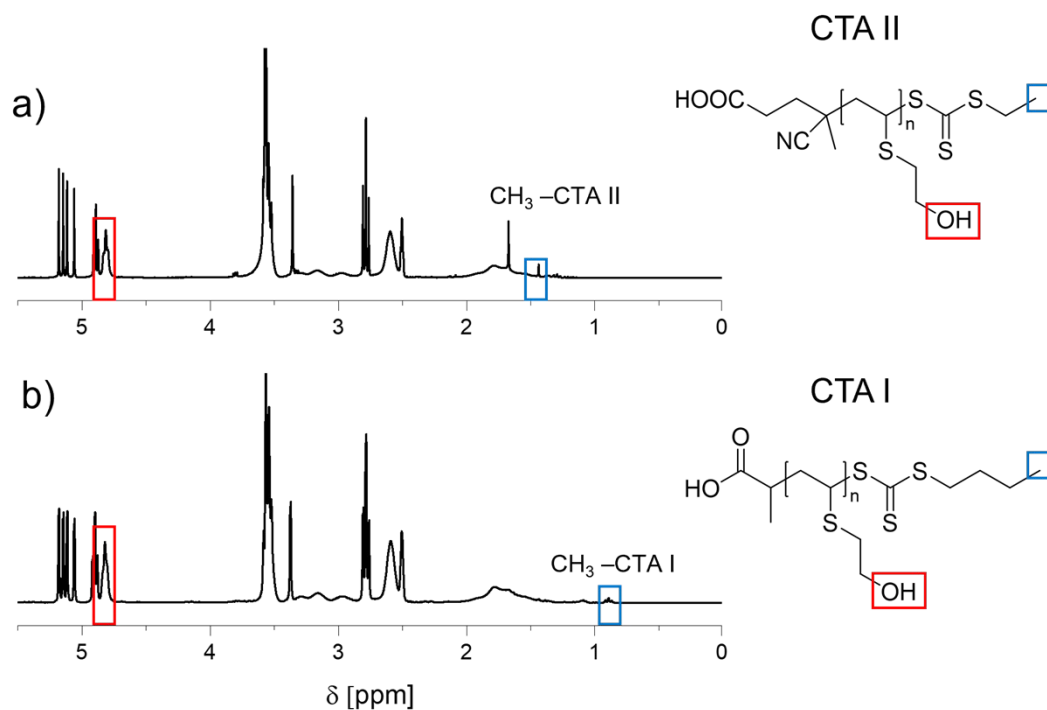
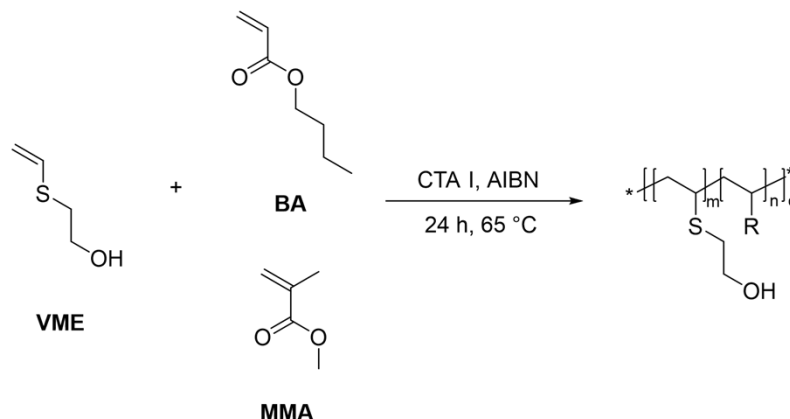


Figure S12: $^1\text{H-NMR}$ spectra (300 MHz, DMSO-d_6) of the kinetic samples of the RAFT polymerization with a) CTA II after 6 h and b) CTA I after 24 h.

Table S7: Determination of M_n via the integrals of the protons in the NMR spectra.

RAFT polymerization	Integral CTA group	Integral OH-group	Repeating units	M_n [g/mol]
CTA I	3	55.63	56	6000
CTA II	3	65.56	66	7100

RAFT-copolymerizations



Scheme S1: Synthesis of random copolymers using RAFT.

Table S8: Conversions, molar masses (M_n) and dispersities (\mathcal{D}) of the copolymers obtained from RAFT copolymerizations with different ratios of the monomers.

	Ratio VME: BA pre-weight	Conversion VME ^a	Conversion BA ^a	M_n [g mol ⁻¹] ^b	\mathcal{D}^b	Degree of polymerization (DP_{calc}) ^c
R1	3:1	47	100	15 800	1.10	74
R2	2:1	54	100	17 700	1.10	77
R3	1:1	76	88	18 300	1.12	82
R4	0.5:1	93	82	17 500	1.14	88

^a ¹H-NMR (300 MHz, CDCl₃) after 24 h, determination *via* standard mesitylene ^b SEC (DMAc (+ 0.21 wt.% LiCl), PMMA standards) after 24 h, ^c Determination from conversion of the monomers.

Table S9: Conversions, molar masses and dispersities of the copolymers obtained from RAFT copolymerizations with different ratios of CTA I and the monomers.

	Targeted DP	Conversion VME ^a	Conversion <i>n</i> -BA ^a	M_n [g mol ⁻¹] ^b	\mathcal{D}^b	DP_{calc} ^c
R5	50	76	85	10 400	1.12	40
R3	100	76	88	18 300	1.12	82
R6	200	88	99	36 700	1.12	187

^a ¹H-NMR (300 MHz, CDCl₃) after 24 h, determination *via* standard mesitylene ^b SEC (DMAc (+ 0.21 wt.% LiCl), PMMA standards) after 24 h ^c Determination from conversion of the monomers..

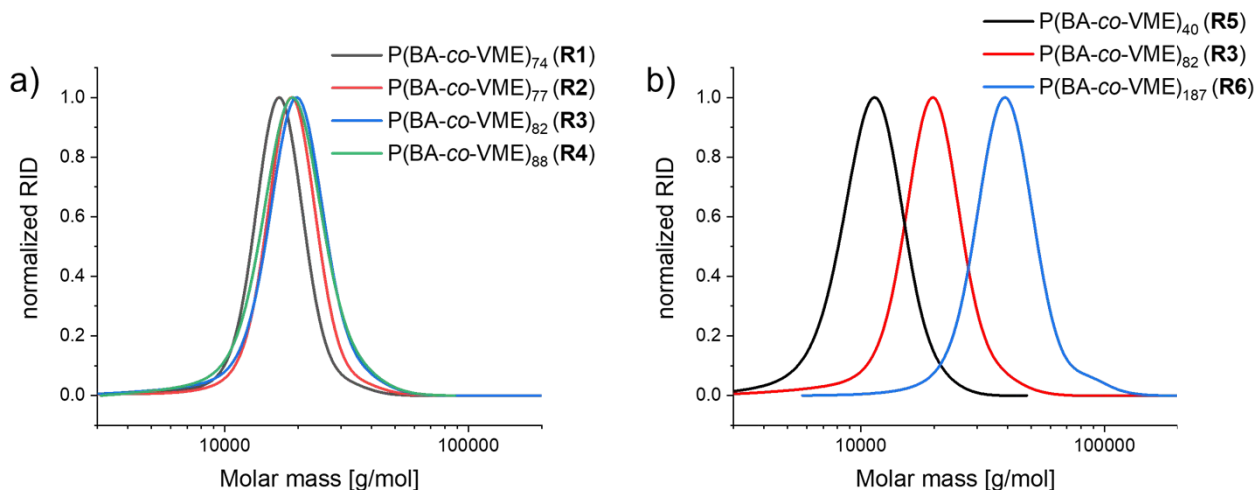


Figure S13: SEC (DMAc (+ 0.21 wt.% LiCl), PMMA standards) traces of the RAFT-polymers R1-R6 after 24 h.

Table S10: Conversions, molar masses and dispersities of the copolymers obtained from the RAFT copolymerizations (CTA I) with different ratios of the monomers.

	Ratio VME: MMA pre-weight	Conversion VME ^a	Conversion MMA ^a	M_n [g mol ⁻¹] ^b	\bar{D}^b	DP_{calc}^c
R7	3:1	61	100	14 900	1.11	81
R8	2:1	58	100	14 200	1.13	79
R9	1:1	63	98	16 500	1.14	81
R10	0.5:1	88	98	16 700	1.14	93

^a ¹H-NMR (300 MHz, DMSO-d₆) after 24 h, determination *via* standard mesitylene ^b SEC (DMAc (+ 0.21 wt.% LiCl), PMMA standards) after 24 h ^c Determination from conversion of the monomers.

Table S11: Conversions, molar masses and dispersities of the copolymers obtained from RAFT copolymerizations with different ratios of CTA I and the monomers.

	Targeted DP	Conversion VME ^a	Conversion MMA ^a	M_n [g mol ⁻¹] ^b	\bar{D}^b	DP_{calc}^c
R11	50	94	99	10 500	1.15	48
R9	100	63	98	16 500	1.14	81
R12	200	61	93	26 700	1.16	154

^a ¹H-NMR (300 MHz, DMSO-d₆) after 24 h, determination *via* standard mesitylene ^b SEC (DMAc (+ 0.21 wt.% LiCl), PMMA standards) after 24 h ^c Determination from conversion of the monomers.

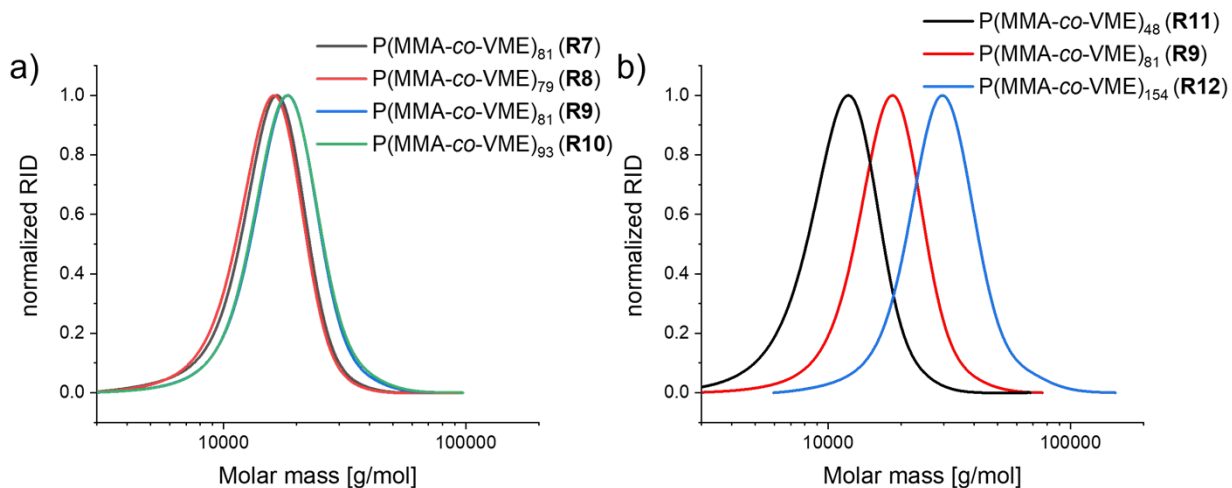


Figure S14: SEC (DMAc (+ 0.21 wt.% LiCl), PMMA standards) traces of the RAFT-polymers R7-R12 after 24 h.

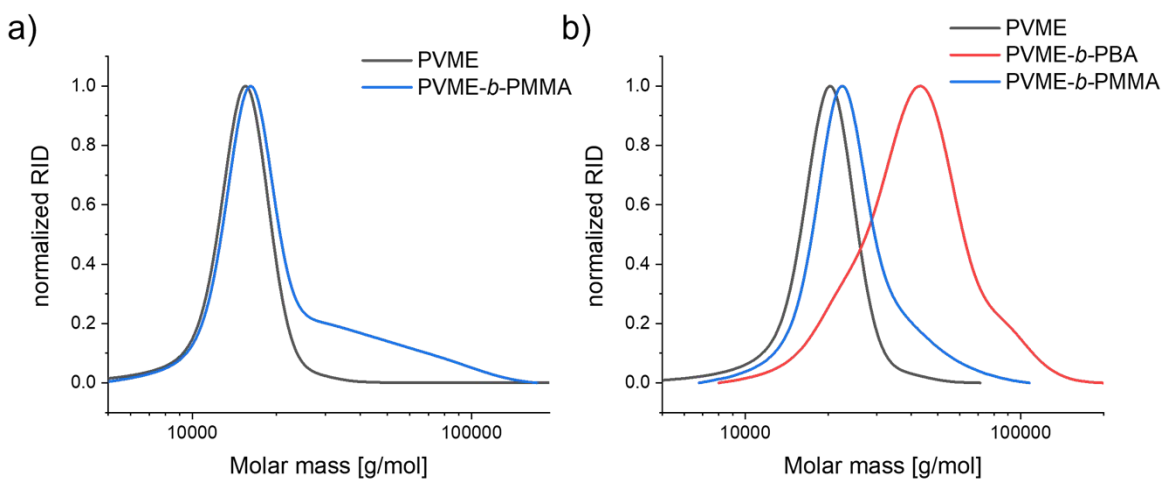


Figure S15: SEC (DMAc (+ 0.21 wt.% LiCl), PMMA standards) traces of a) PVME₆₂ and PVME₆₂-*b*-PMMA with a reaction time of 4 h and b) of the different *block*-copolymers with a reaction time of 24 h.

Modification of homopolymers by oxidation

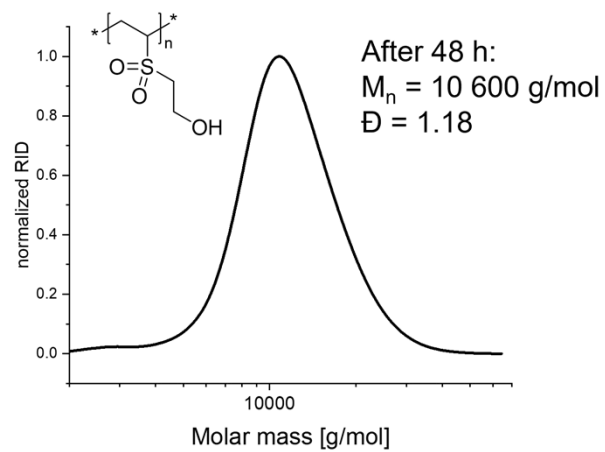


Figure S16: SEC (DMAc (+ 0.21 wt.% LiCl), PMMA standards) traces of PVSE.

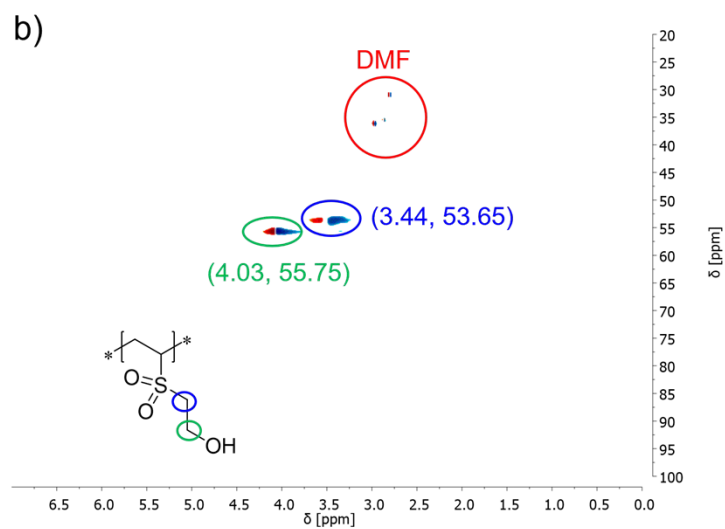
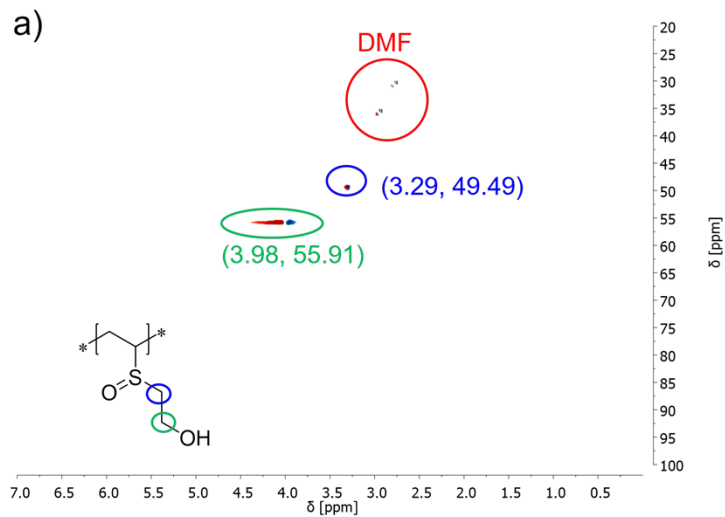
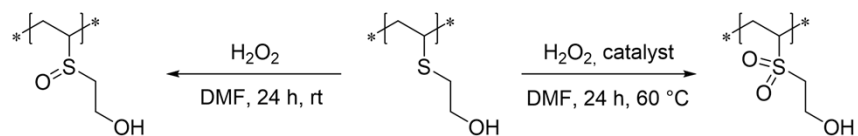


Figure S17: Zoomed HSQC-NMR-spectra (400 MHz, DMF-d₇, 298 K) of the oxidized species prepared a) without any catalyst and b) with the catalyst sodium tungstate.

Thermal properties of the prepared homo- and copolymers

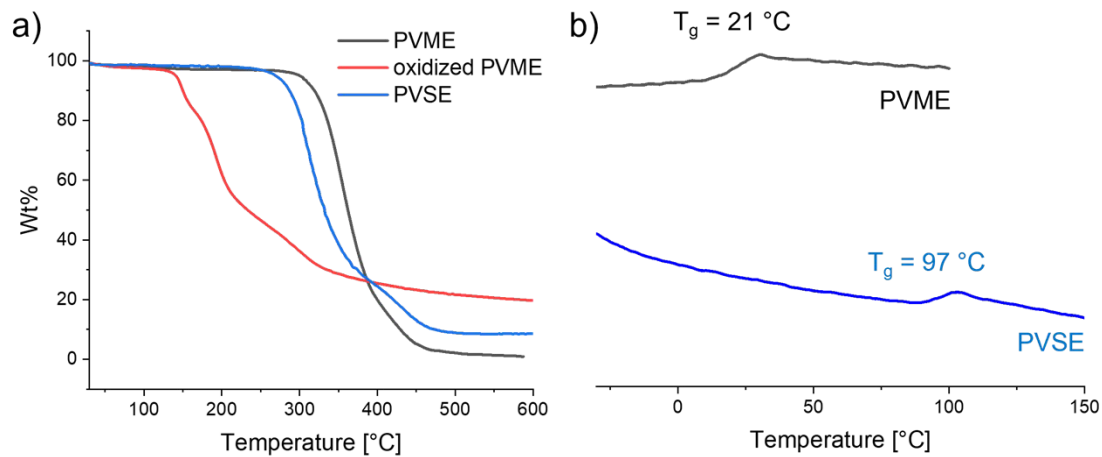


Figure S18: a) TGA-data and b) DSC-data of PVME, the oxidized species of PVME and PVSE.

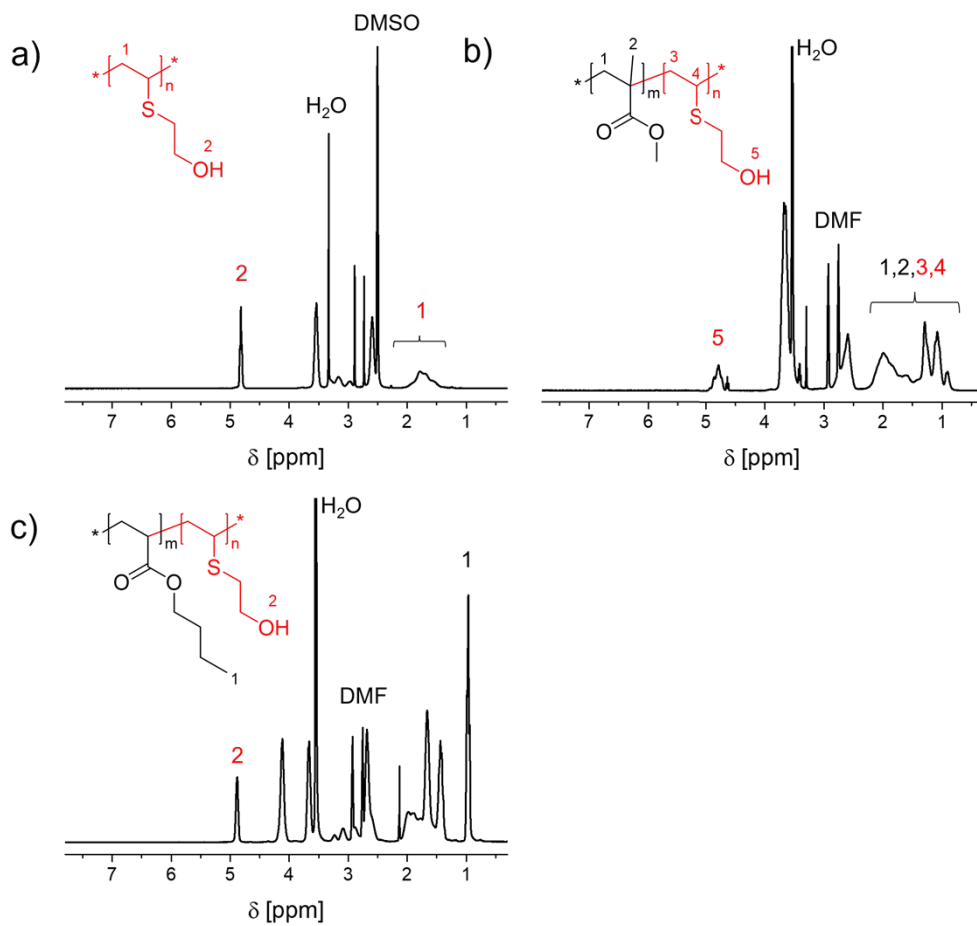


Figure S19: a) $^1\text{H-NMR}$ (300 MHz, DMSO-d_6) spectrum of the homopolymer P1, b) $^1\text{H-NMR}$ (300 MHz, DMF-d_7) spectrum of the copolymer P3, c) $^1\text{H-NMR}$ (300 MHz, DMF-d_7) spectrum of the copolymer P4.

Table S12: Composition, number average molar mass and thermal data of homo and copolymers synthesized *via* free radical polymerization.

Polymer	VME content	M_n	\bar{D}^b	T_g [°C] ^c
	[%] ^a	[kg mol ⁻¹] ^b		
PVME (P1)	100	146 100	2.3	21
P(VME- <i>co</i> -MMA) (P2)	19	272 700	2.0	96
P(VME- <i>co</i> -MMA) (P3)	40	304 800	1.6	69
P(VME- <i>co</i> -BA) (P4)	45	408 700	2.4	- 17

^a Determination via ¹H-NMR (300 MHz)-spectroscopy after precipitation and purification ^b SEC (DMAc (+ 0.21 wt.% LiCl), PMMA standards) ^c Determination from DSC measurements.

Table S13: Composition, number average molar mass and thermal data of random copolymers synthesized *via* RAFT polymerization.

Polymer	VME content	M_n	\bar{D}^b	T_g [°C] ^c
	[%] ^a	[kg mol ⁻¹] ^b		
P(BA- <i>co</i> -VME) ₄₀ (R5)	47	10 100	1.1	- 23
P(BA- <i>co</i> -VME) ₈₂ (R3)	44	19 300	1.1	- 25
P(BA- <i>co</i> -VME) ₁₈₇ (R6)	47	38 100	1.1	- 19
P(MMA- <i>co</i> -VME) ₄₈ (R11)	57	14 600	1.1	57
P(MMA- <i>co</i> -VME) ₈₁ (R9)	44	17 000	1.1	56
P(MMA- <i>co</i> -VME) ₁₅₄ (R12)	44	26 800	1.2	55

^a Determination via ¹H-NMR (300 MHz)-spectroscopy after precipitation and purification ^b SEC (DMAc (+ 0.21 wt.% LiCl), PMMA standards) ^c Determination from DSC measurements.

Table S14: Composition, number average molar mass and thermal data of block-copolymers synthesized via RAFT polymerization.

Polymer	VME content	M_n	\bar{D}^b	T_g [°C] ^c
	[%] ^a	[kg mol ⁻¹] ^b		
PVME ₆₂ (R13)	100	14 600	1.1	12
PVME ₆₂ - <i>b</i> -PBA ₈₃ (R14)	43	22 100	1.1	- 48 7
PBA ₉₂ (R15)	0	13 100	1.1	- 53
PBA ₉₂ - <i>b</i> -PVME ₂₁ (R16)	19	30 700	1.1	- 52 13
PMMA ₉₆ (R17)	0	11 800	1.1	95
PMMA ₉₆ - <i>b</i> -PVME ₃₂ (R18)	25	18 200	1.1	109

^a Determination via ¹H-NMR (300 MHz)-spectroscopy after precipitation and purification ^b SEC (DMAc (+ 0.21 wt.% LiCl), PMMA standards) ^c Determination from DSC measurements.

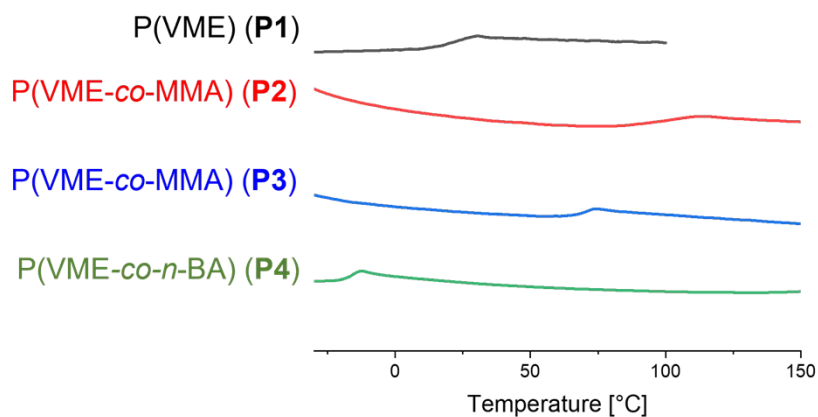


Figure S20: DSC-data of homo- and copolymers P1-P4 synthesized *via* free radical polymerization.

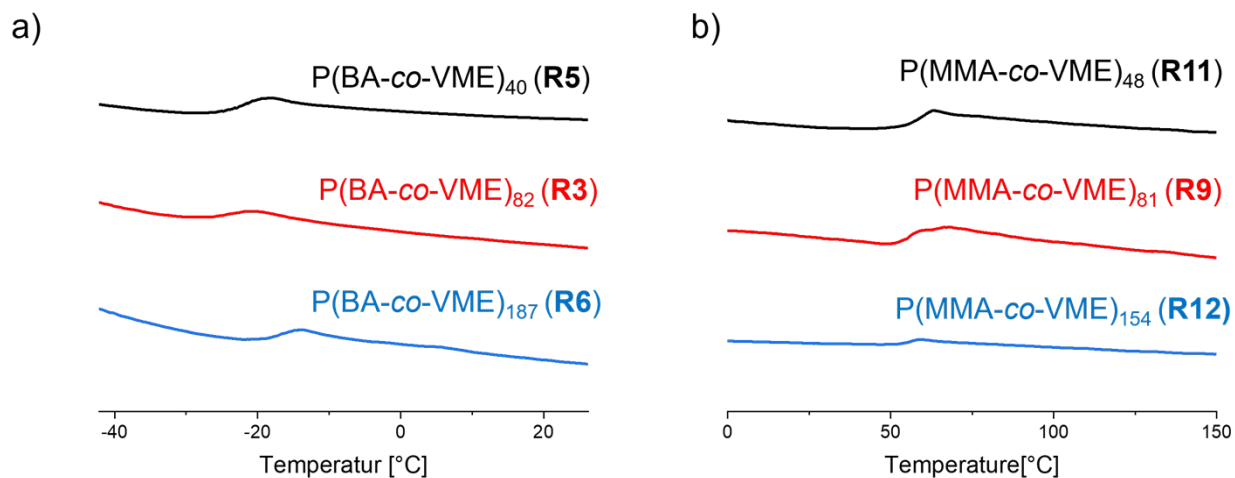


Figure S21: DSC-data of the a) P(BA-*co*-VME) copolymers R3/5/6 and the b) P(MMA-*co*-VME) copolymers R9/11/12 synthesized *via* RAFT polymerization.

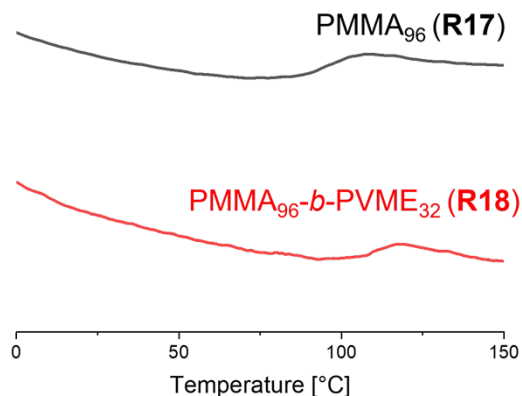


Figure S22: DSC-data of the copolymers R17 and R18.

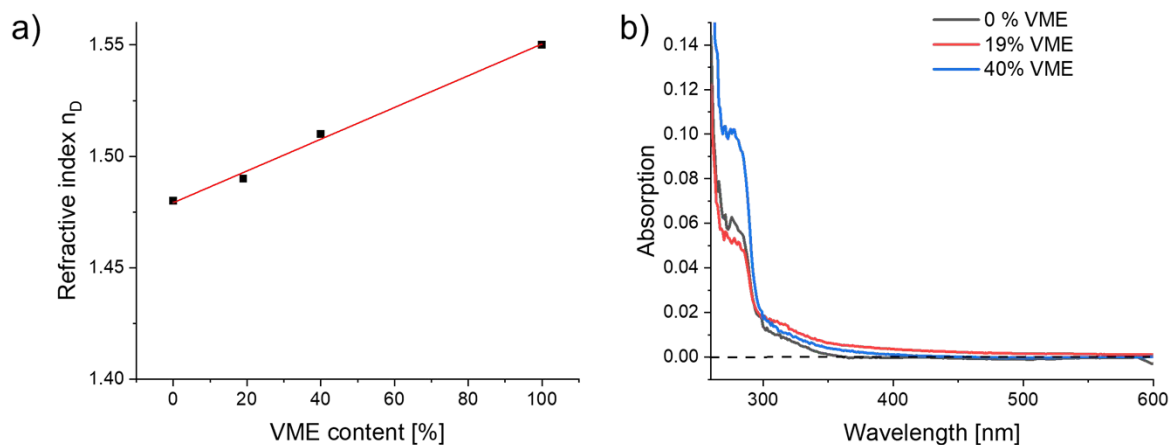


Figure S23: a) Plot of the refractive index vs. the VME content in the polymer b) UV-Vis spectra of the polymer with different amount of VME.

Table S15: Optical and mechanical properties of the different homo-and copolymers.

Copolymer	n_D (632.8 nm) ^a	E- modulus [MPa]	Hardness [MPa]	Creep [nm]
PMMA	1.48	3136 ± 125^b	115 ± 2.6^b	65 ± 2^b
P(VME- <i>co</i> -MMA) (P2)	1.49	2678 ± 93^b	100 ± 2.8^{cb}	72 ± 1^b
P(VME- <i>co</i> -MMA) (P3)	1.51	3209 ± 78^b	99 ± 1.1^b	65 ± 2^b
P(VME- <i>co</i> -BA) (P4)	1.52	2.5 ± 0.3^c	0.1 ± 0.01^c	378 ± 14^c

PVME (P1)	1.55	4.4 ± 0.3^c	0.09 ± 0.003^c	977 ± 16^c
^a Determination <i>via</i> ellipsometry measurements ^b Determination <i>via</i> nano-indenter measurements with a load of 1 mN ^c Determination nano-indenter measurements with a load of 0.3 mN				

1. J. Brandrup, E. H. Immergut and W. A. Grulke, *Polymer Handbook*, John Wiley & Sons, Inc., Hoboken, New Jersey, 1999.
2. G. Beadie, M. Brindza, R. A. Flynn, A. Rosenberg and J. S. Shirk, *Appl. Opt.*, 2015, **54**, F139-F143.

Publication P3

Coordination of noble metals in poly(vinyl mercaptoethanol) particles prepared by precipitation/emulsion polymerization

N. Ziegenbalg, H. F. Ulrich, S. Stumpf, P. Mueller, J. Wiethan, J. Danner, U. S. Schubert, T. Adermann, J. C. Brendel, *Macromol. Chem. Phys.* **2022**, submitted.

Reproduced by permission of H. F. Ulrich, S. Stumpf, P. Mueller, J. Wiethan, J. Danner, U. S. Schubert, T. Adermann, J. C. Brendel.

1 **Coordination of noble metals in poly(vinyl mercaptoethanol) particles** 2 **prepared by precipitation/emulsion polymerization**

3 Nicole Ziegenbalg,^{a,b} Hans F. Ulrich,^{a,b} Steffi Stumpf,^{a,b} Philipp Mueller,^c Jürgen Wiethan,^c Janette
4 Danner,^c Ulrich S. Schubert,^{a,b} Torben Adermann,^c Johannes C. Brendel,^{a,b,*}

5 a Laboratory of Organic and Macromolecular Chemistry (IOMC), Friedrich Schiller University
6 Jena, Humboldtstraße 10, 07743 Jena, Germany

7 b Jena Center for Soft Matter (JCSM), Friedrich Schiller University Jena, Philosophenweg 7,
8 07743 Jena, Germany

9 c BASF SE, Carl-Bosch-Straße 38, 67056 Ludwigshafen/Rhein, Germany

10 d BASF Grenzach GmbH, Koechlinstrasse 1, 79639 Grenzach-Wyhlen, Germany

11 *corresponding author: johannes.brendel@uni-jena.de

12 Keywords: *S*-Vinyl monomer, sulfur-containing polymer, emulsions polymerization, precipitation
13 polymerization, polyvinyl alcohol, metal nanoparticles, antibacterial effect, silver composites, gold
14 composites.

15 **Abstract**

16 *S*-Vinyl monomers react readily in radical polymerizations resulting in polymers with interesting
17 features such as enhanced refractive indices, increased thermal stability, or the ability to coordinate
18 various metals. Among them, vinyl mercaptoethanol (VME) can be produced in industrial scale,
19 but the poor solubility of the resulting homopolymer limits its application. In this contribution, we
20 investigated polymerizations of the monomer in water forming a heterogeneous system. The good
21 solubility of the monomer in water imparts the system with mixed characteristics between a
22 precipitation and an emulsion polymerization. Evaluating various surfactants, only polyvinyl
23 alcohol (PVA) was found to create stable dispersions, although micrometer sized particles are
24 formed with a broad size distribution. Nevertheless, the particles were able to coordinate silver or
25 gold ions. Attempts to reduce the noble metal ions by commercial reducing agents failed. However,

26 exposure to sunlight unexpectedly resulted in a controlled reduction of the metal ions and the
27 formation of composite particles. Silver ion-containing dispersions demonstrated strong
28 antibacterial properties, while the effect was diminished in the corresponding composite. Overall,
29 the precipitation/emulsion polymerization of VME represents a promising pathway to stable sulfur-
30 rich polymer dispersions with the ability to coordinate metal ions or form reactive metal
31 composites.

32 **Introduction**

33 In large-scale production, heterogeneous radical polymerization techniques such as emulsion^[1-6],
34 suspension^[7] or precipitation^[8, 9] polymerizations are often preferred over homogeneous
35 polymerization techniques (bulk or solution polymerization).^[10] In particular, water-based reaction
36 media are used, since they offer the benefit of good heat dissipation, are environmentally benign,
37 and cause only low costs. Furthermore, polymers with higher molar mass and faster polymerization
38 rates can be obtained due to the confinement of the active radicals.^[11-13] In addition, there is the
39 possibility to produce micro- and nanoscale-sized particles and materials instantaneously. The
40 properties of the resulting suspensions or dispersions can be altered by varying the particle size,
41 particle surface chemistry or their composition.^[14-16] Such particles are used, for example, as
42 paints,^[17] coatings,^[18, 19] adhesives,^[20] or imprinted polymers.^[21-23]

43 Such polymer particles can also be used as a host matrix for the coordination of metal salts or
44 nanoparticles, which either allow to introduce additional functionality into the polymers or
45 guarantee stabilization of the metal particles preventing clustering and aggregation.^[24-27] These
46 composites are commonly prepared in two different ways which are referred to as *in situ* or *ex situ*
47 method. In the first, an existing polymer is modified with metal ions or metal nanoparticles, while
48 in the *ex situ* variant the monomer is polymerized in the presence of the nanoparticles or metal
49 salts.^[28] In any case, functional groups are required within the monomers or polymers that feature
50 a high affinity for the corresponding metals. In particular, sulfur-containing polymers have raised
51 considerable attraction,^[29, 30] and they have a high affinity to noble metals such as silver, gold,
52 platinum, but also other metals.^[31-35] Many literature examples are based on polymers comprising
53 sulfonates,^[36] thiolates,^[37] thiols,^[38-43] or thioethers groups,^[38, 44] which coordinate well with these

54 metals. More recently inverse vulcanization using elemental sulfur has raised increasing attention
55 to create sulfur rich polymers,^[45-47] which can further be modified with metal nanoparticles.^[48-51]
56 Vinyl sulfide monomers represent another interesting monomer class to prepare polymers with
57 high sulfur content by straightforward radical polymerization.^[52] The poor availability of such
58 monomers is certainly a limitation, but it is still surprising that reports on emulsion, precipitation,
59 or dispersion polymerizations in aqueous medium are scarcely found in literature, considering the
60 potential to create stable dispersion metal composites in a straightforward and scalable process.

61 Based on our previous work on the radical polymerization of vinyl mercaptoethanol (VME), we
62 investigated in this contribution the possibility of directly generating stable polymer particles from
63 this sulfur-containing monomer.^[53] The monomer itself is fully miscible with water up to a
64 concentration of 105.5 g L⁻¹ (at 20 °C), which differs from common monomers used in emulsion
65 polymerizations. Consequently, polymerization in an aqueous system might feature more
66 characteristics of a precipitation polymerization, although features of an emulsion system might
67 still prevail. Different stabilizing agents, as well as different monomer concentrations, were tested
68 to investigate on the one hand their influence on possible coagulation of the particles and on the
69 other hand their influence on conversion and chain length. Subsequently, we examined the
70 coordination of silver and gold ions within the resulting particles and tested the formation of
71 corresponding nanocomposites to expand the possible range of applications. In particular, with
72 regard to the application of silver nanocomposites, many examples are known in the literature that
73 prove the antibacterial effect of the substances and thus suggest an application in the medical
74 field.^[54-57] Gold nanocomposites, in turn, can also be used in medical applications such as
75 diagnostic imaging and cancer therapy,^[58-62] but are also suitable for catalytic applications.^[63-66]

76 **Results and discussion**

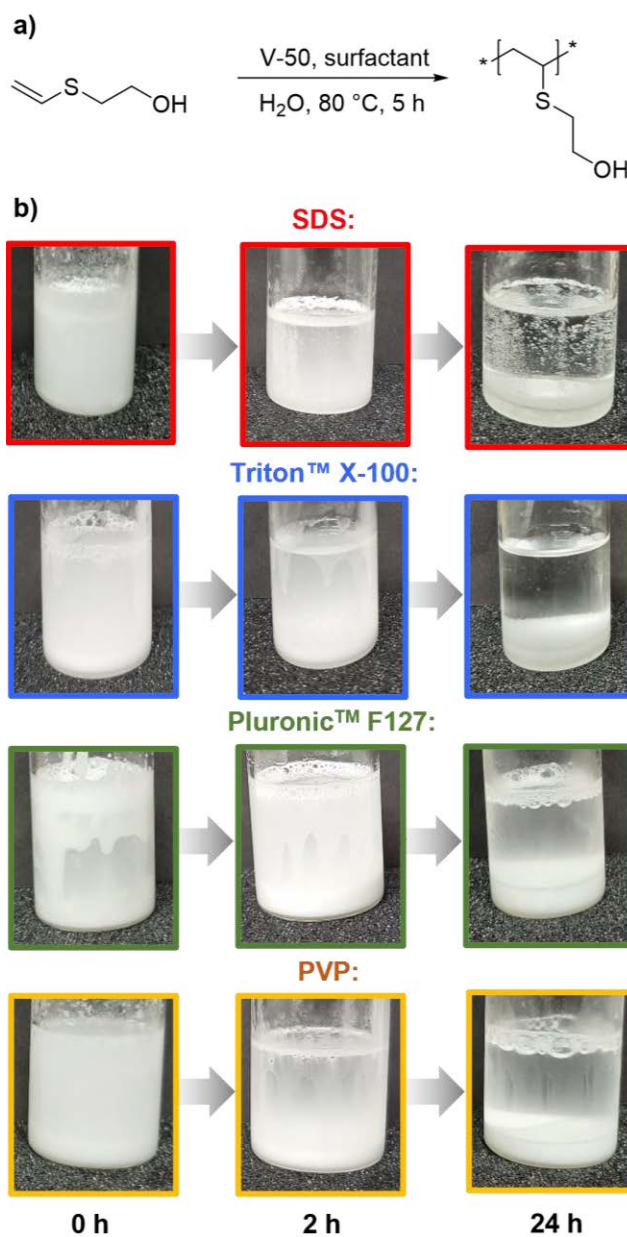
77 *Influence of surfactants*

78 Vinyl mercaptoethanol and the corresponding polymer feature an amphiphilic character induced
79 by the hydrophilic hydroxy moiety and the more hydrophobic thioether group. While the monomer,
80 therefore, has still a rather high solubility in water, the polymer becomes insoluble already at low
81 degrees of polymerization. Nevertheless, the hydroxy groups still cause a significant interaction

82 with water, and due to the polar character, we assume a high degree of swelling of the polymer in
83 water, which makes suitable stabilization of corresponding particles challenging. The first
84 polymerization experiments were all performed at a monomer concentration of 0.22 g/mL, which
85 exceeds the solubility limit. We further used the water-soluble initiator 2,2'-azobis(2-
86 methylpropionamide) dihydrochloride (V-50). Considering that phase-separated monomer
87 droplets are formed in this case, the process certainly resembles some features of an emulsion
88 polymerization although the high solubility might induce most characteristics of a precipitation
89 polymerization. Several different stabilizing reagents are established for heterogeneous
90 polymerizations, which are necessary to prevent coagulation of the particles.^[11] In consequence,
91 we first examined the polymerization of VME dispersed in water containing 1wt% of different
92 surfactants. At first, one of the most common stabilizing reagents, sodium dodecyl sulfate (SDS),
93 was tested. Surprisingly, this surfactant had no significant effect on the stability of the dispersion,
94 since precipitation occurred almost instantaneously with the first polymers formed (**Figure 1**). The
95 results were comparable to the control experiment without any surfactant. Further variations of the
96 conditions resulted in no improvement (data not shown). To exclude that the anionic character of
97 the surfactant induces instability by interacting with the positively charged initiator, we further
98 tested neutral stabilizers. Therefore, polyethylene glycol (PEG) based Tween™ 80 and Triton™
99 X-100 were examined and it seems that these surfactants with alkyl chains are also not suitable to
100 produce stable particles (**Figure 1**). We assume that the aliphatic tails of these surfactants are
101 generally incompatible with the polymer which we relate to the presence of the still rather polar
102 hydroxy groups.

103 In consequence, we further selected surfactants comprising more similar polar groups which were
104 considered to form secondary interactions such as hydrogen bonds with the hydroxyl group of
105 VME and, thus, ensure a better stabilization. Besides the triblock copolymer Pluronic™ F127,
106 commercially available polyvinyl pyrrolidone (PVP 40 000) and polyvinyl alcohol (PVA 31 000)
107 were examined. Unfortunately, Pluronic™ F127 and PVP did not live up to expectations because
108 the resulting particles sedimented still quickly and were not completely redispersible. Nevertheless,
109 some improvements were observed for PVP compared to the previously described surfactants,
110 since the full sedimentation appears slightly delayed and at least a part of the particles was
111 redispersible (for details about conversion and molar mass distribution see **SI Table S6 and Figure**

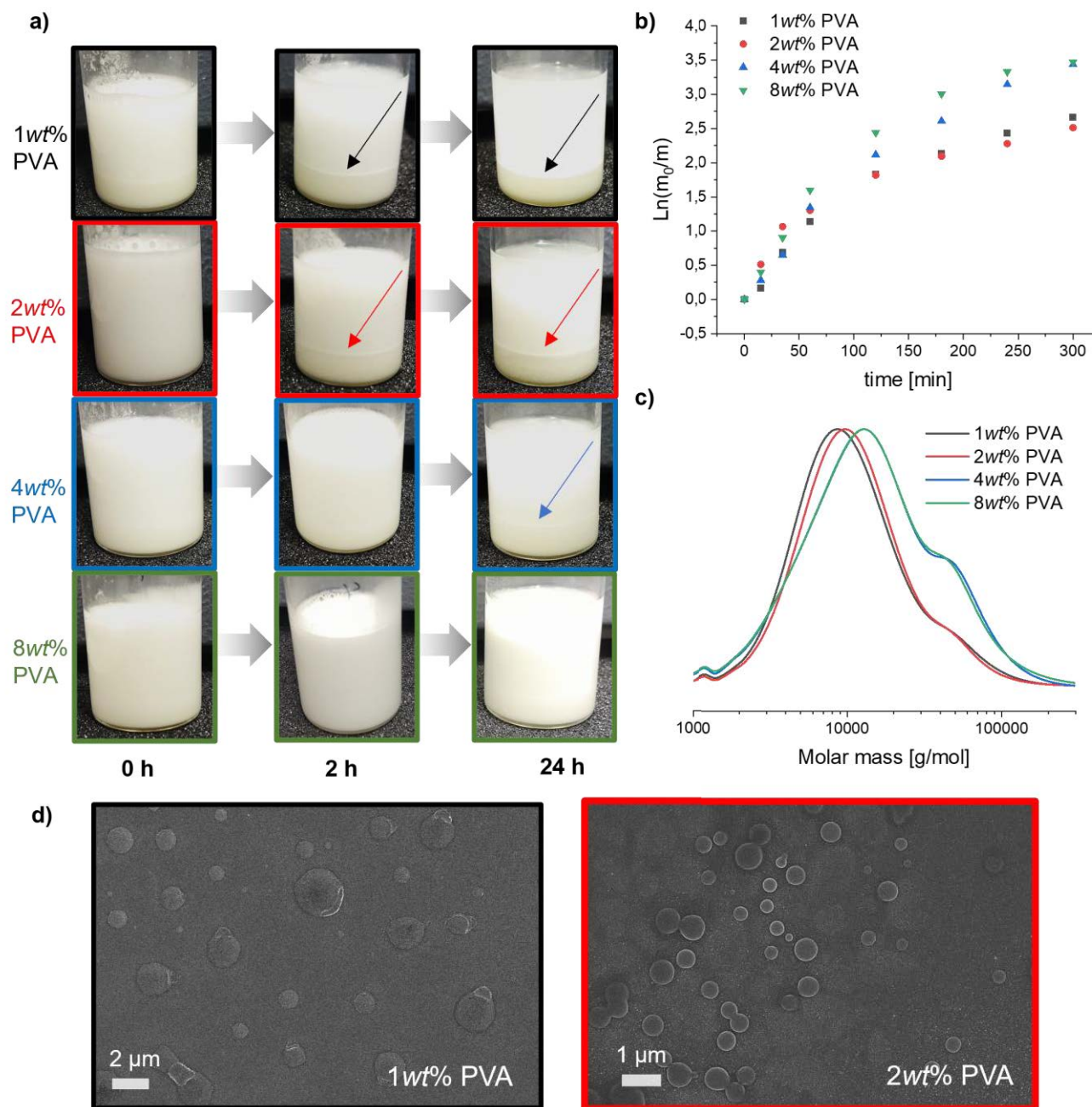
112 **S1)** The DLS-measurements in water performed directly after polymerization confirmed a very
113 broad size distribution of particles with sizes >400 nm for all used surfactants (**SI Figure S2**). The
114 largest aggregates were formed with SDS (≈ 900 nm), while only minimal smaller aggregates were
115 observed with the other three surfactants (400 to 700 nm).



116
117 **Figure 1: Photographs of samples taken at different timepoints after the polymerization of**
118 **VME with different surfactants to illustrate the sedimentation behavior over the time; the**
119 **first image was taken immediately after polymerization.**

120 PVA, on the other hand, proves to be the best stabilizing reagent for this system, because the
121 particles sediment only slowly and are completely redispersible. This behavior could not be
122 observed with any other surfactant. However, even in this case, the DLS-measurements revealed
123 sizes in the range of micrometers (**SI Table S7, Figure S3**). Since the correlogram already give
124 indications of aggregates that are located outside of the measurable range, a very broad distribution
125 can be assumed. Nevertheless, redispersible dispersions are formed with PVA and SEM images
126 prove the spherical shape of the particles formed in the emulsion at a PVA content as low as 1wt%
127 (**Figure 2d**). However, due to the soft nature of the polymer, only collapsed particle structures
128 could be recorded in the SEM images. Subsequently, we investigated the influence of the PVA
129 content as well as the monomer concentration on the conversion, the chain length, and on the
130 stability of the particles. From the data summarized in **Figure 2**, it can be deduced that the
131 polymerization at 1wt% and 2wt% PVA is very similar, as similar conversion rates and molar mass
132 distributions were obtained. The molar mass distribution reveals a bimodal distribution, which is
133 another indication of a mixed polymerization process. However, a slight difference was observed
134 when the PVA content was increased to 4wt%. Both reaction rate and molar mass increase, which
135 might reflect a more heterogeneous character of the system. Interestingly and contrary to our
136 expectations, the DLS-measurements revealed that larger particles are formed at the increased
137 content of PVA (**Figure S3**), which indicates an upper limit even for this surfactant to create stable
138 dispersions. SEM-images prove again the presence of spherical particles (**Figure 2d**) but also
139 confirm broad size distribution of the particles also with higher amount of PVA.

140



141

142 **Figure 2: a) Photographs of samples taken at different timepoints after the polymerization of**
 143 **VME with different content of PVA to illustrate the sedimentation behavior (the arrows**
 144 **indicate the edge of the formed sediment, if present), b) plot of $\ln(m_0/m)$ vs. reaction time, c)**
 145 **SEC (DMAc (+ 0.21 wt% LiCl), PMMA standards) traces of the emulsion polymers after 5 h**
 146 **with different amount of PVA, and d) SEM-images of the particles with 1 wt% and 2 wt%**
 147 **PVA.**

148 Decreasing the monomer concentration had no major impact on the behavior of the polymerization.
149 At lower concentrations, the polymerization rate is decreased (SI Table S8 and Figure S4), but
150 this appears related to dilution rather than any effect of confinement in emulsion particles. At a
151 concentration of 0.06 g mL⁻¹ the monomer fully dissolves in water turning the system into a pure
152 precipitation polymerization. Like the experiments at higher concentrations, redispersible particles
153 are formed, although these appear to sediment slightly faster compared to the previous samples.

154 We further analyzed the thermal properties of the prepared polymers. A decomposition temperature
155 of approximately 270 °C and a glass transition temperature of about 15 °C (SI Table S9, Figure
156 S6) were determined, which are close to the previous measured values for polymers prepared in
157 bulk or solution.^[53] The rather low glass transition might further correlate with the tendency of the
158 particles to agglomerate and fuse together. Overall, stabilization of the particles proved to be
159 difficult, which, as mentioned in the beginning, is mainly due to the amphiphilic character of the
160 monomer and the resulting polymers. Nevertheless, the addition of PVA provided some stability
161 and redispersible microparticles are formed, even though the size distribution was broad.

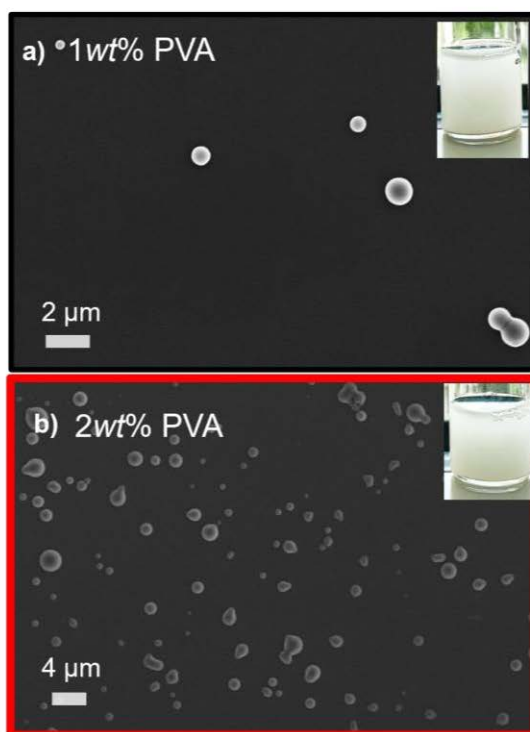
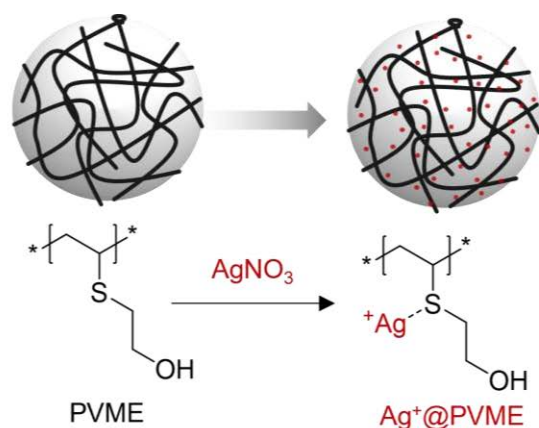
162 *Coordination of silver ions (Ag⁺@PVME) and formation of silver composites (Ag@PVME)*

163 The coordination of various metals or ions is a feature induced by various sulfur compounds, and
164 we considered our dispersions an interesting candidate to create such composites. Initially, we
165 focused on silver ions and the formation of silver nanoparticles within the polymer dispersions.
166 Silver is known to coordinate well with sulfur, and the resulting ion- or metal-loaded polymer
167 particles might be interesting as antibacterial material similar to widely applied silver
168 nanoparticles. It turned out that a direct polymerization in the presence of silver nitrate or acetate
169 and the resulting pre-arrangement of the monomer induced a strong coagulation and was therefore
170 discarded (data not shown). Consequently, we pursued a two-step process, in which polymer
171 particles were first formed as described above (surfactant: PVA) and silver ions were later added
172 to the purified polymer particles.

173 Different amounts (0.02, 0.04 and 0.1 eq.) of silver ions compared to the sulfur atoms in the
174 polymer were added and then dialyzed to remove the excess of non-coordinated silver ions. The
175 successful incorporation of the silver ions into the particles was evaluated by inductively coupled

176 plasma mass spectrometry (ICP-MS) measurements. The analysis revealed that the addition of an
177 increased amount of silver ions at the beginning also resulted in increased incorporation into the
178 polymer particles (**SI Table S10 for details**). At an amount of 0.02 and 0.04 equivalents of silver
179 ions, the determined silver ion concentration in the particles is close to the maximum possible
180 concentration, *i.e.*, almost all silver ions are bound to the sulfur. However, for 0.1 equivalents the
181 values deviate which indicates an oversaturation of the particles with silver and an excess of silver
182 ions is removed during purification. Although 0.1 equivalents appear low considering the strong
183 affinity of the sulfur compounds, it has to be kept in mind that silver ions might coordinate with
184 several sulfur atoms and the particles might not be fully penetrable once the surface is saturated
185 with silver ions.

186 In addition, the influence of the silver ions on the emulsions with different PVA content was also
187 investigated. Interestingly, the silver ions appear to have a stabilizing effect on the particles, as
188 sedimentation was retarded, and DLS-measurements also confirmed a change of size (**see SI**
189 **Figure S7**). An agglomeration of particles might be prevented by the positive charge of the silver
190 ions and the associated repulsion. A positive net charge was confirmed by zeta potential
191 measurements (**see SI Figure S8**) and smaller size distributions are observed. It seems that the best
192 stability can be achieved with a PVA content of 1wt% and the silver ions, while faster
193 sedimentation can again be observed for example with 4wt% or more PVA. Higher amounts of
194 PVA might prevent full incorporation of the silver ions covering the particle surface and a larger
195 amount of silver ions remains then in solution. This assumption is supported by the SEM-images,
196 where coagulation of the silver salts can be observed in the dried sample, but this occurs partly in
197 the polymer particle and partly outside the polymer particle (SEM-images for dispersion with 1wt%
198 and 2wt% PVA see **Figure 4** and SEM-images for dispersion with 4wt% and 8wt% PVA **see SI**
199 **Figure S9**). For this reason, the emulsion with 1wt% was further investigated.

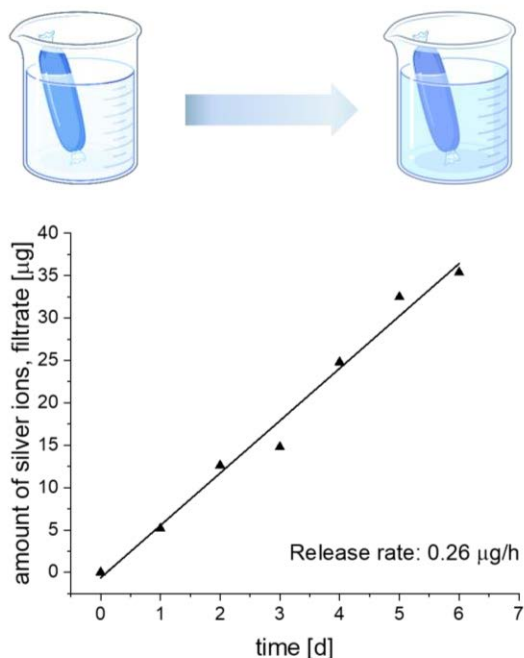


200

201 **Figure 3: SEM images of a) PVME@Ag⁺ with 1wt% PVA, and b) PVME@Ag⁺ with 2wt%**
 202 **PVA.**

203 The stability of the silver ion complexes in the polymer particles was further analyzed over one
 204 week. First, we determined the silver concentration of the sample with 0.04 eq. of silver after initial
 205 dialysis (three days) of the particles to ensure the removal of any excess of free silver ions. Then,
 206 the emulsion was transferred into a controlled dialysis setup and the filtrate was analyzed every
 207 24 h over six days by ICP-MS measurements. This total silver content decreased slightly over the
 208 time indicating already a release of silver ions. A closer look at the filtrate samples taken every day

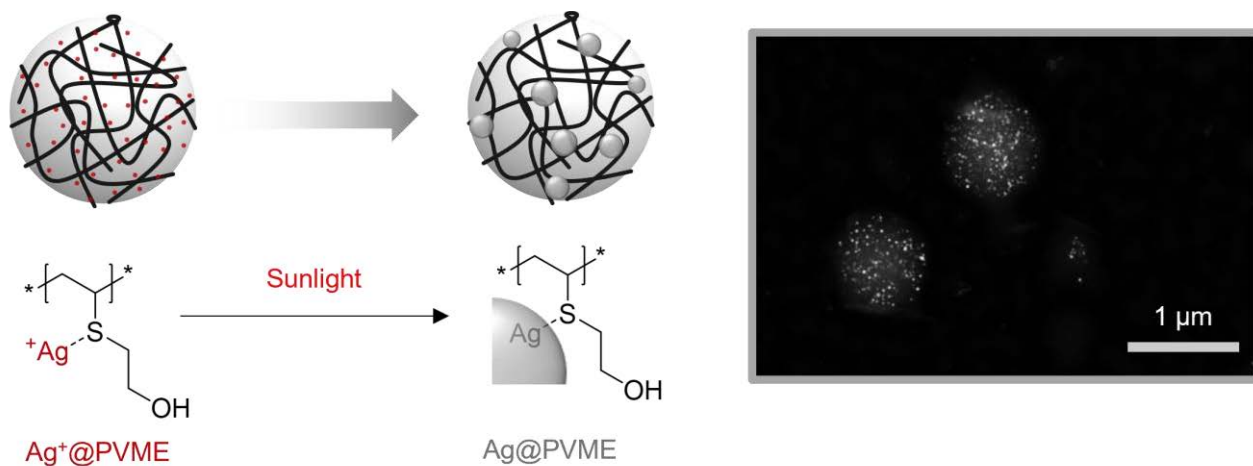
209 confirmed a linear increase of the accumulated silver ions within the dialysis water over the six
210 days (**Figure 4**). Due to the inhomogeneity of the dialysis water, there may be deviations between
211 the concentration values determined for the dialysis water and the concentration loss in the dialysis
212 tube. Nevertheless, a continuous release of silver ions can be observed.



213
214 **Figure 4: Schematic representation of the release experiment (top) and cumulated amount of**
215 **released silver ions in the filtrate over one week.**

216 Since the polymer emulsions were able to coordinate silver ions, we further tested the possibility
217 to create silver nanoparticles inside the polymer emulsions by reduction of the coordinated silver
218 ions. However, the choice of a suitable reducing agent proved to be a major challenge. Initial
219 attempts using conventional reducing agents such as sodium borohydride failed and led to
220 coagulation of the silver and the polymer particles. We consider the rapid formation and
221 competitive coordination of the borohydride salts might cause this instability of the solution, since
222 the coordination of the silver ions in the polymer particle is not sufficiently strong. A gentler
223 reducing agent is ascorbic acid. However, even in this case, silver nanoparticles appeared randomly
224 distributed throughout the sample and both free silver nanoparticles and silver nanoparticles
225 coordinated to the polymer could be detected (**SI Figure S10**). Nevertheless, the emulsion appeared
226 more stable compared to sodium borohydride. Interestingly, an alternative and mild pathway
11

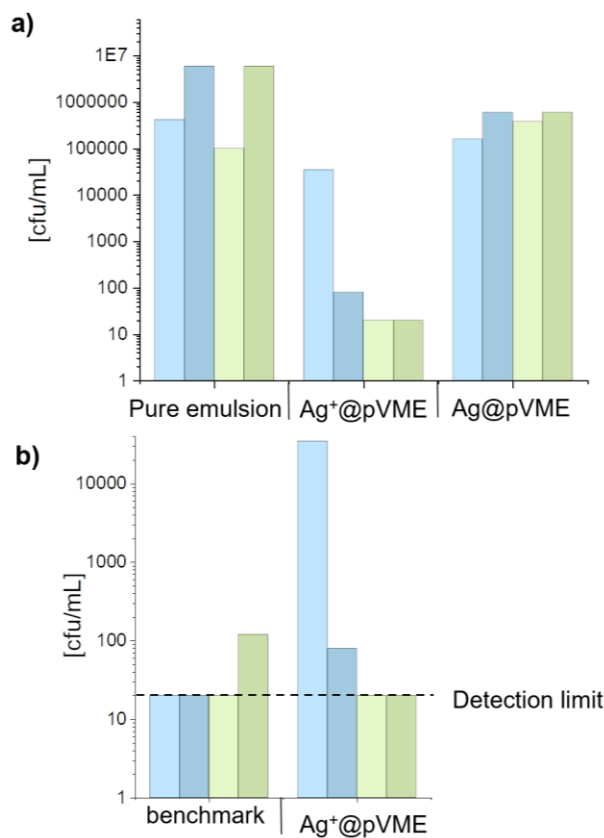
227 opened up during our experiments. Leaving untreated samples on the lab bench in open light
228 induced a color transition of the samples from white to brown indicating the *in-situ* formation of
229 silver nanostructures. We further followed this route using sunlight to induce the reduction. UV-
230 Vis spectra of highly diluted solutions revealed a clear shift of the absorbance of the emulsion to
231 higher wavelengths, which further confirmed the formation of silver nanoparticles (**SI Figure S11**).
232 Kept in sunlight, all emulsions remained stable and only a very slow sedimentation occurred over
233 time. Furthermore, the silver nanoparticles appeared uniformly distributed among the polymer
234 particles as shown by TEM and SEM images of the particles (**Figure 5 and SI Figure 12, DLS**
235 **data Figure S13**). An explanation for the reduction of silver ions by sunlight might be related to
236 the chemical nature of the polymer particle. In this case, the sulfide groups in the repeating unit
237 might act as reducing agents and themselves become oxidized to the corresponding sulfoxide.
238 However, we were not able to directly detect the oxidized product in the composite, despite
239 intensive efforts. Nevertheless, this experiment revealed a straightforward way to create silver
240 nanoparticles within the given polymer emulsions.



241
242 **Figure 3: Schematical representation of the reduction of $Ag^+@PVME$ within the polymer**
243 **particles (left) and corresponding TEM-image of the reduced sample $Ag@PVME$ (right).**

244 As mentioned above, silver nanoparticles are frequently used in antimicrobial coatings or
245 materials.^[54-57, 67] The effect is often related to a continuous release of small amounts of silver ions
246 into the environment, which interfere with microbial growth.^[56, 68, 69] To elucidate whether the
247 polymer particles with silver ions or silver nanoparticles are suitable for antibacterial application,

248 the growth of *E. coli* and *S. aureus* was studied in the presence of the different emulsions (**Figure**
249 **6a**). The pure PVME emulsion showed no antibacterial effect, resulting in unaffected bacterial
250 growth over 24 hours. The modified samples, on the other hand, revealed a significant antibacterial
251 effect. Ag⁺@PVME lead to a strong reduction of bacterial numbers in case of *E. coli* and *S. aureus*
252 after 4 hours of incubation and is maintained up to 24 h. Interestingly, the emulsions with silver
253 nanoparticles were not as effective as the coordinated ions and did not show a clear antibacterial
254 effect under the applied test conditions, which is in contrast to common silver nanoparticle-based
255 systems. We attribute this to the fact that the antibacterial effect is related to the continuous release
256 of silver ions, which was confirmed for Ag⁺@PVME. In case of the silver nanoparticles, the silver
257 content in the test sample with the nanoparticle preparation was significantly lower than in the
258 Ag⁺@PVME test sample and the required oxidation of the metallic silver might be suppressed or
259 the silver ions were too strongly bound to the polymer emulsions.^[70] We finally compared our
260 silver ion containing polymer particles with the benchmark substance Irgaguard B 6000 (**Figure**
261 **6b, for details see Table S11**), which is an antimicrobial agent based on a inorganic silver
262 glass/zeolite composite. At 4 hours incubation, the effect of Ag⁺@PVME on *S. aureus* is slightly
263 diminished compared to the control, but after 24 hours a similar effect is observed, despite the
264 system has not been optimized for this application. More detailed studies might help to improve
265 the effect, but this was beyond the scope of this study.



S. aureus ATCC 6538 (after 4 h and after 24 h)

E. coli DSM 682 (after 4 h and after 24 h)

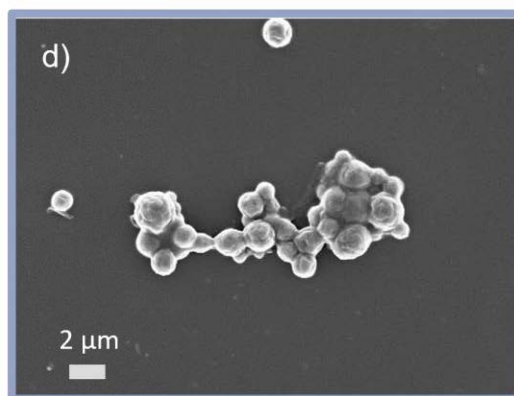
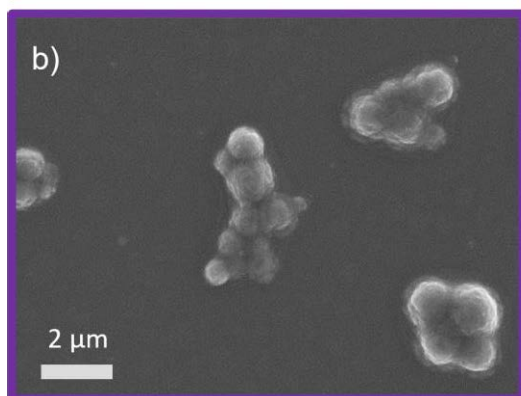
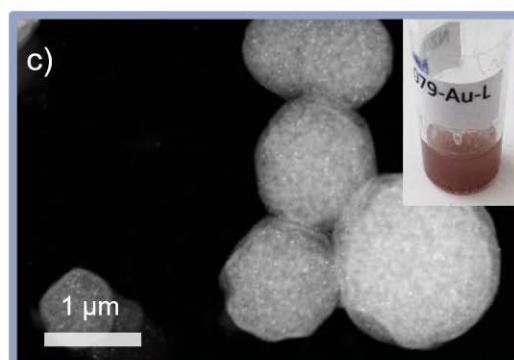
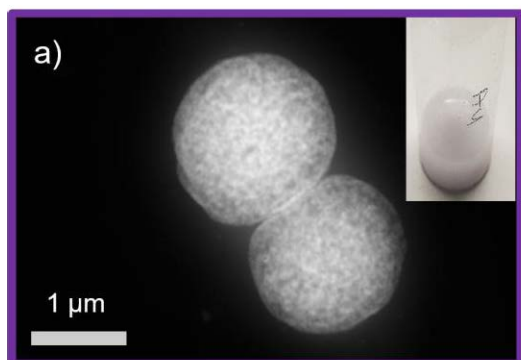
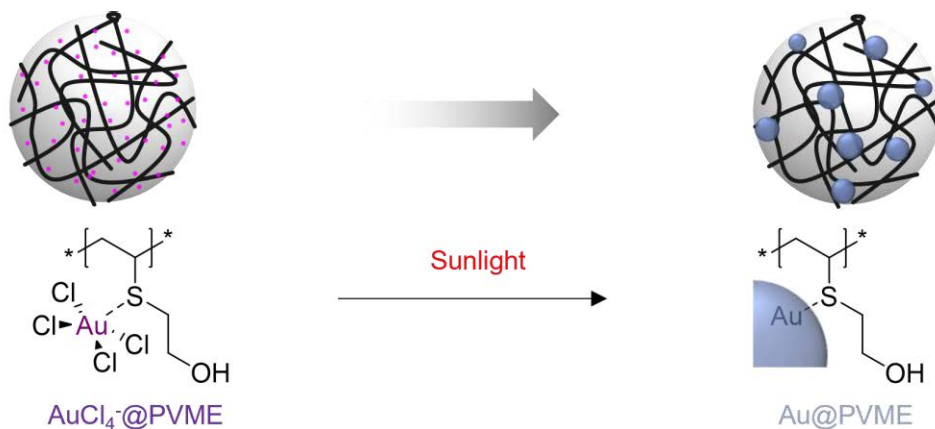
266

267 **Figure 4: a) Results of the tests on antibacterial effects (*S. aureus*: blue, *E. coli*: green) induced**
 268 **by the pure PVME emulsion, the emulsion containing silver ions (Ag⁺@PVME), and**
 269 **emulsions comprising silver nanoparticle (Ag@PVME) after 4 h (light color) and 24 h (dark**
 270 **color) of coincubation and b) Zoomed graph of the results on antibacterial effect for**
 271 **Ag⁺@PVME in comparison to a benchmark.**

272 ***Synthesis of gold composites (Au@PVME)***

273 Besides silver, other noble metals and their ions are known to coordinate well with sulfur
 274 compounds. We therefore tried to extent our approach to gold, focusing again on an *in situ*
 275 formation of polymer integrated nanoparticles. Initially, we tested potassium Au(III) chloride as
 276 precursor, but this did not lead to stable dispersions. The addition of chloroauric acid, however, did
 277 not cause coagulation and a homogeneous distribution of the gold salt could be confirmed by TEM
 278 and SEM images (**Figure 7**). Again, we tested different reducing agents to induce the

279 transformation into metallic gold. However, a broad distribution of gold particles and limited
280 incorporation into the polymer was observed like for the experiments with silver. Consequently,
281 we again tested a light-induced reduction, which resulted in an increasing coloration of the sample
282 turning purple-brown. Interestingly, the subsequent analysis by TEM and SEM revealed slight
283 deformations on the surface of the resulting polymer particles (**Figure 7c**) and confirmed the
284 successful integration of the gold into the polymer. The deformations are most likely a result of the
285 reduction and a homogenous distribution of the initial precursor throughout the outer layers of the
286 polymer particles. We again speculate that the light induces an oxidation of the sulfur in the
287 polymer while the gold precursor is reduced. Overall, the particles appear stable, although a more
288 rapid sedimentation is observed, which we relate to the limited repulsion by charges and an
289 increased density induced by the metallic gold. The polymer particles modified with gold
290 (Au@PVME) are nevertheless still well redispersible if agitated rendering the system an interesting
291 and easily accessible scaffold for integration of noble metal catalysts, which is currently further
292 investigated.



293

294 **Figure 5:** a) TEM-image of $\text{AuCl}_4^- @ \text{PVME}$, b) SEM-image of $\text{AuCl}_4^- @ \text{PVME}$, c) TEM-
 295 image of $\text{Au} @ \text{PVME}$, and d) SEM-image of $\text{Au} @ \text{PVME}$.

296 **Conclusion**

297 In summary, we investigated the possibility of an emulsion polymerization of the electron rich S-
 298 vinyl monomer vinyl mercaptoethanol (VME) testing various surfactants. The monomer itself has
 299 a solubility in water (105.5 g/L) but the polymer becomes insoluble. Due to the high solubility of
 300 the monomer the process resembles characteristics of a precipitation polymerizations although
 16

301 monomer droplets are present at higher concentrations. The stabilization of the resulting polymer
302 particles appeared to be a major challenge in the system. Various added surfactants had no or only
303 limited visible effect on the stability of the formed dispersion, which we relate to the amphiphilic
304 character of the polymer structure comprising hydrophilic hydroxyl-groups next to the hydrophobic
305 thioether groups and the aliphatic backbone. Nevertheless, stable dispersions were obtained
306 applying PVA as surfactant, which might be able to coordinate to the hydroxy groups. In contrast
307 to common emulsion polymerizations, particles of few to several micrometers were obtained
308 depending on the amount of added surfactant. This result again reflects that the process is more
309 related to a precipitation polymerization than a real emulsion system. With a stable dispersion at
310 hand, we further investigated the potential of the particles to coordinate metal ions, particularly of
311 noble metals. First, the coordination of silver ions was examined and both the actual incorporation
312 of silver ions into the particle and the release over time were studied. Up to an amount of 0.04
313 equivalents of silver ions compared to sulfur in the polymer, almost all of the silver ions were
314 incorporated and complexed. Placed in deionized water, the silver ions are continuously released
315 over one week, although the rate is very low. Higher equivalents of silver ions cannot be fully
316 coordinated within the polymer dispersions which indicates that penetration into the polymer
317 particles might be hampered. We further investigated whether metal silver can be formed with the
318 polymer particles from the ion complexes. However, common reducing agents led to agglomeration
319 of the particles and only a limited amount of silver remained coordinated within the polymer.
320 Interestingly, simple irradiation with sunlight resulted in the formation silver nanoparticles, which
321 is presumably due to the fact that the polymer particle itself acts as a gentle reducing agent. In this
322 case, the distribution of silver throughout the polymer particle was more homogeneous and stable
323 dispersions were obtained. Considering a potential antibacterial effect of silver nanoparticles, we
324 further analyzed the effect of our different systems on the growth of *E. coli* and *S. aureus*. In
325 contrast to the pure emulsion, the dispersion comprising coordinated silver ions displayed a strong
326 suppression of bacterial growth almost compatible to an optimized benchmark system. However,
327 the system containing reduced silver nanoparticles had only a minor effect. We relate this to a
328 limited formation of free silver ions by oxidation, which would be required for an antibacterial
329 effect. In addition to silver, we also tested the coordination of gold as another noble metal. Adding
330 chloroauric acid, stable dispersions were formed where the gold ions appear well distributed

331 throughout the polymer particles. The subsequent reduction in sunlight again turned out to be the
332 best method to create metallic gold within the polymer particles. This approach led to micrometer
333 sized polymer dispersions comprising a uniform coverage with metallic gold on the surface.
334 Overall, the presented straightforward approach to create dispersions of the sulfur-rich polymer
335 PVME may open interesting avenues to create host matrices for various metal ions and metal
336 nanoparticles. The resulting dispersions are stable or can easily be redispersed under agitation and
337 the metal particles are accessible at the surface.

338 **Acknowledgements**

339 The presented study is part of a research project funded by BASF SE to identify and develop
340 applications for vinyl mercaptoethanol (VME). JCB and NZ thank the German Science Foundation
341 (DFG) for generous funding within the Emmy Noether Programme (Project-ID: 358263073). In
342 addition, the authors thank Renzo Paulus for the TGA and DSC measurements, Dr Dirk Merten for
343 the ICP-MS measurements and Egon Gisela and Klaus Elfriede for the synthesis of the
344 nanoparticles. The SEM facilities of the Jena Center for Soft Matter (JCSM) were established with
345 a grant from the German Research Council (DFG).

346 **References**

- 347 [1] I. Capek, M. Riza, M. Akashi, *J. Polym. Sci. A Polym. Chem.* **1997**, *35*, 3131.
348 [2] J. M. Saenz, J. M. Asua, *J. Polym. Sci. A Polym. Chem.* **1996**, *34*, 1977.
349 [3] H. Bamnolker, S. Margel, *J. Polym. Sci. A Polym. Chem.* **1996**, *14*, 1857.
350 [4] J. M. Asua, "*Polymer Reaction Engineering*", Blackwell Publishing, Oxford, 2007.
351 [5] J. M. Asua, "*Polymeric Dispersions: Principles and Applications*", Springer, Dordrecht, 1997.
352 [6] C.-S. Chern, "*Principles and Applications of Emulsion Polymerization*", John Wiley & Sons, Hoboken,
353 2008.
354 [7] Y. Saeki, T. Emura, *Prog. Polym. Sci.* **2002**, *27*, 2055.
355 [8] D. Zhang, X. Yang, "Precipitation Polymerization", in *Encyclopedia of Polymeric Nanomaterials*,
356 Springer, Berlin, Heidelberg, 2015, p. 2108.
357 [9] H. J. M. Wolff, M. Kather, H. Breisig, W. Richtering, A. Pich, M. Wessling, *ACS Appl. Mater. Interfaces*
358 **2018**, *10*, 24799.
359 [10] P. Nesvadba, "Radical Polymerization in Industry", in *Encyclopedia of Radicals in Chemistry, Biology*
360 *and Materials*, 2012.
361 [11] P. A. Lovell, F. J. Schork, *Biomacromolecules* **2020**, *21*, 4396.
362 [12] J. M. Asua, *J. Polym. Sci. A Polym. Chem.* **2004**, *42*, 1025.
363 [13] P. B. Zetterlund, Y. Kagawa, M. Okubo, *Chem. Rev.* **2008**, *108*, 3747.
364 [14] P. J. Borm, D. Robbins, S. Haubold, T. Kuhlbusch, H. Fissan, K. Donaldson, R. Schins, V. Stone, W.
365 Kreyling, J. Lademann, J. Krutmann, D. Warheit, E. Oberdorster, *Part. Fibre Toxicol.* **2006**, *3*, 11.

366 [15] I. Khan, K. Saeed, I. Khan, *Arab. J. Chem.* **2019**, *12*, 908.
367 [16] J. Jeevanandam, A. Barhoum, Y. S. Chan, A. Dufresne, M. K. Danquah, *Beilstein J. Nanotechnol.*
368 **2018**, *9*, 1050.
369 [17] Y. Matsuda, K. Uchida, Y. Egami, H. Yamaguchi, T. Niimi, *Sensors* **2016**, *16*, 550.
370 [18] T. Tadros, "Paints and Coatings", in *Encyclopedia of Colloid and Interface Science*, T. Tadros, Ed.,
371 Springer, Berlin, Heidelberg, 2013, p. 821.
372 [19] J. Klier, J. Bohling, M. Keefe, *AIChE J.* **2016**, *62*, 2238.
373 [20] A. C. Taylor, "Adhesives with Nanoparticles", in *Handbook of Adhesion Technology*, Springer, Berlin,
374 Heidelberg, 2011, p. 1437.
375 [21] S. Pardeshi, S. K. Singh, *RSC Adv.* **2016**, *6*, 23525.
376 [22] G. Vasapollo, R. D. Sole, L. Mergola, M. R. Lazzoi, A. Scardino, S. Scorrano, G. Mele, *Int. J. Mol.*
377 *Sci.* **2011**, *12*, 5908.
378 [23] J. Wackerlig, R. Schirhagl, *Anal. Chem.* **2016**, *88*, 250.
379 [24] S. K. Ghosh, "*Functional Coatings: By Polymer Microencapsulation*", Wiley, 2006.
380 [25] S. Förster, M. Antonietti, *Adv. Mater.* **1998**, *10*, 195.
381 [26] S. Förster, M. Konrad, *J. Mater. Chem.* **2003**, *13*, 2671.
382 [27] N. Hadjichristidis, A. Hirao, Y. Tezuka, F. Du Prez, "*Complex Macromolecular Architectures:*
383 *Synthesis, Characterization, and Self-Assembly*", Wiley, 2011.
384 [28] H. Althues, J. Henle, S. Kaskel, *Chem. Soc. Rev.* **2007**, *36*, 1454.
385 [29] X.-H. Zhang, P. Theato, "Sulfur-Containing Polymers: From Synthesis to Functional Materials", Wiley
386 VCH GmbH, Weinheim, 2021.
387 [30] H. Mutlu, E. B. Ceper, X. Li, J. Yang, W. Dong, M. M. Ozmen, P. Theato, *Macromol. Rapid Commun.*
388 **2019**, *40*, e1800650.
389 [31] H. Vahrenkamp, *Angew. Chem. Int. Ed. Engl.* **1975**, *14*, 322.
390 [32] K. Suzuki, K. Yamasaki, *I. Inorg. Nucl. Chem.* **1962**, *24*, 1093.
391 [33] C. Vericat, M. E. Vela, G. Corthey, E. Pensa, E. Cortés, M. H. Fonticelli, F. Ibañez, G. E. Benitez, P.
392 Carro, R. C. Salvarezza, *RSC Adv.* **2014**, *4*, 27730.
393 [34] J. A. Rodriguez, J. Dvorak, T. Jirsak, G. Liu, J. Hrbek, Y. Aray, C. González, *J. Am. Chem. Soc.* **2003**,
394 *125*, 276.
395 [35] R. A. Bell, J. R. Kramer, *Environ. Toxicol. Chem.* **1999**, *18*, 9.
396 [36] A. S. Pozdnyakov, A. A. Ivanova, A. I. Emel'yanov, G. F. Prozorova, *Russ. Chem. Bull.* **2020**, *69*, 715.
397 [37] Y. Zhang, X. Wen, Y. Shi, R. Yue, L. Bai, Q. Liu, X. Ba, *Ind. Eng. Chem. Res.* **2018**, *58*, 1142.
398 [38] H. Xu, J. K. Jin, Y. Mao, J. Z. Sun, F. Yang, W. Z. Yuan, Y. Q. Dong, M. Wang, B. Z. Tang,
399 *Macromolecules* **2008**, *41*, 3874.
400 [39] X. Li, Y. Liu, Z. Xu, H. Yan, *Eur. Polym. J.* **2011**, *47*, 1877.
401 [40] J. A. Akkara, D. L. Kaplan, *Chem. Mater.* **1997**, *9*, 1342.
402 [41] S. Shin, J. Jang, *Chem. Commun.* **2007**, 4230.
403 [42] D. A. Boyd, J. Naciri, J. Fontana, D. B. Pacardo, A. R. Shields, J. Verbarg, C. M. Spillmann, F. S.
404 Ligler, *Macromolecules* **2014**, *47*, 695.
405 [43] J. P. Phillips, N. M. Mackey, B. S. Confait, D. T. Heaps, X. Deng, M. L. Todd, S. Stevenson, H. Zhou,
406 C. E. Hoyle, *Chem. Mat.* **2008**, *20*, 5240.
407 [44] J. Lutz, K. Albrecht, J. Groll, *Adv. NanoBiomed Res.* **2021**, *1*, 2000074.
408 [45] M. E. Duarte, B. Huber, P. Theato, H. Mutlu, *Polym. Chem.* **2020**, *11*, 241.
409 [46] W. J. Chung, J. J. Griebel, E. T. Kim, H. Yoon, A. G. Simmonds, H. J. Ji, P. T. Dirlam, R. S. Glass, J.
410 J. Wie, N. A. Nguyen, B. W. Guralnick, J. Park, Á. Somogyi, P. Theato, M. E. Mackay, Y.-E. Sung, K.
411 Char, J. Pyun, *Nat. Chem.* **2013**, *5*, 518.
412 [47] J. M. Scheiger, C. Direksilp, P. Falkenstein, A. Welle, M. Koenig, S. Heissler, J. Matysik, P. A. Levkin,
413 P. Theato, *Angew. Chem. Int. Ed.* **2020**, *59*, 18639.

- 414 [48] J. C. Bear, W. J. Peveler, P. D. McNaughter, I. P. Parkin, P. O'Brien, C. W. Dunnill, *Chem. Commun.*
415 **2015**, *51*, 10467.
- 416 [49] T. R. Martin, K. A. Mazzio, H. W. Hillhouse, C. K. Luscombe, *Chem. Commun.* **2015**, *51*, 11244.
- 417 [50] N. P. Tarasova, A. A. Zanin, E. G. Krivoborodov, Y. O. Mezhuev, *RSC Adv.* **2021**, *11*, 9008.
- 418 [51] E. T. Kim, W. J. Chung, J. Lim, P. Johe, R. S. Glass, J. Pyun, K. Char, *Polym. Chem.* **2014**, *5*, 3617.
- 419 [52] N. Ziegenbalg, L. Elbinger, U. S. Schubert, J. C. Brendel, *Polym. Chem.* **2022**, *13*, 5019.
- 420 [53] N. Ziegenbalg, F. V. Gruschwitz, T. Adermann, L. Mayr, S. Guriyanova, J. C. Brendel, *Polym. Chem.*
421 **2022**, *13*, 4934.
- 422 [54] G. Franci, A. Falanga, S. Galdiero, L. Palomba, M. Rai, G. Morelli, M. Galdiero, *Molecules* **2015**, *20*,
423 8856.
- 424 [55] N. Durán, M. Durán, M. B. de Jesus, A. B. Seabra, W. J. Fávaro, G. Nakazato, *Nanomedicine:*
425 *Nanotechnology, Biology and Medicine* **2016**, *12*, 789.
- 426 [56] I. A.-O. Yin, J. Zhang, I. A.-O. Zhao, M. L. Mei, Q. Li, C. A.-O. Chu, *Int. J. Nanomedicine* **2020**, *15*,
427 2555.
- 428 [57] C. Marambio-Jones, E. M. V. Hoek, *J. Nanoparticle Res.* **2010**, *12*, 1531.
- 429 [58] L. E. Cole, R. D. Ross, J. M. R. Tilley, T. Vargo-Gogola, R. K. Roeder, *Nanomedicine* **2015**, *10*, 321.
- 430 [59] P. C. Chen, A. K. Mwakwari Sc Fau - Oyelere, A. K. Oyelere, *Nanotechnol. Sci. Appl.* **2008**, *1*, 45.
- 431 [60] W. Cai, H. Gao T Fau - Hong, J. Hong H Fau - Sun, J. Sun, *Nanotechnol. Sci. Appl.* **2008**, *1*, 17.
- 432 [61] X. Huang, P. K. Jain, I. H. El-Sayed, M. A. El-Sayed, *Nanomedicine* **2007**, *2*, 681.
- 433 [62] S. Taghizadeh, V. Alimardani, P. L. Roudbali, Y. Ghasemi, E. Kaviani, *Photodiagnosis Photodyn.*
434 *Ther.* **2019**, *25*, 389.
- 435 [63] P. Paalanen, B. M. Weckhuysen, M. Sankar, *Catal. Sci. Technol.* **2013**, *3*.
- 436 [64] S. S. Dash, I. K. Sen, S. K. Dash, *Int. Nano Lett.* **2022**, *12*, 47.
- 437 [65] J. Zhao, R. Jin, *Nano Today* **2018**, *18*, 86.
- 438 [66] R. Ciriminna, E. Falletta, C. Della Pina, J. H. Teles, M. Pagliaro, *Angew. Chem. Inter. Ed.* **2016**, *55*,
439 14210.
- 440 [67] J. García-Barrasa, J. M. López-de-Luzuriaga, M. Monge, *Central European Journal of Chemistry* **2011**,
441 *9*, 7.
- 442 [68] S. Anees Ahmad, S. Sachi Das, A. Khatoon, M. Tahir Ansari, M. Afzal, M. Saquib Hasnain, A. Kumar
443 Nayak, *Mater. Sci. Energy Techn.* **2020**, *3*, 756.
- 444 [69] A. Kędziora, R. Wiczorek, M. Speruda, I. Matolínová, T. M. Goszczyński, I. Litwin, V. Matolín, G.
445 Bugła-Płoskońska, *Front. Microbiol.* **2021**, *12*.
- 446 [70] J. Liu, D. A. Sonshine, S. Shervani, R. H. Hurt, *ACS Nano* **2010**, *4*, 6903.

447

Supporting Information

Coordination of noble metals in poly(vinyl mercaptoethanol) particles prepared by precipitation/emulsion polymerization

Nicole Ziegenbalg,^{a,b} Hans F. Ulrich,^{a,b} Steffi Stumpf,^{a,b} Philipp Mueller,^c Jürgen Wiethan,^c Janette Danner,^c Ulrich S. Schubert,^{a,b} Torben Adermann,^c Johannes C. Brendel,^{a,b,*}

a Laboratory of Organic and Macromolecular Chemistry (IOMC), Friedrich Schiller University Jena, Humboldtstraße 10, 07743 Jena, Germany

b Jena Center for Soft Matter (JCSM), Friedrich Schiller University Jena, Philosophenweg 7, 07743 Jena, Germany

c BASF SE, Carl-Bosch-Straße 38, 67056 Ludwigshafen/Rhein, Germany

d BASF Grenzach GmbH, Koechlinstrasse 1, 79639 Grenzach-Wyhlen, Germany

*corresponding author: johannes.brendel@uni-jena.de

Experimental part

Materials and Methods

All reagents and solvents were commercially purchased from Sigma-Aldrich, TCI Chemicals, abcr, or were provided by BASF SE and were used without further purification. Table S1 summarizes the molar masses and other important properties of the surfactants used.

19 **Table S1: Overview of the molar masses of the different used surfactants.**

Surfactant	Molar mass [g mol ⁻¹]	Hydrolysis
Triton™ X-100	~ 625	-
Tween™ 80	~1 300	-
Pluronic™ F-127	~12 600	-
PVP	40 000	-
PVA	31 000	86.7 to 88.7mol%

20
 21 ¹H-NMR spectra were measured with a Bruker spectrometer (300 MHz) equipped with an Avance
 22 I console, a dual ¹H and ¹³C sample head and a 60 x BACS automatic sample changer. The chemical
 23 shifts of the peaks were determined by using the residual solvent signal as a reference and are given
 24 in ppm in comparison to TMS. Deuterated solvents were commercially purchased from EURISO-
 25 TOP GmbH.

26 Size-exclusion chromatography (SEC) of polymers was performed on an Agilent system (series
 27 1200) equipped with a PSS degasser, a G1310A pump, a G1362A refractive index detector and a
 28 PSS GRAM 30 and 1000 column with DMAc (+ 0.21wt% LiCl) as eluent at a flow rate of
 29 1 mL/min. The column oven was set to 40 °C and poly(methyl methacrylate) (PMMA) standards
 30 were used for calibration.

31 The differential scanning calorimetry (DSC) measurements were performed on a DSC 204 F1
 32 Phoenix® from Netzsch under a nitrogen atmosphere with a heating rate of 10 K/min. The thermal
 33 gravimetric analysis (TGA) was carried under nitrogen using a Netzsch TG 209F1 Iris®.

34 Dynamic light scattering (DLS) correlograms were measured on a ZetaSizer Nano ZS (Malvern,
 35 Herrenberg, Germany) equipped with a He–Ne laser with a wavelength of $\lambda = 633$ nm at a
 36 scattering angle of 173°. All measurements were conducted in triplicate at 25 °C after an
 37 equilibration time of 10 s and an acquisition time of 30 s.

38 Scanning electron microscopy (SEM) imaging was performed with a Sigma VP Field Emission
 39 Scanning Electron Microscope (Carl-Zeiss AG, Germany) using the InLens detector with an
 40 accelerating voltage of 6 kV. For the sample preparation, the dispersed samples were applied on a

41 mica substrate by drop casting and dried over a few hours. Then the samples were coated with a
42 thin layer of platinum via sputter coating (CCU-010 HV, Safematic, Switzerland) before the
43 measurement. The contrast of the images was increased afterward to make the aggregates more
44 visible.

45 For transmission electron microscopy (TEM), dispersed samples were applied on an ultra-thin
46 carbon-coated grid by the drop-on-grid method. The samples were imaged using a probe-corrected
47 Themis Z® 3.1 machine (Thermo-Fisher, Waltham, USA) in High-Angle Annular Dark-Field
48 (HAADF) Scanning Transmission Electron Microscopy (STEM) mode. Data were analyzed using
49 the Velox 2.1x software. Particle size was manually analyzed with Imagic IMS software (Imagic
50 Bildverarbeitung AG, Glattbrugg, Switzerland).

51 ICP-MS samples were previously filtered and acidified with 2% HNO₃. The measurements were
52 performed on 8900 Triple Quadrupole ICP-MS (FA. Agilent, Waldbronn, Deutschland).

53 Antibacterial tests:

54 Test organisms: *Escherichia coli* DSM 682 (*E. coli*), *Staphylococcus aureus* ATCC 6538 (*S.*
55 *aureus*).

56 Test emulsions: PVME, Ag⁺@PVME and Ag@PVME (with ascorbic acid)

57 Culturing: Two passages of the test organisms were done on Tryptic Soy Agar (TSA) for 24 h at
58 36 °C (+/- 1 °C). Cell material of the second passage was transferred to Tryptic Soy Broth (TSB)
59 for preparation of the inoculation culture (incubation for 24 h at 36 °C).

60 Test procedure: 290 µL of each sample was transferred in a deep-well microtiter plate. Then 10 µL
61 of inoculum was added to each sample resulting in approximately 3.0 x 10E6 cfu mL⁻¹ sample
62 respectively. After mixing each sample with the pipette tip the plate was covered with an adherent
63 film and incubated at 36 °C. After contact times of 4 h and 24 h sampling was done after the
64 following description for each sample: 50 µL were spread directly onto TSA containing neutralizer
65 via Drigalski spatula, another 50 µL were diluted 1:10 in Saponin-Neutralizer, after 20 min
66 neutralizing time 50 µL were plated out onto TSA with a spiral plater, further 1:10 dilutions were
67 performed in deionized water and plated out onto TSA. The TSA plates were incubated for 48–

68 72 hours at 36 °C prior to counting the colonies and calculating the colony forming units (cfu) per
69 mL sample.

70 General procedure for the kinetic experiments of the aqueous polymerizations:

71 2-(Vinylthio)ethanol (4.0 g, 38.3 mmol), the corresponding surfactant, two drops of
72 tetrabutylammonium chloride (internal standard) and water (volume: 11.95 mL) were added in a
73 microwave vial and stirred for 5 min at 40 °C to homogenize the solution. Before polymerization
74 a sample was taken as starting point control. Afterwards, the solution was cooled, and a 10wt%
75 stock solution of V-50 (0.206 g, 0.760 mmol) was added. The dispersion was purged with nitrogen
76 for 20 min and then immersed into an oil bath at 80 °C and stirred (800 rpm) for 5 h. Samples at
77 regular time intervals were taken over the course of the reaction to monitor the progress of the
78 reaction.

79 General procedure for the synthesis of a larger batch of PVME dispersion:

80 2-(Vinylthio)ethanol (20 g, 192 mmol), PVA (200 mg) and V-50 (1058.2 mg, 3.90 mmol) were
81 dispersed water (volume: 69 mL) in a round flask and the dispersion was purged with nitrogen for
82 20 min and then stirred (800 rpm) at 80 °C for 6 h. Afterwards, dialysis (MWCO: 3.5 to 5 kDa)
83 was performed against deionized water for three days including two exchanges of the surrounding
84 water.

85 General procedure for the silver ion release experiments:

86 PVME dispersions (concentration: 142.1 mg mL⁻¹) and a freshly prepared AgNO₃-stock solution
87 (amounts used in the different experiments are given in Table S1) were added to a vial and the
88 dispersion was stirred for 24 h at room temperature. Afterwards, the dispersion was filled into a
89 dialysis tube, (MWCO: 3.5 to 5 kDa), deionized water was added, and the sample was purified
90 against 700 mL of deionized water for three days including two water exchanges to remove an
91 excess of silver ions. A sample of the dispersion was subsequently taken and analyzed *via* ICP-
92 MS-measurements. The dialysis tube was then transferred into fresh water and another sample was
93 taken from the dispersion after 7 d and analyzed by ICP-MS. In case of R2, daily samples were

94 also taken from the filtrate over the course of six days. Quantities of the used chemicals are
 95 summarized in Table S2.

96 **Table S2: Overview of the quantities of chemicals used for release experiments.**

	$c_{Emulsion}$ [mg/mL] ^a	$m_{Emulsion}$ [mg]	m_{AgNO_3} [mg]	c_{AgNO_3} stock solution [mg mL ⁻¹]	Eq. of Ag ⁺ vs. sulfur	m_{water} [mg]
R1	142.0	2019.7	9.6	4.8	0.02	2000
R2	142.0	2004.9	17.7	8.8	0.04	2026
R3	142.0	2008.8	44.2	22.2	0.1	2208

^a Gravimetrically determination of the concentration.

97

98 General procedure for the preparation of Ag@PVME:

99 Ascorbic acid as reducing agent: A freshly prepared AgNO₃ solution was added to the emulsion
 100 and stirred for 3 h, then dialyzed (MWCO: 3.5 to 5 kDa) against deionized water for one day. 5 mL
 101 of ascorbic acid solution were subsequently added, and the solution was stirred overnight under
 102 exclusion of light. The resulting dispersions were again purified by dialysis (MWCO: 3.5 to 5 kDa)
 103 against deionized water for three days including two water exchanges. Quantities of the used
 104 chemicals are summarized in Table S3.

105 **Table S3: Overview of the quantities of chemicals used for synthesis of AgNP@PVME with**
 106 **ascorbic acid.**

$c_{Emulsion}$ [mg/mL] ^a	$m_{Emulsion}$ [mg]	m_{AgNO_3} [mg]	c_{AgNO_3} [mg mL ⁻¹] stock solution	Eq. of Ag ⁺ vs. sulfur	m_{AA} [mg]	c_{AA} stock solution [mg mL ⁻¹]	Eq. of Ag ⁺ vs. sulfur
57.0	5000	44.1	8.8	0.1	45.7	9.1	0.1

^a Gravimetrically determination of the concentration.

107

108 Reduction in sunlight: A freshly prepared AgNO₃ solution was added to the PVME-emulsion and
 109 stirred for 3 h, subsequently dialyzed (MWCO: 3.5 to 5 kDa) against deionized water for one day.
 110 Subsequently, the sample was diluted with deionized water, and the solution was stirred for three
 111 days at room temperature in sunlight. The dispersions were again purified by dialysis (MWCO: 3.5
 112 to 5 kDa) against deionized water for three days including two water exchanges. Several batches
 113 were prepared for all experiments, which are summarized in Table S4.

114 **Table S4: Overview of the quantities of chemicals used for synthesis of AgNP@PVME in**
 115 **sunlight.**

Batch	$C_{Emulsion}$ [mg mL ⁻¹] ^a	$m_{Emulsion}$ [mg]	m_{AgNO3} [mg]	C_{AgNO3} [mg mL ⁻¹] stock solution	m_{water} [mg]	Eq. of Ag ⁺ vs. sulfur
B1 (1% PVA)	68.97	5000	56.2	11.2	5000	0.1
B2 (1% PVA)	142.0	2000	17.7	8.8	2026	0.04
B3(1% PVA)	115.4	2000	33.2	16.6	2000	0.1
B4 (2% PVA)	102.3	2000	30.4	15.2	2000	0.1
B5 (4% PVA)	217.4	2000	58.1	29.1	2000	0.1
B6 (8% PVA)	199.15	2000	50.5	25.3	2000	0.1

^a Gravimetrically determination of the concentration.

116

117 General procedure for the preparation of Au@PVME:

118 A freshly prepared HAuCl₄ solution were added to the PVME-emulsion and stirred for 3 h, then
 119 dialyzed (MWCO: 3.5 to 5 kDa) against deionized water for one day. Afterwards deionized water
 120 was added, and the solution was stirred for three days at room temperature in sunlight. The particles
 121 were purified by dialysis (MWCO: 3.5 to 5 kDa) against deionized water for three days in the
 122 sunlight including two water exchanges. Quantities of the used chemicals are summarized in Table
 123 S5.

124 **Table S5: Overview of the quantities of chemicals used for synthesis of AuNP@PVME in**
 125 **sunlight.**

Batch	$c_{Emulsion}$ [mg mL⁻¹]^a	$m_{Emulsion}$ [mg]	m_{AuCl4} [mg]	c_{AuCl4} [mg mL⁻¹] stock solution	m_{water} [mg]	Eq. of Au⁺ vs. sulfur
C1	57.0	5000	44.1	8.8	5000	0.1

^a Gravimetrically determination of the concentration.

126

127

128 **Results**

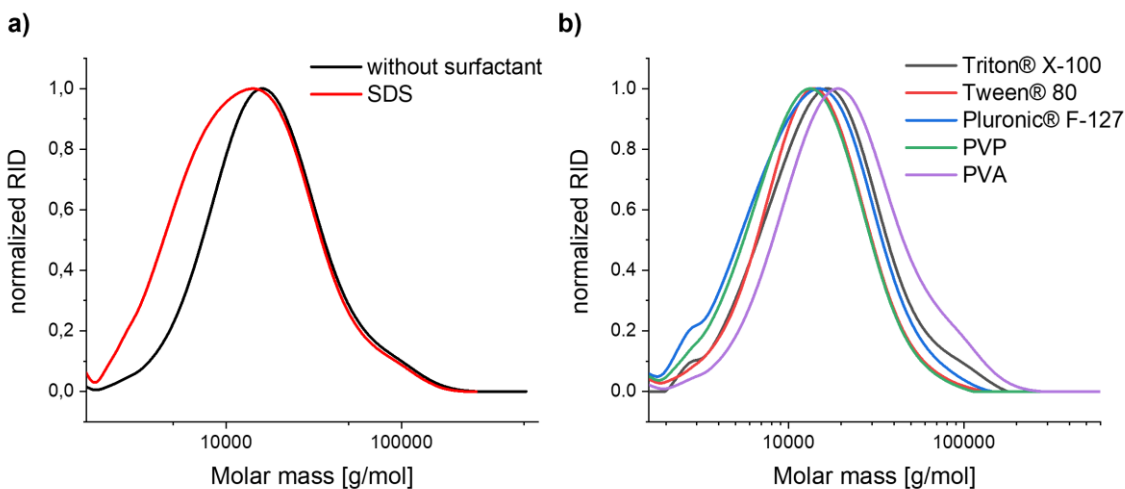
129 Influence of surfactants

130 **Table S6: Conversions and average molar masses of the aqueous polymerizations with**
 131 **different surfactants.**

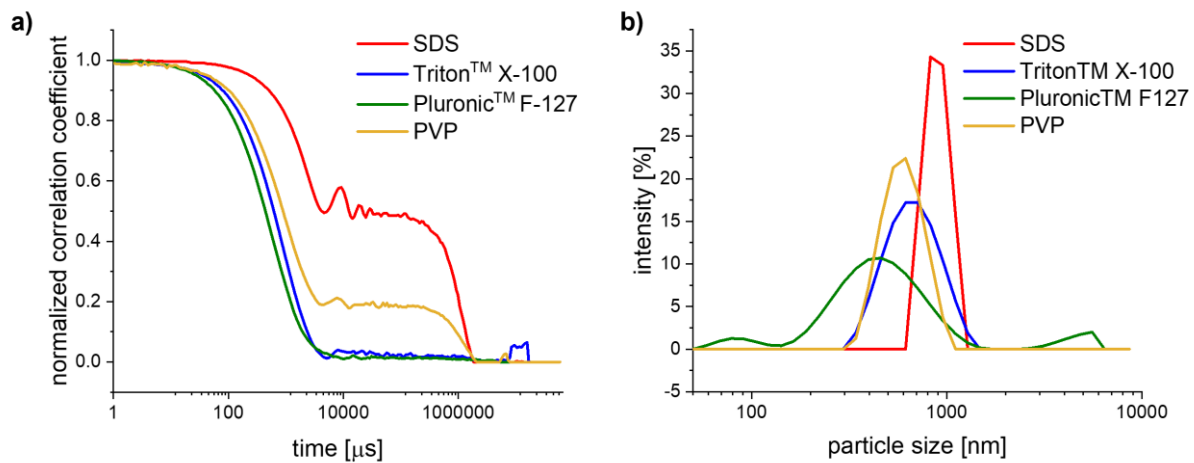
Surfactant	Conversion [%] ^a	Molar mass [g mol ⁻¹] ^b	\bar{M}_w ^b
without	92	13 600	1.68
SDS	93	10 200	1.84
Triton™ X-100	89	12 400	1.78
Tween™ 80	93	11 900	1.43
Pluronic™ F-127	93	10 700	1.70
PVP	93	10 600	1.54

^a Determination via ¹H-NMR (300 MHz, DMSO-d₆)-spectroscopy *via* standard.

^b SEC (DMAc (+ 0.21wt% LiCl), PMMA standards) after 5 h.



132
 133 **Figure S1: SEC (DMAc (+ 0.21wt% LiCl), PMMA standards) traces of the polymers after**
 134 **the aqueous polymerization with 1wt% of different surfactants.**



135

136 **Figure S2: a) Correlograms and b) intensity distributions of the polymer particles after**
 137 **polymerization with different surfactants (DLS measurements in water).**

138

139 Influence of PVA content140 **Table S7: Conversions, molar masses and particle sizes of the emulsion polymerizations with**
141 **different amount of PVA.**

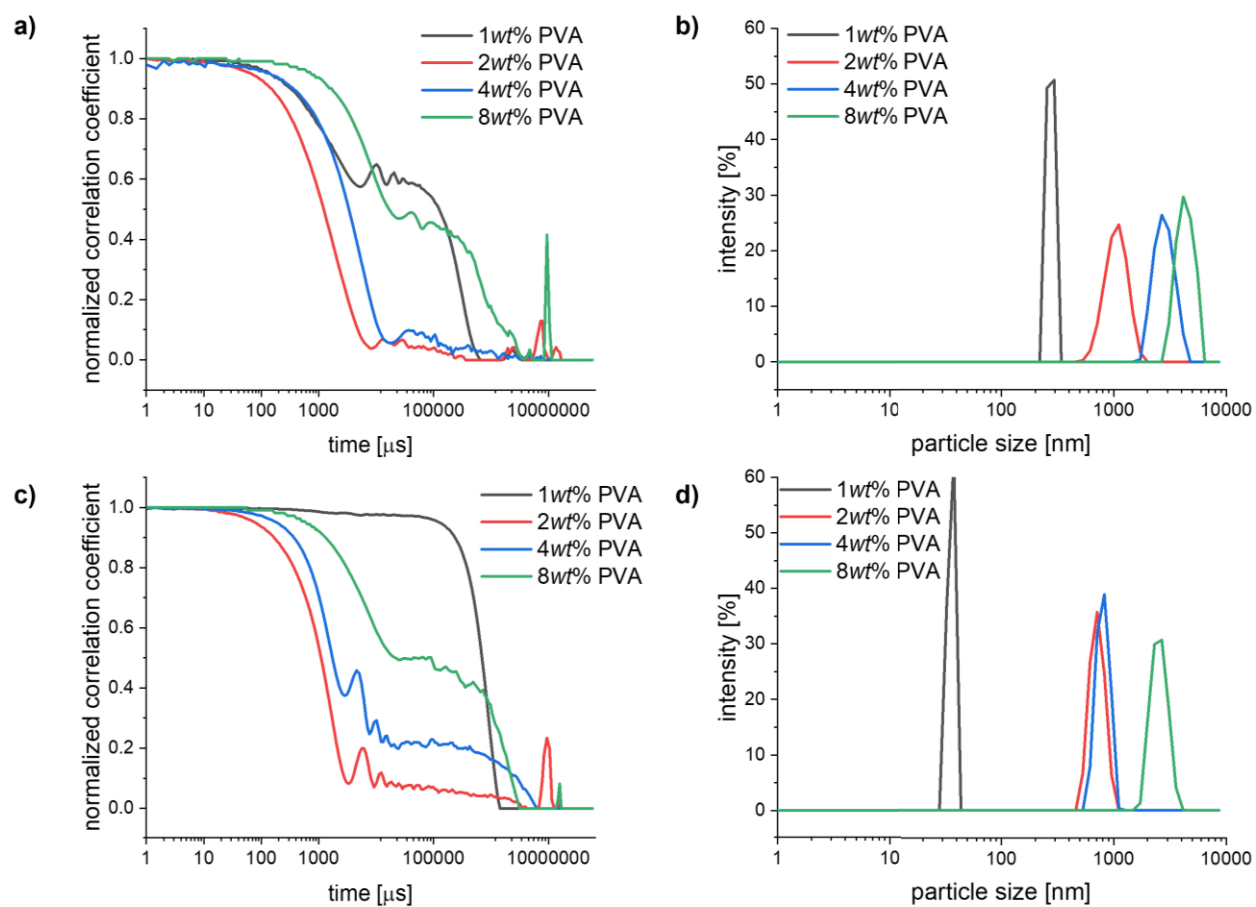
PVA [wt%]	Conversion [%] ^a	Molar mass [g mol ⁻¹] ^b	Đ ^b	Z- average [nm] ^c	PDI ^c	Z-average [nm] ^d	PDI ^d
1	93	7820	1.85	1180	0.64	1870	0.28
2	92	8170	1.80	1080	0.32	890	0.46
4	97	9470	2.24	3140	0.13	1210	0.71
8	97	9480	2.22	5640	0.04	4350	0.29

^a Determination *via* ¹H-NMR (300 MHz, DMSO-d₆)-spectroscopy after 5h with *a* standard.

^b Determination *via* SEC (DMAc (+ 0.21wt% LiCl), PMMA standards) after 5 h.

^c Determination *via* DLS – measurements before purification.

^d Determination *via* DLS – measurements after purification *via* dialysis.



142

143 **Figure S3: a) Correlograms and b) intensity distributions of the polymers after**
 144 **polymerization with different amounts of PVA and c) correlograms and d) intensity**
 145 **distributions after purification of the polymers with different amounts of PVA (DLS**
 146 **measurements in water).**

147

148 **Table S8: Conversions, and molar masses of the polymerizations with 1wt% PVA.**

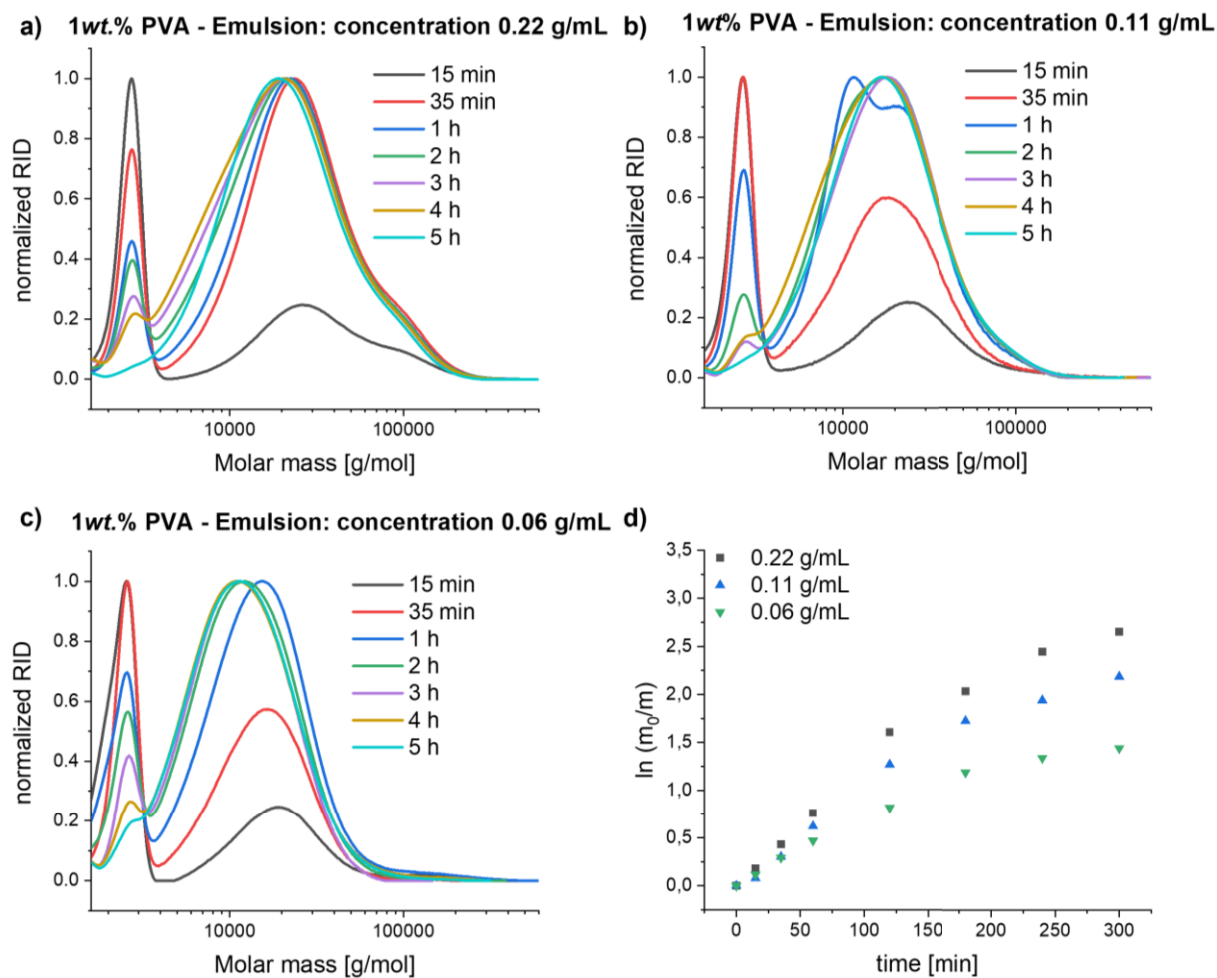
Concentration [g mL ⁻¹]	Conversion [%] ^a	Molar mass [g mol ⁻¹] ^b	\bar{D}^b
0.22	93	15 500	1.75
0.11	89	13 500	1.6
0.06	76	10 800	1.36

^a Determination *via* ¹H-NMR (300 MHz, DMSO-d₆)-spectroscopy after 5 h *via* standard.

^b Determination *via* SEC (DMAc (+ 0.21wt% LiCl), PMMA standards) after 5 h.

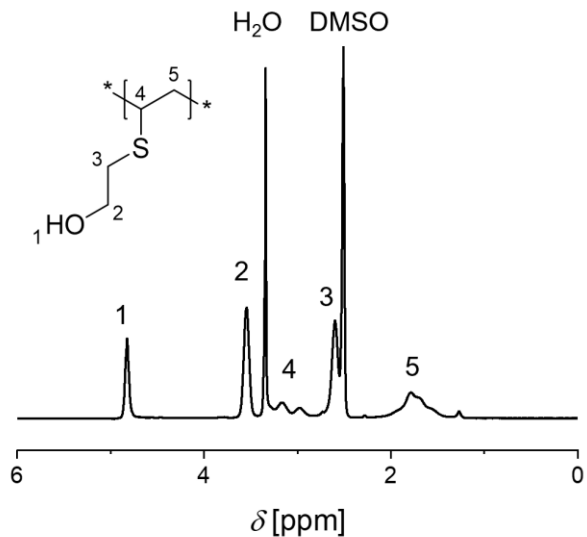
149

150



151

152 **Figure S4: SEC (DMAc (+ 0.21wt% LiCl), PMMA standards) traces of the kinetic samples**
 153 **taken after 15 min, 35 min, 1 h, 2 h, 3 h, 4 h and 5 h of the polymerization at a monomer**
 154 **concentration of a) 0.22 g/mL, b) 0.11 g/mL, c) 0.06 g/mL and d) the plot of $\ln(m_0/m)$ vs.**
 155 **reaction time.**



156

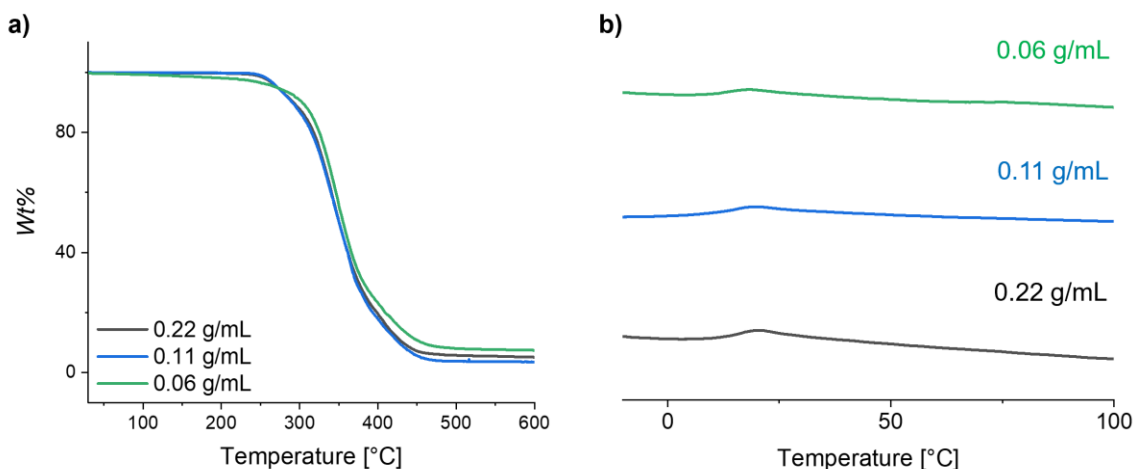
157 **Figure S5: $^1\text{H-NMR}$ spectra (300 MHz, DMSO-d_6) of the purified polymer.**

158 **Table S9: Thermal properties of the polymers prepared at different initial monomer**
 159 **concentrations with 1 wt% PVA.**

Concentration [g mL^{-1}]	T_d [$^{\circ}\text{C}$] ^a	T_g [$^{\circ}\text{C}$] ^b
0.22	271	14.9
0.11	272	13.0
0.06	271	13.7

^a Determination from TGA – measurements.

^b Determination from DSC – measurements.



160
 161 **Figure S6: a) TGA data (N₂) and b) DSC data of PVME prepared at different initial monomer**
 162 **concentrations.**

163

164 Coordination of silver ions (Ag⁺@PVME)

165 **Table S10: Data from silver ion release experiments.**

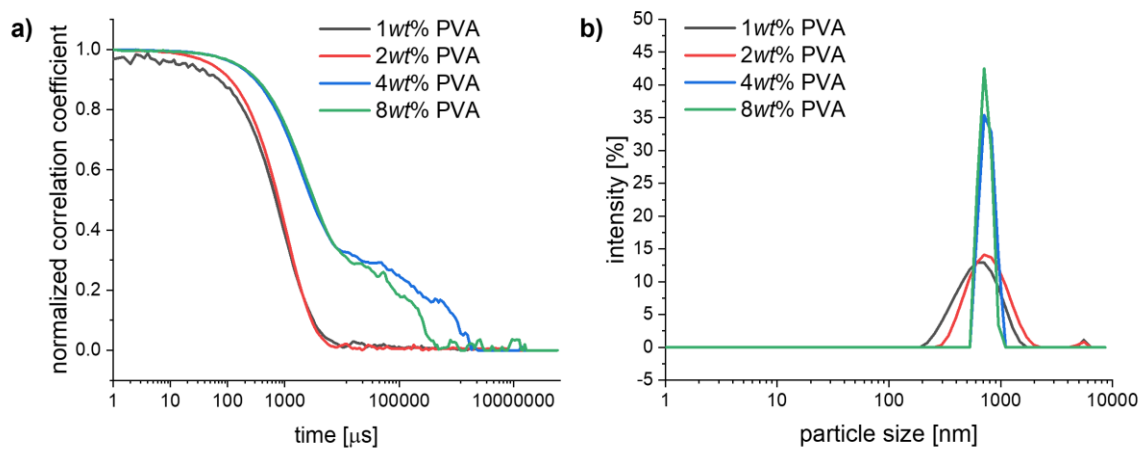
Exp.	Eq. of AgNO ₃ (pre-weight)	c_{Ag^+} [mg/mL] after purification ^a	$c_{Emulsion}$ [mg mL ⁻¹] after 7 d of dialysis ^b	c_{Ag^+} [mg/mL] after 7 d of dialysis ^a	theo. max. c_{Ag^+} [mg mL ⁻¹] after 7 d of dialysis ^d
R1	0.02	0.15	4.2	0,136 ^c	0.086
R2	0.04	0.225	4.3	0.167	0.168
R3	0.1	0.378	6	0.321	0.561

^a Determination *via* ICP – MS measurements.

^b Gravimetrically determination of the concentration.

^c Deviation due to inhomogeneity of the sample.

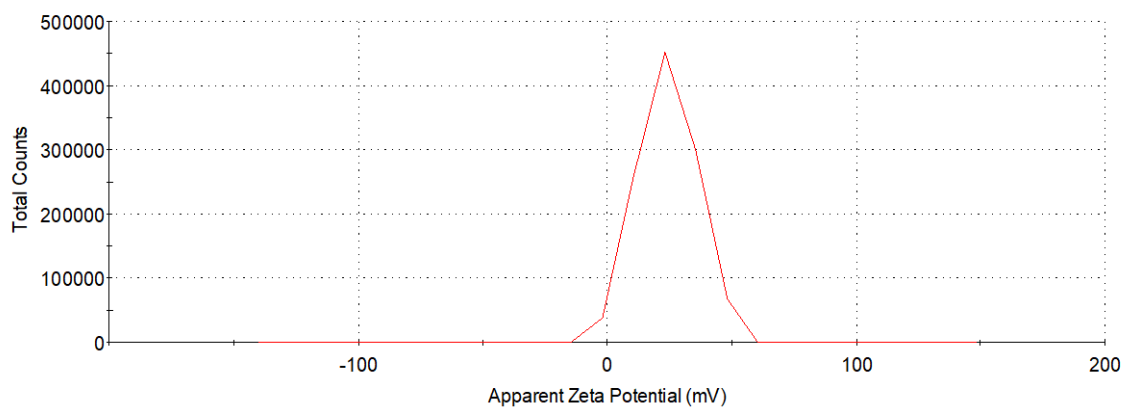
^d Calculation with the determined concentration of the emulsion and the preweighted eq. of the silver salt.



166

167 **Figure S7: a) Correlograms and b) intensity distributions of samples $\text{Ag}^+\text{@PVME}$ (B3-B6)**
 168 **with different amounts of PVA (DLS measurements in water).**

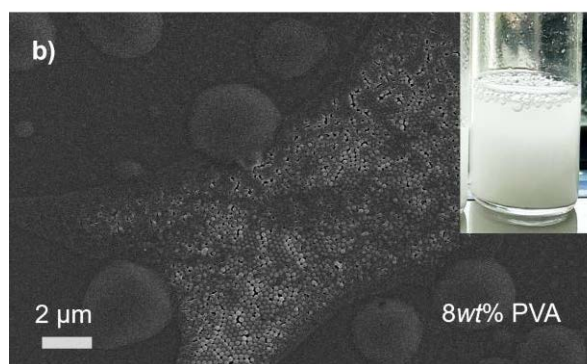
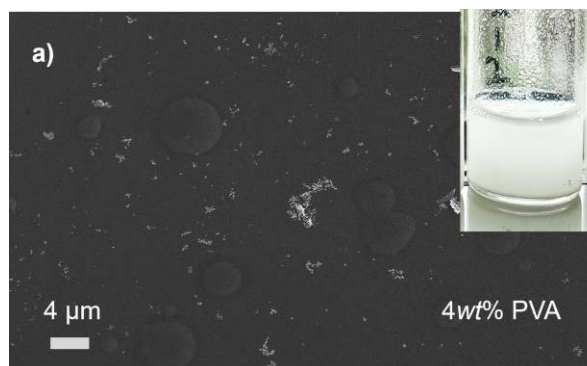
169



170

171 **Figure S8: Zeta-potential of $\text{Ag}^+\text{@PVME}$ (B3) measured in water.**

172

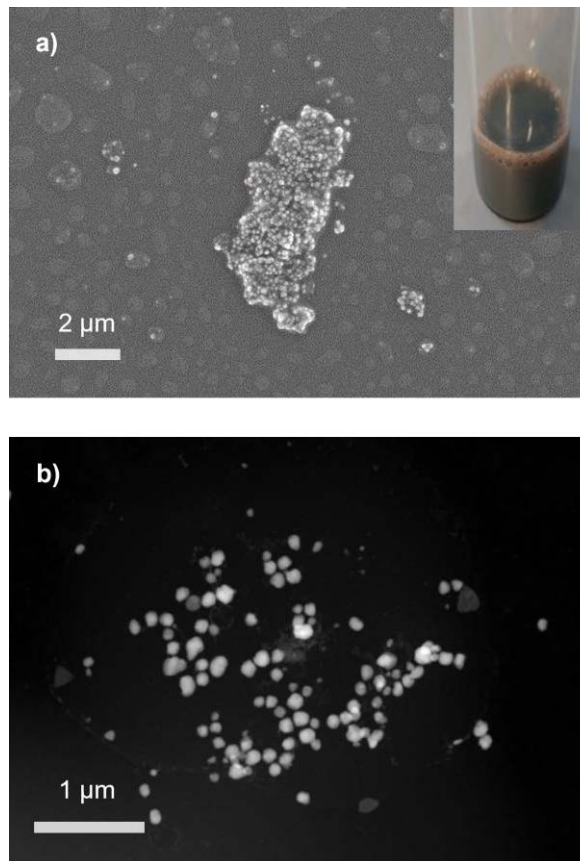


173

174 **Figure S9: SEM images of Ag^+ @PVME a) B5 and b) B6.**

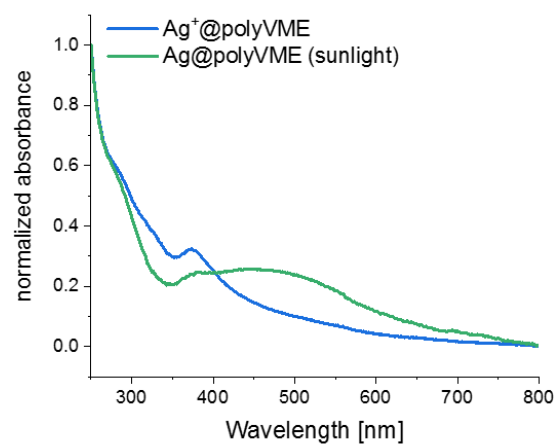
175

176 Formation of silver composites (Ag@PVME)



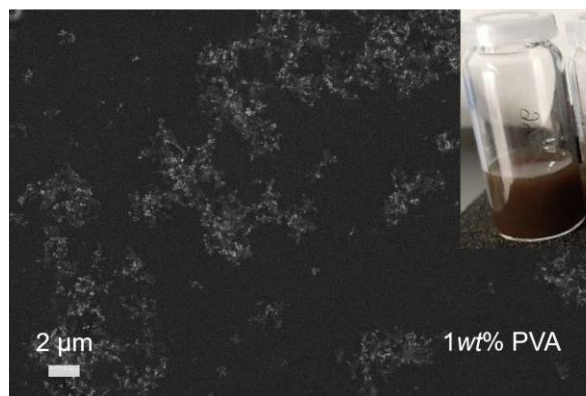
177

178 **Figure S10: a) SEM image of Ag@PVME prepared with ascorbic acid as reducing agent and**
179 **b) corresponding TEM image.**



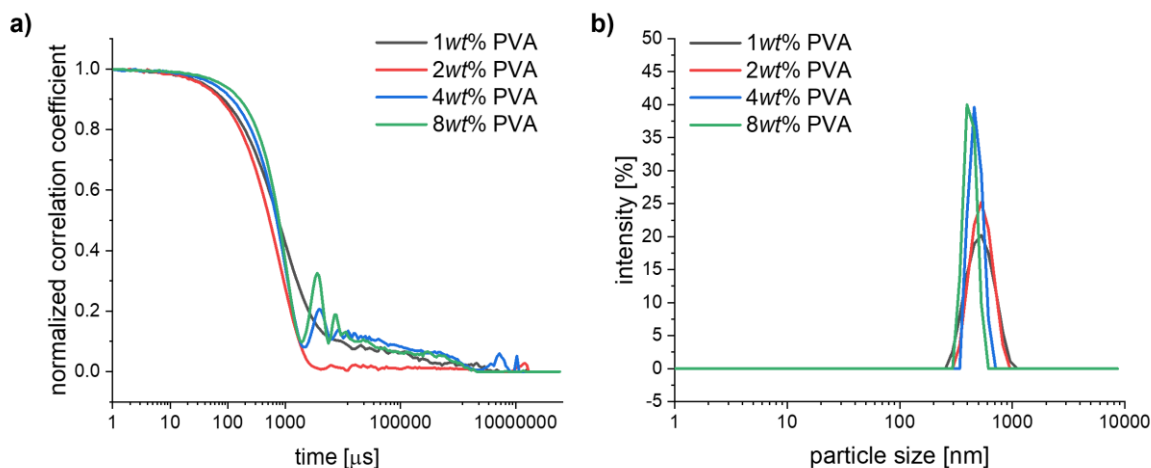
180

181 **Figure S11: UV-Vis spectra of Ag⁺@PVME (R2) and Ag@PVME (B2) synthesized in**
182 **sunlight.**



183

184 **Figure S12: SEM image of Ag@PVME (B2).**



185

186 **Figure S13: a) Correlograms and b) intensity distributions of Ag@PVME (B3-B6) with**
 187 **different amounts of PVA (DLS measurements in water).**

188 **Table S11: Data of the antibacterial tests.**

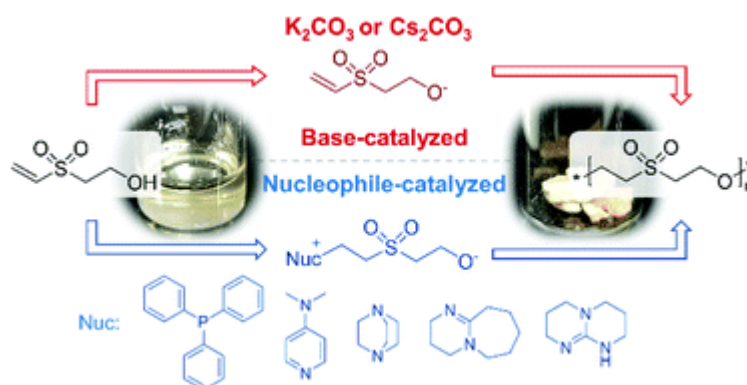
Exp.	Contact time [h]	S. aureus ATCC 6538	E. coli DSM 682
		[cfu mL ⁻¹]	[cfu mL ⁻¹]
Pure emulsion (PVME)	4	4.2E+05	1.0E+05
	24	>6.0E+06	>6.0E+06
Ag ⁺ @PVME	4	3.5E+04	<20
	24	8.0E+01	<20
Ag@PVME	4	1.6E+05	3.8E+05
	24	>6.0E+05	>6.0E+05
Irgaguard B 6000 (benchmark)	4	<20	<20
	24	<20	120

189

Publication P4

“Oxa-Michael polyaddition of vinylsulfonylethanol for aliphatic polyethersulfones”

N. Ziegenbalg, R. Lohwasser, G. D'Andola, T. Adermann and J. C. Brendel, *Polym. Chem.*
2021, *12*, 4337-4346.



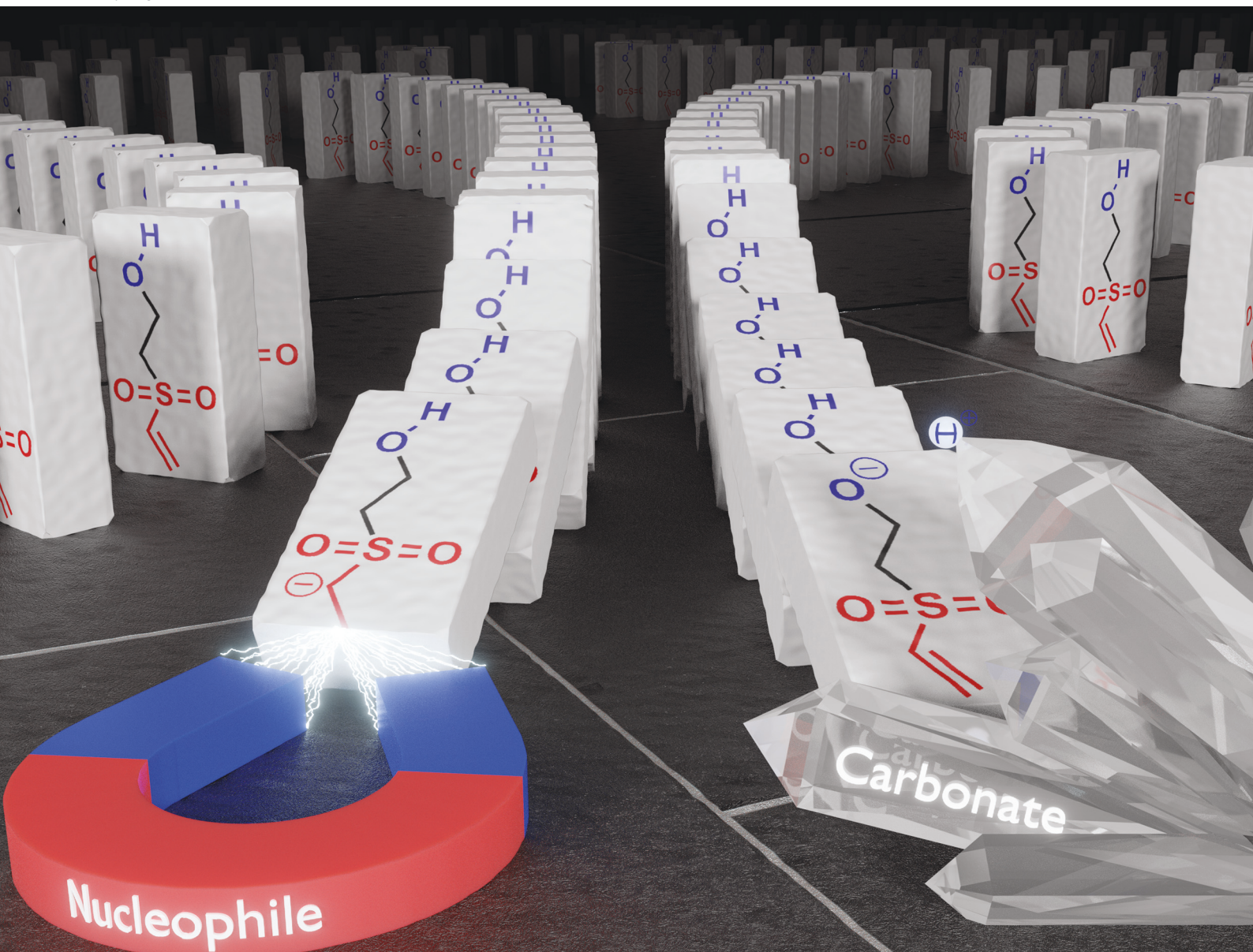
Reproduced by permission of Royal Society of Chemistry. Copyright 2021.

The paper as well as the supporting information is available online:
doi.org/10.1039/D1PY00256B

Polymer Chemistry

Volume 12
Number 30
14 August 2021
Pages 4265-4430

rsc.li/polymers



ISSN 1759-9962

PAPER

Johannes C. Brendel *et al.*
Oxa-Michael polyaddition of vinylsulfonylethanol for
aliphatic polyethersulfones



Cite this: *Polym. Chem.*, 2021, **12**, 4337

Oxa-Michael polyaddition of vinylsulfonylethanol for aliphatic polyethersulfones†

Nicole Ziegenbalg,^{a,b} Ruth Lohwasser,^c Giovanni D'Andola,^c Torben Adermann^c and Johannes C. Brendel^{id} *^{a,b}

Polyethersulfones are an interesting class of polymers for industrial applications due to their unusual properties such as a high refractive index, flame-retardant properties, and high temperature and chemical resistance. The common aromatic polymers however require high temperatures for processing, while alternative aliphatic polyethersulfones remain overall scarce in the literature with only oligomeric materials being reported so far. Nevertheless, these materials have similar promising properties to those observed for their aromatic equivalents. Here, we describe the reactivity of a novel AB-type monomer vinylsulfonylethanol, which enables a successful and straightforward synthesis of aliphatic polyethersulfones. Various organic and inorganic catalysts were tested, and the kinetics of the resulting polymerizations were examined. Rapid conversions were observed resulting in polymers with molar masses in the range of 2000 to 4000 g mol⁻¹ within a few minutes. A closer characterization of the resulting polymers revealed that all organic catalysts initiate the polymerization process by a nucleophilic addition to the vinyl group, even if strong but sterically hindered bases are used. Inorganic bases in turn seem to deprotonate the hydroxy groups to initiate the polymerization, as the vinyl end groups are preserved. The resulting polymers are characterized by excellent heat resistance with degradation temperatures >300 °C in air, which is significantly higher than previous observations for other aliphatic polyolefinsulfones. Further analysis reveals a semi-crystalline nature of the polymer if processed from solvents although recrystallization appears to be kinetically hindered. With the possibility to prepare the starting material vinylsulfonylethanol by a straightforward method and on a large scale, such polymers become easily accessible using the described preparation routes, while the beneficial thermal properties of the polymer may open up interesting opportunities for their application.

Received 24th February 2021
Accepted 30th April 2021

DOI: 10.1039/d1py00256b
rsc.li/polymers

Introduction

At the end of the 19th century Arthur Michael studied the 1,4 addition of stabilized carbanions to α,β -unsaturated carbonyl compounds, which set the basis for one of the most useful synthetic methods in organic chemistry.^{1–4} In recent years, Michael additions were not only used for the synthesis of small intermediates^{5–8} and natural products^{9–11} but also for the synthesis^{12–15} and modification^{16–19} of polymers. In particular, the thiol-Michael polyaddition is often used due to the high reactivity of the monomers.²⁰ Despite their reactivity the

required thiols remain an obstacle in large scale production which is related to their unpleasant odor, their sensitivity to oxidation, and their high reactivity as nucleophiles. As an alternative, the oxa-Michael addition gained increasing attention since alcohols are more accessible and stable compared to thiols, but the reduced nucleophilicity, of course, renders the development of suitable reaction conditions more challenging.

Considering polymerizations based on this oxa-Michael addition, reports remain very scarce due to this limited reactivity. Although in general alcohols are convenient in terms of preparation and storage, until now, only two different approaches for oxa-Michael polyadditions have been reported. In one case, hydroxyl functionalized acrylates^{21–25} are used, which require rather harsh reaction conditions (>80 °C) for a successful polymerization. An interesting alternative approach to improve the yield and reactivity lies in the use of vinyl sulfones or sulfoxides, which are among the most reactive Michael-acceptors. In these reactions divinyl sulfones/divinyl sulfoxides are combined with different bivalent alcohols resulting in an AA/BB-type polyaddition.^{1,26–29} For example, Strasser

^aLaboratory of Organic and Macromolecular Chemistry (IOMC), Friedrich Schiller University Jena, Humboldtstraße 10, 07743 Jena, Germany.

E-mail: johannes.brendel@uni-jena.de

^bJena Center for Soft Matter (JCSM), Friedrich Schiller University Jena, Philosophenweg 7, 07743 Jena, Germany

^cBASF SE, Carl-Bosch-Straße 38, 67056 Ludwigshafen/Rhein, Germany

†Electronic supplementary information (ESI) available. See DOI: 10.1039/d1py00256b

et al. reported a copolymerization of divinyl sulfone and ethylene glycol catalyzed by 4-dimethylaminopyridine (DMAP) at room temperature.²⁷ However, the obtained molar masses remained rather low (<800 g mol⁻¹) and only oligomers are formed, which might be related to the tendency of the intermediates to form cyclic by-products. Nevertheless, their results confirm that oxa-Michael polyadditions can result in the formation of polymers under relatively mild conditions applying the more reactive vinyl sulfone monomers. The resulting polyethersulfones represent an attractive class of materials due to their high polarities, excellent chemical resistance,^{30,31} flame retarding properties,³² and high refractive indices.³³

Nevertheless, an inherent challenge of an AA/BB-type polyaddition is the application of exact equimolar amounts of the respective monomers which is crucial to obtain high degrees of polymerization.^{34,35} An alternative attempt to the above-described reaction of divinyl sulfone and dialcohols therefore lies in the design of a similar reactive AB-type monomer. A promising candidate is vinylsulfonylethanol, which contains both a Michael acceptor and Michael donor. However, applications of vinylsulfonylethanol can only be found sporadically in the literature^{36,37} which is most likely related to a limited large-scale availability of this compound. Synthetic routes may start from thiodiglycol but then either require a selective mono-dehydration or proceed *via* toxic halogenated derivatives.^{38–40} An alternative synthesis is based on vinylmercaptoethanol (VME), which is readily oxidized to the corresponding sulfone. The first reported reactions to form VME used vinyl bromide, which was converted to the desired intermediate using the corresponding sodium thiolate as the nucleophile.⁴¹ More recently, an efficient direct vinylation of mercaptoethanol could be demonstrated following the well-established protocols for vinyl compounds according to Reppe,^{41,42} enabling a cost-effective access to VME on an industrial scale.^{43,44}

With the key intermediate VME being made available by BASF SE, the aim of this work was to develop an efficient oxidation process to prepare the AB-type monomer vinylsulfonylethanol and evaluate its ability to form aliphatic polyethersulfones in a straightforward oxa-Michael polyaddition. In this regard, several potential catalysts were screened to initiate the polymerization. Further in-depth investigations of selected polymerizations were conducted to provide more information on the underlying polymerization mechanism. The resulting polymers were finally examined to determine their composition and properties.

Results and discussion

Synthesis of the monomer

Starting from vinylmercaptoethanol, the direct oxidation was attempted with hydrogen peroxide (1 eq.) and sodium tungstate (Na₂WO₄) as a catalyst, which should first give the corresponding sulfoxide and finally the sulfone. While the sulfoxide is formed rather quickly and does not necessarily require a

catalyst, the full conversion to the sulfone requires elevated temperatures (60 °C). However, it was observed that a careful adjustment of the reaction temperature is required to reduce undesired side reactions which include among others the uncontrolled polymerization. Therefore, the addition of small amounts of a radical scavenger, *e.g.* hydroxyanisol, was found to prevent any undesired polymerization of the vinyl groups. The NMR signals of the vinyl bands shifted from $\delta = 6.42$ and 5.13 ppm to $\delta = 6.93$ and 6.18 ppm, respectively, indicating a successful and complete oxidation (see Fig. 1, for the ¹³C-NMR spectrum see ESI Fig. S1†). Following this procedure, the product is obtained directly with high purity (>96%) and quantitative yields without the need for further purification after quenching the excess of hydrogen peroxide over manganese(IV) oxide.

Despite the presence of a strong Michael acceptor in conjugation with a primary hydroxyl group, the obtained AB-type monomer is stable for more than a year if stored at 4 °C. No signs of side reactions or additions between these complementary groups are observed.

Oxa-Michael polyaddition – bulk polymerizations

After the successful oxidation of VME, various potential catalysts were tested for the oxa-Michael polyaddition in bulk. Two different mechanisms are reported in the literature to initiate the polymerization (see Scheme 1).²⁶ The first one is characterized by a nucleophilic addition to the double bond and a subsequent intra- or intermolecular proton transfer to initiate the reaction cascade. The second possibility is a base-catalyzed mechanism, where the hydroxyl group is directly deprotonated. Subsequently, in both mechanisms, the resulting negatively charged oxygen can attack the vinyl group of another monomer molecule, which is then followed by another intra- or intermolecular proton transfer.

All selected catalysts (Fig. 2) are commercially available and have demonstrated the ability to catalyze Michael

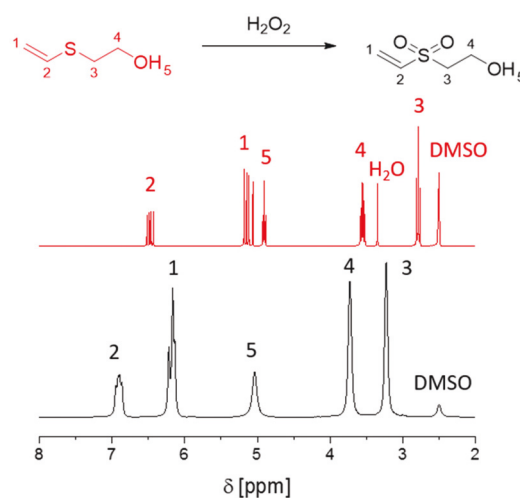
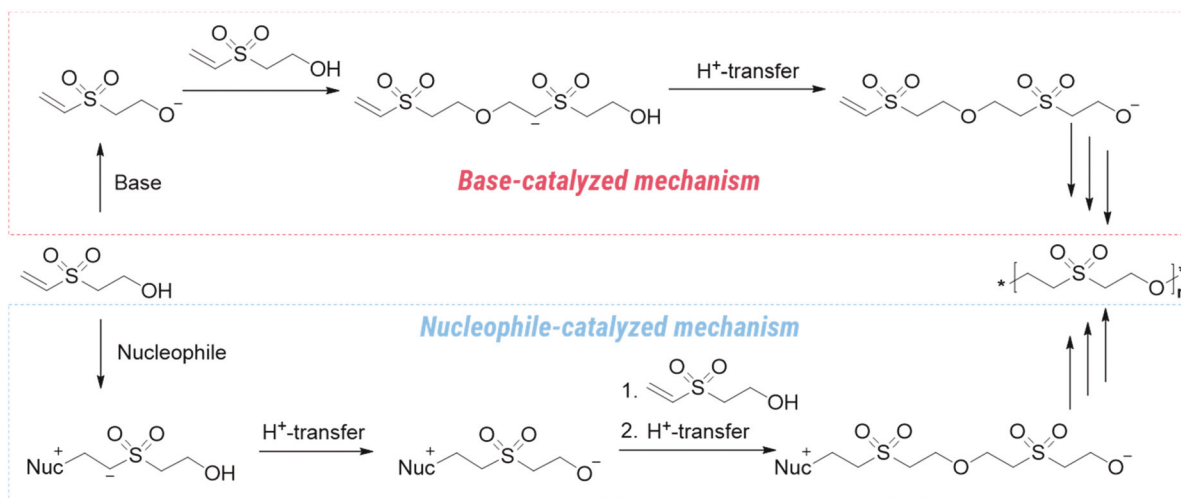


Fig. 1 ¹H-NMR spectrum (300 MHz, DMSO-d₆, 298 K) of vinylmercaptoethanol (red) and vinylsulfonylethanol (black).



Scheme 1 Base-catalyzed and nucleophile-catalyzed mechanisms of the oxa-Michael addition of vinylsulfonylethanol.

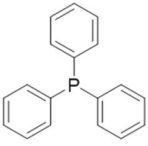
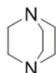
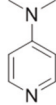
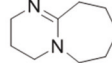
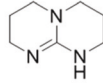
organic catalysts					
					
Triphenylphosphine (PPh ₃)	Triethylenediamin (TEDA)	4-(Dimethylamino)- pyridin (DMAP)	1,8-Diazabicyclo[5.4.0]- undec-7-en (DBU)	1,5,7-Triazabicyclo(4.4.0)- dec-5-en (TBD)	
pKa	2.7	3.0 8.7	9.7	13.5	15.2
inorganic catalysts					
	Potassium carbonate (K ₂ CO ₃)	Cesium carbonate (Cs ₂ CO ₃)			
pKa	10.3	10.3			

Fig. 2 Organic and inorganic catalysts (with the corresponding pK_a-values^{52–56}) used for the oxa-Michael polyaddition.

additions.^{20,26,27,45–51} Due to the fact that some of these catalysts can react both as the nucleophile and base, classification is done according to their organic and inorganic nature (Fig. 2).

The first bulk polymerizations were initiated by addition of the monomer to pre-weighed amounts of the catalysts (0.1 eq.). The exact equivalents of the active catalyst could not be determined in most cases, as the solid catalysts did not completely dissolve over the course of the reaction. Nevertheless, in all cases, a change in color was observed and the viscosity increased significantly after only a few minutes indicating a successful polymerization. More detailed investigations using NMR spectroscopy confirmed the formation of a polymer by oxa-Michael polyaddition as exemplarily displayed for the Cs₂CO₃-catalyzed reaction after 1 h (Fig. 3, the NMR spectra of the other reactions can be found in the ESI, Fig. S3†). To determine the conversion of the functional vinyl groups, the corre-

sponding signal of the =CH₂ moiety (δ = 6.21 ppm) was compared to the –CH₂–signal in the polymer backbone (δ = 3.42 ppm) (for further information see ESI, Fig. S2†).

After 24 h conversions of the vinyl group of >94% were obtained for all tested polymerizations, which confirms the high reactivity of the monomer (Table 1). In general, there are few differences in the conversion and chain length within the kinetics of the polymerizations with different catalysts (see ESI, Fig. S4/5/6†). Interestingly, dispersities between 1.2 and 1.5 were observed for the final polymers, which are relatively low compared to those from other step growth reactions. The low values might be related to the relatively low molar masses or the formation of cyclic structures, which cannot be excluded during the reaction. In addition, the final samples (24 h) were characterized by MALDI-ToF-MS. The obtained number average molar masses were lower compared to the SEC values, in particular for the carbonate catalyst samples. Interestingly,

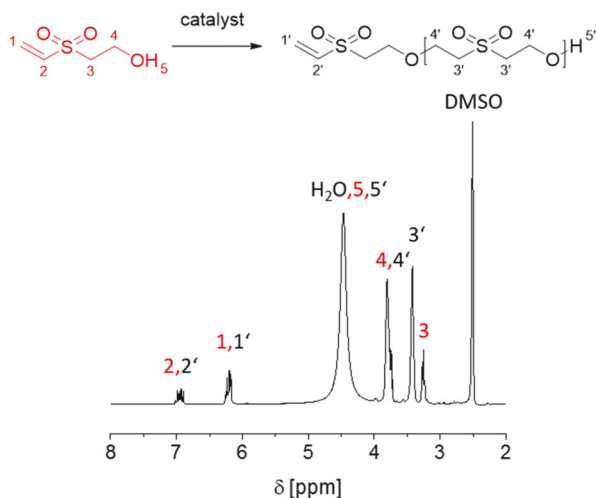


Fig. 3 $^1\text{H-NMR}$ spectrum (300 MHz, DMSO-d_6 , 298 K) of the Cs_2CO_3 -catalyzed polymerization mixture after 1 h.

much better signal-to-noise ratios were obtained for the polymers catalyzed by the organic compounds and a closer look revealed that the main signals can only be assigned if the catalyst is added to the polymer either as a salt or as a covalently bound product (Fig. S8–S14[†]). The different possibilities were further investigated on the purified polymers (*vide infra*). These unexpected differences between the samples also indicate that some polymers might only be insufficiently ionized, which limits the accuracy of the determination of M_n by MALDI-ToF-MS.

A closer look at the kinetic samples reveals differences between the bulky PPh_3 and the other catalysts in the first few minutes of the reaction. A retarded initiation due to the steric demand of the phenyl groups of PPh_3 was observed. However, as soon as this initiation period is overcome, a fast propagation of the polymerization occurs and conversions of >95% are achieved within 1 hour. Interestingly, the liquid catalyst DBU did not result in a significant increase in the reaction rates compared to the other polymerizations, although it appeared to fully mix with the monomer and thus the amount of available catalyst should theoretically be higher.

The course of the reaction was further monitored by SEC measurements. PEG-standards were used for calibration of the

SEC and, therefore, these values will not reflect the absolute molar mass values, but could provide a good approximation due to the structural similarity of the polymers. In all cases, a continuous increase of the molar mass with the reaction time (Fig. S5/S6[†]) was observed. Interestingly, the samples catalyzed by DBU and PPh_3 revealed rather high molar masses already in the early stage of the polymerization. This could be a result of the better miscibility of the first but contrasts with the expected evolution of a typical AB-type polycondensation. For polymerizations that follow such a mechanism and under neglect of by-products, it is possible to use the Carothers equation to estimate the expected degree of polymerization \bar{X}_n for a specific conversion p according to:⁵⁷

$$\bar{X}_n = \frac{1}{1-p} \quad (1)$$

Plotting the measured M_n versus the conversion allowed a direct comparison with the theoretical expected molar masses according to the Carothers equation (eqn (1)) as exemplarily shown for PPh_3 and Cs_2CO_3 in Fig. 4 (the other polymerizations are given in the ESI, Fig. S7[†]).

The direct comparison of the obtained molar masses with the theoretical values according to eqn (1) reveals clear differences for several polymerizations, which cannot be only related to deviations caused by the calibration of the SEC with PEG. In particular, the final molar mass of the polymers obtained from the organic catalysts is expected to be one order of magnitude larger according to theory. Therefore, we assume that a significant ratio of cyclic products is formed during these reactions. A comparison of the $^1\text{H-NMR}$ spectrum of the polymer and the commercially available compound 4,4-dioxo-1,4-oxathiane was performed and the signals were found to overlap partially (see ESI, Fig. S32[†]). With increasing size of the cyclic structures, their signals will be more shifted towards the observed polymer signal and, thus, impede a clear differentiation. In contrast, the inorganic bases resulted in overall lower final conversions but similar number average molar masses, which are closer to the theoretical values calculated from the Carothers equation. Nevertheless, cyclic by-products cannot be excluded in these cases.

For a more detailed characterization of the final polymers, a second batch of polymers was prepared and quenched by addition of trifluoroacetic acid (TFA) after the polymerization.

Table 1 Conversions, number average molar masses (M_n) and dispersities (D) of oxa-Michael polyaddition of vinylsulfonyl ethanol after 24 hours

Polymer	Catalyst	Conversion ^a [%]	M_n [g mol ⁻¹] (theo.) ^b	M_n [g mol ⁻¹] (SEC) ^c	D ^c	M_n [g mol ⁻¹] (MALDI) ^d
P1	PPh_3	99	13 620	3670	1.50	2050
P2	TEDA	98	6810	2330	1.38	1990
P3	DMAP	97	4540	2570	1.46	1880
P4	DBU	99	13 620	2200	1.58	2150
P5	TBD	99	13 620	3360	1.28	2310
P6	K_2CO_3	95	2720	2070	1.38	1040
P7	Cs_2CO_3	96	3400	2890	1.45	1770

^a $^1\text{H-NMR}$ (300 MHz, DMSO-d_6 , 298 K) after 24 h, determination *via* vinyl groups. ^b Determination with the Carothers equation. ^c SEC (DMAc (+0.21 wt% LiCl), PEG standards) after 24 h. ^d Determination from MALDI-ToF-MS spectra.

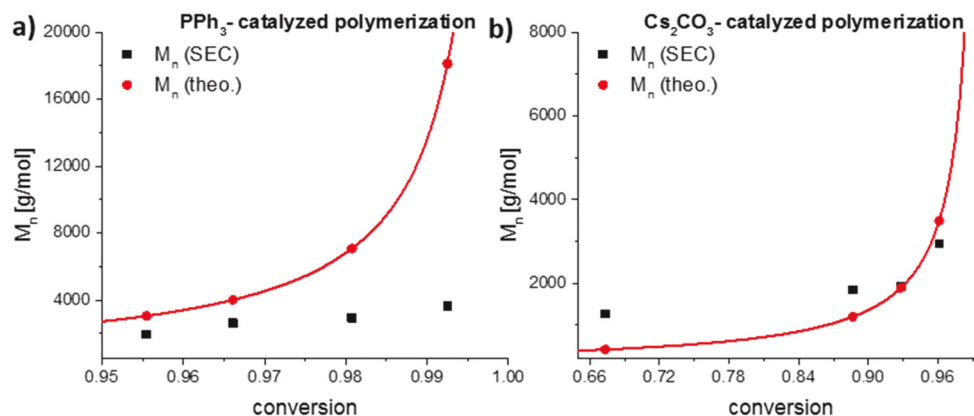


Fig. 4 Plot of M_n versus conversion for the (a) PPh_3 -catalyzed polymerization and (b) Cs_2CO_3 -catalyzed polymerization.

Subsequently, the material was precipitated in methanol to remove the excess catalyst, any unreacted monomer, or small oligomeric cycles. The obtained molar masses were found to be comparable to those of the first batch (see ESI, Table S5 and Fig. S33[†]). However, the precipitation and purification of the compounds allowed us to use vapor pressure osmometry to determine the absolute molar masses (ESI Fig. S27[†]). The exemplarily determined molar mass for the sample prepared with K_2CO_3 of 2110 g mol^{-1} confirms the good approximation of the SEC measurements ($M_n = 2230 \text{ g mol}^{-1}$). The NMR-spectra of these purified polymers displayed clear signals for the vinyl end groups as depicted in Fig. 5 for Cs_2CO_3 and PPh_3 (see ESI Fig. S15–28[†] for the other NMR spectra and MALDI-ToF-spectra). The inorganic bases are therefore considered to follow the above-mentioned process of deprotonation of the hydroxyl groups and a subsequent addition to the vinyl units. However, further signals are visible in the case of the organic compounds, which indicates the presence of the remaining catalyst. Therefore, these samples were not considered for analysis by vapor pressure osmometry, as the

remaining catalyst units affect the results. A closer look at the sample initiated by PPh_3 reveals that the signals are slightly shifted compared to the pure catalyst (see ESI for representative spectra, Fig. S15[†]). Also, a protonation of PPh_3 can be excluded as the acid strength of TFA is not sufficient for the protonation of PPh_3 . We therefore conclude that this polymerization is mainly initiated by a nucleophilic addition of PPh_3 to the reactive vinyl bond followed by a proton transfer as described above. This process is corroborated by the low basicity of this catalyst excluding a deprotonation of the hydroxyl groups. PPh_3 and the other organic compounds can therefore be considered to act as initiators instead of catalysts, although they might still be partially recovered by substitution reactions. For simplicity we stick to the term catalyst in the following. This irreversible addition further explains the observed deviations from the Carothers equation (1) in the case of this compound, as it disrupts the exact equimolarity of the AB-type monomer.

Assuming an irreversible addition of PPh_3 , the presence of vinyl end groups also proves an intermolecular proton transfer

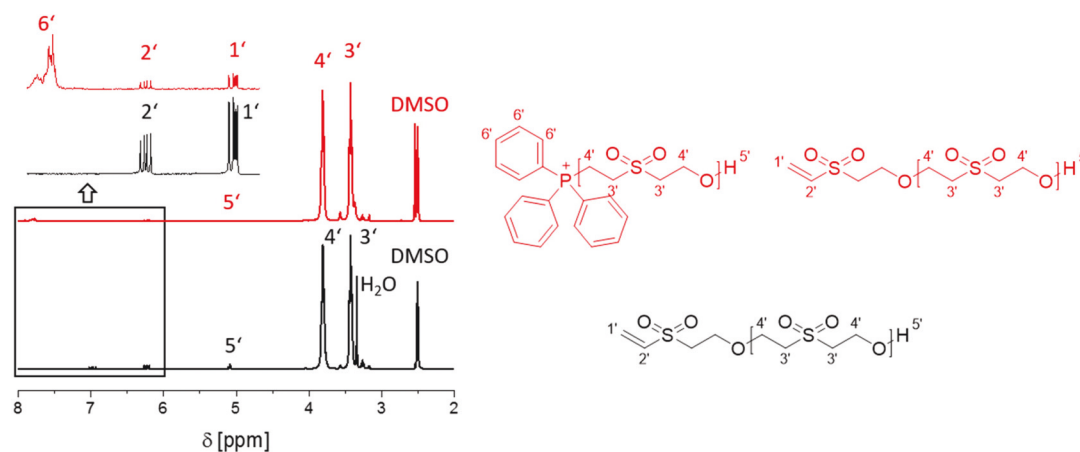


Fig. 5 ^1H -NMR spectrum (300 MHz, DMSO-d_6 , 298 K) of the purified polymer obtained with PPh_3 (P1, red) and the purified polymer obtained with Cs_2CO_3 (P7, black).

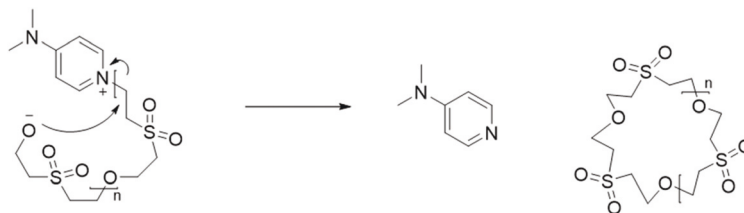
during the reaction and not only an intramolecular proton transfer, which could have been imagined considering the favorable arrangement of the groups. Interestingly, similar results are obtained for the nitrogen-based compounds which is particularly surprising for sterically very demanding or non-nucleophilic bases such as DBU or DMAP. Besides the NMR analysis, further MALDI-ToF-MS measurements confirm the presence of the respective cationic end groups. These results support a mechanism based on a first nucleophilic addition of the catalyst which is in agreement with previous results obtained by Strasser *et al.*^{26,27} In contrast to the phosphonium moiety formed by PPh_3 , the respective nitrogen compounds represent more reactive leaving groups making these end groups more susceptible to nucleophilic substitutions. In these cases, intramolecular reactions should be more favored, because of an attractive interaction between the negatively charged oxygen atom of the end of the chain after the proton transfer and the positively charged nitrogen atom at the beginning of the chains (Scheme 2). Therefore, the formation of cyclic compounds might be enhanced in these cases, which explains the observed lower final molar masses for DMAP- or TEDA-catalyzed systems compared to the ones using PPh_3 , despite similarly high conversions. Unfortunately, viscosity measurements could not provide a clear indication for the enhanced cyclization in these cases (see ESI Fig. S30/S31†). Even the mass spectra cannot unambiguously prove the presence of the cycles because the cycles have the same molar masses as the corresponding linear polymers with the vinyl end groups. Interestingly, the formation of the corresponding thioxane sulfone from an activated monomer does not seem to occur frequently, as confirmed by comparison of the NMR-spectra of the kinetic samples with that of the commercially available compound (Fig. S32†). Despite the favored six-membered structure, the addition of a second monomer seems to be preferred. Unfortunately, no other favored ring-sizes could be further identified in the NMR-spectra.

A closer look at the MALDI measurements further revealed the presence of a second peak series for several samples (see ESI Fig. S16–S19†). In the case of the inorganic bases, the different series can be assigned to the different attached ions (Na^+ or K^+). However, the use of PPh_3 , TEDA, DMAP, and TBD resulted in a second peak series, which cannot be explained by the different ions present. Interestingly, this second peak series is shifted by m/z values of 18 for all samples prepared with the nitrogen compounds, which corresponds to a release of water and most likely arises from a modification of the end

group of the polymers. Considering the increased acidity of the methylene groups next to the sulfone moiety an elimination of the resulting hydroxyl end group might occur during the course of the reaction in the presence of an excess of the applied bases. As a result an additional vinyl group is formed which might still participate in the polyaddition. The PPh_3 -catalyzed polymers, however, are different, since here the second and much more pronounced peak series is shifted by m/z values of 44 towards higher masses compared to the main series. This increase of molar mass could not be unequivocally assigned to a specific species. The mass difference corresponds to the addition of an ethylene oxide unit, which could only arise from a very unlikely hydrolysis of a sulfone unit and a C–S bond breakage. Another possibility is the incorporation of a single CO_2 molecule into the chain, which could be catalyzed by the phosphonium end group as reported for similar compounds, but usually requires increased CO_2 pressure. We therefore cannot unambiguously explain this second series for PPh_3 in the current stage, but further studies are in preparation to test the influence of different conditions.

Oxa-Michael polyaddition – solution polymerizations

A critical aspect during the previously described bulk polymerizations is the limited solubility of many catalysts and subsequently the indeterminable quantity of catalyst which initiates the polymerization process. In consequence, the most effective catalysts were further tested in solution. DMSO was chosen as the solvent due to the good solubility of the polymers and most catalysts. The inorganic catalysts, however, were not soluble under these conditions and therefore not considered in these tests. PPh_3 , DMAP and DBU were selected as organic catalysts and a monomer concentration of 3.3 M was chosen for the following experiments. The DBU- and PPh_3 -catalyzed polymerizations show similarly high conversions and chain lengths after 1 h (see Fig. 6 and ESI Fig. S35†). However, it is noticeable that the conversion after 5 min is again significantly lower for PPh_3 (64%) in comparison to DBU (91%), which is similarly related to the steric demand and the resulting retardation in the initiation step. The conversions after 1 h are already >93% and hardly change with further reaction time, which is in agreement with the obtained SEC traces and the determined molar masses at the different time points in solution. Due to the high conversions, the typical step-growth behavior for the PPh_3 and DBU-catalyzed polymerization cannot be identified unequivocally in the SEC data. However, the polymerization catalyzed by DMAP represents an exception



Scheme 2 Possible mechanism for the formation of cycles in the case of the DMAP-catalyzed polymerization.

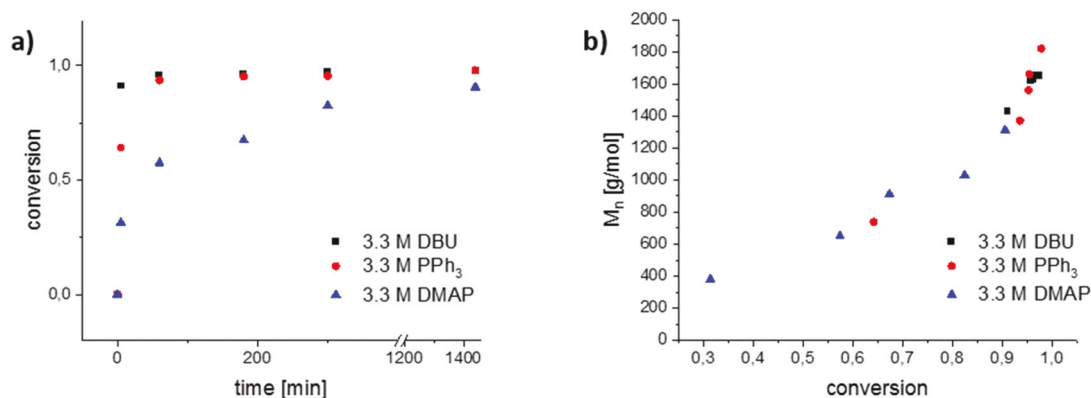


Fig. 6 (a) Conversion versus reaction time and (b) M_n versus conversion for different polymerizations in solution.

with conversions being significantly lower over the course of the reaction. In this case it was possible to monitor the continuous increase of the chain length with reaction time, revealing the typical progress expected for a step growth mechanism (Fig. 6b). In theory, the formation of cyclic byproducts should be enhanced in solution compared to the bulk polymerizations due to the increased dilution of the reactive groups. However, the similarities in the determined molar masses of the different polymers did not imply an increase in the occurrence of shorter cyclic polymers. Nevertheless, cyclic products still occur but the exact ratios could still not be quantified, and similar to the previous bulk polymerizations no preferential ring size could be determined either.

Furthermore, the polymerization at different monomer concentrations was tested using DBU as the catalyst (see ESI, Fig. S34 and S35[†]) but all conversions remained at similar levels revealing no significant influence of the concentration. Interestingly, the reaction rate appears higher in comparison to the bulk polymerization which is most likely related to the lower viscosity of the solution promoting the polymerization and conversion.

With the guaranteed homogeneous reaction conditions in solution, it was possible to investigate the influence of the catalyst quantity on the polymerization. In a first experiment, the impact of reduced amounts of PPh_3 on the final polymer length was evaluated, since for the bulk polymerizations we speculated that the amount of attached catalyst as the end group might cause a deviation of the stoichiometry of the reactive end groups and thus cause reduced molar masses compared to theory. However, the SEC analysis of the different polymerizations after 24 h did not reveal any significant differences in the molar mass of the polymers (Fig. S36[†]). A more detailed examination of the NMR-spectra after precipitation revealed an increase of vinyl and hydroxy end groups compared to bound PPh_3 with decreasing catalyst content (Fig. S37[†]). Consequently, the unequal stoichiometry obtained by the addition reaction of the catalyst is not the main limitation for the chain length and other factors such as reactivity must be taken into account. Similar molar masses were

further obtained with different amounts of DBU as catalyst (compare Fig. S35c with Fig. S38[†]). Interestingly, the kinetic analysis revealed conversions already exceeding 85% after 1 h even with such low amounts of catalyst. We therefore monitored the progress of the reaction directly in the NMR instrument and the spectra were recorded every minute over 35 minutes. For comparison, the course of the reaction was similarly monitored for DMAP as another exemplarily chosen catalyst. For each time point conversions were calculated as indicated above (Fig. 7). In general, a higher amount of catalyst resulted in faster polymerization. The kinetics for DMAP revealed a moderate reaction rate, which further decreases with time, most likely due to an increasing viscosity in the concentrated solution impeding the movement of the chains. A conversion of 49% for the 0.1 eq. DMAP catalyzed polymerization can be observed after 35 minutes, which correlates with the previous results. In comparison, the stronger base DBU results in a much faster polymerization and conversions of >80% are observed in less than 5 min for 0.1 eq. of catalyst. Even with half the amount of catalyst the reaction rate is still very high, displaying a similar course. Only with a low catalyst amount of 0.03 eq. a significant reduction of the polymerization rate is observed, which nevertheless leads to high conversions of >70% after 35 minutes.

Properties of the polymers

Commercial polyether sulfones based on aromatic units are particularly valued for their high thermal and chemical resistance. However, the high glass transition temperatures require high processing temperatures.⁵⁸ Aliphatic equivalents have barely been studied in this context. The available references report on potential elimination reactions and release of sulfur dioxide which occurred already at rather low temperatures for similar poly(olefin sulfones).^{59,60} Surprisingly, thermogravimetric analysis (TGA) of the herein synthesized precipitated poly(vinylsulfonylethanol) shows degradation temperatures T_D (5 wt% loss, air) of more than 300 °C for polymers that had been prepared with inorganic bases (Fig. 8, see ESI Fig. S39[†] for the TGA-data of the other polymers and the

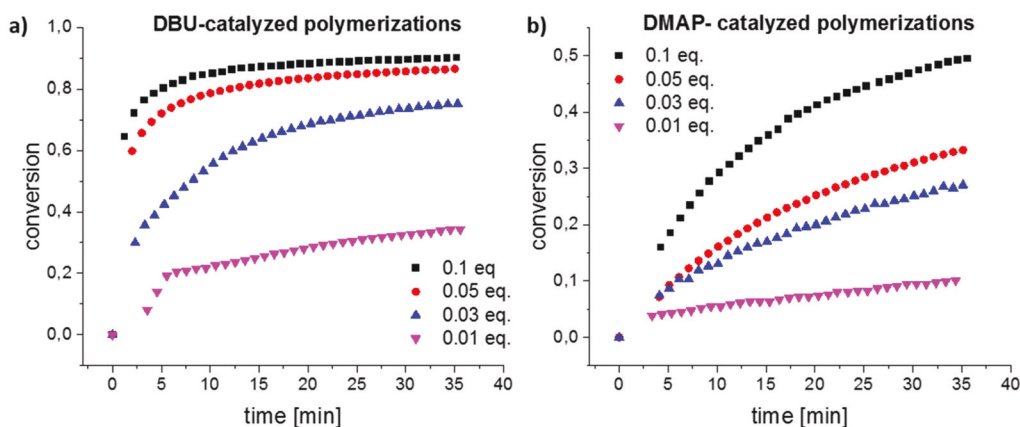


Fig. 7 Conversion versus reaction time of the (a) DBU- and (b) DMAP-catalyzed polymerizations with different amounts of catalyst.

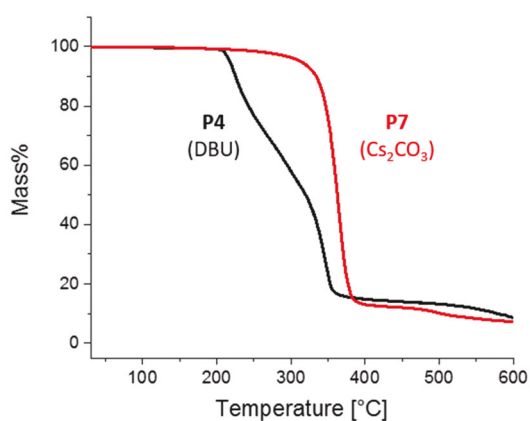


Fig. 8 TGA-data of the polymers P4 and P7.

measurements in N₂) even if the molar masses are considerably lower than those of commercial aromatic polyether sulfones ($M_n > 10\,000\text{ g mol}^{-1}$). Interestingly, the stability is sig-

nificantly affected by the applied catalyst and the conditions, as the organo-catalyzed polymerizations in bulk yield materials with lower degradation temperature. As NMR and mass spectrometry confirmed the presence of catalyst moieties as the polymer end groups, one hypothesis is that these units influence the thermal stability of the polymers and catalyze their thermal degradation. However, if the same polymerizations were conducted in solution, a high stability is maintained, which is especially noticeable for the PPh₃ catalyzed sample. In contrast to the sample polymerized in bulk the T_D (5 wt% loss, N₂) is shifted by almost 100 °C and the stability becomes similar as for the polymers prepared with inorganic bases. A comparison of the NMR-spectra of the precipitated polymers prepared in bulk or solution (Fig. S41†) did not corroborate an enhanced degradation by catalyst derived end groups as similar amounts of PPh₃ are found in both samples. The difference in stability must therefore be based on a structural difference, which could not be identified yet. In all cases, except for the PPh₃-based materials, a nearly complete decomposition is observed with almost no residual side pro-

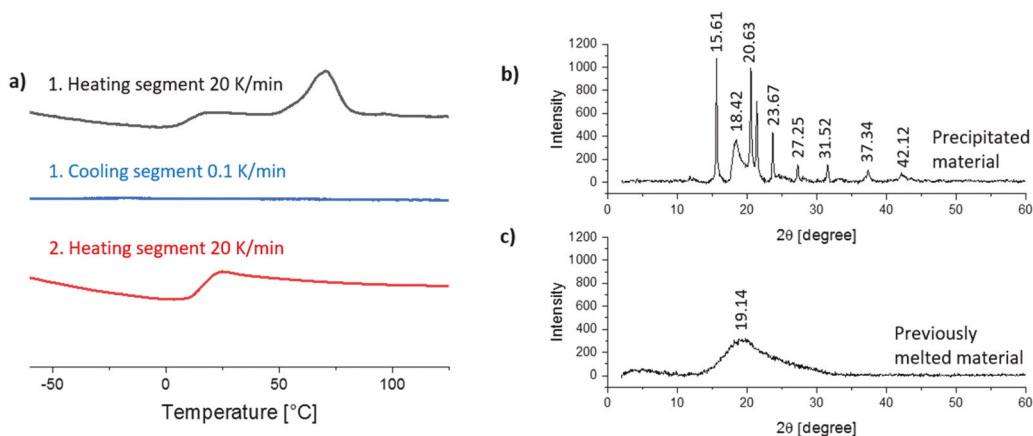


Fig. 9 (a) DSC-traces of P1 with different heating and cooling segments, (b) XRD-spectrum of P1 after precipitation, and (c) XRD-spectrum of P1 after precipitation and melting.

ducts left behind at temperatures above 400 °C. We assume a depolymerization by a retro Michael addition which can be accelerated by the remaining strong bases in the materials.⁶¹ Nevertheless, a more detailed analysis is required to identify the volatile compounds expelled during the degradation.

In contrast to the aromatic polyethersulfones, the glass transition temperature (T_g) of the presented polymers is considerably lower with values between 10 and 22 °C and no major differences were found between the polymers from bulk and those from solution polymerization (Fig. S39, S40 and Tables S5, S6†). However, the first heating cycle in the differential scanning calorimetry (DSC) revealed a strong endothermic signal at 70 °C indicating a melting point (Fig. 9a). Indeed, the purified and precipitated polymers appear rather brittle considering the low T_g which corroborates a semi-crystalline nature. However, no recrystallization was observed even at very low cooling rates of 0.1 K min⁻¹ (Fig. 9a) or extended annealing for 24 h at 50 °C (Fig. S42†), which hints at a kinetic inhibition of the crystallization from the melt. The semi-crystalline nature of the polymers could be confirmed by X-ray powder diffraction (XRD)-measurements (Fig. 9b) giving sharp and strong signals indicative of a highly crystalline polymer. These sharp signals disappear when measuring the material after melting and only a broad signal corresponding to an amorphous halo remains, which clearly proves the absence of any recrystallization in the bulk (Fig. 9c).

Conclusion

A novel aliphatic polyethersulfone was successfully prepared by oxa-Michael polyaddition using a variety of organic and inorganic catalysts. In contrast to previous reports based on an AA/BB-type polyaddition, the AB-type monomer vinylsulfonyl-ethanol was used. Vinylsulfonyl-ethanol is conveniently prepared from vinylmercaptoethanol in quantitative yields by oxidation with hydrogen peroxide using readily scalable procedures. The unique combination of a strong Michael acceptor (vinyl sulfone) and a Michael donor (aliphatic alcohol) within this AB-type monomer leads to a long shelf-life at 4 °C on the one hand, and high reactivity in oxa-Michael polyaddition, if triggered by moderate to strong organic or inorganic bases. Interestingly, even sterically hindered amine bases and PPh₃ appear to react by a nucleophilic addition to the vinyl sulfone moiety and a subsequent intra/intermolecular proton transfer. Polymers with average molar masses between 2000 g mol⁻¹ and 4000 g mol⁻¹ were obtained despite nearly quantitative conversions of the vinyl end groups in the case of highly reactive organic catalysts. This deviation from the theory according to Carothers is most likely related to the formation of cyclic structures or a partially irreversible addition of the organic catalysts. The obtained molar masses are clearly lower than those of commercial aromatic polyethersulfones with molar masses exceeding 10 000 g mol⁻¹. Nevertheless, the resulting polymers revealed an unexpected good thermal stability with decomposition temperatures exceeding 300 °C for the inorganic carbon-

ate catalyzed materials. In contrast to common aromatic polyethersulfones, the glass transition temperatures of the aliphatic polyethersulfones are much lower ranging from 10 to 20 °C and they feature a semi-crystalline nature with a melting point at 70 °C. The latter can however only be observed for materials processed from solvents, while a recrystallization from the melt appears to be kinetically hindered. Overall, the described aliphatic polyethersulfones represent an attractive class of materials with an unexpected good stability and interesting thermal properties, which certainly require more detailed investigations. With straightforward access to the monomer vinylsulfonyl-ethanol, the polymer can conveniently be prepared on larger scales and a thorough investigation of the mechanical properties is expected to open up opportunities for industrial applications.

Conflicts of interest

There are no conflicts to declare.

Acknowledgements

The presented study is part of an ongoing research project funded by BASF SE to identify and develop applications for vinylmercaptoethanol (VME). JCB thanks the German Science Foundation (DFG) for generous funding within the Emmy-Noether Programme (Project-ID: 358263073). Prof. U. S. Schubert is furthermore acknowledged for his continuous support and access to excellent research facilities. In addition, the authors thank Willi Tobiaschus and Nicole Fritz for the MS measurements, Rica Patzschke for the NMR measurements, Antje Wermann for the XRD measurements and Renzo Paulus for the TGA and DSC measurements.

References

- 1 A. Michael and P. C. Freer, *J. Prakt. Chem.*, 1891, **43**, 390–395.
- 2 A. Michael and O. Schulthess, *J. Prakt. Chem.*, 1892, **45**, 55–63.
- 3 A. Michael, *J. Prakt. Chem.*, 1887, **35**, 349–356.
- 4 A. Michael, *J. Prakt. Chem.*, 1894, **49**, 20–25.
- 5 J. Aleman, A. Nunez, L. Marzo, V. Marcos, C. Alvarado and J. L. Garcia Ruano, *Chem. – Eur. J.*, 2010, **16**, 9453–9456.
- 6 A. J. Boersma, D. Coquiere, D. Geerdink, F. Rosati, B. L. Feringa and G. Roelfes, *Nat. Chem.*, 2010, **2**, 991–995.
- 7 E. M. Phillips, M. Riedrich and K. A. Scheidt, *J. Am. Chem. Soc.*, 2010, **132**, 13179–13181.
- 8 L. Wang, X. Liu, Z. Dong, X. Fu and X. Feng, *Angew. Chem., Int. Ed.*, 2008, **47**, 8670–8673.
- 9 B.-C. Hong, P. Kotame, C.-W. Tsai and J.-H. Liao, *Org. Lett.*, 2010, **12**, 776–779.

- 10 H. Imagawa, H. Saijo, T. Kurisaki, H. Yamamoto, M. Kubo, Y. Fukuyama and M. Nishizawa, *Org. Lett.*, 2009, **11**, 1253–1255.
- 11 I. N. Lykakis, I. P. Zaravinos, C. Raptis and M. Stratakis, *J. Org. Chem.*, 2009, **74**, 6339–6342.
- 12 L. R. Dix, J. R. Ebdon and P. Hodge, *Eur. Polym. J.*, 1995, **31**, 647–652.
- 13 P. Ferruti, E. Ranucci, F. Trotta, E. Gianasi, E. G. Evagorou, M. Wasil, G. Wilsona and R. Duncan, *Macromol. Chem. Phys.*, 1999, **200**, 1644–1654.
- 14 D. M. Lynn and R. Langer, *J. Am. Chem. Soc.*, 2000, **122**, 10761–10768.
- 15 T. Saegusa, S. Kobayashi and Y. Kimura, *Macromolecules*, 1974, **7**, 256–258.
- 16 C. J. Atkins, G. Patias, J. S. Town, A. M. Wemyss, A. M. Eissa, A. Shegiwal and D. M. Haddleton, *Polym. Chem.*, 2019, **10**, 646–655.
- 17 T. J. Farmer, D. J. Macquarrie, J. W. Comerford, A. Pellis and J. H. Clark, *J. Polym. Sci., Part A: Polym. Chem.*, 2018, **56**, 1935–1945.
- 18 A. Guarneri, V. Cutifani, M. Cespuogli, A. Pellis, R. Vassallo, F. Asaro, C. Ebert and L. Gardossi, *Adv. Synth. Catal.*, 2019, **361**, 2559–2573.
- 19 S.-i. Matsuoka, Y. Kamijo and M. Suzuki, *Polym. J.*, 2017, **49**, 423–428.
- 20 D. P. Nair, M. Podgórski, S. Chatani, T. Gong, W. Xi, C. R. Fenoli and C. N. Bowman, *Chem. Mater.*, 2014, **26**, 724–744.
- 21 T. Murase, S.-i. Matsuoka and M. Suzuki, *Polym. Chem.*, 2018, **9**, 2984–2990.
- 22 T. Saegusa, S. Kobayashi and Y. Kimura, *Macromolecules*, 1975, **8**, 950–952.
- 23 T. Saegusa, S. Kobayashi and Y. Kimura, *Macromolecules*, 1974, **7**, 256–258.
- 24 S. Matsuoka, S. Namera and M. Suzuki, *Polym. Chem.*, 2015, **6**, 294–301.
- 25 M. Gibas and A. Korytkowska-Walach, *Polymer*, 2003, **44**, 3811–3816.
- 26 S. Strasser and C. Slugovc, *Catal. Sci. Technol.*, 2015, **5**, 5091–5094.
- 27 S. Strasser, C. Wappl and C. Slugovc, *Polym. Chem.*, 2017, **8**, 1797–1804.
- 28 H. Wang, F. Cheng, W. He, J. Zhu, G. Cheng and J. Qu, *Biointerphases*, 2017, **12**, 02C414-1–02C414-8.
- 29 H. Yang, Y. Zuo, J. Zhang, Y. Song, W. Huang, X. Xue, Q. Jiang, A. Sun and B. Jiang, *Polym. Chem.*, 2018, **9**, 4716–4723.
- 30 J. Black and G. Hastings, *Handbook of Biomaterial Properties*, Springer, New York, 1998.
- 31 G. S. Sur, H. L. Sun, S. G. Lyu and J. E. Mark, *Polymer*, 2001, **42**, 9783–9789.
- 32 T. Schwab, *US Pat*, WO2008/059004A1, 2007.
- 33 S. S. Lane, R. L. Lindstrom, P. A. Williams and C. W. Lindstrom, *J. Refractive Surg.*, 1985, **1**, 207–216.
- 34 J. K. Stille, *J. Chem. Educ.*, 1981, **58**, 862–866.
- 35 T. Higashihara and M. Ueda, *Encyclopedia of Polymer Science and Technology*, 2013.
- 36 J. Morales-Sanfrutos, F. J. Lopez-Jaramillo, F. Hernandez-Mateo and F. Santoyo-Gonzalez, *J. Org. Chem.*, 2010, **75**, 4039–4047.
- 37 B. L. Ekerdt, D. V. Schaffer, R. Segalman and Y. Lei, *US Pat*, WO2017/062375A1, 2017.
- 38 R. M. Black, K. Brewster, J. M. Harrison and N. Stansfield, *Phosphorus, Sulfur Silicon Relat. Elem.*, 2006, **71**, 31–47.
- 39 A. H. Ford-Moore, *J. Chem. Soc.*, 1949, 2433–2440.
- 40 C. C. Price and O. H. Bullitt, *J. Org. Chem.*, 1947, **12**, 238–248.
- 41 A. Schöberl and M. Biedermann, *Justus Liebigs Ann. Chem.*, 1968, **716**, 37–46.
- 42 W. Reppe, *Acetylene chemistry*, CA Meyer, 1949.
- 43 V. Wascholowski, F. N. Windlin, P. Tuzina and P. Fournier, *German Pat*, WO/2018/036848, 2018.
- 44 R. Lohwasser, P. Tuzina, F. Bienewald and D. P. Kunsmann-Keitel, *German Pat*, WO/2020/221607, 2020.
- 45 N. Azizi, A. Khajeh-Amiri, H. Ghafuri and M. Bolourtchian, *Green Chem. Lett. Rev.*, 2009, **2**, 43–46.
- 46 J. W. Chan, C. E. Hoyle, A. B. Lowe and M. Bowman, *Macromolecules*, 2010, **43**, 6381–6388.
- 47 T. Flessner and S. Doye, *J. Prakt. Chem.*, 1999, **341**, 186–190.
- 48 S.-H. Guo, S.-Z. Xing, S. Mao, Y.-R. Gao, W.-L. Chen and Y.-Q. Wang, *Tetrahedron Lett.*, 2014, **55**, 6718–6720.
- 49 C. F. Nising and S. Bräse, *Chem. Soc. Rev.*, 2012, **41**, 988–999.
- 50 W. Xi, C. Wang, C. J. Kloxin and C. N. Bowman, *ACS Macro Lett.*, 2012, **1**, 811–814.
- 51 C.-E. Yeom, M. J. Kim and B. M. Kim, *Tetrahedron*, 2007, **63**, 904–909.
- 52 D. J. Darensbourg, M. S. Zimmer, P. Rainey and D. L. Larkins, *Inorg. Chem.*, 2000, **39**, 1578–1585.
- 53 D. Gimenez, A. Dose, N. L. Robson, G. Sandford, S. L. Cobb and C. R. Coxon, *Org. Biomol. Chem.*, 2017, **15**, 4081–4085.
- 54 D. A. Guzonas and D. E. Irish, *Can. J. Chem.*, 1988, **66**, 1249–1257.
- 55 W. M. Haynes and D. R. Lide, *CRC handbook of chemistry and physics : a ready-reference book of chemical and physical data*, CRC Press, Boca Raton, 2010.
- 56 K. Kaupmees, A. Trummal and I. Leito, *Croat. Chem. Acta*, 2014, **87**, 385–395.
- 57 C. H. Carothers, *Trans. Faraday Soc.*, 1936, **32**, 39–49.
- 58 J. Brandrup, E. H. Immergut and E. A. Grulke, *Polymer Handbook*, John Wiley & Sons, 2004.
- 59 E. Kiran, J. K. Gillham and E. Gipstein, *J. Appl. Polym. Sci.*, 1977, **21**, 1159–1176.
- 60 C. M. Possanza Casey and J. S. Moore, *ACS Macro Lett.*, 2016, **5**, 1257–1260.
- 61 T. Sasaki, T. Kondo, M. Noro, K. Saida, H. Yaguchi and Y. Naka, *J. Polym. Sci., Part A: Polym. Chem.*, 2012, **50**, 1462–1468.

Supplementary Information for

Oxa-Michael polyaddition of vinylsulfonylethanol for aliphatic polyethersulfones

Nicole Ziegenbalg,^{a,b} Ruth Lohwasser,^c Giovanni D'Andola,^c Torben Adermann,^c Johannes C. Brendel,^{a,b,*}

a Laboratory of Organic and Macromolecular Chemistry (IOMC), Friedrich Schiller University Jena, Humboldtstraße 10, 07743 Jena, Germany

b Jena Center for Soft Matter (JCSM), Friedrich Schiller University Jena, Philosophenweg 7, 07743 Jena, Germany

c BASF SE, Carl-Bosch-Straße 38, 67056 Ludwigshafen/Rhein, Germany

*corresponding author: johannes.brendel@uni-jena.de

Experimental part

Materials and Methods

All reagents and solvents were commercially purchased from Sigma-Aldrich, TCI Chemicals, and abcr. and were used without further purification. Vinylmercaptoethanol was provided by BASF SE.

¹H-NMR spectra were measured with a Bruker spectrometer (300 MHz) equipped with an Avance I console, a dual ¹H and ¹³C sample head and a 60 x BACS automatic sample changer, and a Bruker spectrometer (400 MHz) equipped with an Avance III console, a BBFO sample head, and a 60 x BACS automatic sample changer. The chemical shifts of the peaks were determined by using the residual solvent signal as a reference and are given in ppm in comparison to TMS. Deuterated solvents were commercially purchased from EURISO-TOP GmbH.

Size-exclusion chromatography (SEC) of polymers was performed on an Agilent system (series 1200) equipped with a PSS degasser, a G1310A pump, a G1362A refractive index detector and a PSS GRAM 30 and 1000 column with DMAc (+ 0.21 wt.% LiCl) as eluent at a flow rate of 1 mL/min. The column oven was set to 40 °C and poly(ethylene glycol) (PEG) standards were used for calibration.

Matrix-assisted laser desorption ionization mass spectrometry (MALDI-MS) measurements were carried out using an Ultraflex III ToF/ToF instrument (Bruker Daltonics) equipped with an Nd-YAG laser. All these spectra were measured in the positive mode using alpha-Cyano-4-hydroxycinnamic acid (CHCA) as a matrix.

The differential scanning calorimetry (DSC) measurements were performed on a DSC 204 F1 Phoenix from Netzsch under a nitrogen atmosphere with a heating rate of 10 K/min. The thermal gravimetric analysis (TGA) was carried under nitrogen using a Netzsch TG 209F1.

The density and viscosity measurements were carried out on a Density meter: DMA 4100 M and an AMVn (Automated Micro Viscometer) from Anton Paar. A glass capillary with a diameter of 0.9 mm and a 0.3μ-gold plated ball (density 7.484 g/cm³) with a diameter of 0.794 mm was used. All viscosity measurements were performed in DMSO.

The X-ray diffraction (XRD) measurements were performed on the STOE Transmission Diffractometer System STADI P with Cu-K α radiation (40 kV, 15 mA, $\lambda = 1.5406 \text{ \AA}$).

The vapor pressure osmometry measurements were performed on the Vapor Pressure Osmometer K-7000 from Knauer. A calibration with PEG-standard ($M_n = 2800 \text{ g/mol}$) was executed and the polymer was measured in 4 different concentration. An extrapolation of the measurements data reveals the absolute molar mass of the polymers.

Synthetic procedures

Vinylsulfonylethanol: Vinylmercaptoethanol (30.00 g, 288 mmol, 1 eq.), sodium tungstate (0.04 g, 0.12 mmol, 0.0004 eq.) and hydroxyanisol (0.05 g, 0.40 mmol, 0.001 eq.) were dispersed in water (15 mL). Afterwards, 50% hydrogen peroxide solution (19.61 g, 288 mmol, 1 eq.) was added dropwise so that 40 °C was not exceeded. Then the solution was stirred for 1 h at 40 °C. Subsequently, 50% hydrogen peroxide solution (19.61 g, 288 mmol, 1 eq.) was added dropwise at 40 °C and then the solution was stirred overnight at 60 °C. Finally, manganese oxide was added, the solution was centrifuged and the solvent was removed in a gas flow at 40 °C.

$^1\text{H-NMR}$ (300 MHz, DMSO): δ [ppm] = 6.93 (dd, $J = 16.2, 9.8 \text{ Hz}$, 1H), 6.18 (dd, $J = 12.7, 8.9 \text{ Hz}$, 2H), 5.06 (s, 1H), 3.74 (s, 2H), 3.24 (s, 2H).

$^{13}\text{C-NMR}$ (75 MHz, DMSO) δ [ppm] = 138.09, 128.30, 56.19, 54.84.

General procedure for the bulk-polymerizations: Vinylsulfonylethanol (1 eq.) was added to the respective catalyst (0.1 eq.) and the reaction was agitated for 24 h at 40 °C. To monitor kinetics samples were taken at different time points. To quench the catalyst an excess of TFA was added. For purification, the polymer was subsequently dissolved in DMSO, precipitated in methanol and dried under vacuum. Details of the applied amounts can be found in Table S1.

Table S1: Applied amount of monomer and catalysts for the bulk polymerizations.

Polymer	Catalyst	m_{catalyst} [g]	n_{catalyst} [mmol]	m_{monomer} [g]	n_{monomer} [mmol]
P1	PPh ₃	0.39	1.47	2.01	14.73
P2	TEDA	0.17	1.48	2.00	14.70
P3	DMAP	0.18	1.48	2.00	14.68

P4	DBU	0.22	1.47	2.00	14.68
P5	TBD	0.20	1.47	2.01	14.73
P6	K ₂ CO ₃	0.20	1.47	2.00	14.69
P7	Cs ₂ CO ₃	0.48	1.47	2.00	14.68

General procedure for the solution polymerization: The catalyst was dissolved in DMSO. Vinylsulfonylethanol (1 eq.) was added to the respective catalyst and the reaction was agitated for 24 h at 40 °C. To monitor kinetics samples were taken at different time points. To quench the catalyst an excess of TFA was added. For purification, the polymer was subsequently dissolved in DMSO, precipitated in methanol and dried under vacuum. Details of the applied amounts can be found in Table S2.

Table S2: Applied amount of monomer and catalysts for the solution polymerizations.

Polymer	Catalyst	m _{catalyst} [mg]	n _{catalyst} [mmol]	m _{monomer} [mg]	n _{monomer} [mmol]	m _{DMSO} [mg]
P8	PPh ₃	58.0	0.22	302.9	2.22	471.1
P9	PPh ₃	29.1	0.11	310.2	2.28	474.6
P10	PPh ₃	15.1	0.06	310.1	2.28	470.3
P11	DMAP	26.9	0.22	303.1	2.22	476.0
P12	DBU	34.1	0.22	301.2	2.21	475.4
P13	DBU	34.1	0.22	306.5	2.23	341.7
P14	DBU	34.1	0.22	301.0	2.21	171.0
P15	DBU	10.1	0.07	302.8	2.22	474.9
P16	DBU	3.3	0.02	307.0	2.26	476.0

General procedure for the kinetic experiments in the NMR (solution-polymerizations using DBU as catalyst): Vinylsulfonylethanol (200 mg, 1.47 mmol, 1 eq.) and DBU were each dissolved in 0.15 mL DMSO-d₆. The solution was mixed in an NMR-tube and inserted into the preheated NMR-instrument at 40 °C. Every minute, an ¹H-NMR-spectrum was measured. Details of the applied amounts of catalyst are listed in Table S3.

Table S3: Applied amount of DBU for the NMR-experiments.

m _{catalyst} [mg]	n _{catalyst} [mmol]	Eq.
22.4	0.15	0.10

11.1	0.07	0.05
6.7	0.04	0.03
2.2	0.01	0.01

General procedure for the kinetic experiments in the NMR (solution-polymerizations using DMAP as catalyst): DMAP was dissolved in 0.3 mL DMSO-d₆. Vinylsulfonylethanol (200 mg, 1.47 mmol, 1 eq.) and the DMAP-solution were mixed in an NMR-tube and heated to 40 °C in an NMR-instrument. Every minute, an ¹H-NMR-spectrum was measured. Details of the applied amounts of catalyst are listed in S4.

Table S4: Applied amount of DMAP for the NMR-experiments.

m_{catalyst} [mg]	n_{catalyst} [mmol]	Eq.
18.0	0.15	0.10
8.9	0.07	0.05
5.4	0.04	0.03
1.7	0.01	0.01

Monomer

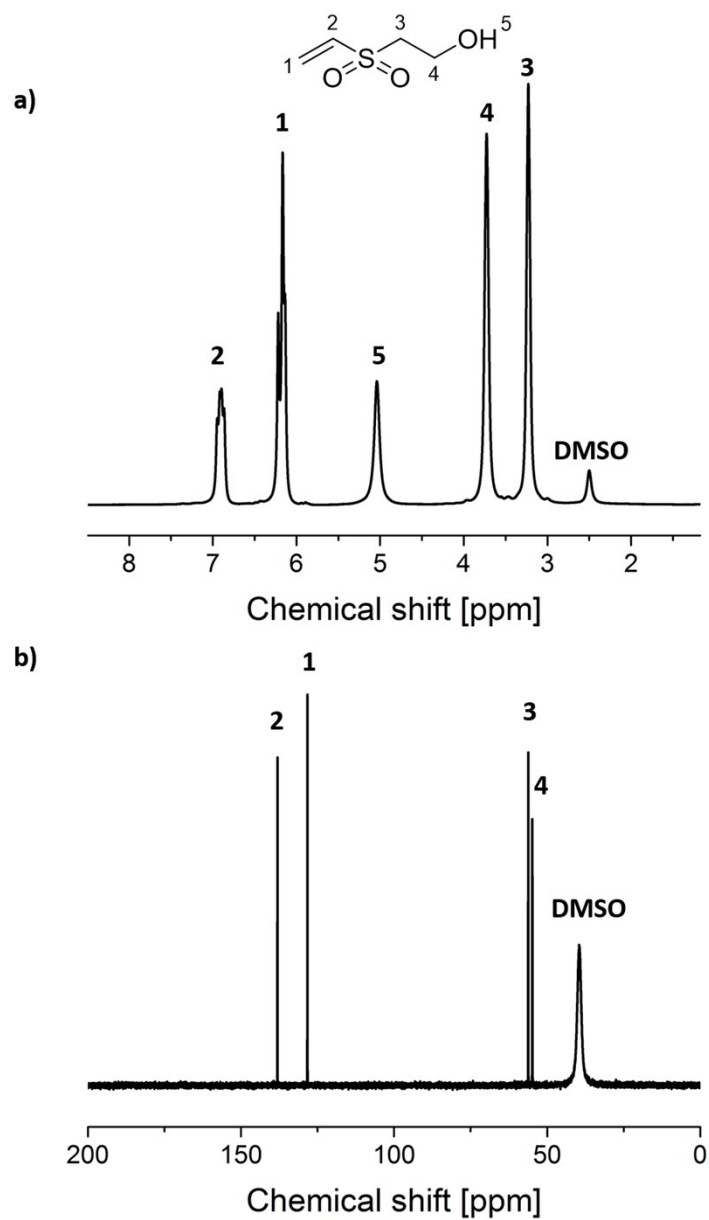


Figure S1: a) $^1\text{H-NMR}$ (300 MHz, DMSO-d_6) spectrum and b) $^{13}\text{C-NMR}$ (75 MHz, DMSO-d_6) spectrum of vinylsulfonylethanol.

Determination of conversion

The conversion of the end-groups was determined from the comparison of the NMR spectra before and after the reaction. Setting the integral of the signal at $\delta = 6.21$ ppm to 2, which reflects protons in residual monomer and end-group, the integral of the second signal at $\delta = 3.42$ ppm, which comprises only protons of the polymer chain, can be used to determine the conversion according to

$$\text{conversion} = \frac{I(\text{polymer signal } 3')/2}{I(\text{end - group monomer signal } 1) + I(\text{polymer signal } 3')/2}$$

The chemical shift of the water signal depends on the concentration of the compounds. Because of this, there may be an overlap between the water signal and the polymer signal at $\delta = 3.42$ ppm. If this is the case, the other polymer signal $\delta = 3.80$ ppm was used for the determination of the conversion. This signal comprises the protons of the polymer chain and the monomer and so the conversion was determined according to the following equation:

$$\text{conversion} = \frac{I(\text{polymer signal } 4' - 2)/2}{I(\text{end - group monomer signal } 1) + I(\text{polymer signal } 4' - 2)/2}$$

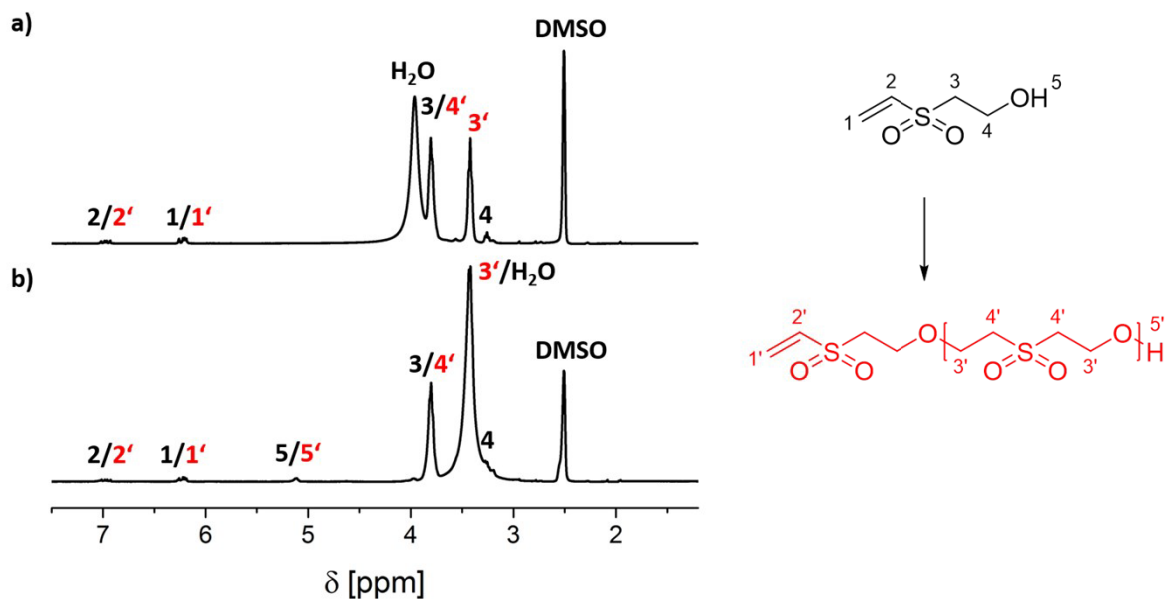


Figure S2: a) $^1\text{H-NMR}$ (300 MHz, DMSO-d_6) spectrum of the kinetic sample of the K_2CO_3 -catalyzed polymerization after 3 h and b) $^1\text{H-NMR}$ (300 MHz, DMSO-d_6) spectrum of the kinetic sample of the PPh_3 -catalyzed polymerization after 3 h.

Bulk-polymerization

Kinetic samples after 1 h

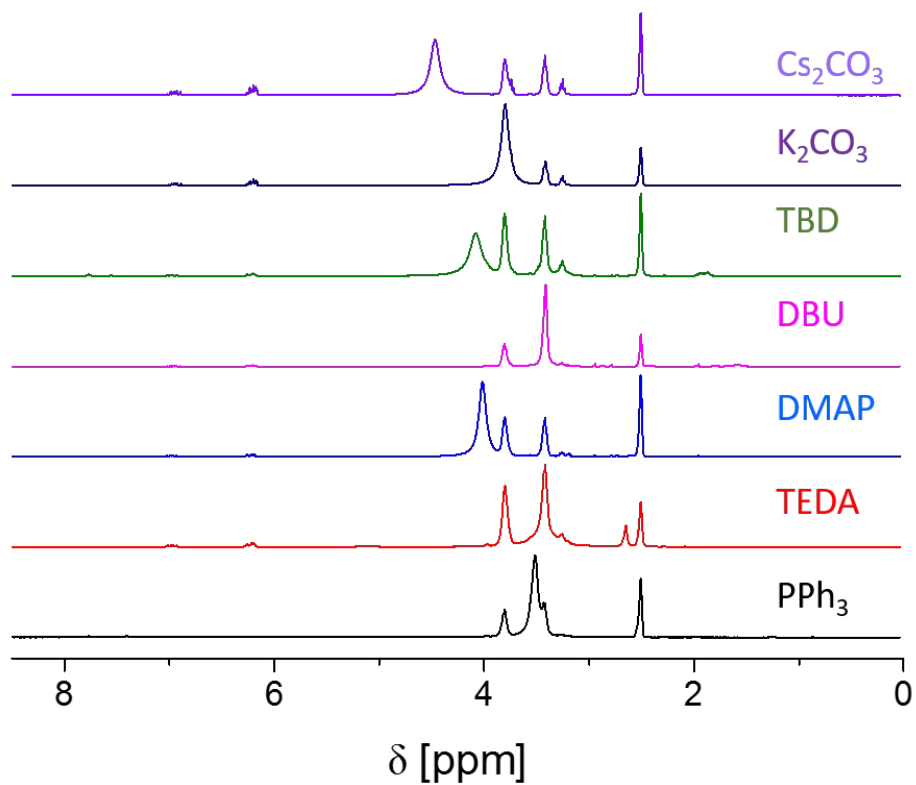


Figure S3: ¹H-NMR (300 MHz, DMSO-d₆) spectra of the polymerization with different catalysts after 1 h.

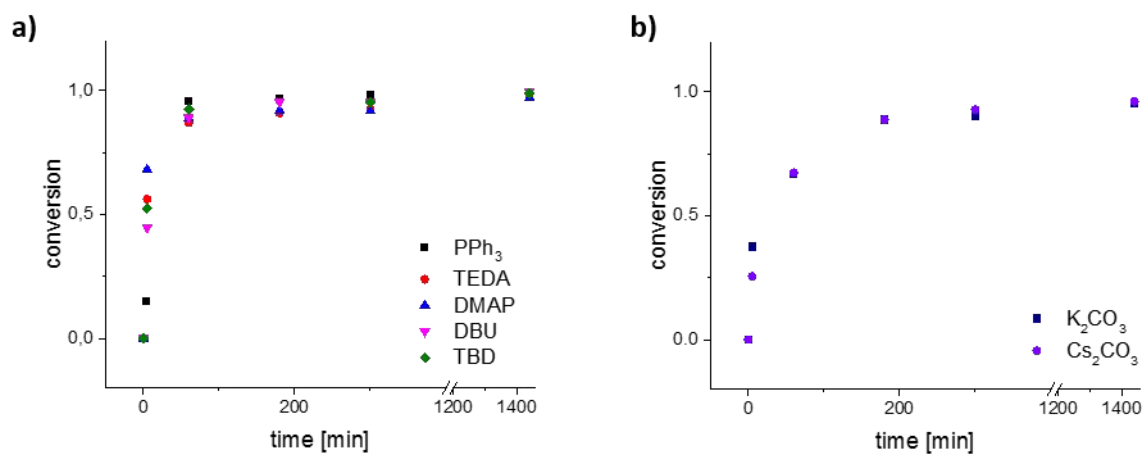


Figure S4: Conversion vs. reaction time for different polymerizations: a) comparison of different organic catalysts; b) comparison of different inorganic catalysts.

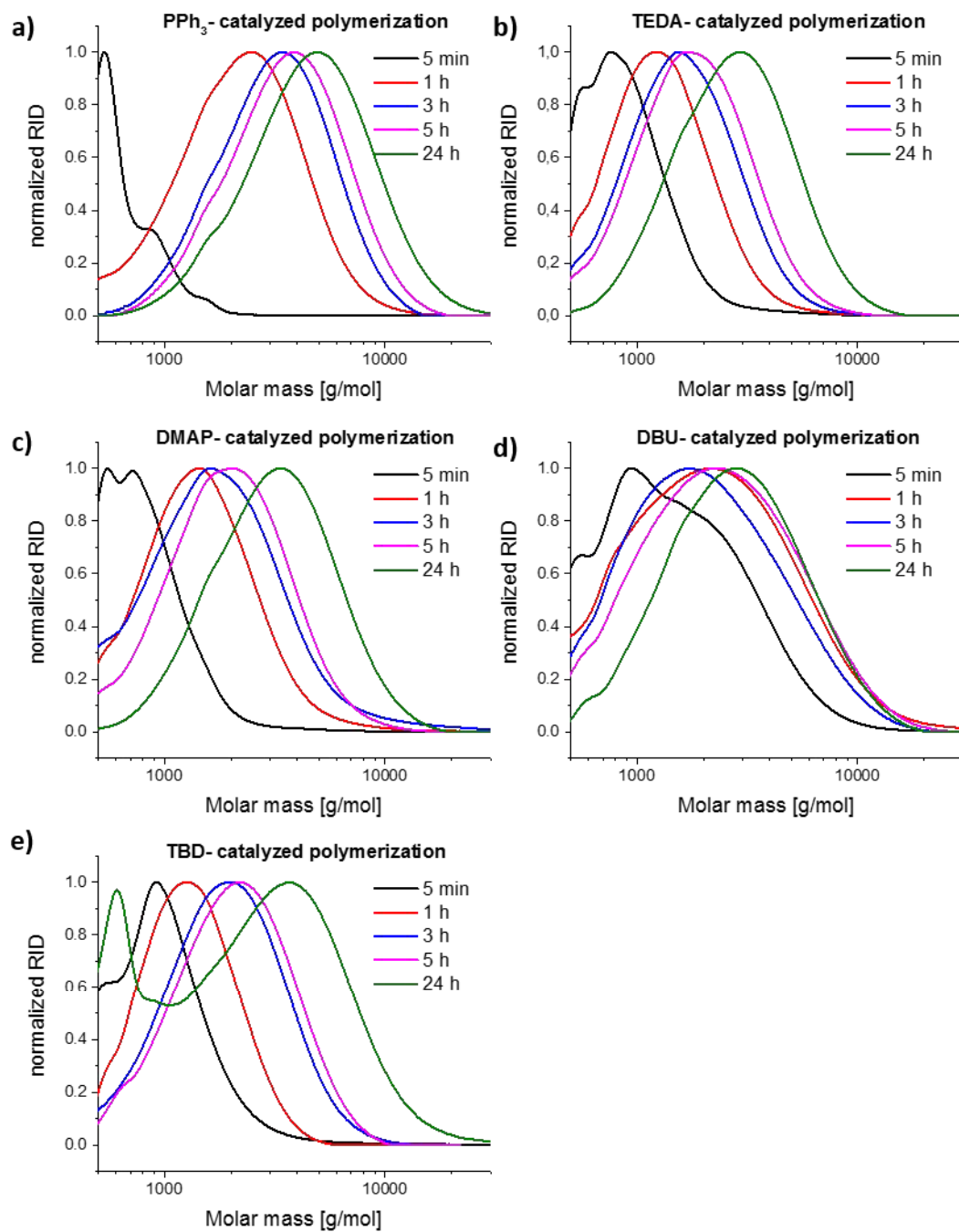


Figure S5: SEC (DMAc (+ 0.21 wt.% LiCl), PEG standards) traces of the kinetic samples taken after 5 min, 1 h, 3 h and 24 h of the polymerization catalyzed with a) triphenylphosphine, b) TEDA, c) DMAP, d) DBU, e) TBD.

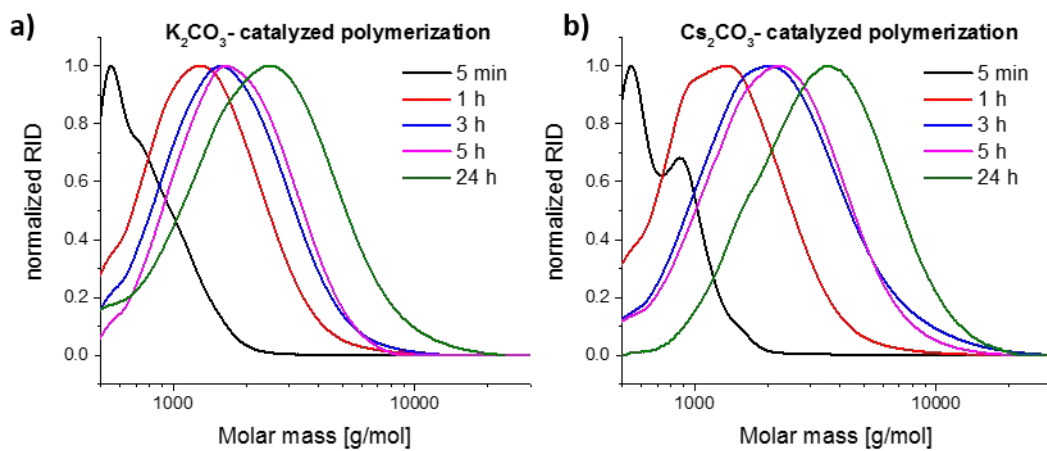


Figure S6: SEC (DMAc (+ 0.21 wt.% LiCl), PEG standards) traces of the kinetic samples taken after 5 min, 1 h, 3 h and 24 h of the polymerization catalyzed with a) K₂CO₃, and b) Cs₂CO₃

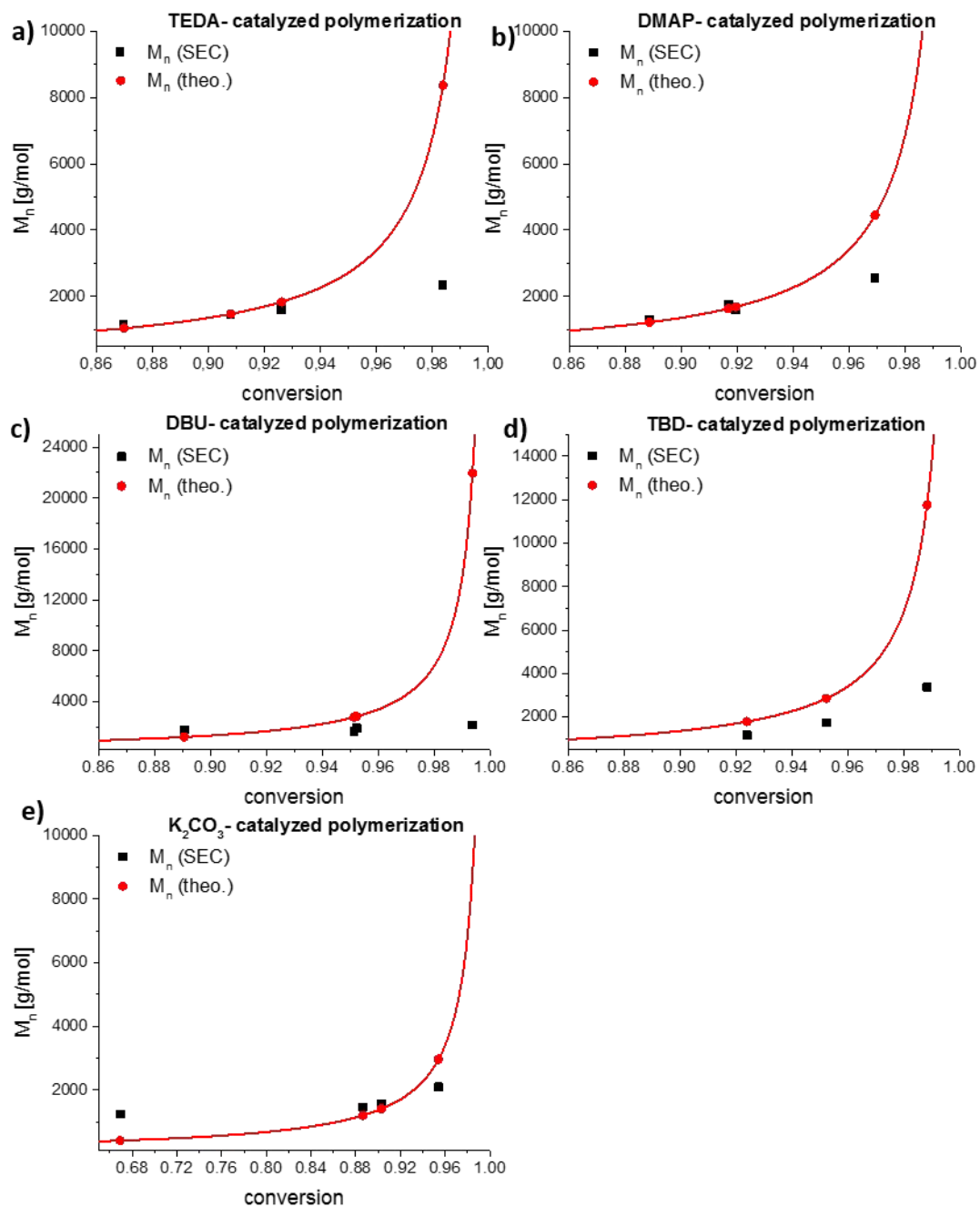


Figure S7: Plot of M_n versus conversion (red: theoretically values according to Carothers equation; black: experimental data from SEC measurements) for the polymerizations catalyzed by a) TEDA, b) DMAP, c) DBU, d) TBD, e) K_2CO_3 .

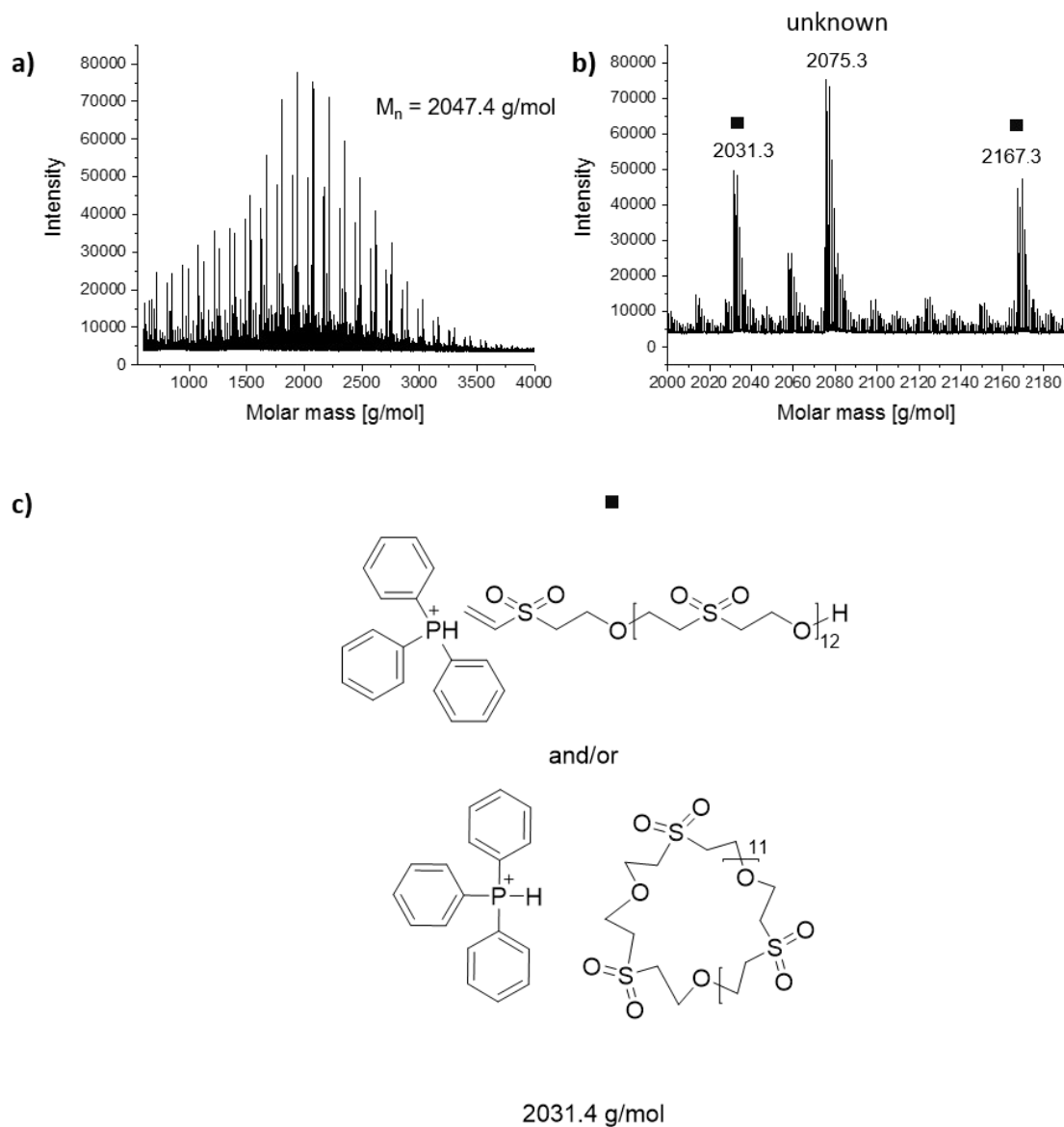


Figure S8: a) MALDI-ToF-spectrum of PPh_3 -catalyzed polymer after 24 h; b) Enlarged section of the MALDI ToF-spectrum of PPh_3 -catalyzed polymer after 24 h; c) potential chemical structures of detected species.

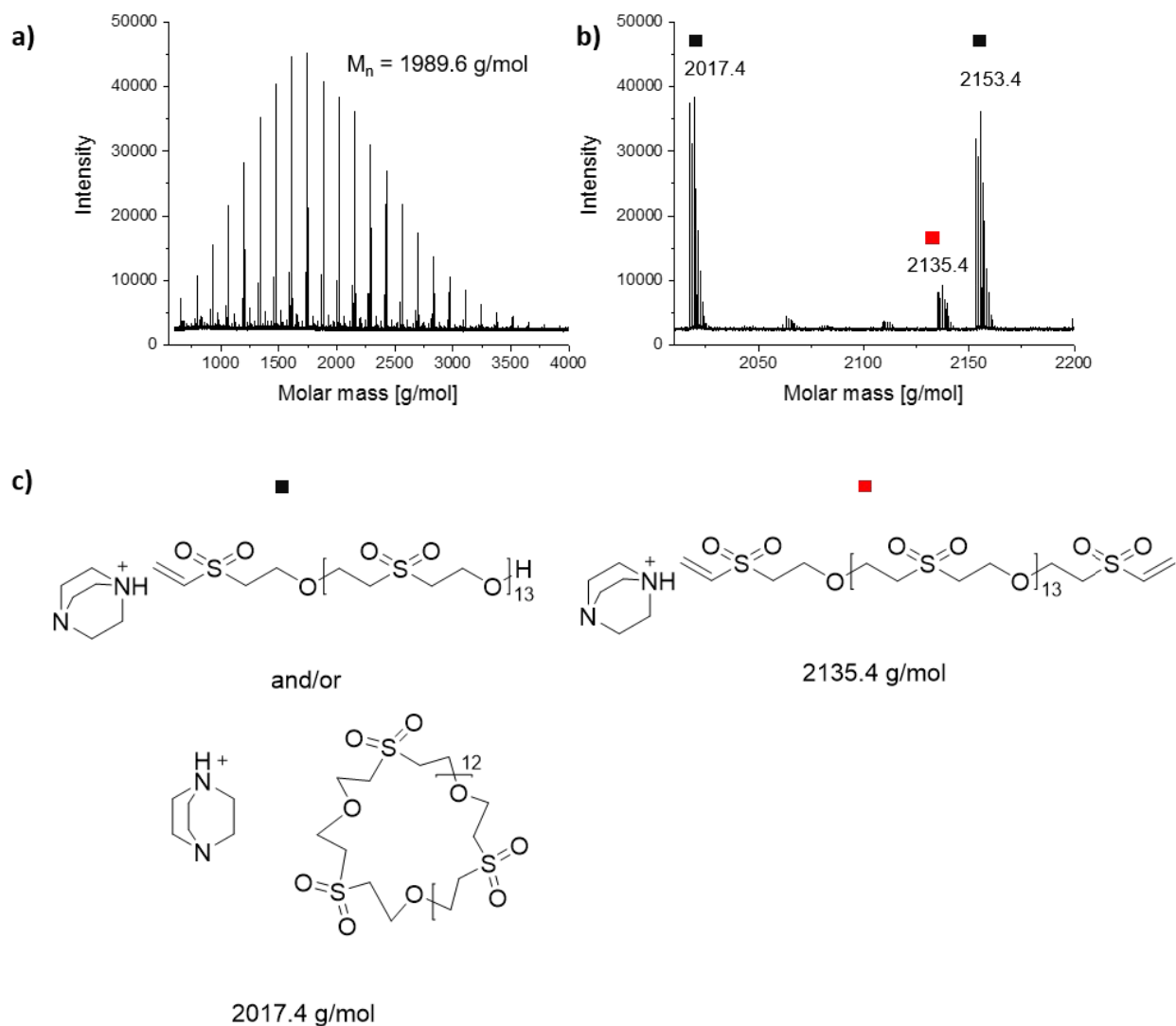


Figure S9: a) MALDI-ToF-spectrum of TEDA-catalyzed polymer after 24 h; b) Enlarged section of the MALDI ToF-spectrum of TEDA-catalyzed polymer after 24 h; c) potential chemical structures of detected species.

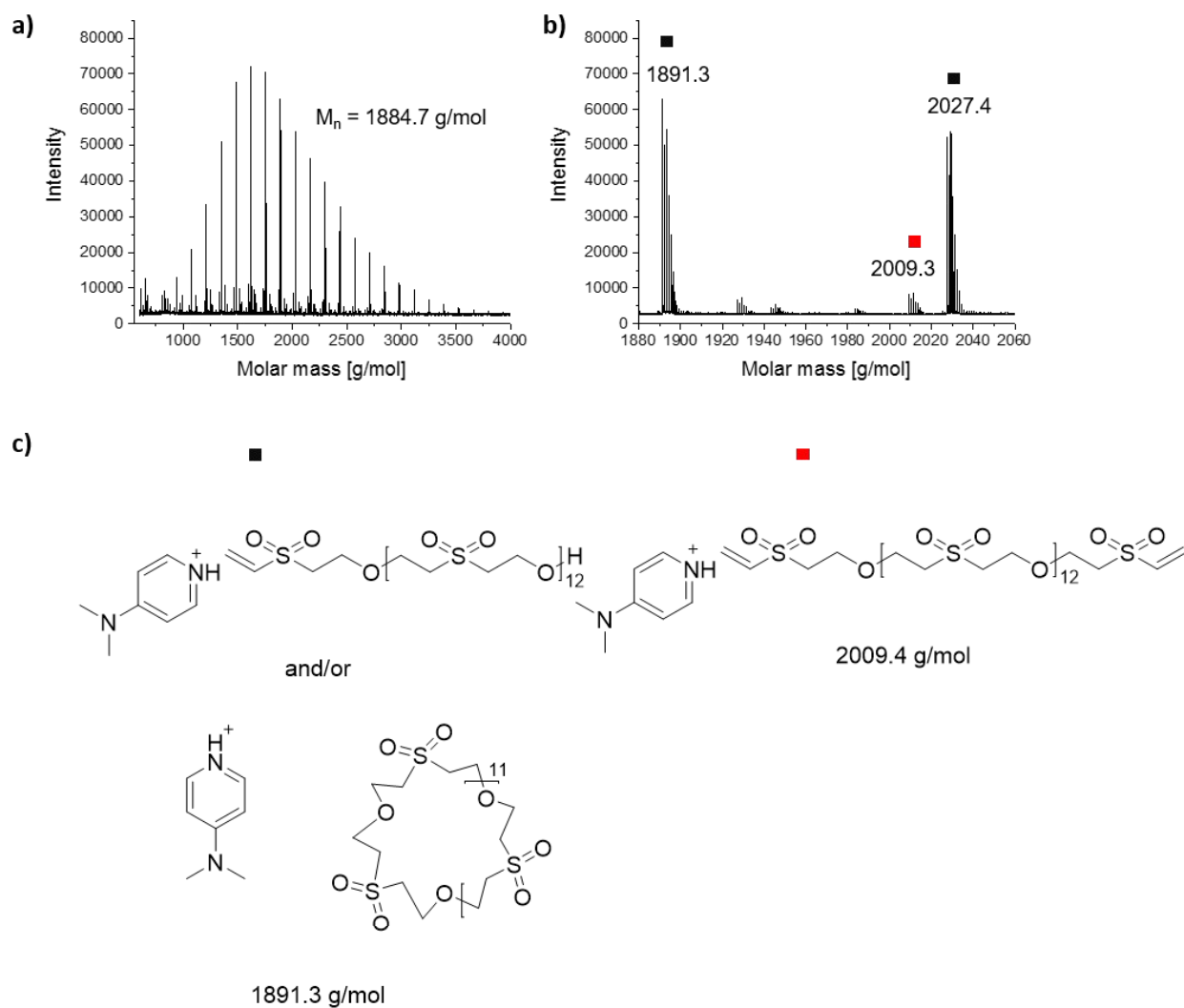


Figure S10: a) MALDI-ToF-spectrum of DMAP-catalyzed polymer after 24 h; b) Enlarged section of the MALDI ToF-spectrum of DMAP-catalyzed polymer after 24 h; c) potential chemical structures of detected species.

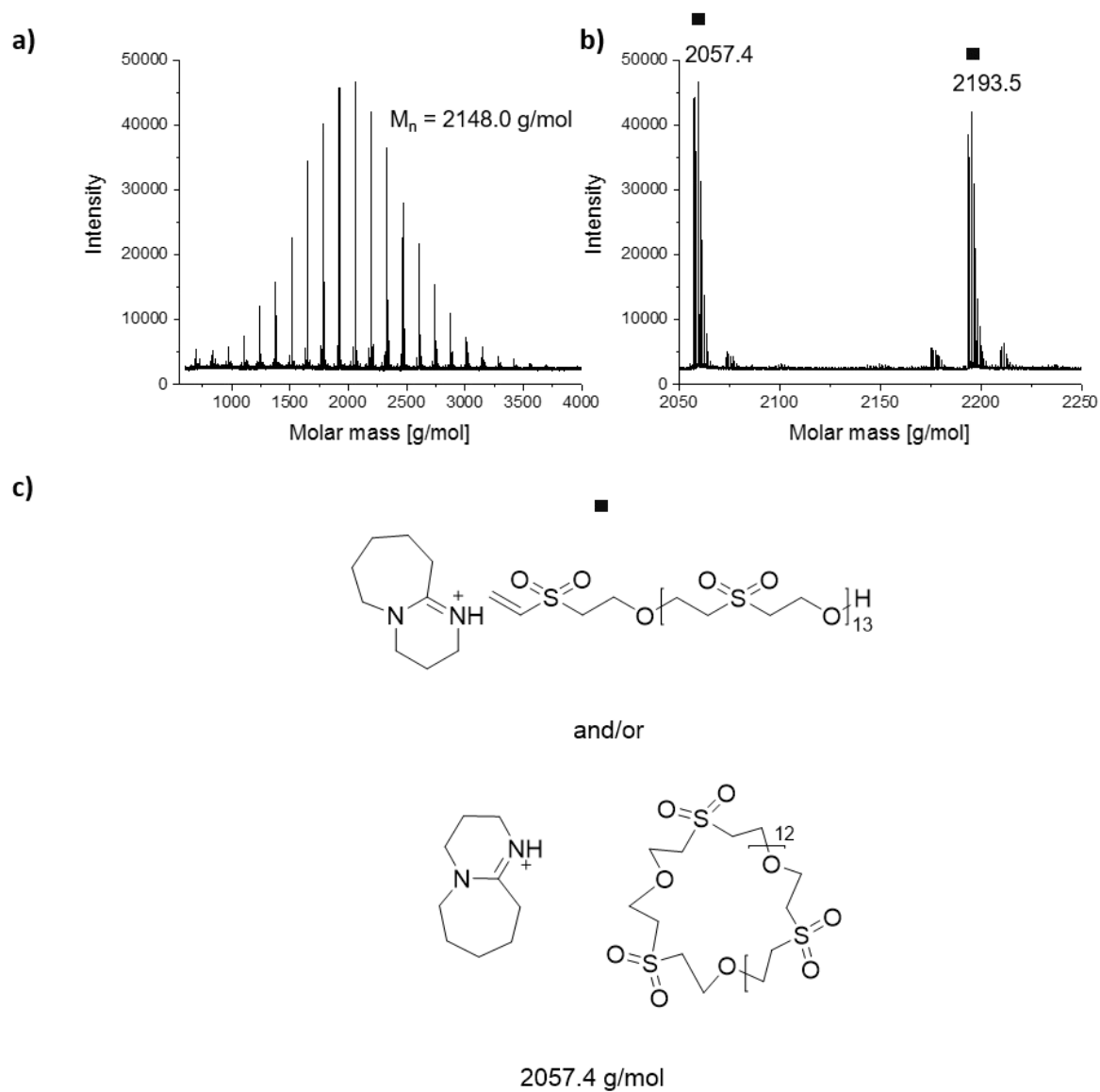


Figure S11: a) MALDI-ToF-spectrum of DBU-catalyzed polymer after 24 h; b) Enlarged section of the MALDI ToF-spectrum of DBU-catalyzed polymer after 24 h; c) potential chemical structures of detected species.

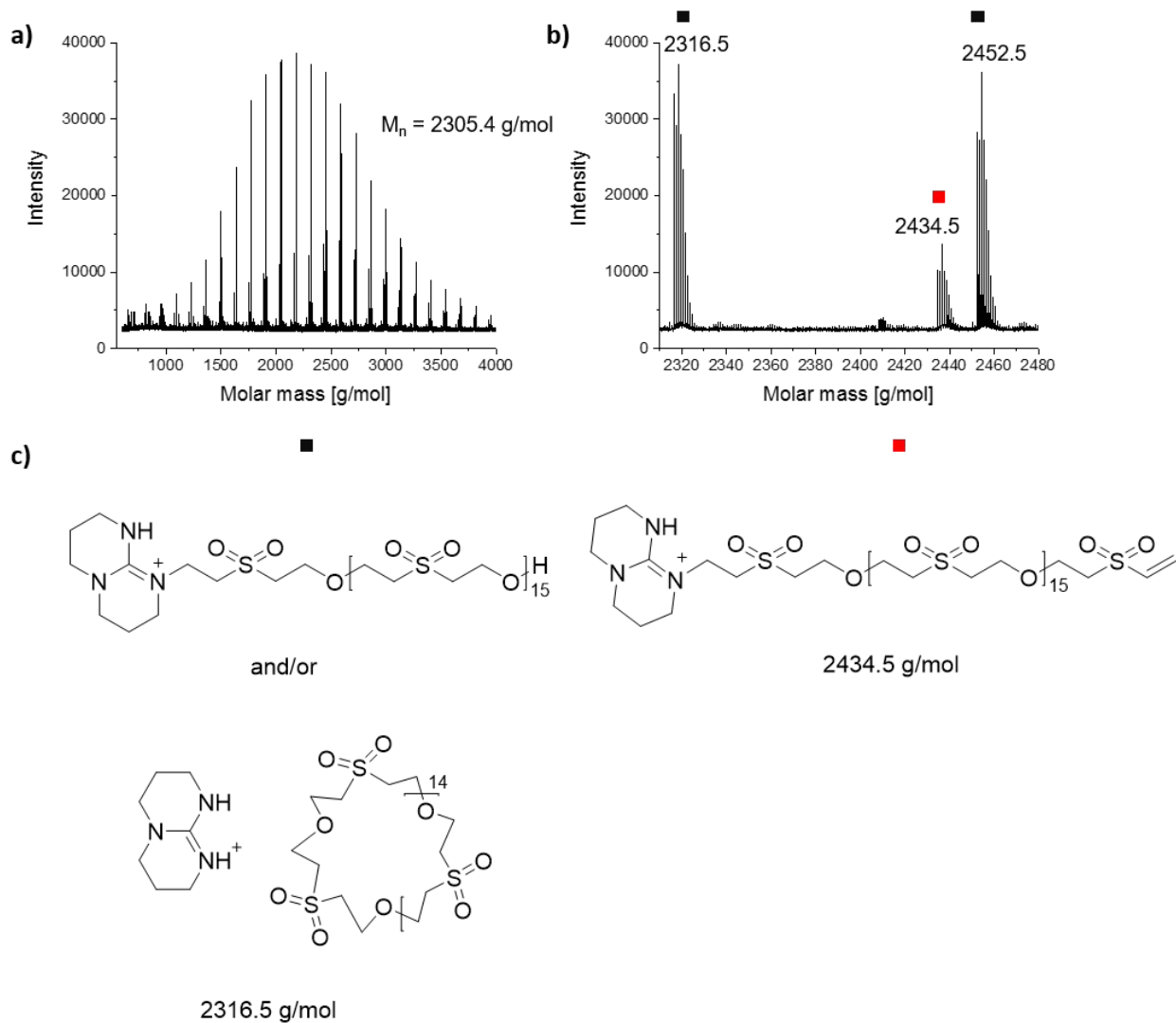


Figure S12: a) MALDI-ToF-spectrum of TBD-catalyzed polymer after 24 h; b) Enlarged section of the MALDI ToF-spectrum of TBD-catalyzed polymer after 24 h; c) potential chemical structures of detected species.

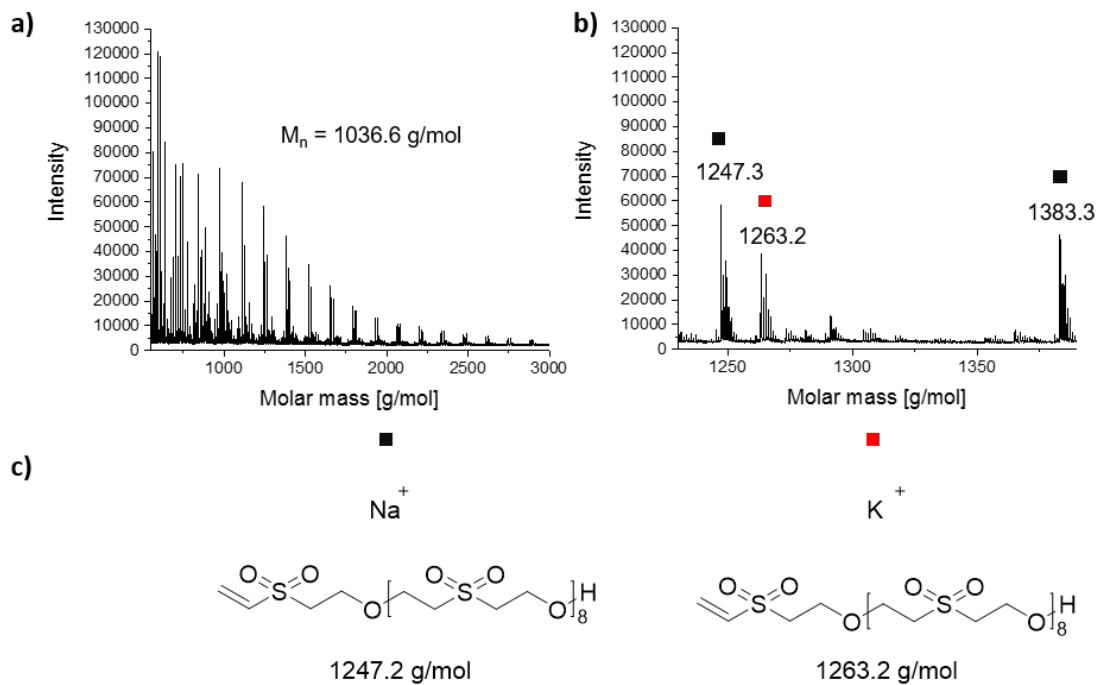


Figure S13: a) MALDI-ToF-spectrum of K_2CO_3 -catalyzed polymer after 24 h; b) Enlarged section of the MALDI ToF-spectrum of K_2CO_3 -catalyzed polymer after 24 h; c) potential chemical structures of detected species.

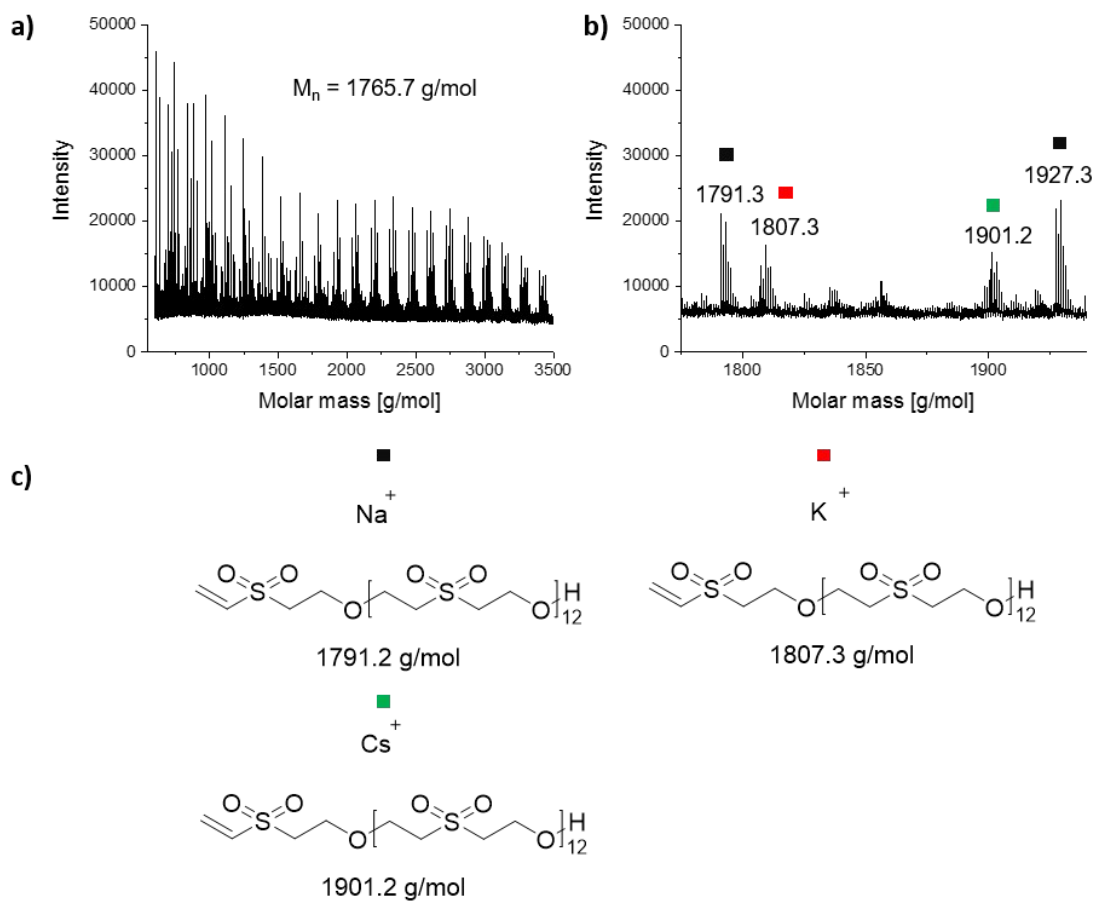


Figure S14: a) MALDI-ToF-spectrum of Cs₂CO₃-catalyzed polymer after 24 h; b) Enlarged section of the MALDI ToF-spectrum of Cs₂CO₃-catalyzed polymer after 24 h; c) potential chemical structures of detected species.

Purified Polymers (2nd batch)

Polymer P1 (PPh₃):

¹H-NMR (300 MHz, DMSO-d₆) δ [ppm] = 7.99 – 7.71 (m), 6.98 (dd, J = 16.6, 10.0 Hz), 6.31 – 6.17 (m), 5.08 (s), 3.81 (t, J = 5.2 Hz), 3.43 (t, J = 5.3 Hz).

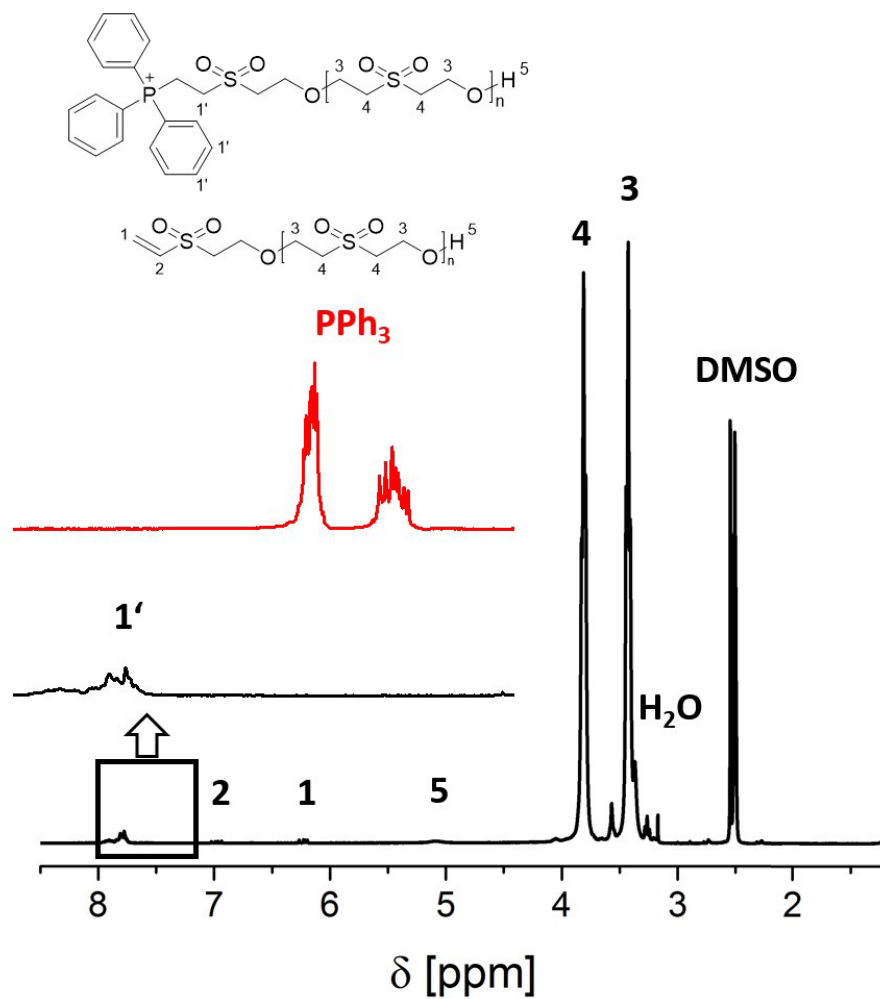


Figure S15: ¹H-NMR-spectrum (300 MHz, DMSO-d₆) of P1 (black) and PPh₃ (red).

MALDI-ToF-MS:

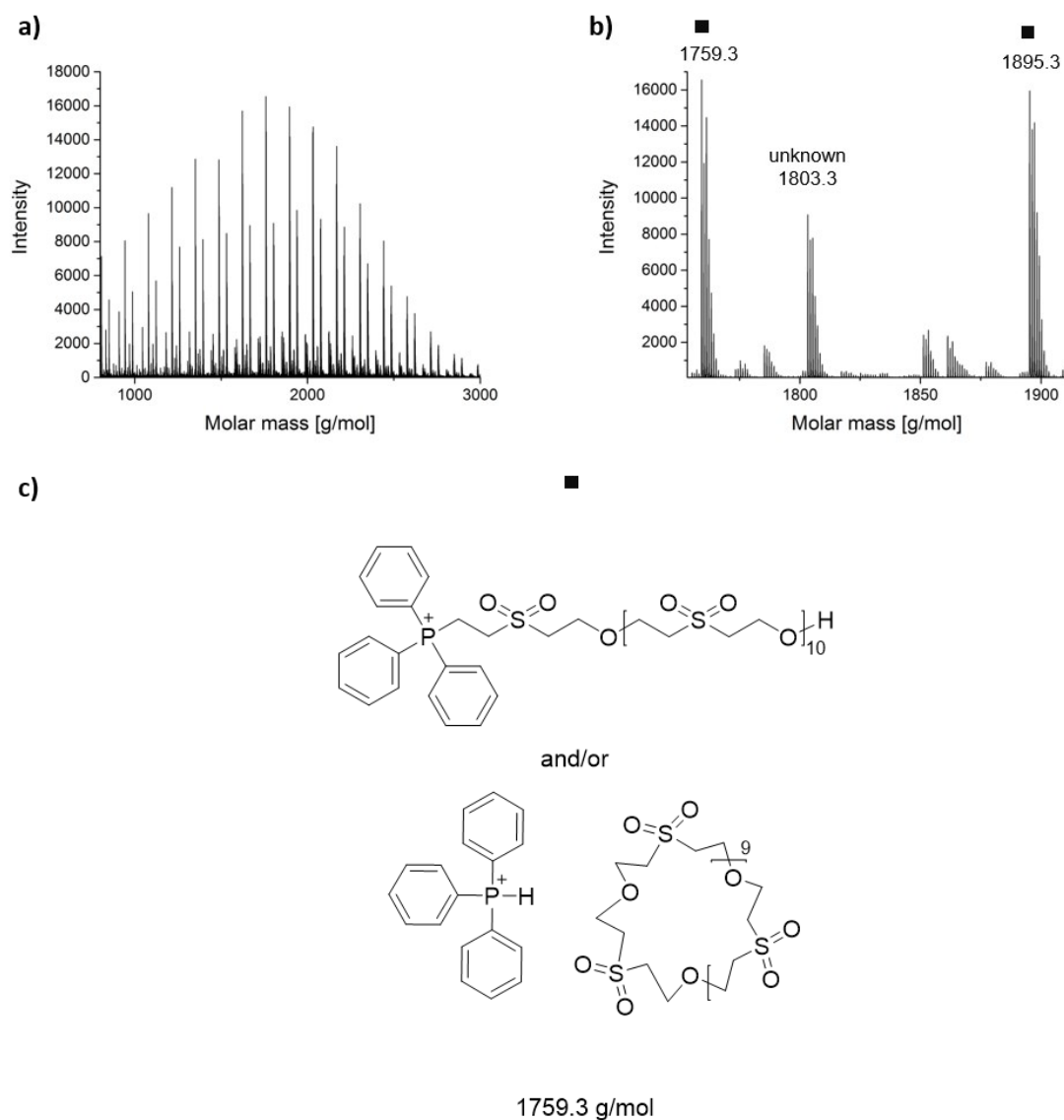


Figure S16: a) MALDI-ToF-spectrum of P1; b) Enlarged section of the MALDI ToF-spectrum of P1; c) potential chemical structures of detected species for P1 with consideration of the ^1H -NMR spectrum.

Polymer P2 (TEDA):

$^1\text{H-NMR}$ (300 MHz, DMSO-d_6) δ [ppm] = 6.98 (dd, $J = 16.6, 10.0$ Hz), 6.22 (dd, $J = 13.3, 8.0$ Hz), 5.09 (t, $J = 5.0$ Hz), 3.81 (t, $J = 5.2$ Hz), 3.43 (t, $J = 5.2$ Hz), 3.26 (t, $J = 5.8$ Hz), 3.05 (s).

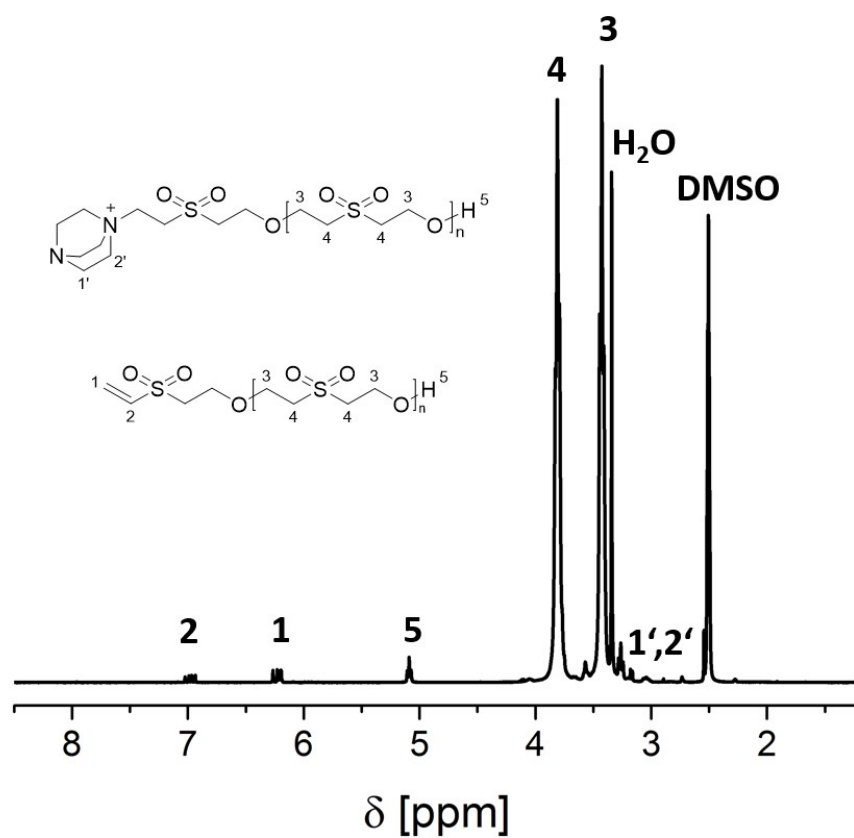


Figure S17: $^1\text{H-NMR}$ -spectrum (300 MHz, DMSO-d_6) of P2.

MALDI-ToF-MS:

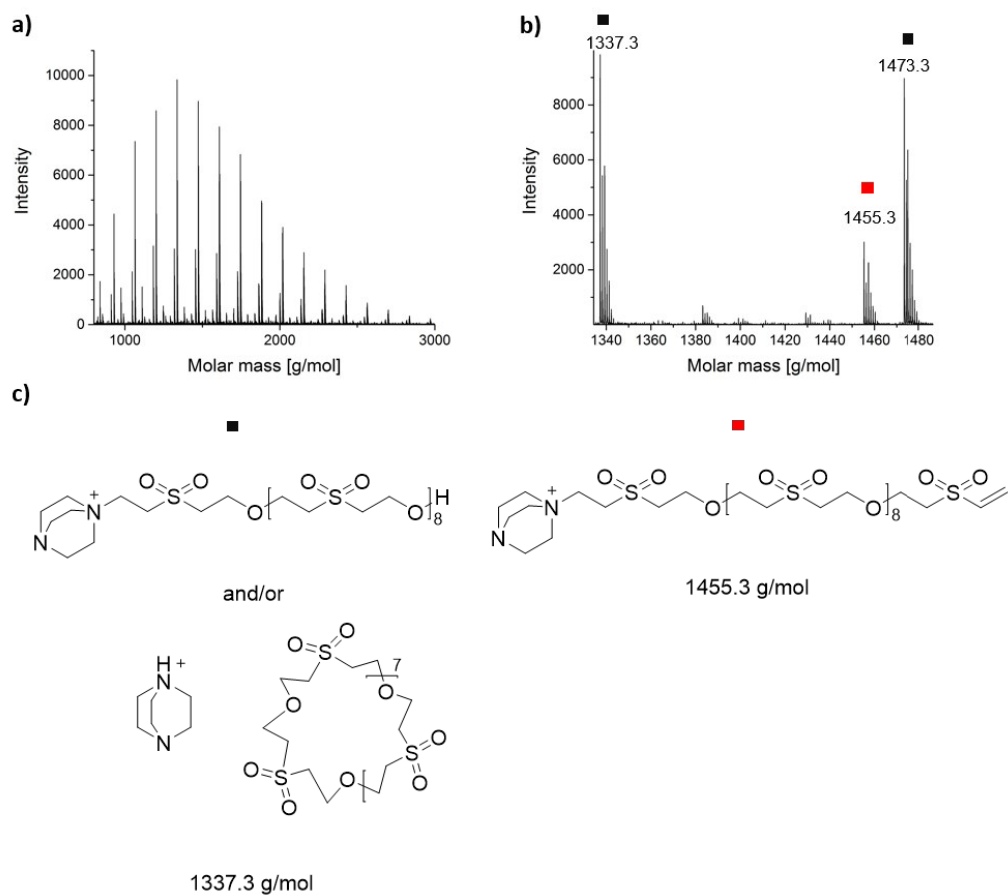


Figure S18: a) MALDI-ToF-spectrum of P2 b) Enlarged section of the MALDI ToF-spectrum of P3 c) potential chemical structures of detected species for P2 with consideration of the ^1H -NMR spectrum.

Polymer P3 (DMAP):

$^1\text{H-NMR}$ (300 MHz, DMSO-d_6): δ [ppm] = 8.28 (s), 7.08 – 6.89 (m), 6.22 (dd, $J = 13.3, 8.4$ Hz), 5.08 (t, $J = 5.0$ Hz), 3.80 (t, $J = 5.2$ Hz), 3.42 (t, $J = 5.2$ Hz).

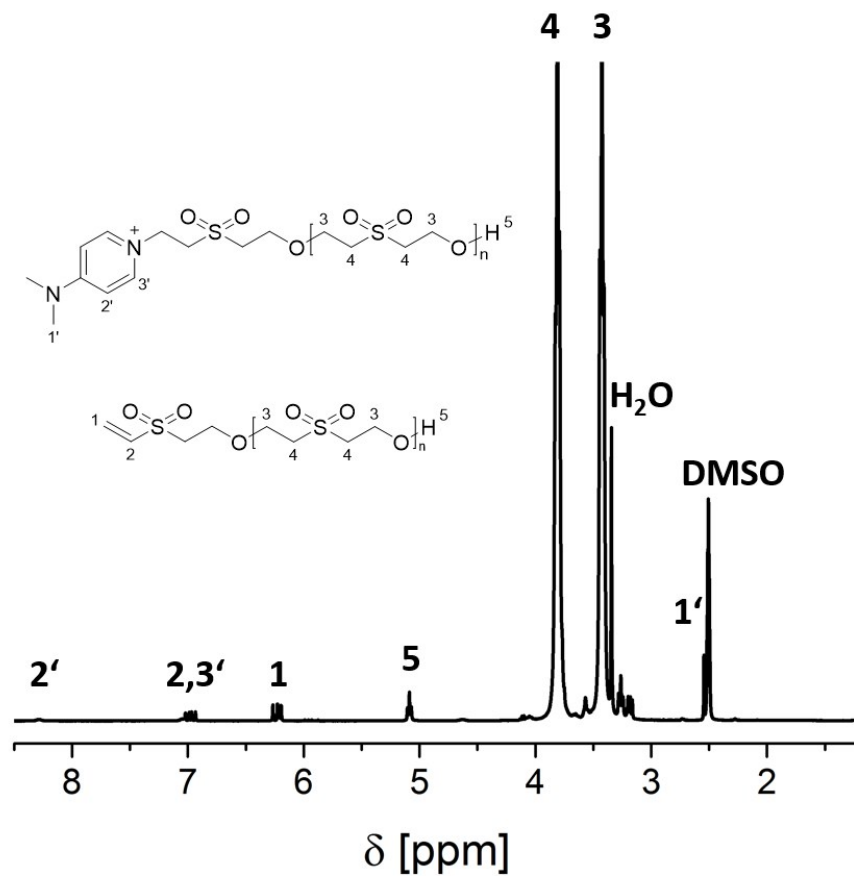


Figure S19: $^1\text{H-NMR}$ -spectrum (300 MHz, DMSO-d_6) of P3.

MALDI-ToF-MS:

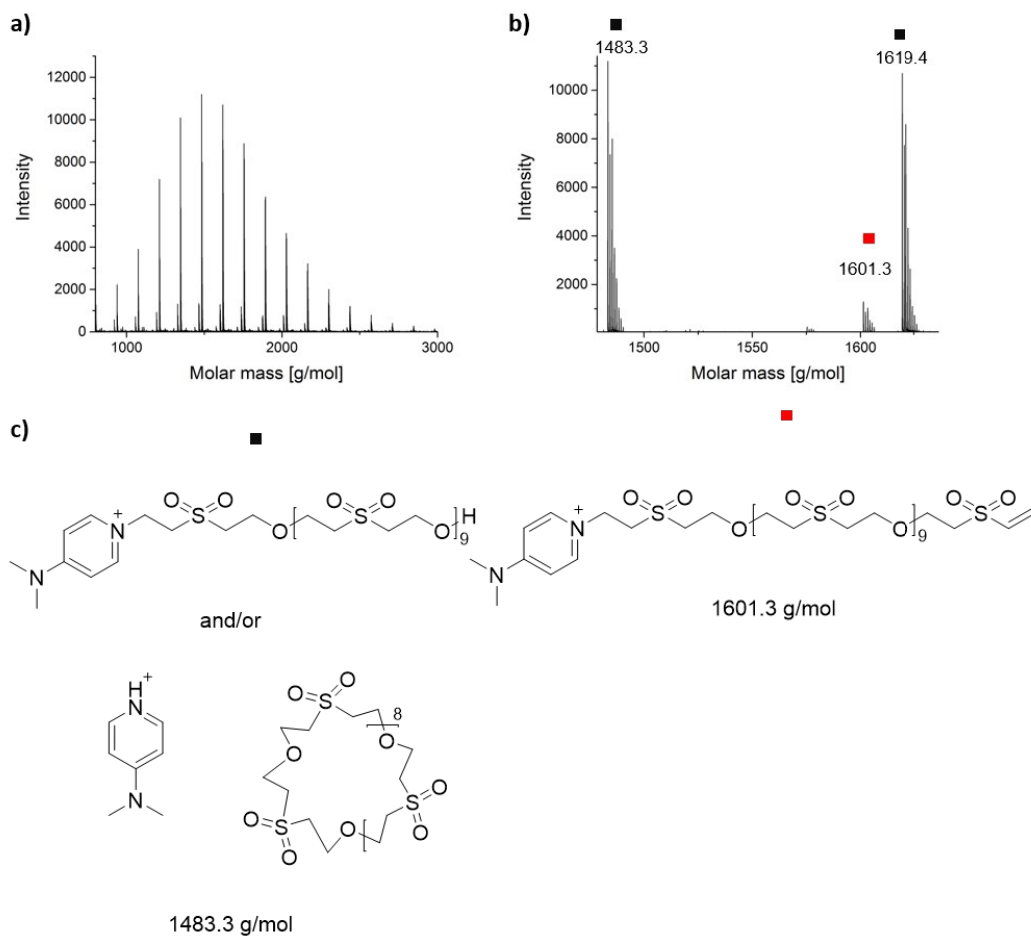


Figure S20: a) MALDI-ToF-spectrum of P3 b) Enlarged section of the MALDI ToF-spectrum of P3 c) potential chemical structures of detected species for P3 with consideration of the ^1H -NMR spectrum.

Polymer P4 (DBU):

$^1\text{H-NMR}$ (300 MHz, DMSO-d_6) δ [ppm] = 7.10 – 6.91 (m), 6.22 (dd, $J = 13.3, 8.1$ Hz), 5.09 (t, $J = 4.9$ Hz), 3.81 (t, $J = 5.2$ Hz), 3.43 (t, $J = 5.3$ Hz).

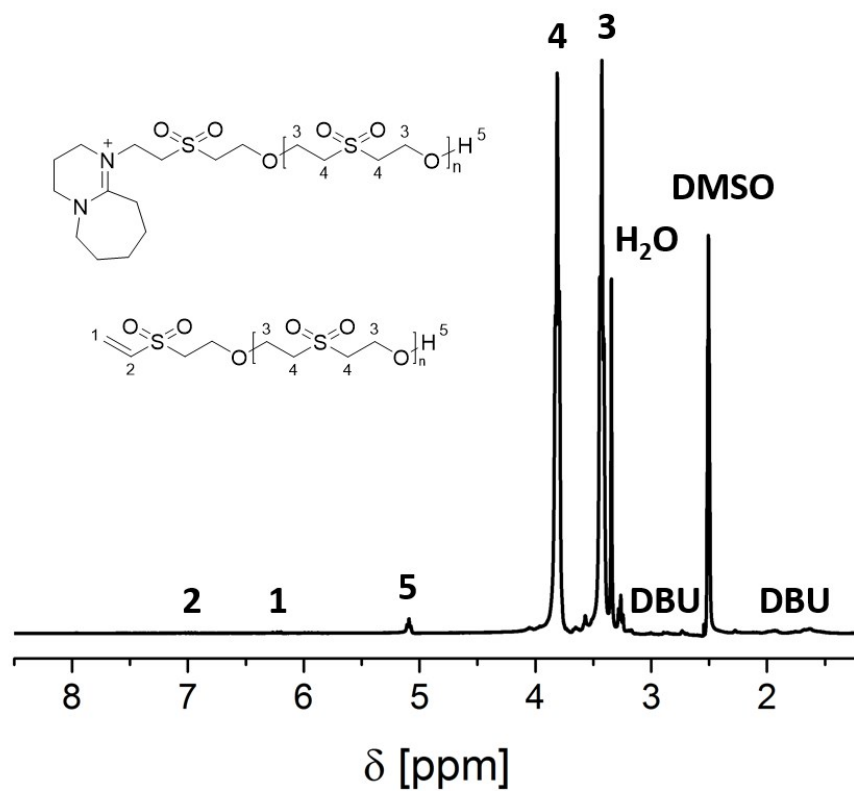


Figure S21: $^1\text{H-NMR}$ -spectrum (300 MHz, DMSO) of P4.

MALDI-ToF-MS:

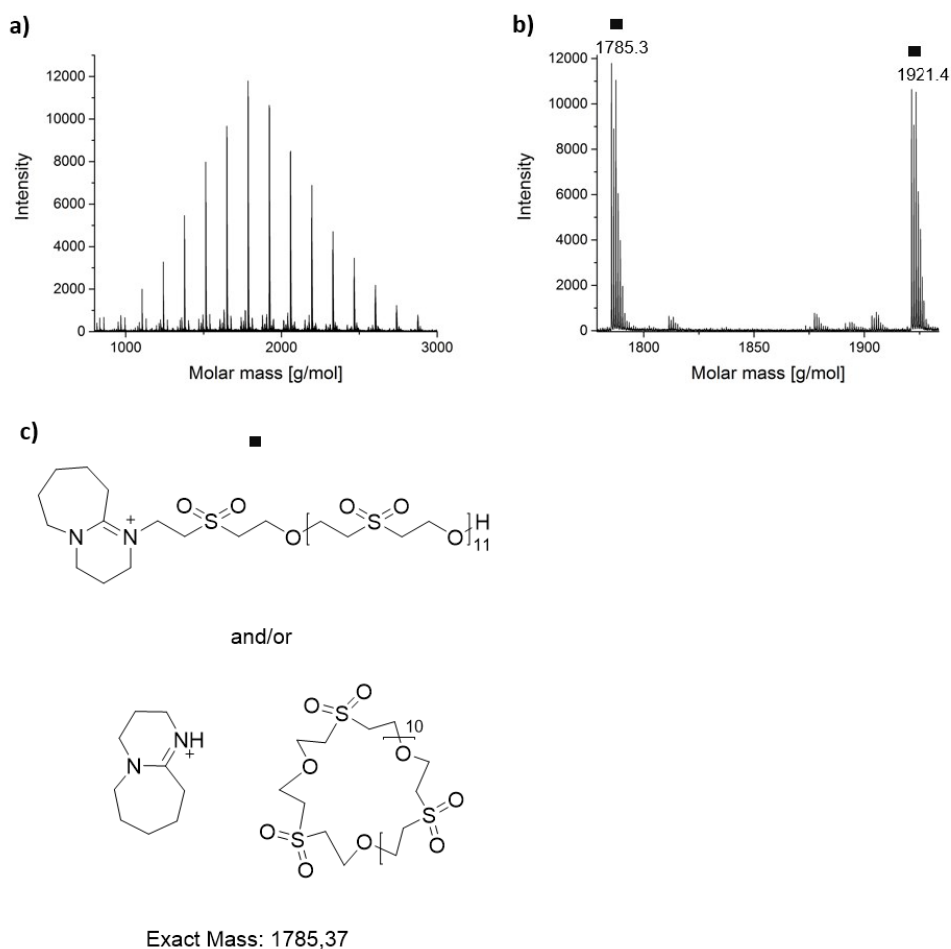


Figure S22: a) MALDI-ToF-spectrum of P4 b) Enlarged section of the MALDI ToF-spectrum of P4 c) potential chemical structures of detected species for P4 with consideration of the ^1H -NMR spectrum.

Polymer P5 (TBD):

$^1\text{H-NMR}$ (300 MHz, DMSO-d_6) δ [ppm] = 6.98 (dd, $J = 16.6, 9.9$ Hz), 6.22 (dd, $J = 13.3, 8.0$ Hz), 5.09 (s), 3.81 (t, $J = 5.1$ Hz), 3.43 (t, $J = 5.3$ Hz).

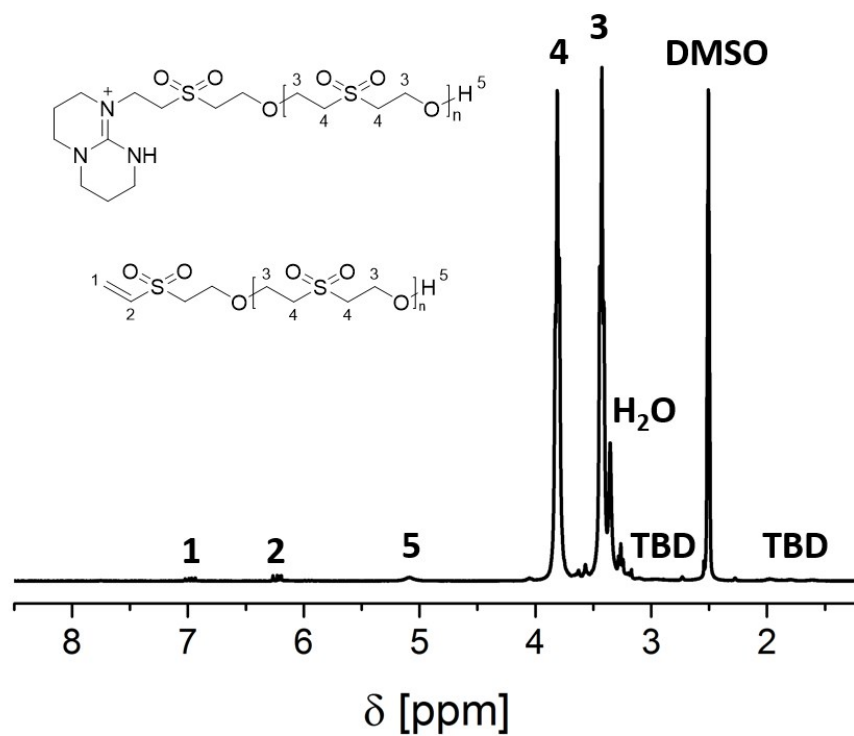


Figure S23: $^1\text{H-NMR}$ -spectrum (300 MHz, DMSO-d_6) of P5.

MALDI-ToF-MS:

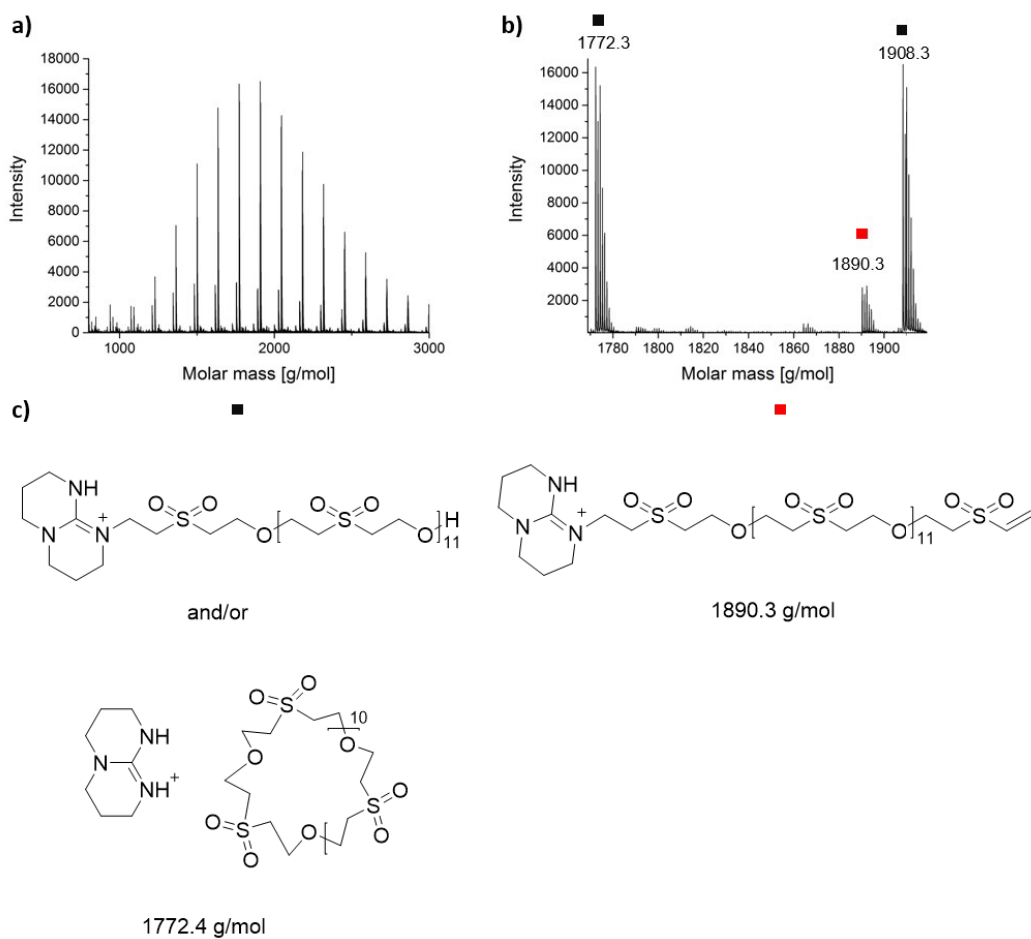


Figure S24: a) MALDI-ToF-spectrum of P5 b) Enlarged section of the MALDI ToF-spectrum of P5 c) potential chemical structures of detected species for P5 with consideration of the ^1H -NMR spectrum.

Polymer P6 (K₂CO₃):

¹H-NMR (300 MHz, DMSO-d₆) δ [ppm] = 6.98 (dd, J = 16.6, 10.0 Hz), 6.22 (dd, J = 13.3, 8.1 Hz), 5.09 (t, J = 4.9 Hz), 3.81 (t, J = 5.1 Hz), 3.43 (t, J = 5.1 Hz).

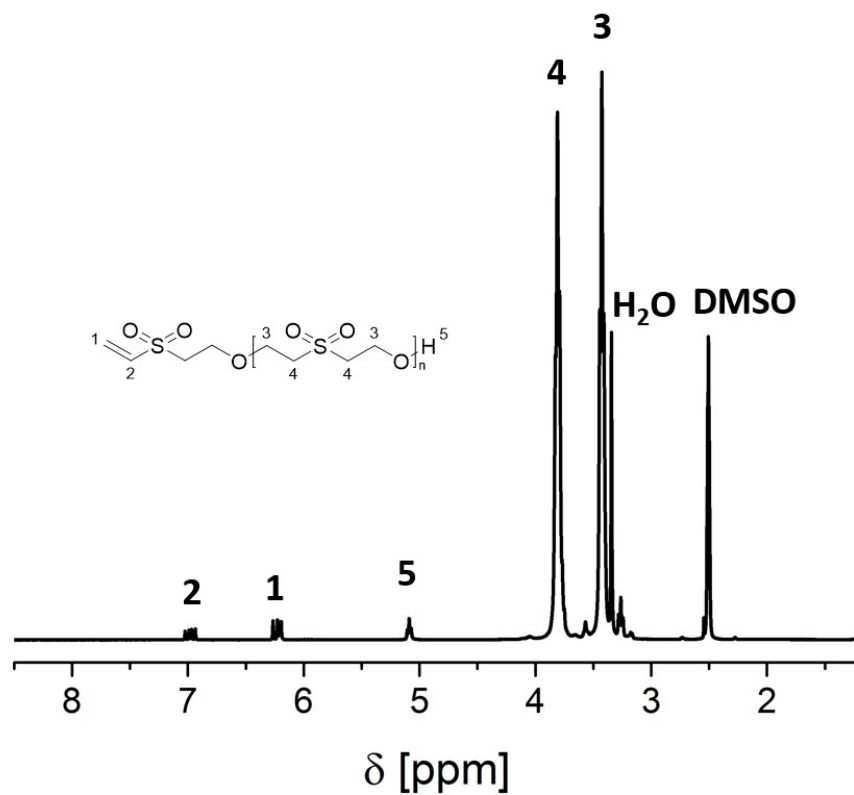


Figure S25: ¹H-NMR-spectrum (300 MHz, DMSO-d₆) of P6.

MALDI-ToF-MS:

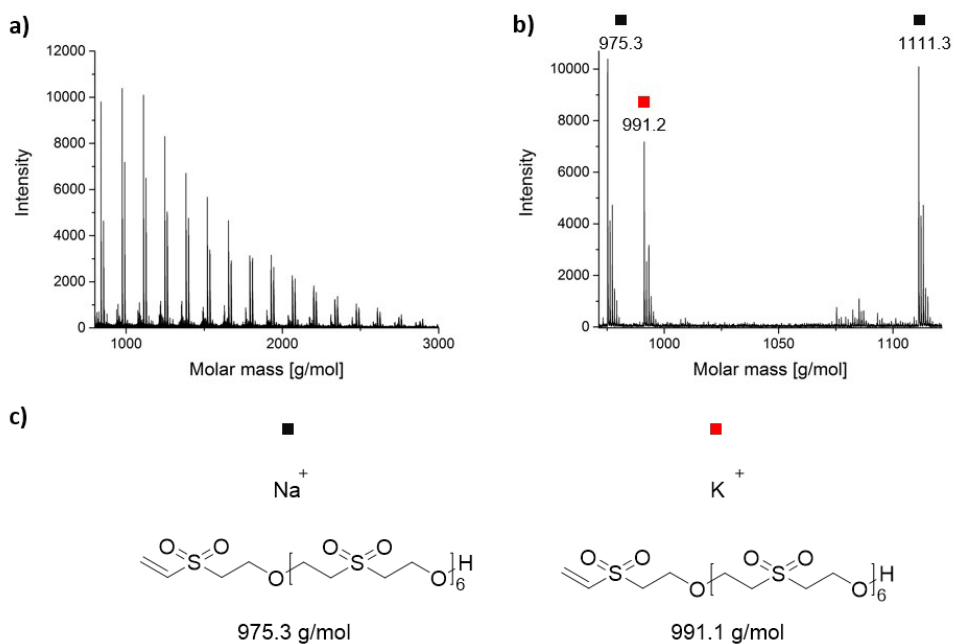


Figure S26: a) MALDI-ToF-spectrum of P6 b) Enlarged section of the MALDI ToF-spectrum of P6 c) potential chemical structures of detected species for P6.

Vapor pressure osmometry:

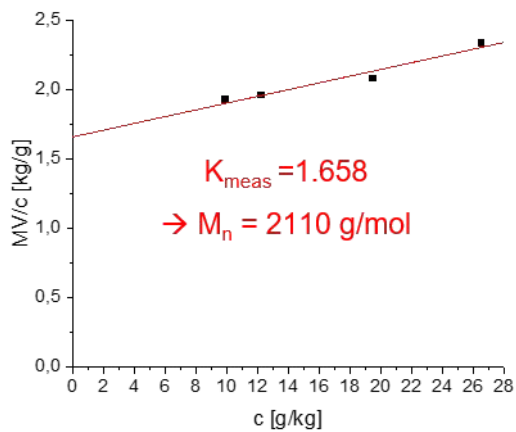


Figure S27: Plot of the vapor pressure osmometry measurement (PEG M_n = 2800 g/mol was used for the calibration)

Polymer P7 (Cs₂CO₃):

¹H-NMR (300 MHz, DMSO-d₆) δ [ppm] = 6.98 (dd, J = 16.6, 10.0 Hz), 6.22 (dd, J = 13.3, 8.0 Hz), 5.09 (t, J = 5.0 Hz), 3.81 (t, J = 5.2 Hz), 3.43 (t, J = 5.2 Hz).

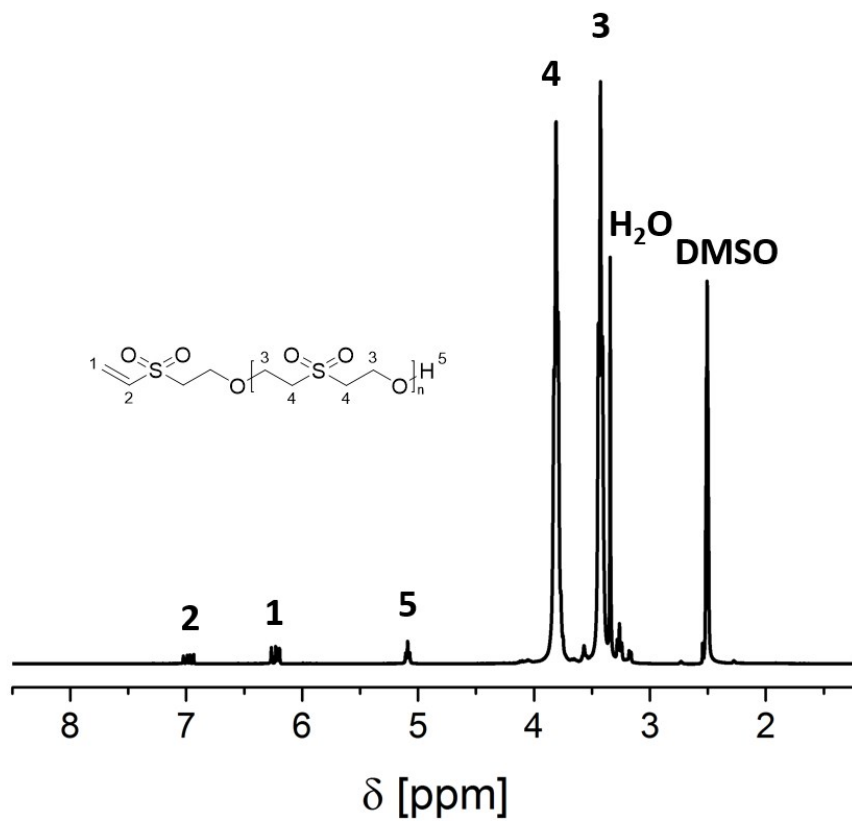


Figure S28: ¹H-NMR-spectrum (300 MHz, DMSO-d₆) of P7.

MALDI-ToF-MS:

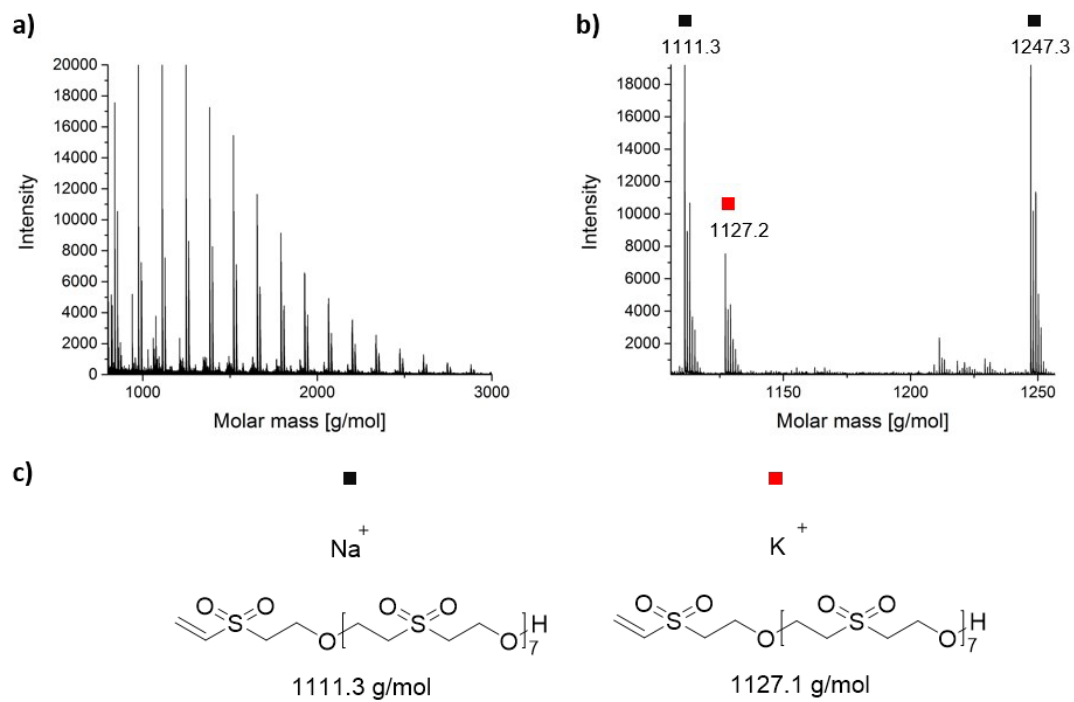


Figure S29: a) MALDI-ToF-spectrum of P7 b) Enlarged section of the MALDI ToF-spectrum of P7 c) potential chemical structures of detected species for P7.

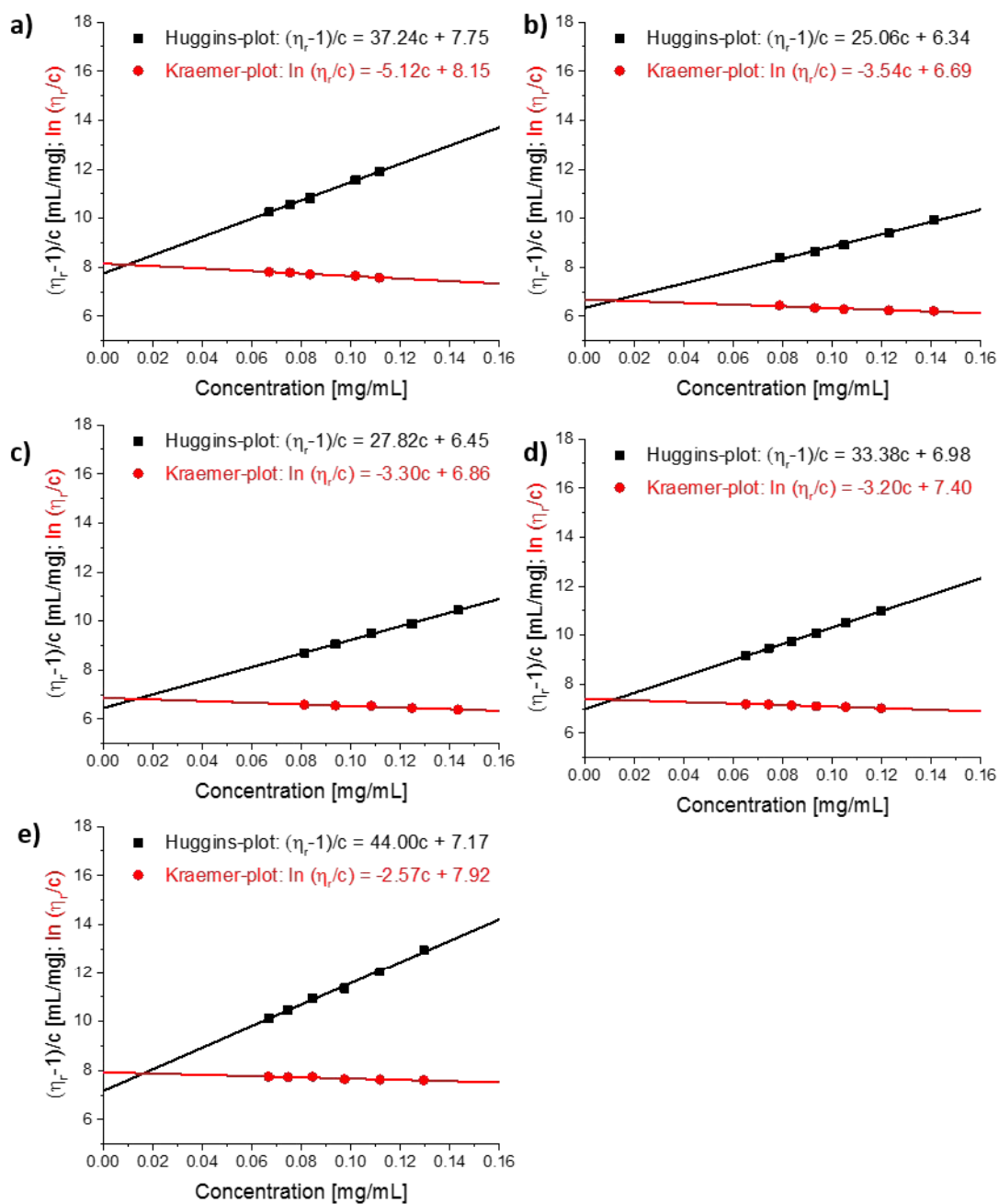


Figure S30: Huggins (black dots and line) and Kraemer (red dots and line) plots for the viscosity measurements of different concentrations of a) P1 b) P2 c) P3 d) P4 e) P5 in DMSO.

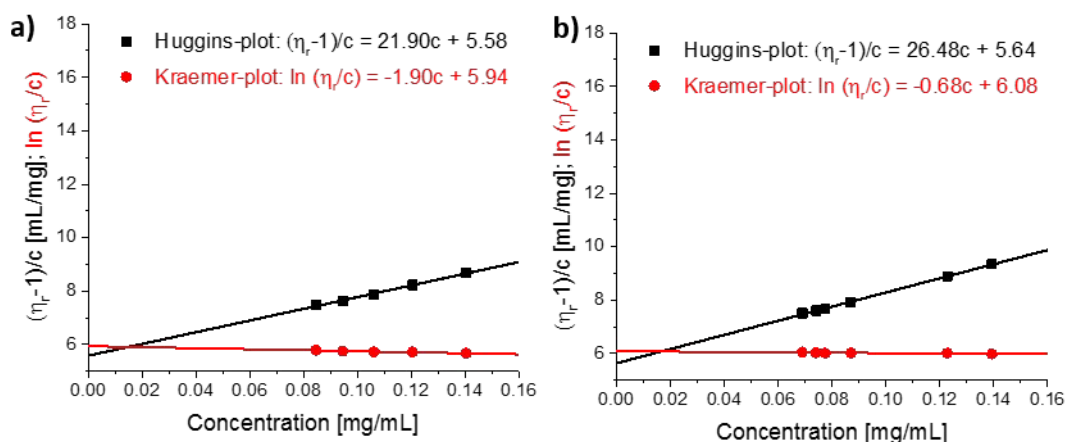


Figure S31: Huggins (black dots and line) and Kraemer (red dots and line) plots for the viscosity measurements of different concentrations of a) P6 b) P7 in DMSO.

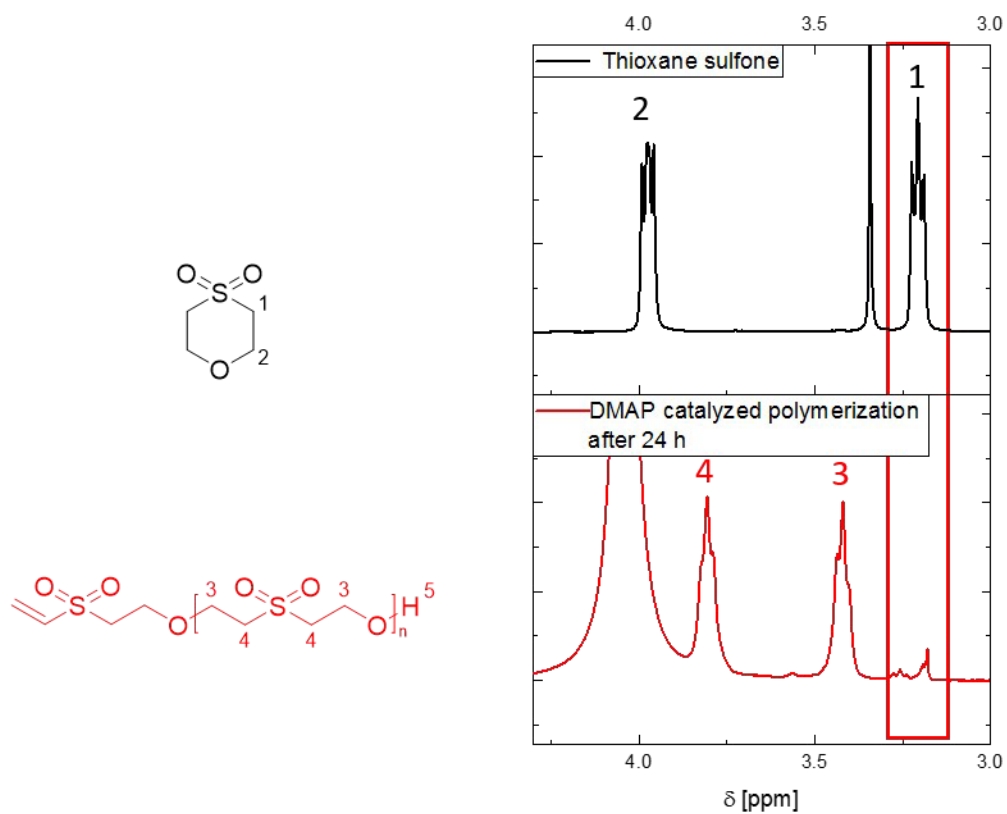
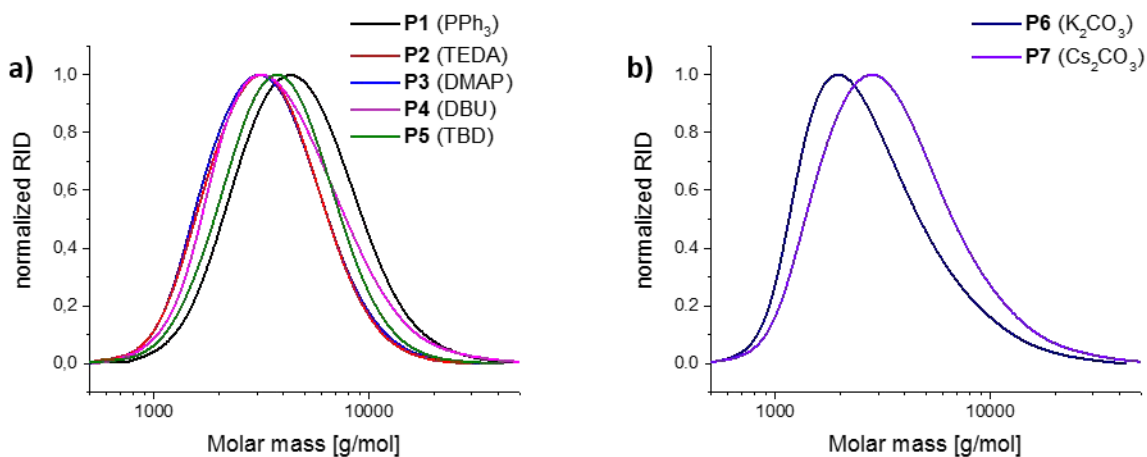


Figure S32: $^1\text{H-NMR}$ (300 MHz, DMSO-d_6) spectra of thioxane sulfone and the kinetic sample of the DMAP- catalyzed polymerization after 24 h.

Table S5: SEC-data and thermal properties of the purified polymers.

Polymer	M_n (SEC) [g/mol] ^a	\bar{D} ^a	M_n (MALDI) [g/mol] ^b	5% mass loss [°C] ^c	5% mass loss [°C] ^d	T_g [°C] ^e
P1	3750	1.49	1890	213	213	13.6
P2	2750	1.40	1790	295	281	14.5
P3	2750	1.41	1680	265	261	10.3
P4	3120	1.40	2080	217	217	21.7
P5	3200	1.56	2230	217	224	18.6
P6	2230 (2110) ^f	1.56	1780	310	298	17.1
P7	2730	1.64	1680	318	313	12.6

^a SEC (DMAc (+ 0.21 wt.% LiCl), PEG standards); ^b Determination from MALDI-ToF-spectra; ^c Determination from TGA measurements (N_2); ^d Determination from TGA measurements (Air); ^e Determination from DSC measurements; ^f the absolute M_n for P6 was exemplarily determined by vapor pressure osmometry.

**Figure S33: SEC (DMAc (+ 0.21 wt.% LiCl), PEG standards) traces of the purified polymers a) P1-P5 and b) P6/P7.**

Solution-polymerization

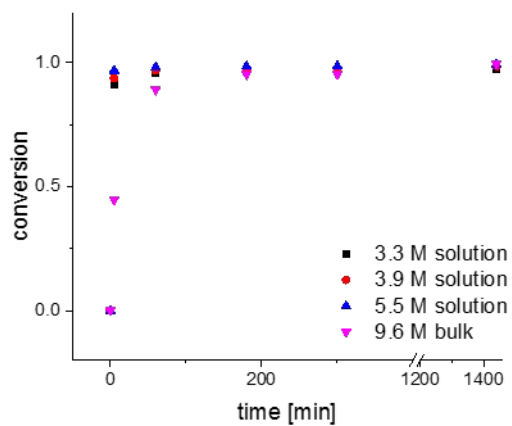


Figure S34: Conversion vs. reaction time for polymerizations with different monomer concentrations (catalyst: DBU)

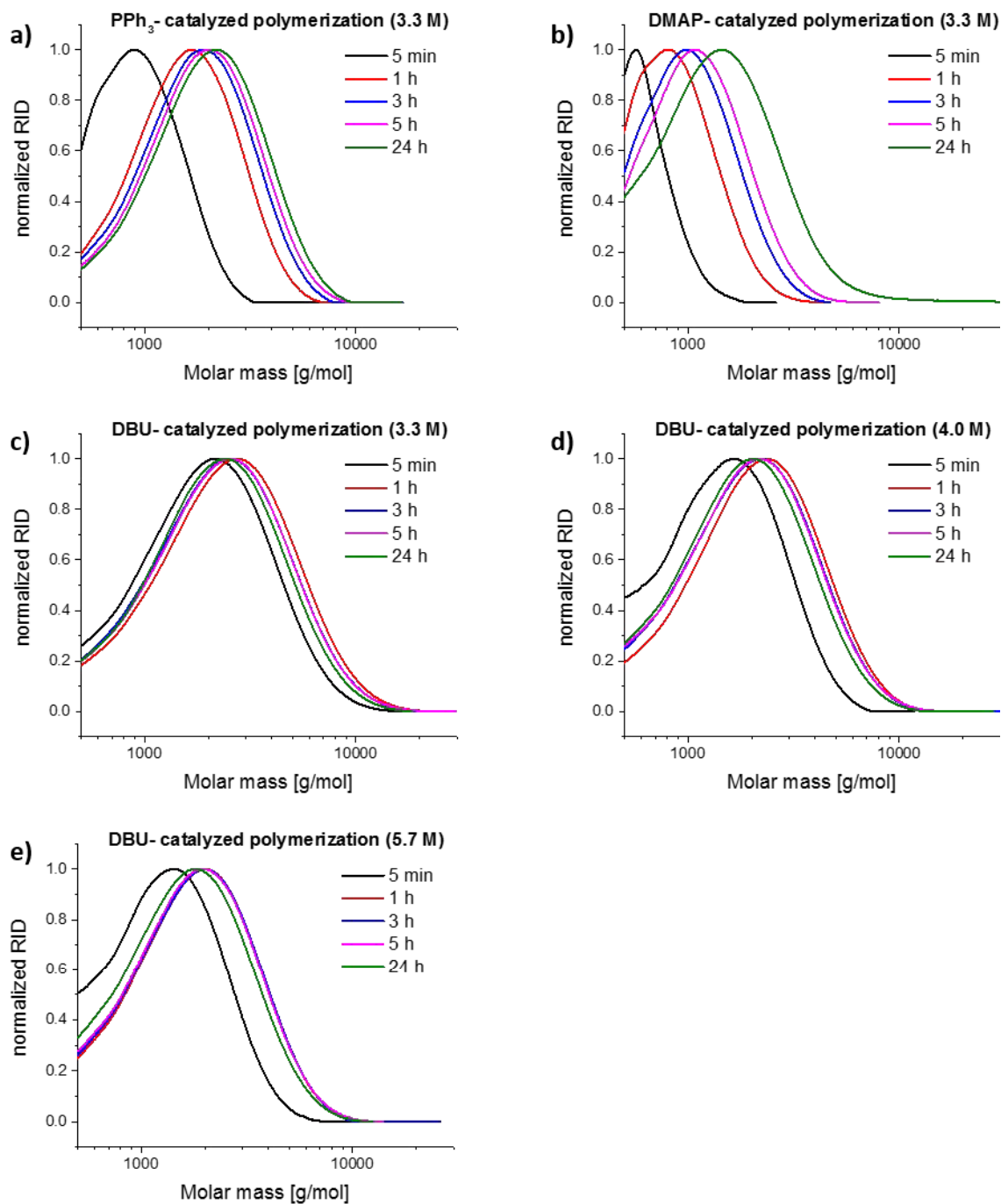


Figure S35: SEC (DMAc (+ 0.21 wt.% LiCl), PEG standards) traces of the kinetic samples taken after 5 min, 1 h, 3 h and 24 h of the polymerization catalyzed with a) PPh₃ (3.3 M) b) DMAP (3.3 M), c) DBU (3.3 M), d) DBU (4.0 M), e) DBU (5.7 M) in DMSO.

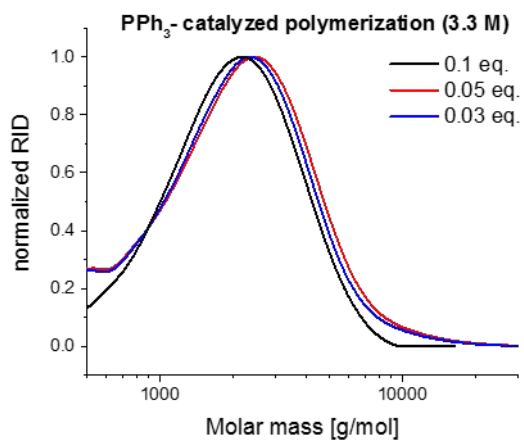


Figure S36: SEC (DMAc (+ 0.21 wt.% LiCl), PEG standards) traces of the kinetic samples taken after 24 h of the polymerization catalyzed with PPh₃ in DMSO.

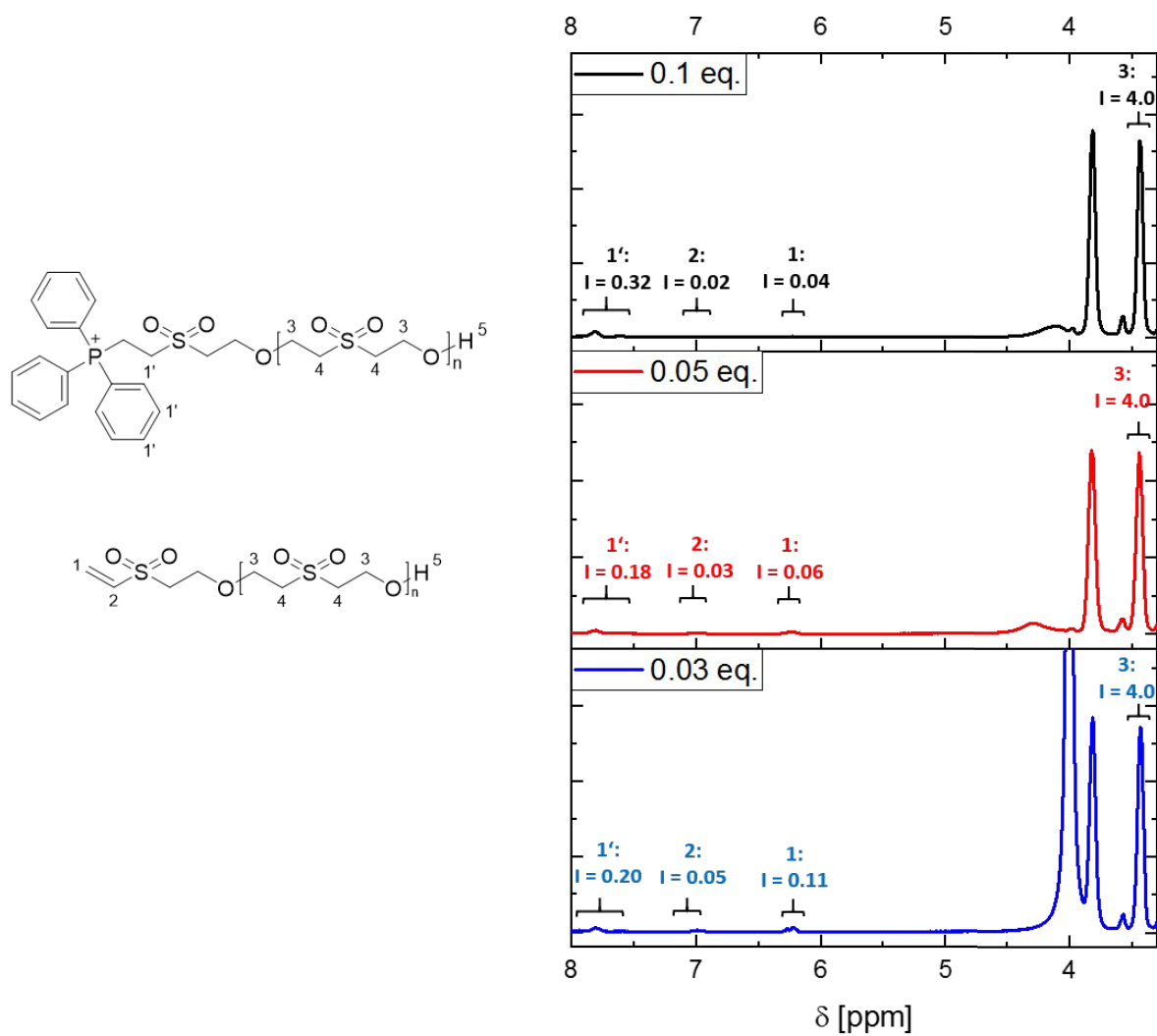


Figure S37: $^1\text{H-NMR}$ (300 MHz, DMSO-d_6) spectra of the PPh_3 - catalyzed polymers with different amounts of PPh_3 after precipitation.

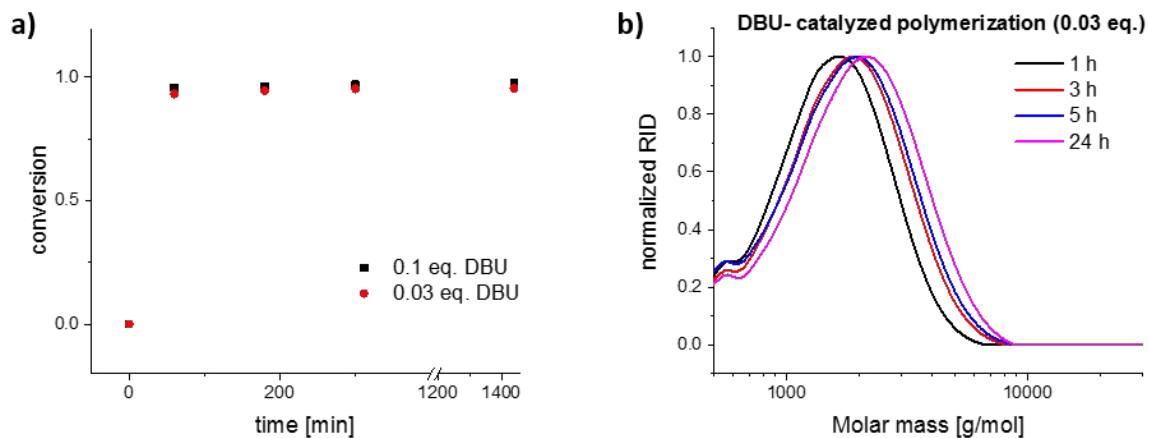


Figure S38: a) Conversion vs. reaction time for different polymerizations: comparison of different amount of catalyst (catalyst: DBU) b) SEC (DMAc (+ 0.21 wt.% LiCl), PEG standards) traces of the kinetic samples taken after 1 h, 3 h and 24 h of the polymerization catalyzed with 0.03 eq. DBU in DMSO.

Thermal properties of the polymers

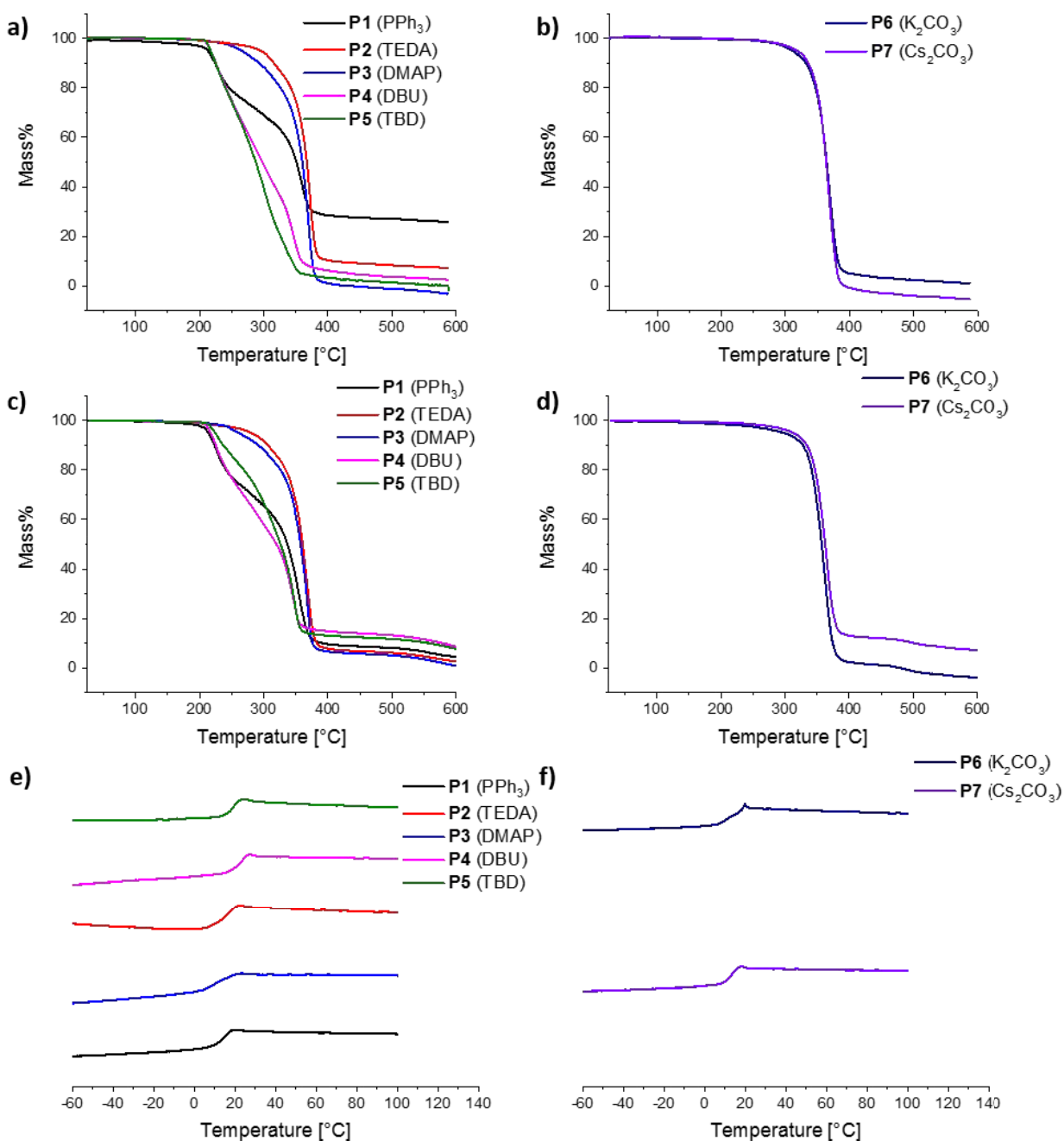


Figure S39: a) TGA-data of the polymers P1-P5 (N₂) b) TGA-data of the polymers P6/P7 (N₂) c) TGA-data of the polymers P1-P5 (Air) d) TGA-data of the polymers P6/P7 (Air) e) DSC-data of the polymers P1-P5 f) DSC-data of the polymers P6/P7.

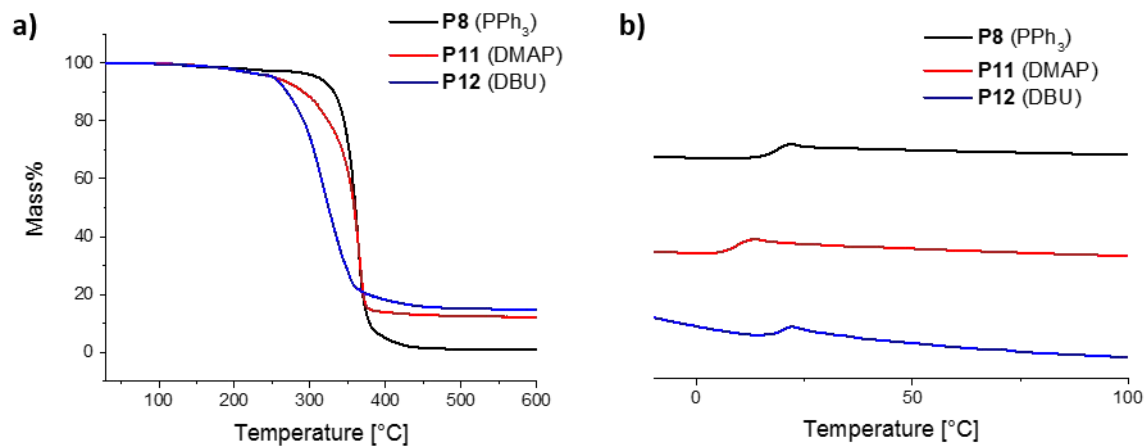


Figure S40: a) TGA-data of the polymers P8/11/12 (N₂) b) DSC-data of the polymers P8/11/12.

Table S6: SEC-data and thermal properties of the purified polymers.

Polymer	5% mass loss [°C] ^b	T _g [°C] ^d
P8	311	17.8
P11	253	9.2
P12	252	18.2

^a Determination from TGA measurements (N₂) ^b Determination from DSC measurements.

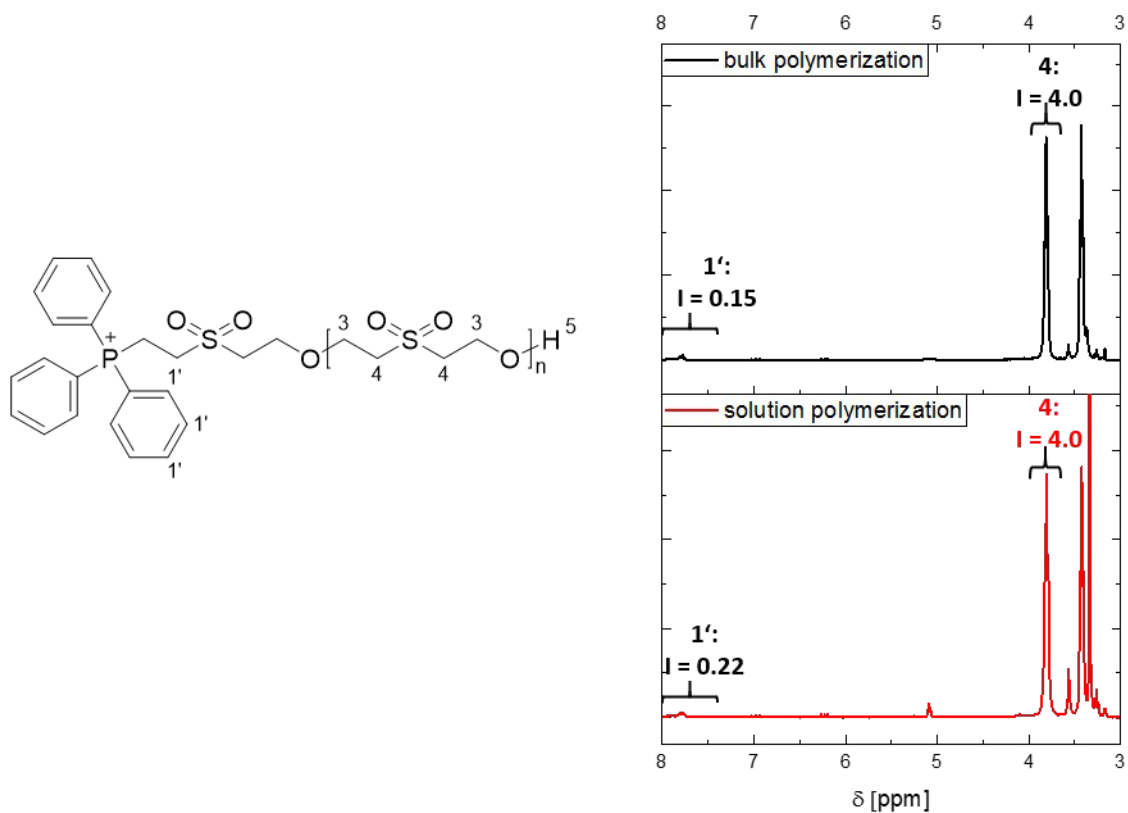


Figure S41: $^1\text{H-NMR}$ (300 MHz, DMSO-d_6) spectra of the PPh_3 - catalyzed polymers *via* bulk- and solution polymerization after precipitation.

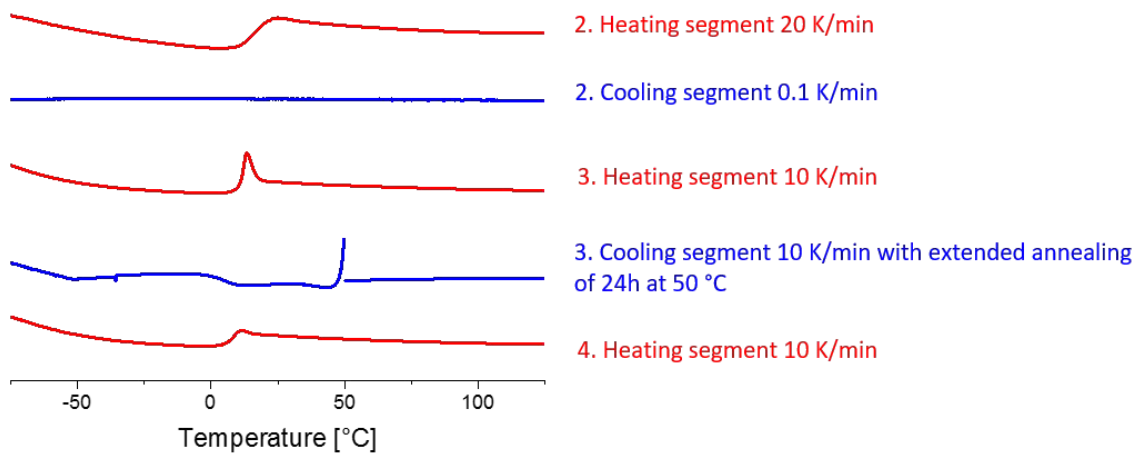


Figure S42: DSC-traces of P1 with different heating and cooling rates.

Appendix 2

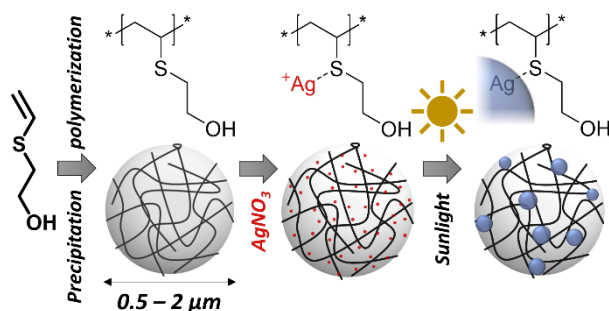
Publication P3

Note: Publication P3 was accepted by Macromol. Chem. Phys. in the meantime and published in the following form:

Publication P3

Coordination of noble metals in poly(vinyl mercaptoethanol) particles prepared by precipitation/emulsion polymerization

N. Ziegenbalg, H. F. Ulrich, S. Stumpf, P. Mueller, J. Wiethan, J. Danner, U. S. Schubert, T. Adermann, J. C. Brendel, *Macromol. Chem. Phys.* **2023**, 224, 2200379.



Reproduced by permissions of Jons Wiley and Sons. Copyright 2023.

The paper as well as the supporting information is available online:

doi.org/10.1002/macp.202200379

Coordination of Noble Metals in Poly(vinyl mercaptoethanol) Particles Prepared by Precipitation/Emulsion Polymerization

Nicole Ziegenbalg, Hans F. Ulrich, Steffi Stumpf, Philipp Mueller, Jürgen Wiethan, Janette Danner, Ulrich S. Schubert, Torben Adermann, and Johannes C. Brendel*

S-Vinyl monomers react readily in radical polymerizations resulting in polymers with interesting features such as enhanced refractive indices, increased thermal stability, or the ability to coordinate various metals. Among them, vinyl mercaptoethanol (VME) can be produced in industrial scale, but the poor solubility of the resulting homopolymer limits its application. In this contribution, polymerizations of the monomer are investigated in water forming a heterogeneous system. The good solubility of the monomer in water imparts the system with mixed characteristics between a precipitation and an emulsion polymerization. Evaluating various surfactants, only polyvinyl alcohol (PVA) is found to create stable dispersions, although micrometer-sized particles are formed with a broad size distribution. Nevertheless, the particles are able to coordinate silver or gold ions. Attempts to reduce the noble metal ions by commercial reducing agents fail. However, exposure to sunlight unexpectedly results in a controlled reduction of the metal ions and the formation of composite particles. Silver ion-containing dispersions demonstrate strong antibacterial properties, while the effect is diminished in the corresponding composite. Overall, the precipitation/emulsion polymerization of VME represents a promising pathway to stable sulfur-rich polymer dispersions with the ability to coordinate metal ions or form reactive metal composites.

precipitation^[8,9] polymerizations are often preferred over homogeneous polymerization techniques (bulk or solution polymerization).^[10] In particular, water-based reaction media are used, since they offer the benefit of good heat dissipation, are environmentally benign, and cause only low costs. Furthermore, polymers with higher molar mass and faster polymerization rates can be obtained due to the confinement of the active radicals.^[11–13] In addition, there is the possibility to produce micro- and nanoscale-sized particles and materials instantaneously. The properties of the resulting suspensions or dispersions can be altered by varying the particle size, particle surface chemistry or their composition.^[14–16] Such particles are used, for example, as paints,^[17] coatings,^[18,19] adhesives,^[20] or imprinted polymers.^[21–23]

Such polymer particles can also be used as a host matrix for the coordination of metal salts or nanoparticles, which either allow to introduce additional functionality into the polymers or guarantee stabilization of the metal particles preventing clustering and aggregation.^[24–27] These composites

are commonly prepared in two different ways which are referred to as in situ or ex situ method. In the first, an existing polymer is modified with metal ions or metal nanoparticles, while in the ex situ variant the monomer is polymerized in the presence of the

1. Introduction

In large-scale production, heterogeneous radical polymerization techniques such as emulsion,^[1–6] suspension,^[7] or

N. Ziegenbalg, H. F. Ulrich, S. Stumpf, U. S. Schubert, J. C. Brendel
 Laboratory of Organic and Macromolecular Chemistry (IOMC)
 Friedrich Schiller University Jena
 Humboldtstraße 10, 07743 Jena, Germany
 E-mail: johannes.brendel@uni-jena.de

N. Ziegenbalg, H. F. Ulrich, S. Stumpf, U. S. Schubert, J. C. Brendel
 Jena Center for Soft Matter (JCSM)
 Friedrich Schiller University Jena
 Philosophenweg 7, 07743 Jena, Germany
 P. Mueller, T. Adermann
 BASF SE
 Carl-Bosch-Straße 38, 67056 Ludwigshafen, Rhein Germany
 J. Wiethan, J. Danner
 BASF Grenzach GmbH
 Koechlinstraße 1, 79639 Grenzach-Wyhlen, Germany

The ORCID identification number(s) for the author(s) of this article can be found under <https://doi.org/10.1002/macp.202200379>

© 2023 The Authors. Macromolecular Chemistry and Physics published by Wiley-VCH GmbH. This is an open access article under the terms of the Creative Commons Attribution-NonCommercial License, which permits use, distribution and reproduction in any medium, provided the original work is properly cited and is not used for commercial purposes.

DOI: 10.1002/macp.202200379

nanoparticles or metal salts.^[28] In any case, functional groups are required within the monomers or polymers that feature a high affinity for the corresponding metals. In particular, sulfur-containing polymers have raised considerable attraction,^[29,30] and they have a high affinity to noble metals such as silver, gold, platinum, but also other metals.^[31–35] Many literature examples are based on polymers comprising sulfonates,^[36] thiolates,^[37] thiols,^[38–43] or thioether groups,^[38,44] which coordinate well with these metals. More recently inverse vulcanization using elemental sulfur has raised increasing attention to create sulfur-rich polymers,^[45–47] which can further be modified with metal nanoparticles.^[48–51] Aqueous dispersions of materials with high sulfur content are often based on ring opening polymerizations or step growth polymerizations.^[52–54] Interestingly, aqueous emulsion, precipitation, or dispersion polymerizations of thioether-containing vinyl monomers have so far scarcely been reported in literature, despite the industrial relevance of the processes and the convenient access to ready dispersions.^[55,56] In particular, vinyl sulfides should enable access to polymers with high sulfur content by corresponding radical polymerization techniques,^[57] but to the best of our knowledge no dispersion processes based on these monomers have been reported, yet. Keeping the potential in mind to create stable dispersions of sulfur-rich polymers in a straightforward and scalable process, we here aimed at establishing suitable conditions for the heterogeneous polymerization of vinyl mercaptoethanol (VME) as an industrially available *S*-vinyl monomer. In this regard, peculiarities of these monomers have to be kept in mind, such as the sensitivity to oxidants,^[58] but once suitable conditions are established they could be transferred and applied to other vinyl sulfides.

VME has a similar reactivity as (meth)acrylates, but in comparison the vinyl group is considered electron rich.^[59] Unfortunately, the low solubility of the polymer severely limits any possible applications. Establishing suitable conditions for heterogeneous polymerization processes has, therefore, further potential to circumvent this issue and create a processible material. The monomer itself is fully miscible with water up to a concentration of 105.5 g L⁻¹ (at 20 °C), which differs from common monomers used in emulsion polymerizations. Consequently, polymerization in an aqueous system might feature more characteristics of a precipitation polymerization, although features of an emulsion system might still prevail at sufficient monomer concentrations. Since only limited information was available on heterogeneous processes using such monomers, we first investigated different stabilizing agents and different monomer concentrations. Their influence on possible coagulation of the particles was evaluated and kinetics of the polymerization were analyzed. As a first proof of concept, we further extended the study to test a potential coordination of silver and gold ions within the resulting particles and the subsequent formation of nanocomposites by reduction of the coordinated ions. With regard to potential applications, such silver nanocomposites are frequently tested for their antibacterial effect.^[60–63] We therefore examined the activity of our particles in first experiments, which revealed an unexpected behavior of particles with coordinated ions and corresponding composites. Gold nanocomposites, in turn, can also be used in medical applications such as diagnostic imaging and cancer therapy,^[64–68] but are also suitable for catalytic applications.^[69–72]

2. Results and Discussion

2.1. Influence of Surfactants

VME and the corresponding polymer feature an amphiphilic character induced by the hydrophilic hydroxy moiety and the more hydrophobic thioether group. While the monomer, therefore, has still a rather high solubility in water, the polymer becomes insoluble already at low degrees of polymerization. Nevertheless, the hydroxy groups still cause a significant interaction with water, and due to the polar character, we assume a high degree of swelling of the polymer in water, which makes suitable stabilization of corresponding particles challenging. The first polymerization experiments were all performed at a monomer concentration of 0.22 g mL⁻¹, which exceeds the solubility limit. We further used the water-soluble initiator 2,2'-azobis(2-methylpropionamide) dihydrochloride (V-50). Considering that phase-separated monomer droplets are formed in this case, the process certainly resembles some features of an emulsion polymerization although the high solubility might induce most characteristics of a precipitation polymerization. Several different stabilizing reagents are established for heterogeneous polymerizations, which are necessary to prevent coagulation of the particles.^[11] In consequence, we first examined the polymerization of VME dispersed in water containing 1 wt.% of different surfactants. At first, one of the most common stabilizing reagents, sodium dodecyl sulfate (SDS), was tested. Surprisingly, this surfactant had no significant effect on the stability of the dispersion, since precipitation occurred almost instantaneously with the first polymers formed (**Figure 1**). The results were comparable to the control experiment without any surfactant. Further variations of the conditions resulted in no improvement (data not shown). To exclude that the anionic character of the surfactant induces instability by interacting with the positively charged initiator, we further tested neutral stabilizers. Therefore, polyethylene glycol (PEG) based Tween 80 and Triton X-100 were examined and it seems that these surfactants with alkyl chains are also not suitable to produce stable particles (**Figure 1**). We assume that the aliphatic tails of these surfactants are generally incompatible with the polymer which we relate to the presence of the still rather polar hydroxy groups.

In consequence, we further selected surfactants comprising more similar polar groups which were considered to form secondary interactions such as hydrogen bonds with the hydroxyl group of VME and, thus, ensure a better stabilization. Besides the triblock copolymer Pluronic F127, commercially available polyvinyl pyrrolidone (PVP, 40 000 g mol⁻¹) and polyvinyl alcohol (PVA, 31 000 g mol⁻¹) were examined. Unfortunately, Pluronic F127 and PVP did not live up to expectations because the resulting particles sedimented still quickly and were not completely redispersible. Nevertheless, some improvements were observed for PVP compared to the previously described surfactants, since the full sedimentation appears slightly delayed and at least a part of the particles was redispersible (for details about conversion and molar mass distribution see Table S6 and **Figure S1**, Supporting Information). Interestingly, the molar masses of the polymers (10 600 g mol⁻¹, 2 mol% initiator V-50, 40 °C) are much lower compared to the polymers prepared in bulk (95 000 g mol⁻¹ 1 mol% initiator azobisisobutyronitrile

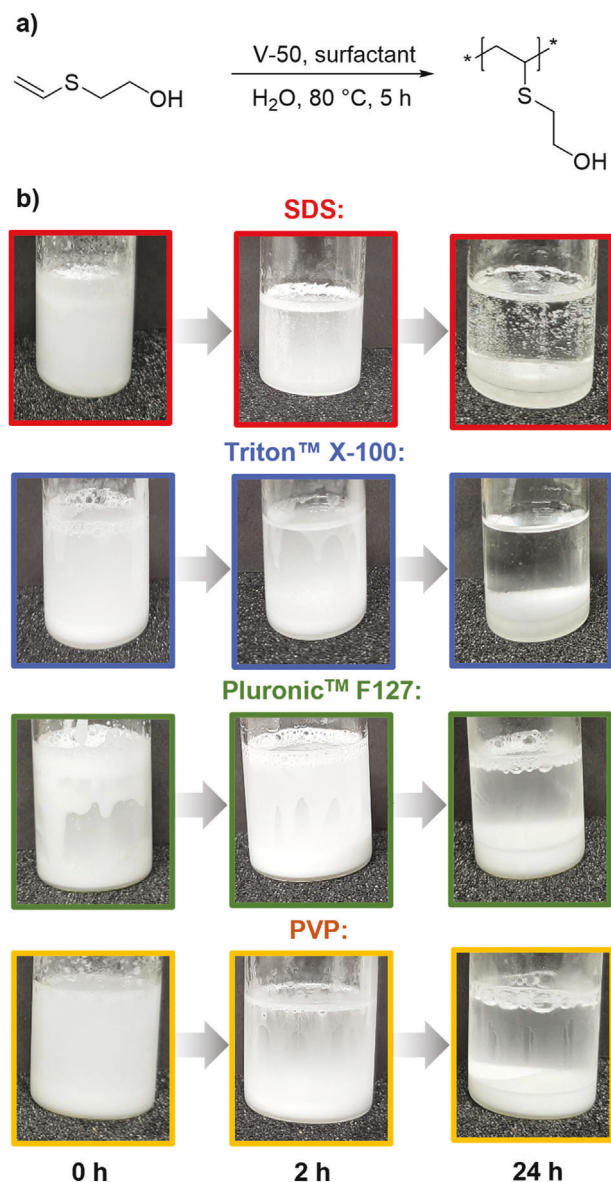


Figure 1. Photographs of samples taken at different timepoints after the polymerization of VME with different surfactants to illustrate the sedimentation behavior over the time; the first image was taken immediately after polymerization.

(AIBN), 55 °C).^[59] The lower molar masses must be a consequence of either a retarded propagation rate or an increased termination rate. While water should enhance the propagation rate of radical polymerizations in homogenous solutions,^[73] the precipitation might hamper the diffusion of monomer to the reactive chain end and increase the probability of termination reactions in the local confinement. Therefore, the kinetic chain length might be restricted once precipitation occurs. However, it has to be kept in mind that the reaction conditions differ significantly from the reported bulk polymerizations. Dynamic light scattering (DLS) measurements in water performed directly after polymerization confirmed a very broad size distribution of particles with sizes >400 nm for all used surfactants (Figure S2,

Supporting Information). The largest aggregates were formed with SDS (≈ 900 nm), while only minimal smaller aggregates were observed with the other three surfactants (400 to 700 nm).

PVA, on the other hand, proves to be the best stabilizing reagent for this system, because the particles sediment only slowly and are completely redispersible. This behavior could not be observed with any other surfactant. However, even in this case, the DLS measurements revealed sizes in the range of micrometers (Table S7 and Figure S3, Supporting Information). Since the correlogram already give indications of aggregates that are located outside of the measurable range, a very broad distribution can be assumed. Nevertheless, redispersible dispersions are formed with PVA and scanning electron microscopy (SEM) images prove the spherical shape of the particles formed in the dispersion at a PVA content as low as 1 wt.% (Figure 2d). However, due to the soft nature of the polymer, only collapsed particle structures could be observed in the SEM images. Subsequently, we investigated the influence of the PVA content as well as the monomer concentration on the conversion, the chain length, and on the stability of the particles. From the data summarized in Figure 2, it can be deduced that the polymerization at 1 wt.% and 2 wt.% PVA is very similar, as similar conversion rates and molar mass distributions were obtained. The molar mass distribution reveals a bimodal distribution, which is another indication of a mixed polymerization process. However, a slight difference was observed when the PVA content was increased to 4 wt.%. Both reaction rate and molar mass increase, which might reflect a more heterogeneous character of the system. Interestingly and contrary to our expectations, the DLS measurements revealed that larger particles are formed at the increased content of PVA (Figure S3, Supporting Information), which indicates an upper limit even for this surfactant to create stable dispersions. SEM images prove again the presence of spherical particles (Figure 2d) but also confirm broad size distribution of the particles also with higher amount of PVA.

Decreasing the monomer concentration had no major impact on the behavior of the polymerization. At lower concentrations, the polymerization rate is decreased (Figure 3a) but this appears related to dilution rather than any effect of confinement in emulsion particles. Similarly, the average molar masses of the polymers decrease, which correlates well with the decreased propagation rate at the lower concentration (Figure S4 and Table S8, Supporting Information). At a concentration of 0.06 g mL^{-1} the monomer fully dissolves in water turning the system into a pure precipitation polymerization. Since no significant changes were observed when crossing from a dispersed to a homogenous starting solution, we conclude that overall all polymerizations feature more characteristics of precipitation polymerizations rather than those of an emulsion system. The homogenous starting solution at a concentration of 0.06 g mL^{-1} enabled a closer look at the kinetics of the particle formation, since no concealing scattering from monomer droplets occurs. Although some datapoints appear somewhat scattered, which is most likely to different degrees of particle sedimentation in the samples, the scattering intensity or the derived count rate, respectively, increases continuously over 2 h until it saturates. A similar trend can be observed for the average size of the particles, although this data has to be taken with more care, since stronger deviations due to partial sedimentations are more likely. It is noteworthy to mention that

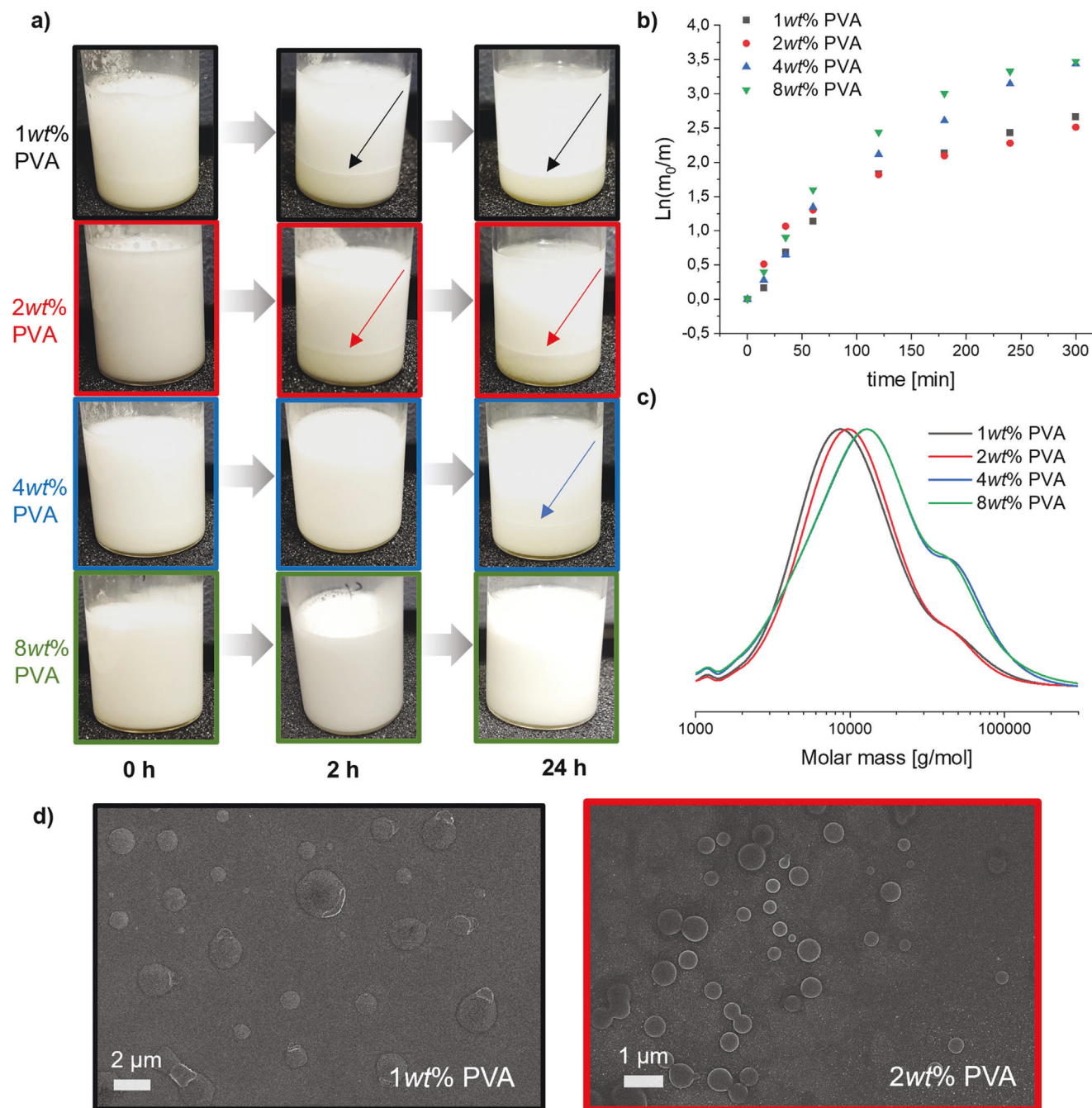


Figure 2. a) Photographs of samples taken at different timepoints after the polymerization of VME with different content of PVA to illustrate the sedimentation behavior (the arrows indicate the edge of the formed sediment, if present), b) plot of $\ln(m_0/m)$ versus reaction time, c) SEC (DMAC (+0.21 wt.% LiCl), PMMA standards) traces of the emulsion polymers after 5 h with different amount of PVA, and d) SEM images of the particles with 1 wt.% and 2 wt.% PVA.

particle formation occurs instantly with first conversion of the monomer, which again reflects the characteristics of a precipitation polymerization and the limited solubility of the polymer in water. Although the size of the resulting particles seems to increase with further progress of the polymerization, quite large particles ($>2 \mu\text{m}$) are already formed after 10 min of polymerization. Over time, coagulation might further cause particle growth

but the increase in scattering intensity is certainly due to an increase of overall particle concentration.

We further analyzed the thermal properties of the prepared polymers. A decomposition temperature of approximately $270 \text{ }^\circ\text{C}$ and a glass transition temperature of about $15 \text{ }^\circ\text{C}$ (Table S9 and Figure S6, Supporting Information) were determined, which are close to the previous measured values for polymers prepared in

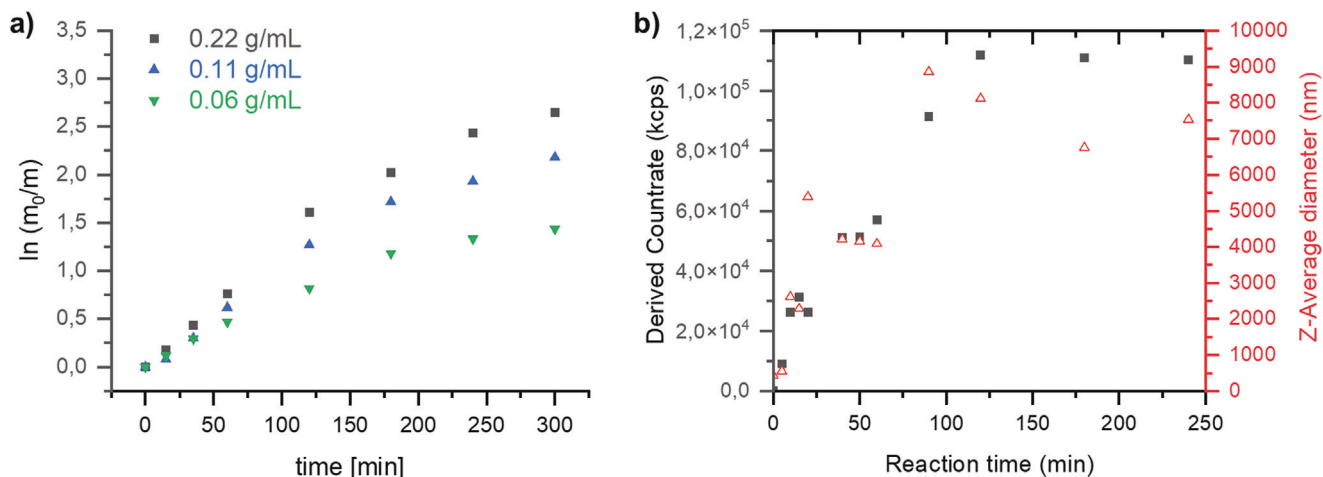


Figure 3. a) Polymerization kinetics at different monomer concentrations and b) derived count rates as well as average sizes of particles at different time points (obtained from DLS measurements in water).

bulk or solution.^[59] The rather low glass transition might further correlate with the tendency of the particles to agglomerate and fuse together. Overall, stabilization of the particles proved to be difficult, which, as mentioned in the beginning, is mainly due to the amphiphilic character of the monomer and the resulting polymers. Nevertheless, the addition of PVA provided some stability and redispersible microparticles are formed, even though the size distribution was broad.

2.2. Coordination of Silver Ions (Ag^+ @PVME) and Formation of Silver Composites (Ag @PVME)

The coordination of various metals or ions is a feature induced by various sulfur compounds, and we considered our dispersions an interesting candidate to create such composites. Initially, we focused on silver ions and the formation of silver nanoparticles within the polymer dispersions. Silver is known to coordinate well with sulfur, and the resulting ion or metal loaded polymer particles might be interesting as antibacterial material similar to widely applied silver nanoparticles. It turned out that a direct polymerization in the presence of silver nitrate or acetate is not possible, and the resulting pre-arrangement of the monomer induced a strong coagulation, which why it was discarded (data not shown). Consequently, we pursued a two-step process, in which polymer particles were formed as described above (surfactant: PVA) and silver ions were subsequently added to the purified polymer particles.

Different amounts (0.02, 0.04 and 0.1 eq.) of silver ions compared to the sulfur atoms in the polymer were added and then dialyzed to remove the excess of non-coordinated silver ions. The successful incorporation of the silver ions into the particles was evaluated by inductively coupled plasma mass spectrometry (ICP-MS) measurements. The analysis revealed that the addition of an increased amount of silver ions at the beginning also resulted in increased incorporation into the polymer particles (Table S10, Supporting Information, for details). At an amount of 0.02 and 0.04 equivalents of silver ions, the determined silver ion concentration in the particles is close to the maximum possible

concentration, i.e., almost all silver ions are bound to the sulfur. However, for 0.1 equivalents the values deviate which indicates an oversaturation of the particles with silver and an excess of silver ions is removed during purification. Although 0.1 equivalents appear low considering the strong affinity of the sulfur compounds, it has to be kept in mind that silver ions might coordinate with several sulfur atoms and the particles might not be fully penetrable once the surface is saturated with silver ions.

In addition, the influence of the silver ions on the emulsions with different PVA content was also investigated. Interestingly, the silver ions appear to have a stabilizing effect on the particles, as sedimentation was retarded, and DLS measurements also confirmed a change of size (Figure S7, Supporting Information). An agglomeration of particles might be prevented by the positive charge of the silver ions and the associated repulsion. It seems that the best stability can be achieved with a PVA content of 1 wt.% and the silver ions, while faster sedimentation can again be observed for example with 4 wt.% or more PVA. Higher amounts of PVA might prevent full incorporation of the silver ions covering the particle surface and a larger amount of silver ions remains than in solution. This assumption is supported by the SEM images, where coagulation of the silver salts can be observed in the dried sample, but this occurs partly in the polymer particle and partly outside the polymer particle (SEM images for dispersion with 1 wt.% and 2 wt.% PVA see Figure 4 and SEM images for dispersion with 4 wt.% and 8 wt.% PVA see Figure S8, Supporting Information). For this reason, the dispersion with 1 wt.% was further investigated.

The stability of the silver ion complexes in the polymer particles was further analyzed over one week. First, we determined the silver concentration of the sample with 0.04 eq. of silver after initial dialysis (three days) of the particles to ensure the removal of any excess of free silver ions. Then, the dispersion was transferred into a controlled dialysis setup and the filtrate was analyzed every 24 h over six days by ICP-MS measurements. The total silver content decreased slightly over the time indicating already a release of silver ions. A closer look at the filtrate samples taken every day confirmed a linear increase of the accumulated silver ions within the dialysis water over the six days (Figure 5). Due to

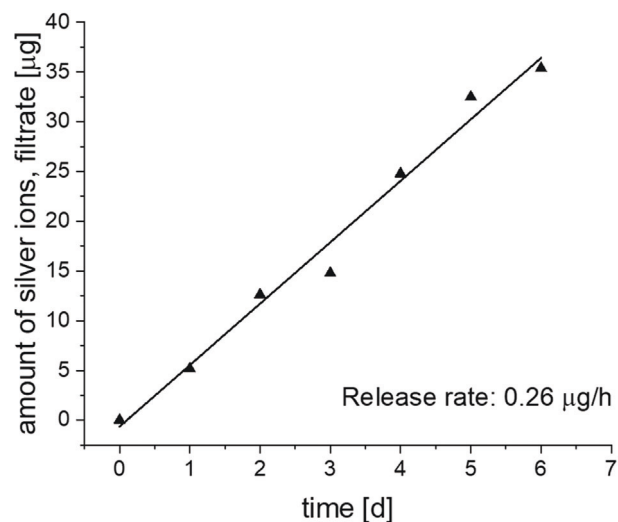
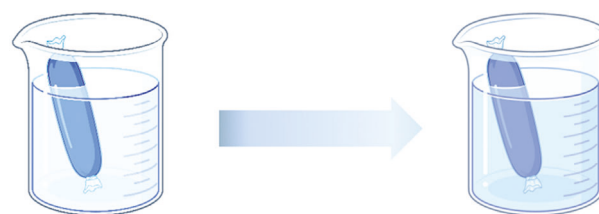
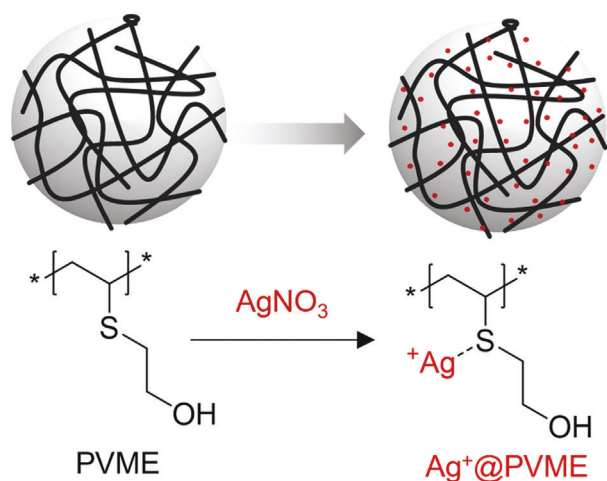


Figure 5. Schematic representation of the release experiment (top) and cumulated amount of released silver ions in the filtrate over one week.

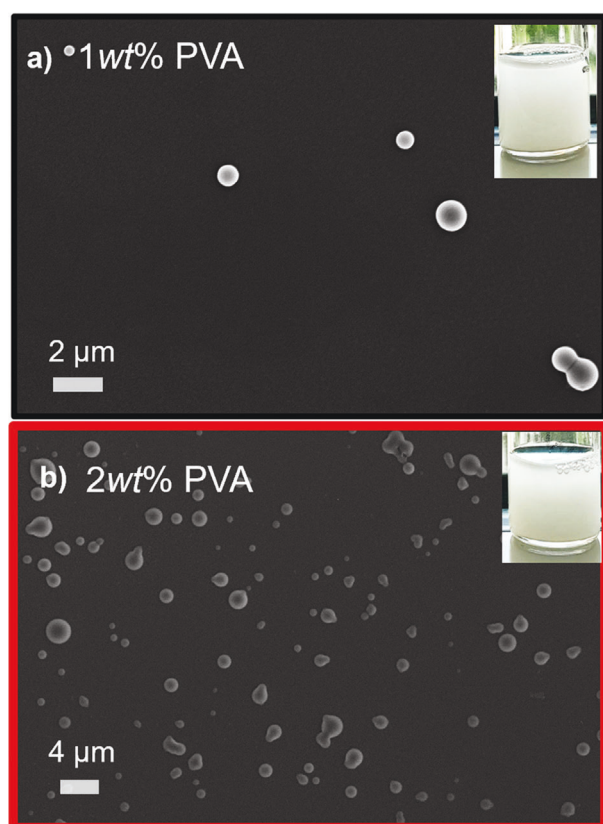


Figure 4. SEM images of a) PVME@Ag⁺ with 1 wt.% PVA, and b) PVME@Ag⁺ with 2 wt.% PVA.

the inhomogeneity of the dialysis water, there may be deviations between the concentration values determined for the dialysis water and the concentration loss in the dialysis tube. Nevertheless, a continuous release of silver ions can be observed.

Since the polymer emulsions were able to coordinate silver ions, we further tested the possibility to create silver nanoparticles inside the polymer emulsions by reduction of the coordinated silver ions. However, the choice of a suitable reducing agent proved to be a major challenge. Initial attempts using conven-

tional reducing agents such as sodium borohydride failed and led to coagulation of the silver and the polymer particles. We consider the rapid formation and competitive coordination of the borohydride salts might cause this instability of the solution, since the coordination of the silver ions in the polymer particle is not sufficiently strong. A gentler reducing agent is ascorbic acid. However, even in this case, silver nanoparticles appeared randomly distributed throughout the sample and both free silver nanoparticles and silver nanoparticles coordinated to the polymer could be detected (Figure S9, Supporting Information). Nevertheless, the emulsion appeared more stable compared to sodium borohydride. Interestingly, an alternative and mild pathway opened up during our experiments. Leaving untreated samples on the lab bench in open light induced a color transition of the samples from white to brown indicating the in situ formation of silver nanostructures. We further followed this route using sunlight to induce the reduction. Therefore, the samples were kept behind a double-glazed window at room temperature for overall 3 days to induce the reaction. UV-vis spectra of highly diluted solutions revealed a clear shift of the absorbance of the emulsion to higher wavelengths, which further confirmed the formation of silver nanoparticles (Figure S10, Supporting Information). Kept in sunlight, all emulsions remained stable and only a very slow sedimentation occurred over time. Furthermore, the silver nanoparticles appeared uniformly distributed among the polymer particles as shown by transmission electron microscopy (TEM) and SEM images of the particles (Figure 6; Figure S11, DLS data Figure S13, Supporting Information). An explanation for the reduction

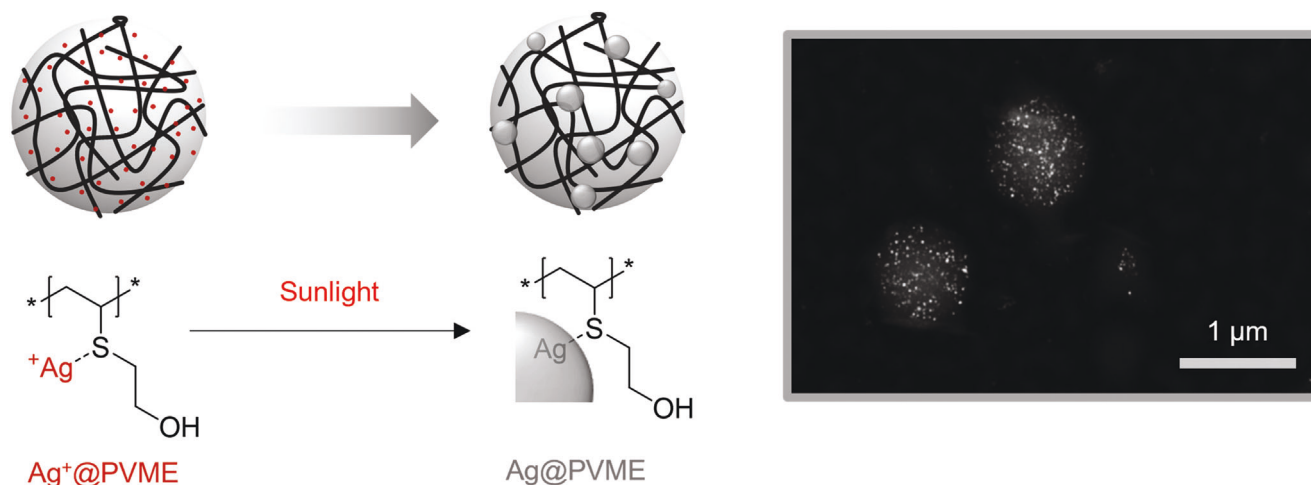


Figure 6. Schematical representation of the reduction of Ag^+ @PVME within the polymer particles (left) and corresponding TEM image of the reduced sample Ag@PVME (right).

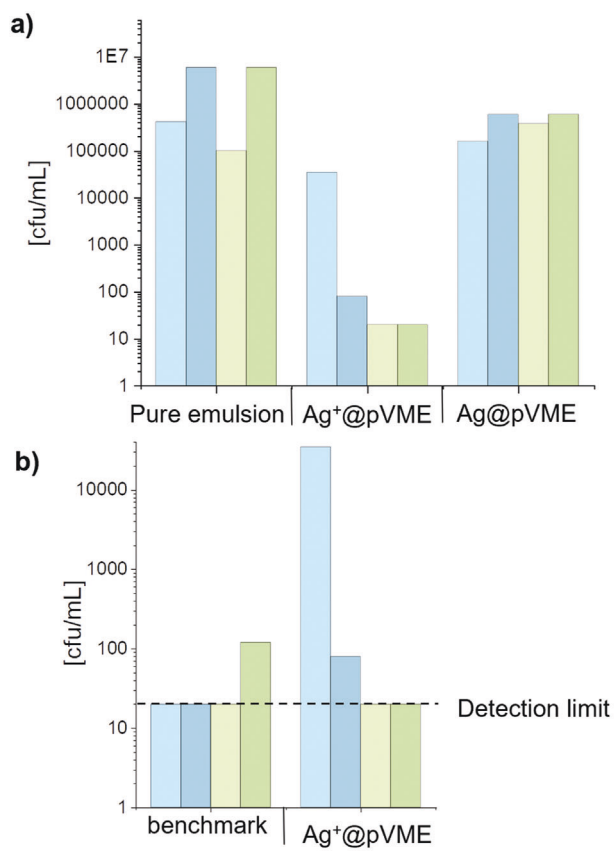
of silver ions by sunlight might be related to the chemical nature of the polymer particle. In this case, the thioether groups in the repeating unit might act as reducing agents and themselves become oxidized to the corresponding sulfoxide. As a control experiment a silver nitrate solution was kept under identical environmental conditions but in the absence of the polymer. No change of color was observed in this case, supporting the theory that the silver ions must interact with the polymer to induce the reaction. In an attempt to analyze the changes on the particles induced by the reaction, we investigated the zeta potential of the pure emulsion and the emulsions modified with silver ions and silver nanoparticles (Figure S12, Supporting Information). Unfortunately, in all cases a positive zeta potential was observed and the modification of the particles with silver ions had only a negligible effect on the measurements. The positive zeta potential of the initial dispersions can be attributed to the presence of cationic polymer end groups, which are introduced by the applied initiator. Therefore, we were not able to detect any oxidized groups in the composite and verify the proposed mechanism.

In further experiments, we altered the conditions to determine the effect of the reaction environment on the reaction. In addition to the treatment by sunlight, we tested UV-irradiation (UV-cube) or irradiation by a daylight lamp (color spectrum: 400 nm to 800 nm) lacking the UV spectrum (Figure S14, Supporting Information). In the first case, a color change was observed after one hour of irradiation, but at the same time agglomeration of the particles occurred at the bottom of the vial. The increased temperatures and the intense radiation generated in the UV cube seems to negatively affect the stability of the particles (Figure S14, Supporting Information), which is why we did not pursue this study further. The daylight lamp (Intensity: 10 000 lux at 10 cm distance), on the other hand, appears to induce a more controlled reaction and a color change could be observed after 24 h, while the dispersion remained stable. Unfortunately, an extended reaction time of three days could not be realized due to overheating of the lamp, but the experiment confirmed that UV-light appears not to be necessary to induce the reaction. Although further investigations are required to reveal the exact mechanism of this

reaction, the easily accessible irradiation with visible light or sunlight represents a convenient route to stable dispersions of silver nanocomposites on polymers.

As mentioned above, silver nanoparticles are frequently used in antimicrobial coatings or materials.^[60–63,74] The effect is often related to a continuous release of small amounts of silver ions into the environment, which interfere with microbial growth.^[62,75,76] To elucidate whether the polymer particles with silver ions or silver nanoparticles are suitable for antibacterial application, the growth of *E. coli* and *S. aureus* was studied in the presence of the different emulsions (Figure 7a). The pure PVME emulsion showed no antibacterial effect, resulting in unaffected bacterial growth over 24 h. The modified samples, on the other hand, revealed a significant antibacterial effect. Ag^+ @PVME leads to a strong reduction of bacterial numbers in case of *E. coli* and *S. aureus* after 4 h of incubation and is maintained up to 24 h. Interestingly, the emulsions with silver nanoparticles were not as effective as the coordinated ions and did not show a clear antibacterial effect under the applied test conditions, which is in contrast to common silver nanoparticle-based systems. We attribute this to the fact that the antibacterial effect is related to the continuous release of silver ions, which was confirmed for Ag^+ @PVME. In case of the silver nanoparticles, the silver content in the test sample with the nanoparticle preparation was significantly lower than in the Ag^+ @PVME test sample and the required oxidation of the metallic silver might be suppressed or the silver ions were too strongly bound to the polymer emulsions.^[77] We finally compared our silver ion containing polymer particles with the benchmark substance Irgaguard B 6000 (Figure 7b; for details see Table S11, Supporting Information), which is an antimicrobial agent based on an inorganic silver glass/zeolite composite. At 4 h incubation, the effect of Ag^+ @PVME on *S. aureus* is slightly diminished compared to the control, but after 24 h a similar effect is observed, despite the system has not been optimized for this application.

In summary, the slow release of silver ions from the polymer particle induces a significant antibacterial effect without the need to create a silver nanocomposite. In contrast, the reduced sam-



S. aureus ATCC 6538 (after 4 h and after 24 h)

E. coli DSM 682 (after 4 h and after 24 h)

Figure 7. a) Results of the tests on antibacterial effects (*S. aureus*: blue, *E. coli*: green) induced by the pure PVME emulsion, the emulsion containing silver ions (Ag⁺@PVME), and emulsions comprising silver nanoparticle (Ag@PVME) after 4 h (light color) and 24 h (dark color) of coincubation and b) zoomed graph of the results on antibacterial effect for Ag⁺@PVME in comparison to a benchmark.

ples containing metallic silver had almost no antibacterial effect. The strong coordination of the silver and an inhibition of a reoxidation of Ag(0) to Ag(I) might prevent the release of ions, which are essential to induce the antibacterial effect in other composite materials. More detailed studies could certainly improve the efficiency of the here presented materials, but this was beyond the scope of this study.

2.3. Synthesis of Gold Composites (Au@PVME)

Besides silver, other noble metals and their ions are known to coordinate well with sulfur compounds. We therefore tried to extend our approach to gold, focusing again on an in situ formation of polymer-integrated nanoparticles. Initially, we tested potassium Au(III) chloride as precursor, but this did not lead to stable dispersions. The addition of chloroauric acid, however, did not cause coagulation and a homogeneous distribution of the gold salt could be confirmed by TEM and SEM images (Figure 8). Again, we

tested different reducing agents to induce the transformation into metallic gold. However, a broad distribution of gold particles and limited incorporation into the polymer was observed like for the experiments with silver. Consequently, we again tested a light-induced reduction, which resulted in an increasing coloration of the sample turning purple-brown. Interestingly, the subsequent analysis by TEM and SEM revealed slight deformations on the surface of the resulting polymer particles (Figure 8c) and confirmed the successful integration of the gold into the polymer. The deformations are most likely a result of the reduction and a homogenous distribution of the initial precursor throughout the outer layers of the polymer particles. We again speculate that the light induces an oxidation of the sulfur in the polymer while the gold precursor is reduced. Overall, the particles appear stable, although a more rapid sedimentation is observed, which we relate to the limited repulsion by charges and an increased density induced by the metallic gold. The polymer particles modified with gold (Au@PVME) are nevertheless still well redispersible if agitated rendering the system an interesting and easily accessible scaffold for integration of noble metal catalysts, which is currently further investigated.

3. Conclusion

In summary, we investigated the possibility of an emulsion polymerization of the electron-rich *S*-vinyl monomer vinyl mercaptoethanol (VME) testing various surfactants. The monomer itself has a solubility in water (105.5 g L⁻¹) but the polymer becomes insoluble. Due to the high solubility of the monomer the process resembles characteristics of a precipitation polymerizations although monomer droplets are present at higher concentrations. The stabilization of the resulting polymer particles appeared to be a major challenge in the system. Various added surfactants had no or only limited visible effect on the stability of the formed dispersion, which we relate to the amphiphilic character of the polymer structure comprising hydrophilic hydroxyl-groups next to the hydrophobic thioether groups and the aliphatic backbone. Nevertheless, stable dispersions were obtained applying PVA as surfactant, which might be able to coordinate to the hydroxy groups. In contrast to common emulsion polymerizations, particles of few to several micrometers were obtained depending on the amount of added surfactant. This result again reflects that the process is more related to a precipitation polymerization than a real emulsion system. With a stable dispersion at hand, we further investigated the potential of the particles to coordinate metal ions, particularly of noble metals. First, the coordination of silver ions was examined and both the actual incorporation of silver ions into the particle and the release over time were studied. Up to an amount of 0.04 equivalents of silver ions compared to sulfur in the polymer, almost all of the silver ions were incorporated and complexed. Placed in deionized water, the silver ions are continuously released over one week, although the rate is very low. Higher equivalents of silver ions cannot be fully coordinated within the polymer dispersions which indicates that penetration into the polymer particles might be hampered. We further investigated whether metal silver can be formed with the polymer particles from the ion complexes. However, common reducing agents led to agglomeration of the particles and only a limited amount of silver remained coordinated within the poly-

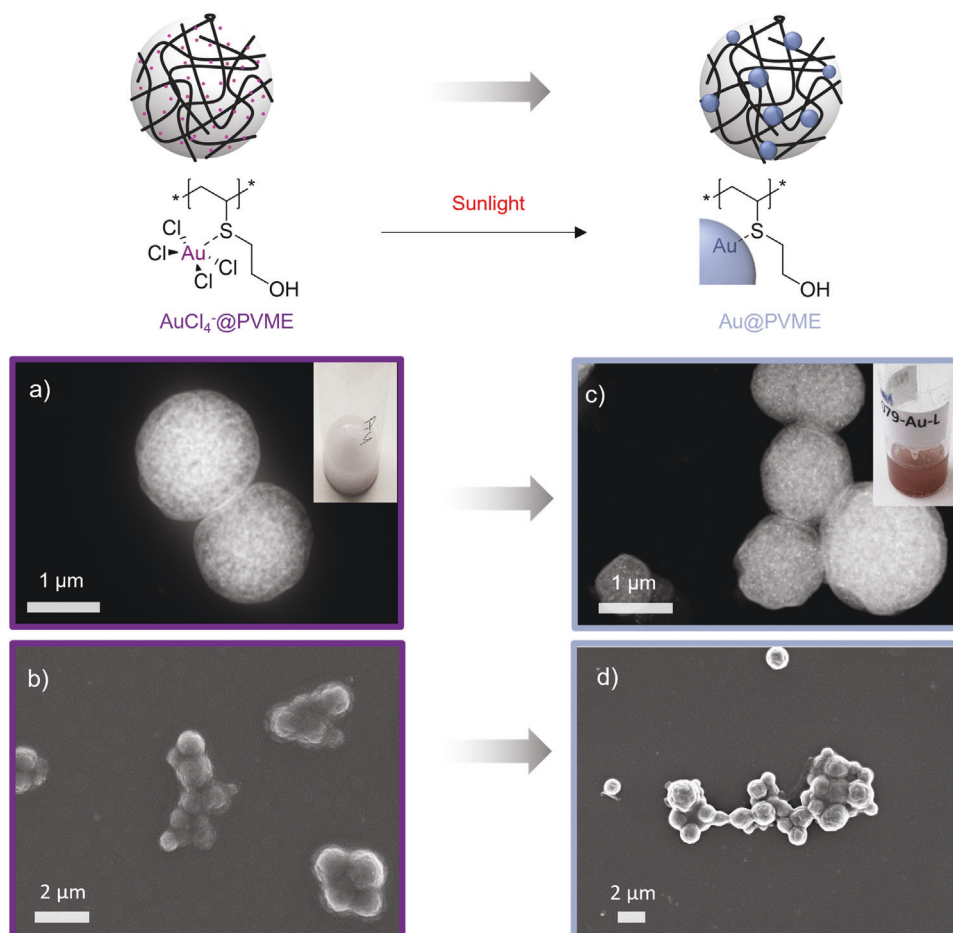


Figure 8. a) TEM image of AuCl_4^- @PVME, b) SEM image of AuCl_4^- @PVME, c) TEM image of Au@PVME, and d) SEM image of Au@PVME.

mer. Interestingly, simple irradiation with sunlight resulted in the formation of silver nanoparticles, which is presumably due to the fact that the polymer particle itself acts as a gentle reducing agent. In this case, the distribution of silver throughout the polymer particle was more homogeneous and stable dispersions were obtained. Considering a potential antibacterial effect of silver nanoparticles, we further analyzed the effect of our different systems on the growth of *E. coli* and *S. aureus*. In contrast to the pure dispersion, the dispersion comprising coordinated silver ions displayed a strong suppression of bacterial growth almost compatible to an optimized benchmark system. However, the system containing reduced silver nanoparticles had only a minor effect. We relate this to a limited formation of free silver ions by oxidation, which would be required for an antibacterial effect. In addition to silver, we also tested the coordination of gold as another noble metal. Adding chloroauric acid, stable dispersions were formed where the gold ions appear well distributed throughout the polymer particles. The subsequent reduction in sunlight again turned out to be the best method to create metallic gold within the polymer particles. This approach led to micrometer-sized polymer dispersions comprising a uniform coverage with metallic gold on the surface. Overall, the presented straightforward approach to create dispersions of the sulfur-rich polymer PVME may open interesting avenues to create host matrices for

various metal ions and metal nanoparticles. The resulting dispersions are stable or can easily be redispersed under agitation and the metal particles are accessible at the surface.

Supporting Information

Supporting Information is available from the Wiley Online Library or from the author.

Acknowledgements

The presented study was part of a research project funded by BASF SE to identify and develop applications for vinyl mercaptoethanol (VME). J.C.B. and N.Z. thank the German Science Foundation (DFG) for generous funding within the Emmy Noether Programme (Project-ID: 358263073). In addition, the authors thank Renzo Paulus for the TGA and DSC measurements, Dr. Dirk Merten for the ICP-MS measurements and Egon Gisela and Klaus Elfriede for the synthesis of the nanoparticles. The SEM facilities of the Jena Center for Soft Matter (JCSM) were established with a grant from the DFG.

Open access funding enabled and organized by Projekt DEAL.

Conflict of Interest

The authors declare no conflict of interest.

Data Availability Statement

The data that support the findings of this study are available on request from the corresponding author. The data are not publicly available due to privacy or ethical restrictions.

Keywords

antibacterial effect, emulsions polymerization, gold composites, metal nanoparticles, polyvinyl alcohol, precipitation polymerization, silver composites, sulfur-containing polymer, S-Vinyl monomer

Received: October 17, 2022

Revised: December 14, 2022

Published online: January 1, 2023

- [1] I. Capek, M. Riza, M. Akashi, *J. Polym. Sci., Part A: Polym. Chem.* **1997**, *35*, 3131.
- [2] J. M. Saenz, J. M. Asua, *J. Polym. Sci., Part A: Polym. Chem.* **1996**, *34*, 1977.
- [3] H. Bamnolker, S. Margel, *J. Polym. Sci., Part A: Polym. Chem.* **1996**, *34*, 1857.
- [4] J. M. Asua, "Polymer Reaction Engineering", Blackwell Publishing, Oxford, **2007**.
- [5] J. M. Asua, "Polymeric Dispersions: Principles and Applications", Springer, Dordrecht, **1997**.
- [6] C.-S. Chern, "Principles and Applications of Emulsion Polymerization", John Wiley & Sons, Hoboken, **2008**.
- [7] Y. Saeki, T. Emura, *Prog. Polym. Sci.* **2002**, *27*, 2055.
- [8] D. Zhang, X. Yang, in *Encyclopedia of Polymeric Nanomaterials*, Springer, Berlin, Heidelberg, **2015**, p. 2108.
- [9] H. J. M. Wolff, M. Kather, H. Breisig, W. Richtering, A. Pich, M. Wessling, *ACS Appl. Mater. Interfaces* **2018**, *10*, 24799.
- [10] P. Nesvadba, *Encyclopedia of Radicals in Chemistry, Biology and Materials*, **2012**.
- [11] P. A. Lovell, F. J. Schork, *Biomacromolecules* **2020**, *21*, 4396.
- [12] J. M. Asua, *J. Polym. Sci., Part A: Polym. Chem.* **2004**, *42*, 1025.
- [13] P. B. Zetterlund, Y. Kagawa, M. Okubo, *Chem. Rev.* **2008**, *108*, 3747.
- [14] P. J. Borm, D. Robbins, S. Haubold, T. Kuhlbusch, H. Fissan, K. Donaldson, R. Schins, V. Stone, W. Kreyling, J. Lademann, J. Krutmann, D. Warheit, E. Oberdorster, *Part. Fibre Toxicol.* **2006**, *3*, 11.
- [15] I. Khan, K. Saeed, I. Khan, *Arab. J. Chem.* **2019**, *12*, 908.
- [16] J. Jeevanandam, A. Barhoum, Y. S. Chan, A. Dufresne, M. K. Danquah, *Beilstein J. Nanotechnol.* **2018**, *9*, 1050.
- [17] Y. Matsuda, K. Uchida, Y. Egami, H. Yamaguchi, T. Niimi, *Sensors* **2016**, *16*, 550.
- [18] T. Tadros, in *Encyclopedia of Colloid and Interface Science*, T. Tadros, Springer, Berlin, Heidelberg, **2013**, p. 821.
- [19] J. Klier, J. Bohling, M. Keefe, *AIChE J.* **2016**, *62*, 2238.
- [20] A. C. Taylor, in *Handbook of Adhesion Technology*, Springer, Berlin, Heidelberg, **2011**, p. 1437.
- [21] S. Pardeshi, S. K. Singh, *RSC Adv.* **2016**, *6*, 23525.
- [22] G. Vasapollo, R. D. Sole, L. Mergola, M. R. Lazzoi, A. Scardino, S. Scorrano, G. Mele, *Int. J. Mol. Sci.* **2011**, *12*, 5908.
- [23] J. Wackerlig, R. Schirhagl, *Anal. Chem.* **2016**, *88*, 250.
- [24] S. K. Ghosh, "Functional Coatings: By Polymer Microencapsulation", Wiley, Weinheim, **2006**.
- [25] S. Förster, M. Antonietti, *Adv. Mater.* **1998**, *10*, 195.
- [26] S. Förster, M. Konrad, *J. Mater. Chem.* **2003**, *13*, 2671.
- [27] N. Hadjichristidis, A. Hirao, Y. Tezuka, F. D. u Prez, "Complex Macromolecular Architectures: Synthesis, Characterization, and Self-Assembly", Wiley, Weinheim, **2011**.
- [28] H. Althues, J. Henle, S. Kaskel, *Chem. Soc. Rev.* **2007**, *36*, 1454.
- [29] X.-H. Zhang, P. Theato, "Sulfur-Containing Polymers: From Synthesis to Functional Materials", Wiley VCH GmbH, Weinheim, **2021**.
- [30] H. Mutlu, E. B. Ceper, X. Li, J. Yang, W. Dong, M. M. Ozmen, P. Theato, *Macromol. Rapid Commun.* **2019**, *40*, 1800650.
- [31] H. Vahrenkamp, *Angew. Chem. Int. Ed. Engl.* **1975**, *14*, 322.
- [32] K. Suzuki, K. Yamasaki, I. Inorg, *Nucl. Chem.* **1962**, *24*, 1093.
- [33] C. Vericat, M. E. Vela, G. Corthey, E. Pensa, E. Cortés, M. H. Fonticelli, F. Ibañez, G. E. Benitez, P. Carro, R. C. Salvezza, *RSC Adv.* **2014**, *4*, 27730.
- [34] J. A. Rodriguez, J. Dvorak, T. Jirsak, G. Liu, J. Hrbek, Y. Aray, C. González, *J. Am. Chem. Soc.* **2003**, *125*, 276.
- [35] R. A. Bell, J. R. Kramer, *Environ. Toxicol. Chem.* **1999**, *18*, 9.
- [36] A. S. Pozdnyakov, A. A. Ivanova, A. I. Emel'yanov, G. F. Prozorova, *Russ. Chem. Bull.* **2020**, *69*, 715.
- [37] Y. Zhang, X. Wen, Y. Shi, R. Yue, L. Bai, Q. Liu, X. Ba, *Ind. Eng. Chem. Res.* **2018**, *58*, 1142.
- [38] H. Xu, J. K. Jin, Y. Mao, J. Z. Sun, F. Yang, W. Z. Yuan, Y. Q. Dong, M. Wang, B. Z. Tang, *Macromolecules* **2008**, *41*, 3874.
- [39] X. Li, Y. Liu, Z. Xu, H. Yan, *Eur. Polym. J.* **2011**, *47*, 1877.
- [40] J. A. Akkara, D. L. Kaplan, *Chem. Mater.* **1997**, *9*, 1342.
- [41] S. Shin, J. Jang, *Chem. Commun.* **2007**, 4230.
- [42] D. A. Boyd, J. Naciri, J. Fontana, D. B. Pacardo, A. R. Shields, J. Verbarg, C. M. Spillmann, F. S. Ligler, *Macromolecules* **2014**, *47*, 695.
- [43] J. P. Phillips, N. M. Mackey, B. S. Confait, D. T. Heaps, X. Deng, M. L. Todd, S. Stevenson, H. Zhou, C. E. Hoyle, *Chem. Mat.* **2008**, *20*, 5240.
- [44] J. Lutz, K. Albrecht, J. Groll, *Adv. NanoBiomed Res.* **2021**, *1*, 2000074.
- [45] M. E. Duarte, B. Huber, P. Theato, H. Mutlu, *Polym. Chem.* **2020**, *11*, 241.
- [46] W. J. Chung, J. J. Griebel, E. T. Kim, H. Yoon, A. G. Simmonds, H. J. Ji, P. T. Dirlam, R. S. Glass, J. J. Wie, N. A. Nguyen, B. W. Guralnick, J. Park, Á. Somogyi, P. Theato, M. E. Mackay, Y.-E. Sung, K. Char, J. Pyun, *Nat. Chem.* **2013**, *5*, 518.
- [47] J. M. Scheiger, C. Direksilp, P. Falkenstein, A. Welle, M. Koenig, S. Heissler, J. Matysik, P. A. Levkin, P. Theato, *Angew. Chem., Int. Ed.* **2020**, *59*, 18639.
- [48] J. C. Bear, W. J. Peveler, P. D. McNaughtner, I. P. Parkin, P. O'Brien, C. W. Dunnill, *Chem. Commun.* **2015**, *51*, 10467.
- [49] T. R. Martin, K. A. Mazzi, H. W. Hillhouse, C. K. Luscombe, *Chem. Commun.* **2015**, *51*, 11244.
- [50] N. P. Tarasova, A. A. Zanin, E. G. Krivoborodov, Y. O. Mezhuev, *RSC Adv.* **2021**, *11*, 9008.
- [51] E. T. Kim, W. J. Chung, J. Lim, P. Johe, R. S. Glass, J. Pyun, K. Char, *Polym. Chem.* **2014**, *5*, 3617.
- [52] M. Geven, R. d'Arcy, Z. Y. Turhan, F. El-Mohtadi, A. Alshamsan, N. Tirelli, *Eur. Polym. J.* **2021**, *149*, 110387.
- [53] A. Rehor, N. Tirelli, J. A. Hubbell, *Macromolecules* **2002**, *35*, 8688.
- [54] L. I. Teixeira, K. Landfester, H. Thérien-Aubin, *Macromolecules* **2021**, *54*, 3659.
- [55] S. Xu, G. Ng, J. Xu, R. P. Kuchel, J. Yeow, C. Boyer, *ACS Macro Lett.* **2017**, *6*, 1237.
- [56] S. Hemvasdukij, W. Ngeontae, A. Imyim, *J. Appl. Polym. Sci.* **2011**, *120*, 3098.
- [57] N. Ziegenbalg, L. Elbinger, U. S. Schubert, J. C. Brendel, *Polym. Chem.* **2022**, *13*, 5019.
- [58] V. K. Gollmer, H. Ringsdorf, *Makromol. Chem.* **1969**, *121*, 227.
- [59] N. Ziegenbalg, F. V. Gruschwitz, T. Adermann, L. Mayr, S. Guriyanova, J. C. Brendel, *Polym. Chem.* **2022**, *13*, 4934.
- [60] G. Franci, A. Falanga, S. Galdiero, L. Palomba, M. Rai, G. Morelli, M. Galdiero, *Molecules* **2015**, *20*, 8856.
- [61] N. Durán, M. Durán, M. B. de Jesus, A. B. Seabra, W. J. Fávaro, G. Nakazato, *Nanomedicine* **2016**, *12*, 789.

- [62] I. A.-O. Yin, J. Zhang, I. A.-O. Zhao, M. L. Mei, Q. Li, C. A.-O. Chu, *Int. J. Nanomed.* **2020**, *15*, 2555.
- [63] C. Marambio-Jones, E. M. V. Hoek, *J. Nanoparticle Res.* **2010**, *12*, 1531.
- [64] L. E. Cole, R. D. Ross, J. M. R. Tilley, T. Vargo-Gogola, R. K. Roeder, *Nanomedicine* **2015**, *10*, 321.
- [65] P. C. Chen, A. K. Mwakwari Sc Fau – Oyelere, A. K. Oyelere, *Nanotechnol. Sci. Appl.* **2008**, *1*, 45.
- [66] W. Cai, H. Gao T Fau – Hong, J. Hong H Fau – Sun, J. Sun, *Nanotechnol. Sci. Appl.* **2008**, *1*, 17.
- [67] X. Huang, P. K. Jain, I. H. El-Sayed, M. A. El-Sayed, *Nanomedicine* **2007**, *2*, 681.
- [68] S. Taghizadeh, V. Alimardani, P. L. Roudbali, Y. Ghasemi, E. Kaviani, *Photodiagnosis Photodyn. Ther.* **2019**, *25*, 389.
- [69] P. Paalanen, B. M. Weckhuysen, M. Sankar, *Catal. Sci. Technol.* **2013**, *3*, 2869.
- [70] S. S. Dash, I. K. Sen, S. K. Dash, *Int. Nano Lett.* **2022**, *12*, 47.
- [71] J. Zhao, R. Jin, *Nano Today* **2018**, *18*, 86.
- [72] R. Ciriminna, E. Falletta, C. Della Pina, J. H. Teles, M. Pagliaro, *Angew. Chem. Inter. Ed.* **2016**, *55*, 14210.
- [73] A. Valdebenito, M. V. Encinas, *Polym. Int.* **2010**, *59*, 1246.
- [74] J. García-Barrasa, J. M. López-de-Luzuriaga, M. Monge, *Cent. Eur. J. Chem.* **2011**, *9*, 7.
- [75] S. Anees Ahmad, S. Sachi Das, A. Khatoon, M. Tahir Ansari, M. Afzal, M. Saquib Hasnain, A. Kumar Nayak, *Mater. Sci. Energy Techn.* **2020**, *3*, 756.
- [76] A. Kędziora, R. Wieczorek, M. Speruda, I. Matolínová, T. M. Goszczyński, I. Litwin, V. Matolín, G. Bugla-Płoskońska, *Front. Microbiol.* **2021**, *12*, 659614.
- [77] J. Liu, D. A. Sonshine, S. Shervani, R. H. Hurt, *ACS Nano* **2010**, *4*, 6903.

[M]acro-
olecular
Chemistry and Physics

Supporting Information

for *Macromol. Chem. Phys.*, DOI 10.1002/macp.202200379

Coordination of Noble Metals in Poly(vinyl mercaptoethanol) Particles Prepared by
Precipitation/Emulsion Polymerization

*Nicole Ziegenbalg, Hans F. Ulrich, Steffi Stumpf, Philipp Mueller, Jürgen Wiethan, Janette
Danner, Ulrich S. Schubert, Torben Adermann and Johannes C. Brendel**

Supporting Information

Coordination of noble metals in poly(vinyl mercaptoethanol) particles prepared by precipitation/emulsion polymerization

Nicole Ziegenbalg,^{a,b} Hans F. Ulrich,^{a,b} Steffi Stumpf,^{a,b} Philipp Mueller,^c Jürgen Wiethan,^d Janette Danner,^d Ulrich S. Schubert,^{a,b} Torben Adermann,^c Johannes C. Brendel,^{a,b,*}

- a Laboratory of Organic and Macromolecular Chemistry (IOMC), Friedrich Schiller University Jena, Humboldtstraße 10, 07743 Jena, Germany
- b Jena Center for Soft Matter (JCSM), Friedrich Schiller University Jena, Philosophenweg 7, 07743 Jena, Germany
- c BASF SE, Carl-Bosch-Straße 38, 67056 Ludwigshafen/Rhein, Germany
- d BASF Grenzach GmbH, Koechlinstrasse 1, 79639 Grenzach-Wyhlen, Germany

*corresponding author: johannes.brendel@uni-jena.de

Experimental part

Materials and Methods

All reagents and solvents were commercially purchased from Sigma-Aldrich, TCI Chemicals, abcr, or were provided by BASF SE and were used without further purification. Table S1 summarizes the molar masses and other important properties of the surfactants used.

Table S1: Overview of the molar masses of the different used surfactants.

Surfactant	Molar mass [g mol ⁻¹]	Hydrolysis
Triton™ X-100	~ 625	-
Tween™ 80	~1 300	-
Pluronic™ F-127	~12 600	-
PVP	40 000	-
PVA	31 000	86.7 to 88.7mol%

¹H-NMR spectra were measured with a Bruker spectrometer (300 MHz) equipped with an Avance I console, a dual ¹H and ¹³C sample head and a 60 x BACS automatic sample changer. The chemical shifts of the peaks were determined by using the residual solvent signal as a reference and are given in ppm in comparison to TMS. Deuterated solvents were commercially purchased from EURISO-TOP GmbH.

Size-exclusion chromatography (SEC) of polymers was performed on an Agilent system (series 1200) equipped with a PSS degasser, a G1310A pump, a G1362A refractive index detector and a PSS GRAM 30 and 1000 column with DMAc (+ 0.21wt% LiCl) as eluent at a flow rate of 1 mL/min. The column oven was set to 40 °C and poly(methyl methacrylate) (PMMA) standards were used for calibration.

The differential scanning calorimetry (DSC) measurements were performed on a DSC 204 F1 Phoenix® from Netzsch under a nitrogen atmosphere with a heating rate of 10 K/min. The thermal gravimetric analysis (TGA) was carried under nitrogen using a Netzsch TG 209F1 Iris®.

Dynamic light scattering (DLS) correlograms were measured on a ZetaSizer Nano ZS (Malvern, Herrenberg, Germany) equipped with a He–Ne laser with a wavelength of $\lambda = 633$ nm at a scattering angle of 173°. All measurements were conducted in triplicate at 25 °C after an equilibration time of 10 s and an acquisition time of 30 s.

Scanning electron microscopy (SEM) imaging was performed with a Sigma VP Field Emission Scanning Electron Microscope (Carl-Zeiss AG, Germany) using the InLens detector with an accelerating voltage of 6 kV. For the sample preparation, the dispersed samples were applied on a mica substrate by drop casting and dried over a few hours. Then the samples were coated with a thin layer of platinum via sputter coating (CCU-010 HV, Safematic, Switzerland) before the measurement. The contrast of the images was increased afterward to make the aggregates more visible.

For transmission electron microscopy (TEM), dispersed samples were applied on an ultra-thin carbon-coated grid by the drop-on-grid method. The samples were imaged using a probe-corrected Themis Z® 3.1 machine (Thermo-Fisher, Waltham, USA) in High-Angle Annular Dark-Field (HAADF) Scanning Transmission Electron Microscopy (STEM) mode. Data were analyzed using the Velox 2.1x software. Particle size was manually analyzed with Imagic IMS software (Imagic Bildverarbeitung AG, Glattbrugg, Switzerland).

ICP-MS samples were previously filtered and acidified with 2% HNO₃. The measurements were performed on 8900 Triple Quadrupole ICP-MS (FA. Agilent, Waldbronn, Deutschland).

Antibacterial tests:

Test organisms: *Escherichia coli* DSM 682 (*E. coli*), *Staphylococcus aureus* ATCC 6538 (*S. aureus*).

Test emulsions: PVME, Ag⁺@PVME and Ag@PVME (with ascorbic acid)

Culturing: Two passages of the test organisms were done on Tryptic Soy Agar (TSA) for 24 h at 36 °C (+/- 1 °C). Cell material of the second passage was transferred to Tryptic Soy Broth (TSB) for preparation of the inoculation culture (incubation for 24 h at 36 °C).

Test procedure: 290 µL of each sample was transferred in a deep-well microtiter plate. Then 10 µL of inoculum was added to each sample resulting in approximately 3.0 x 10⁶ cfu mL⁻¹ sample respectively. After mixing each sample with the pipette tip the plate was covered with an adherent film and incubated at 36 °C. After contact times of 4 h and 24 h sampling was done after the following description for each sample: 50 µL were spread directly onto TSA containing neutralizer via Drigalski spatula, another 50 µL were diluted 1:10 in Saponin-Neutralizer, after 20 min neutralizing time 50 µL were plated out onto TSA with a spiral plater, further 1:10 dilutions were performed in deionized water and plated out onto TSA. The TSA plates were incubated for 48–72 hours at 36 °C prior to counting the colonies and calculating the colony forming units (cfu) per mL sample.

General procedure for the kinetic experiments of the aqueous polymerizations:

Vinyl mercaptoethanol (2-(Vinylthio)ethanol, 4.0 g, 38.3 mmol), the corresponding surfactant, two drops of tetrabutylammonium chloride (internal standard) and water (volume: 11.95 mL) were added in a microwave vial and stirred for 5 min at 40 °C to homogenize the solution. Before polymerization a sample was taken as starting point control. Afterwards, the solution was cooled, and a 10wt% stock solution of V-50 (0.206 g, 0.760 mmol) was added. The dispersion was purged with nitrogen for 20 min and then immersed into an oil bath at 80 °C and stirred (800 rpm) for 5 h. Samples at regular time intervals were taken over the course of the reaction to monitor the progress of the reaction.

General procedure for the synthesis of a larger batch of PVME dispersion:

Vinyl mercaptoethanol (2-(Vinylthio)ethanol, 20 g, 192 mmol), PVA (200 mg) and V-50 (1058.2 mg, 3.90 mmol) were dispersed water (volume: 69 mL) in a round flask and the dispersion was purged with nitrogen for 20 min and then stirred (800 rpm) at 80 °C for 6 h. Afterwards, dialysis (MWCO: 3.5 to 5 kDa) was performed against deionized water for three days including two exchanges of the surrounding water.

General procedure for the silver ion release experiments:

PVME dispersions (concentration: 142.1 mg mL⁻¹) and a freshly prepared AgNO₃-stock solution (amounts used in the different experiments are given in Table S1) were added to a vial and the dispersion was

stirred for 24 h at room temperature. Afterwards, the dispersion was filled into a dialysis tube, (MWCO: 3.5 to 5 kDa), deionized water was added, and the sample was purified against 700 mL of deionized water for three days including two water exchanges to remove an excess of silver ions. A sample of the dispersion was subsequently taken and analyzed *via* ICP-MS-measurements. The dialysis tube was then transferred into fresh water and another sample was taken from the dispersion after 7 d and analyzed by ICP-MS. In case of R2, daily samples were also taken from the filtrate over the course of six days. Quantities of the used chemicals are summarized in Table S2.

Table S2: Overview of the quantities of chemicals used for release experiments.

	$C_{Emulsion}$ [mg mL ⁻¹] ^a	$m_{Emulsion}$ [mg]	m_{AgNO_3} [mg]	C_{AgNO_3} stock solution [mg mL ⁻¹]	Eq. of Ag ⁺ vs. sulfur	m_{water} [mg]
R1	142.0	2019.7	9.6	4.8	0.02	2000
R2	142.0	2004.9	17.7	8.8	0.04	2026
R3	142.0	2008.8	44.2	22.2	0.1	2208

^a Gravimetrically determination of the concentration.

General procedure for the preparation of Ag@PVME:

Ascorbic acid as reducing agent: A freshly prepared AgNO₃ solution was added to the emulsion and stirred for 3 h, then dialyzed (MWCO: 3.5 to 5 kDa) against deionized water for one day. 5 mL of ascorbic acid solution were subsequently added, and the solution was stirred overnight under exclusion of light. The resulting dispersions were again purified by dialysis (MWCO: 3.5 to 5 kDa) against deionized water for three days including two water exchanges. Quantities of the used chemicals are summarized in Table S3.

Table S3: Overview of the quantities of chemicals used for synthesis of AgNP@PVME with ascorbic acid.

$C_{Emulsion}$ [mg mL ⁻¹] ^a	$m_{Emulsion}$ [mg]	m_{AgNO_3} [mg]	C_{AgNO_3} [mg mL ⁻¹] stock solution	Eq. of Ag ⁺ vs. sulfur	m_{AA} [mg]	C_{AA} stock solution [mg mL ⁻¹]	Eq. of Ag ⁺ vs. sulfur
57.0	5000	44.1	8.8	0.1	45.7	9.1	0.1

^a Gravimetrically determination of the concentration.

Reduction in sunlight: A freshly prepared AgNO₃ solution was added to the PVME-emulsion and stirred for 3 h, subsequently dialyzed (MWCO: 3.5 to 5 kDa) against deionized water for one day. Subsequently, the sample was diluted with deionized water, and the solution was stirred for three days at room temperature in sunlight. The dispersions were again purified by dialysis (MWCO: 3.5 to 5 kDa) against deionized water for three days including two water exchanges. Several batches were prepared for all experiments, which are summarized in Table S4.

Table S4: Overview of the quantities of chemicals used for synthesis of AgNP@PVME in sunlight.

Batch	$C_{Emulsion}$ [mg mL⁻¹]^a	$m_{Emulsion}$ [mg]	m_{AgNO_3} [mg]	C_{AgNO_3} [mg mL⁻¹] stock solution	m_{water} [mg]	Eq. of Ag⁺ vs. sulfur
B1 (1% PVA)	68.97	5000	56.2	11.2	5000	0.1
B2 (1% PVA)	142.0	2000	17.7	8.8	2026	0.04
B3(1% PVA)	115.4	2000	33.2	16.6	2000	0.1
B4 (2% PVA)	102.3	2000	30.4	15.2	2000	0.1
B5 (4% PVA)	217.4	2000	58.1	29.1	2000	0.1
B6 (8% PVA)	199.15	2000	50.5	25.3	2000	0.1

^a Gravimetrically determination of the concentration.

General procedure for the preparation of Au@PVME:

A freshly prepared HAuCl₄ solution were added to the PVME-emulsion and stirred for 3 h, then dialyzed (MWCO: 3.5 to 5 kDa) against deionized water for one day. Afterwards deionized water was added, and the solution was stirred for three days at room temperature in sunlight. The particles were purified by dialysis (MWCO: 3.5 to 5 kDa) against deionized water for three days in the sunlight including two water exchanges. Quantities of the used chemicals are summarized in Table S5.

Table S5: Overview of the quantities of chemicals used for synthesis of AuNP@PVME in sunlight.

Batch	$C_{Emulsion}$ [mg mL⁻¹]^a	$m_{Emulsion}$ [mg]	m_{AuCl_4} [mg]	C_{AuCl_4} [mg mL⁻¹] stock solution	m_{water} [mg]	Eq. of Au⁺ vs. sulfur
C1	57.0	5000	44.1	8.8	5000	0.1

^a Gravimetrically determination of the concentration.

Results

Influence of surfactants

Table S6: Conversions and average molar masses of the aqueous polymerizations with different surfactants.

Surfactant	Conversion [%] ^a	Molar mass [g mol ⁻¹] ^b	\bar{D} ^b
without	92	13 600	1.68
SDS	93	10 200	1.84
Triton™ X-100	89	12 400	1.78
Tween™ 80	93	11 900	1.43
Pluoronic™ F-127	93	10 700	1.70
PVP	93	10 600	1.54

^a Determination via ¹H-NMR (300 MHz, DMSO-d₆)-spectroscopy *via* standard.

^b SEC (DMAc (+ 0.21wt% LiCl), PMMA standards) after 5 h.

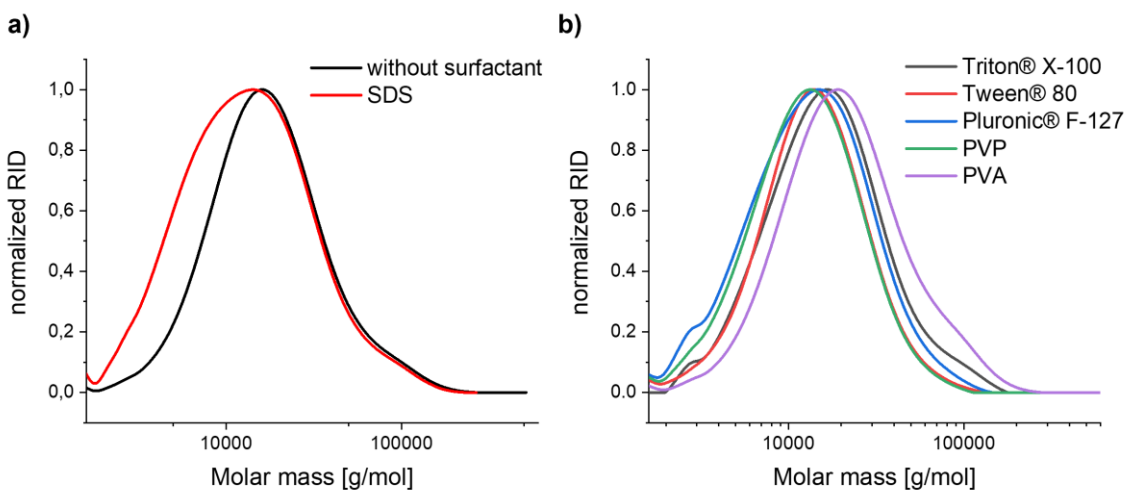


Figure S1: SEC (DMAc (+ 0.21wt% LiCl), PMMA standards) traces of the polymers after the aqueous polymerization with 1wt% of different surfactants.

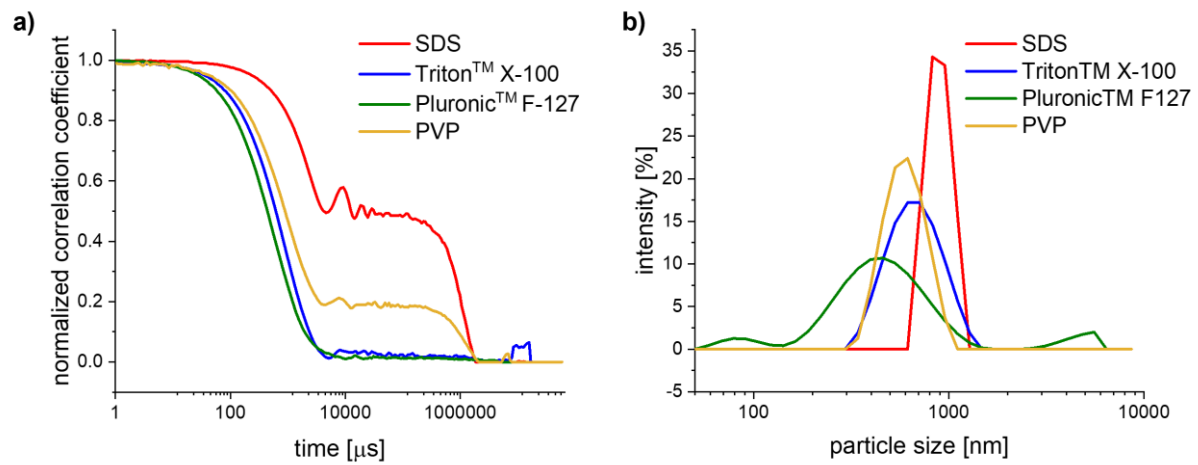


Figure S2: a) Correlograms and b) intensity distributions of the polymer particles after polymerization with different surfactants (DLS measurements in water).

Influence of PVA content

Table S7: Conversions, molar masses and particle sizes of the emulsion polymerizations with different amount of PVA.

PVA [wt%]	Conversion [%] ^a	Molar mass [g mol ⁻¹] ^b	\bar{D} ^b	Z- average [nm] ^c	PDI ^c	Z-average [nm] ^d	PDI ^d
1	93	7820	1.85	1180	0.64	1870	0.28
2	92	8170	1.80	1080	0.32	890	0.46
4	97	9470	2.24	3140	0.13	1210	0.71
8	97	9480	2.22	5640	0.04	4350	0.29

^a Determination *via* ¹H-NMR (300 MHz, DMSO-d₆)-spectroscopy after 5h with *a* standard.

^b Determination *via* SEC (DMAc (+ 0.21wt% LiCl), PMMA standards) after 5 h.

^c Determination *via* DLS – measurements before purification.

^d Determination *via* DLS – measurements after purification *via* dialysis.

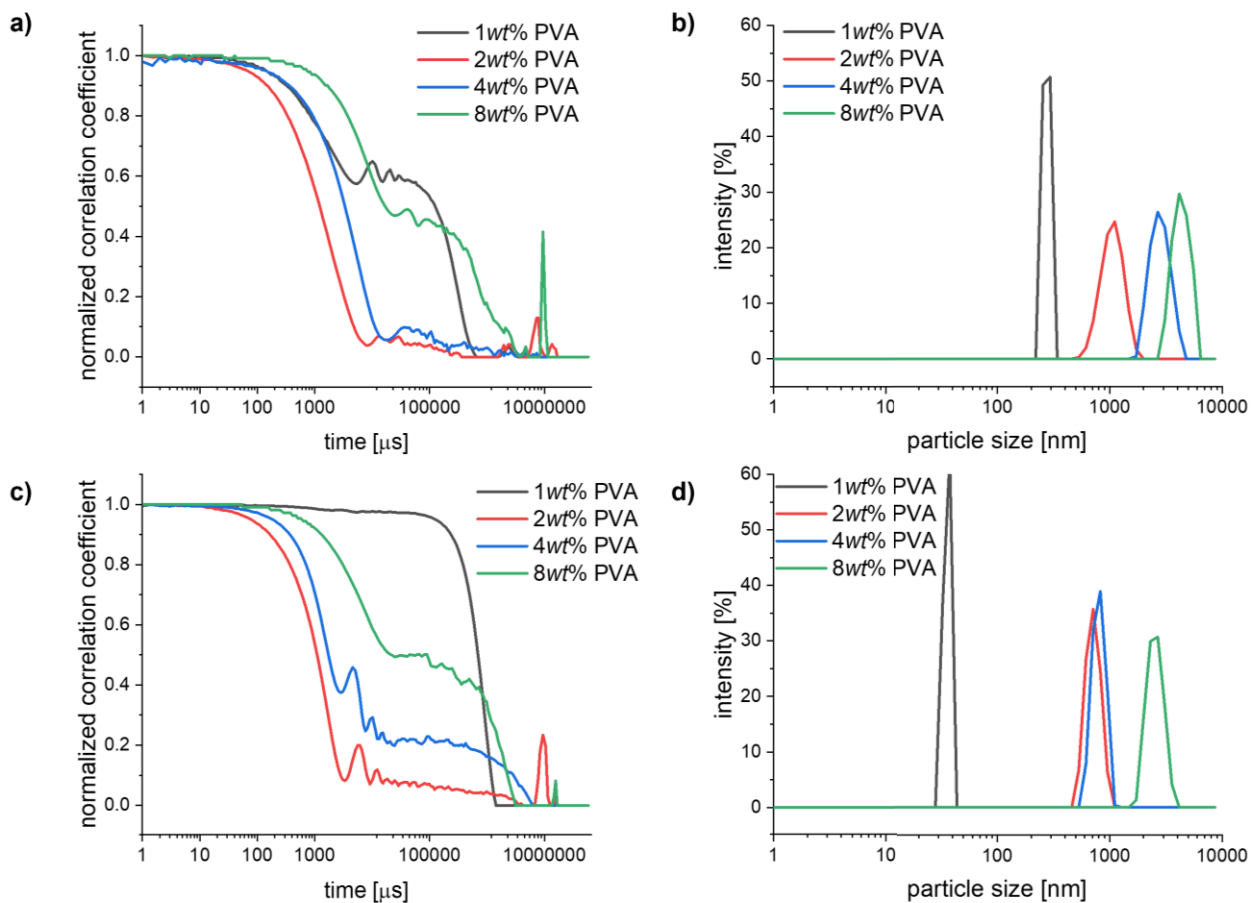


Figure S3: a) Correlograms and b) intensity distributions of the polymers after polymerization with different amounts of PVA and c) correlograms and d) intensity distributions after purification of the polymers with different amounts of PVA (DLS measurements in water).

Table S8: Conversions, and molar masses of the polymerizations with 1wt% PVA.

Concentration [g mL ⁻¹]	Conversion [%] ^a	Molar mass [g mol ⁻¹] ^b	\bar{M}_n ^b
0.22	93	15 500	1.75
0.11	89	13 500	1.6
0.06	76	10 800	1.36

^a Determination *via* ¹H-NMR (300 MHz, DMSO-d₆)-spectroscopy after 5 h *via* standard.

^b Determination *via* SEC (DMAc (+ 0.21wt% LiCl), PMMA standards) after 5 h.

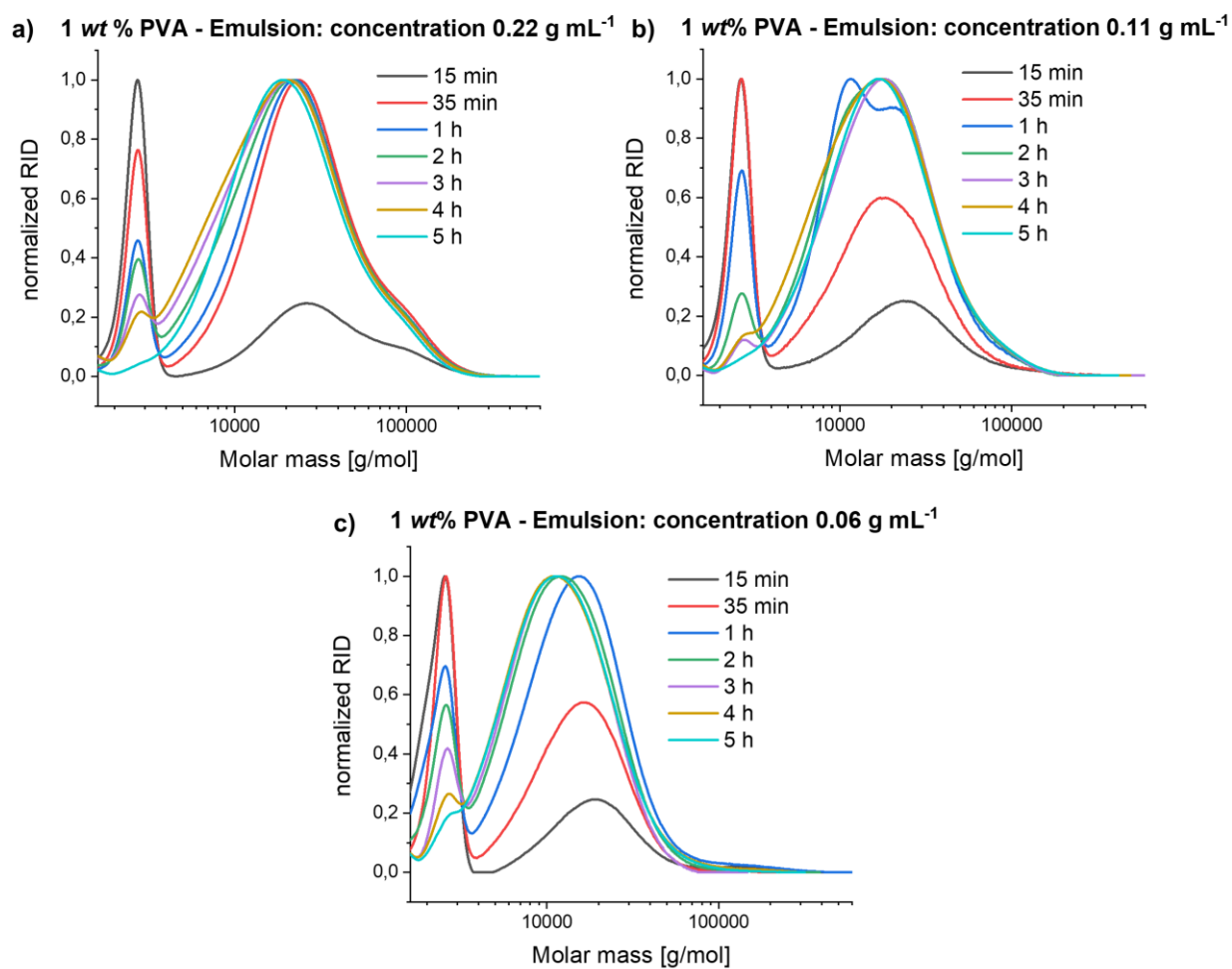


Figure S4: SEC (DMAc (+ 0.21wt% LiCl), PMMA standards) traces of the kinetic samples taken after 15 min, 35 min, 1 h, 2 h, 3 h, 4 h and 5 h of the polymerization at a monomer concentration of a) 0.22 g mL⁻¹, b) 0.11 g mL⁻¹, and c) 0.06 g mL⁻¹.

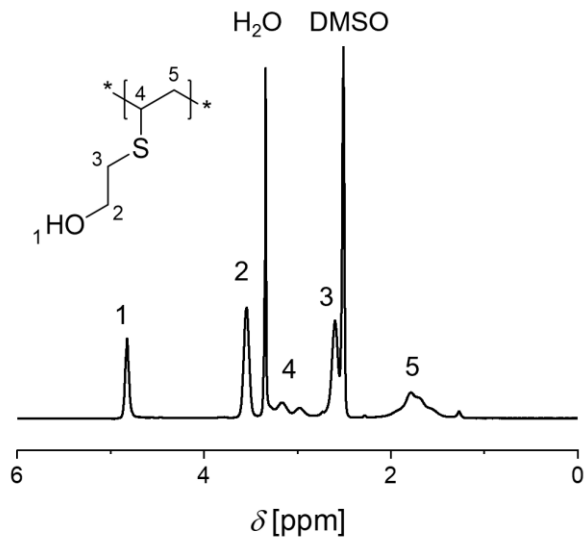


Figure S5: $^1\text{H-NMR}$ spectra (300 MHz, DMSO-d_6) of the purified polymer.

Table S9: Thermal properties of the polymers prepared at different initial monomer concentrations with 1wt% PVA.

Concentration [g mL^{-1}]	T_d [$^{\circ}\text{C}$] ^a	T_g [$^{\circ}\text{C}$] ^b
0.22	271	14.9
0.11	272	13.0
0.06	271	13.7

^a Determination from TGA – measurements.

^b Determination from DSC – measurements.

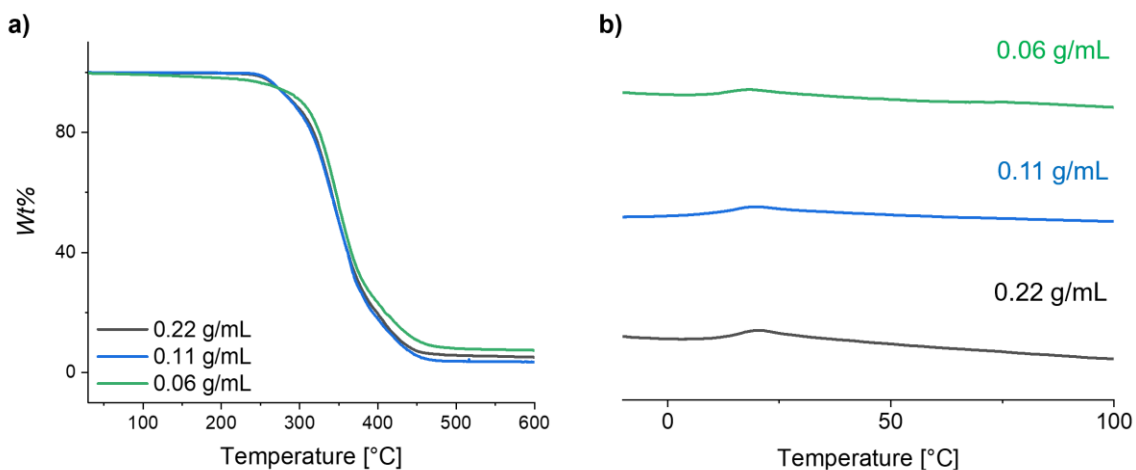


Figure S6: a) TGA data (N_2) and b) DSC data of PVME prepared at different initial monomer concentrations.

Coordination of silver ions (Ag^+ @PVME)

Table S10: Data from silver ion release experiments.

Exp.	Eq. of AgNO_3 (pre-weight)	c_{Ag^+} [mg mL ⁻¹] after purification ^a	c_{Emulsion} [mg mL ⁻¹] after 7 d of dialysis ^b	c_{Ag^+} [mg mL ⁻¹] after 7 d of dialysis ^a	theo. max. c_{Ag^+} [mg mL ⁻¹] after 7 d of dialysis ^d
R1	0.02	0.15	4.2	0,136 ^c	0.086
R2	0.04	0.225	4.3	0.167	0.168
R3	0.1	0.378	6	0.321	0.561

^a Determination *via* ICP – MS measurements.

^b Gravimetrically determination of the concentration.

^c Deviation due to inhomogeneity of the sample.

^d Calculation with the determined concentration of the emulsion and the preweighted eq. of the silver salt.

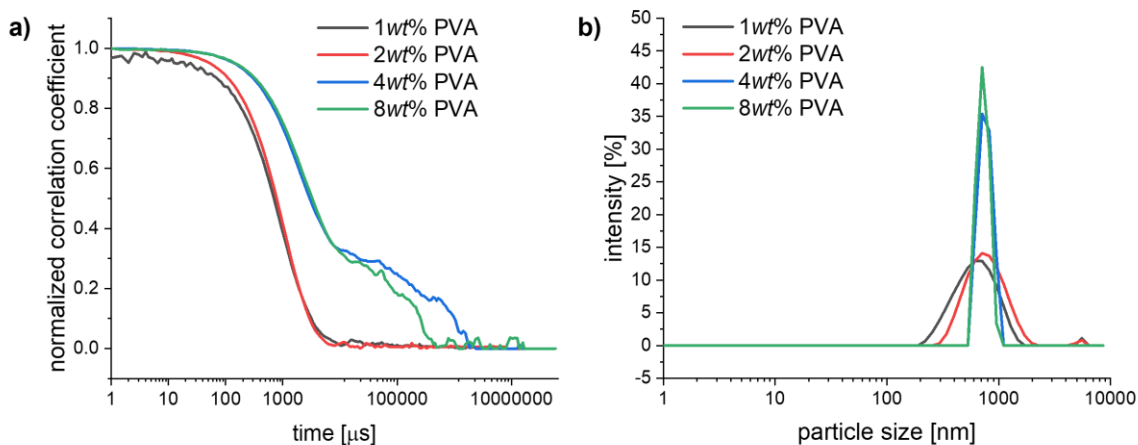


Figure S7: a) Correlograms and b) intensity distributions of samples Ag^+ @PVME (B3-B6) with different amounts of PVA (DLS measurements in water).

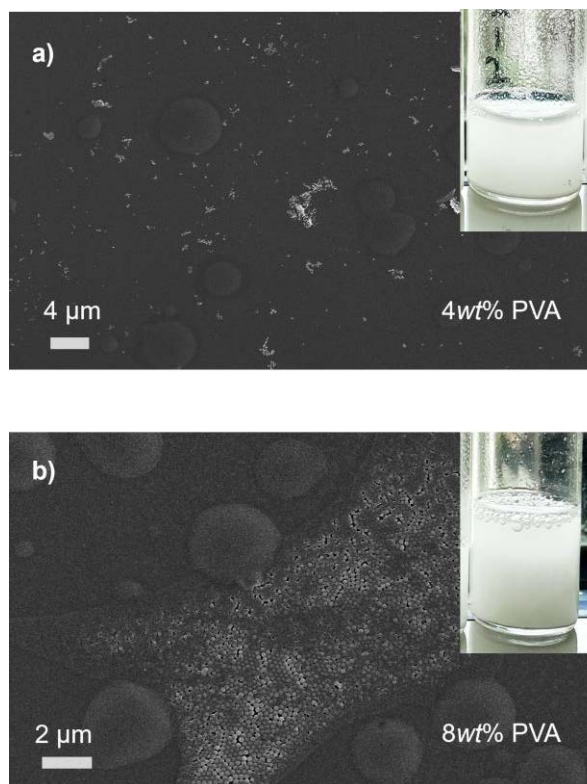


Figure S8: SEM images of Ag⁺@PVME a) B5 and b) B6.

Formation of silver composites (Ag@PVME)

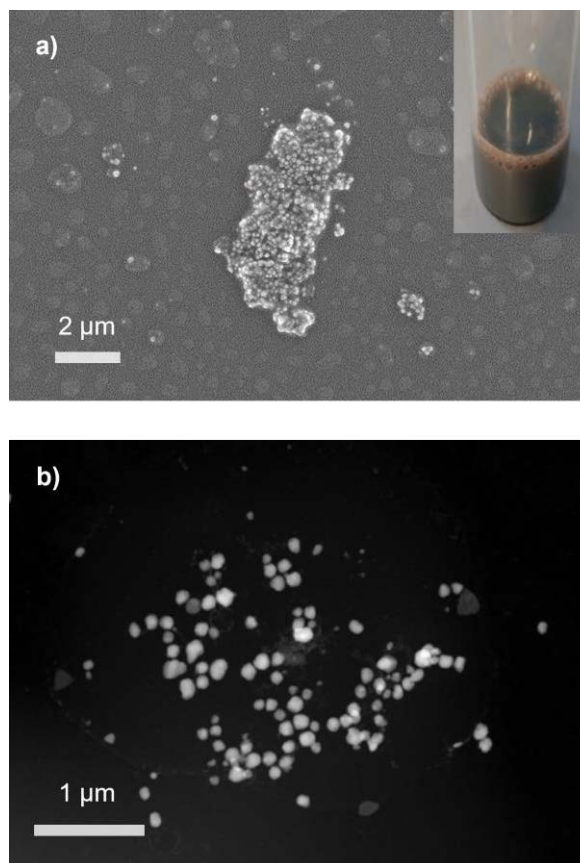


Figure S9: a) SEM image of Ag@PVME prepared with ascorbic acid as reducing agent and b) corresponding TEM image.

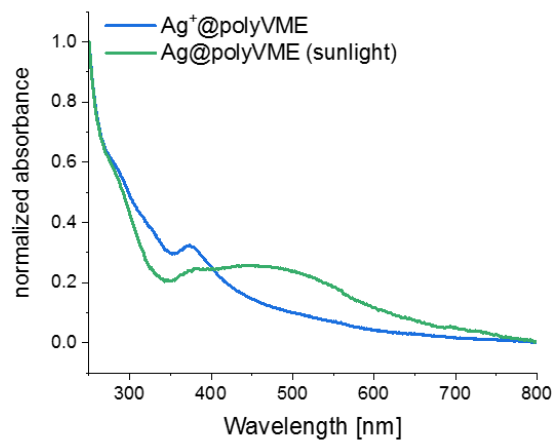


Figure S10: UV-Vis spectra of Ag⁺@PVME (R2) and Ag@PVME (B2) synthesized in sunlight.

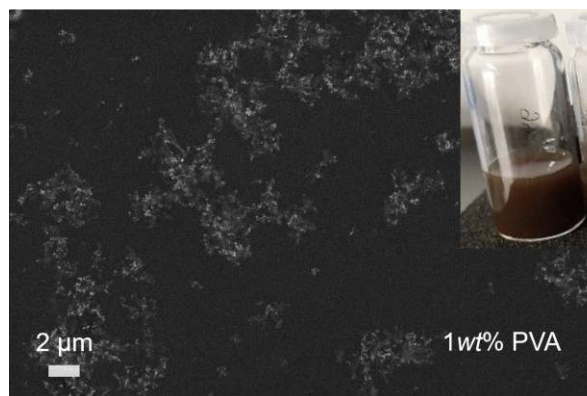


Figure S11: SEM image of Ag@PVME (B2).

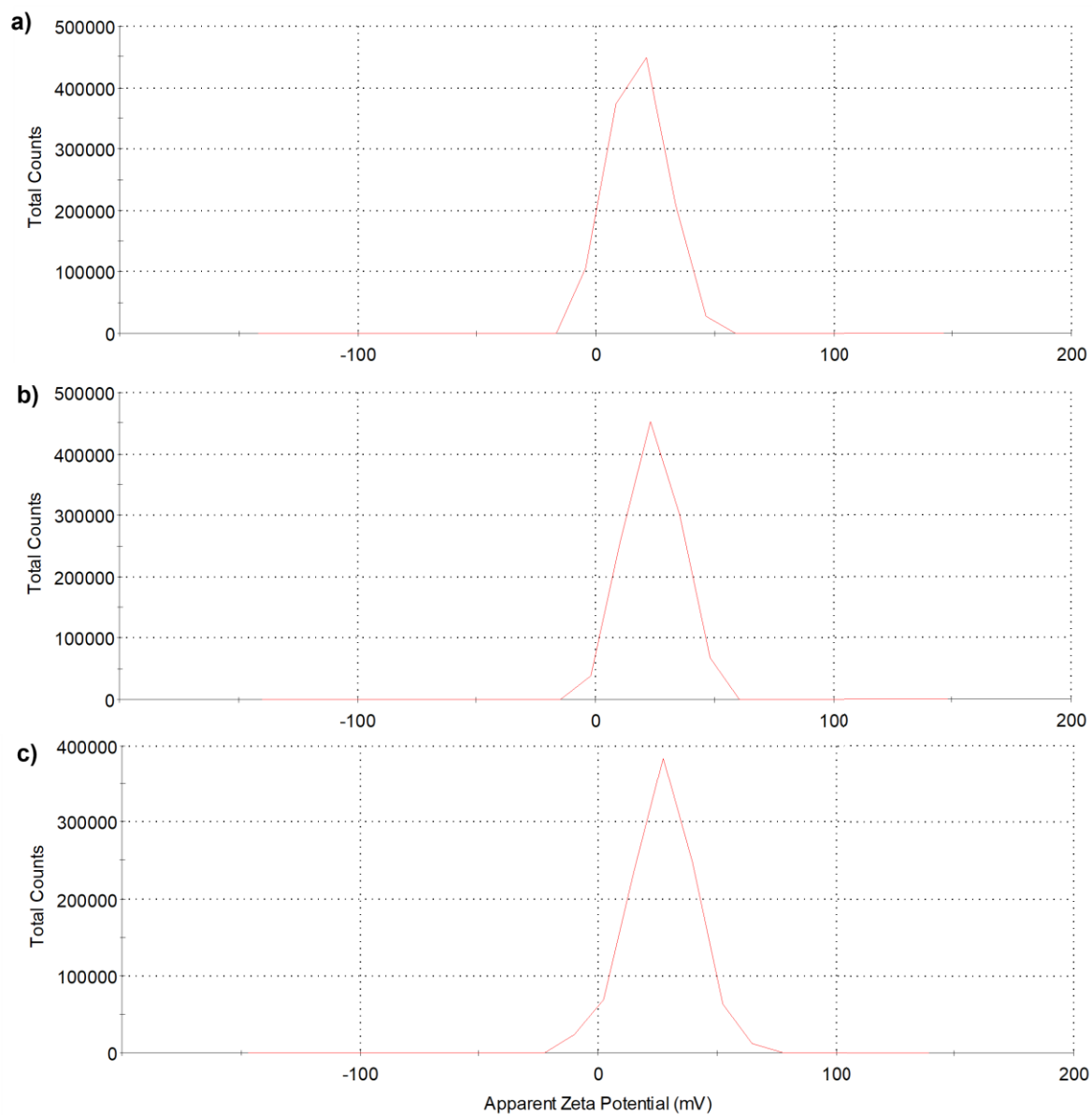


Figure S12: Zeta-potential of a) PVME, b) Ag⁺@PVME (B3) and c) Ag@PVME (B3) measured in water.

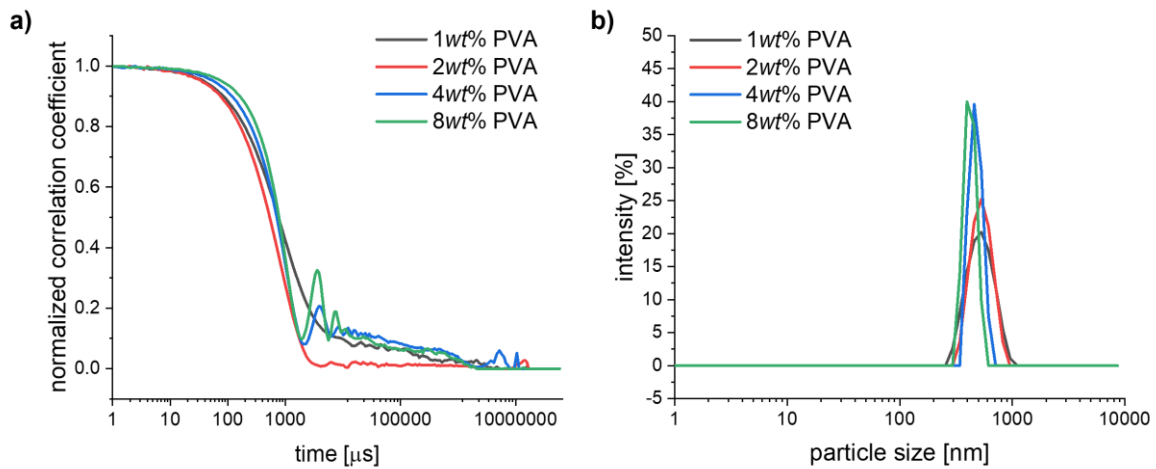


Figure S13: a) Correlograms and b) intensity distributions of Ag@PVME (B3-B6) with different amounts of PVA (DLS measurements in water).

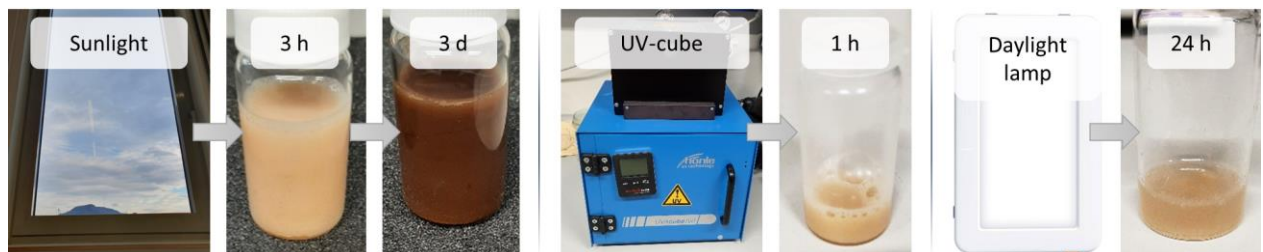


Figure S14: Influence of different reaction environment for the reduction of silver ions.

Table S11: Data of the antibacterial tests.

Exp.	Contact time [h]	S. aureus ATCC 6538 [cfu mL⁻¹]	E. coli DSM 682 [cfu mL⁻¹]
Pure emulsion (PVME)	4	4.2E+05	1.0E+05
	24	>6.0E+06	>6.0E+06
Ag ⁺ @PVME	4	3.5E+04	<20
	24	8.0E+01	<20
Ag@PVME	4	1.6E+05	3.8E+05
	24	>6.0E+05	>6.0E+05
Irgaguard B 6000 (benchmark)	4	<20	<20
	24	<20	120